Molecular Assembly in Crystals and Thin Films of Novel Metal-Organic Compounds and Optical Second Harmonic Generation Studies

A Thesis Submitted for the Degree of
DOCTOR OF PHILOSOPHY

by

S. Philip Anthony

School of Chemistry
University of Hyderabad
Hyderabad 500 046
INDIA

March 2005

Dedicated to
My Parents

CONTENTS

DECLARATION

I hereby declare that the matter embodied in this thesis is the result of investigations carried out by me in the School of Chemistry, University of Hyderabad, Hyderabad under the supervision of Prof. T. P. Radhakrishnan.

In keeping with the general practice of reporting scientific observations, due acknowledgements have been made wherever the work described is based on the findings of other investigators.

S. Philip Anthony

CERTIFICATE

This is to certify that the work described in this thesis entitled "**Molecular Assembly in Crystals and Thin Films of Novel Metal-Organic Compounds and Optical Second Harmonic Generation Studies**" has been carried out by S. Philip Anthony, under my supervision and the same has not been submitted elsewhere for any degree.

Prof. T. P. Radhakrishnan
(Thesis Supervisor)

DEAN
School of Chemistry
University of Hyderabad
Hyderabad 500 046

ACKNOWLEDGEMENTS

I express a deep sense of gratitude to Prof. T. P. Radhakrishnan, my research supervisor for his constant guidance, encouragement and for the freedom he gave me in carrying out my research. His commitment to the work with a great sense of discipline and patience are highly admirable and very inspiring. My association with him is a memorable one in my life.

I am deeply indebted to Prof. D. Narayana Rao, School of Physics, for his cooperation and valuable guidance in carrying out the SHG experiments. Without his help and involvement I couldn't have completed my work effectively. Association with him is always motivating.

I thank Prof. E. D. Jemmis, Dean School of Chemistry, former Deans and other faculty members of the school for their support and help on various occasions. Special thanks are due to late Prof. Bhaskar G. Maiya, Prof. K. C. Kumaraswamy and Prof. S. Pal. I thank DST for the National Single Crystal X-ray Diffractometer Facility at our School and CSIR for the financial support.

I take this opportunity to thank all my teachers in school and college, especially V. Kalyanasundaram, M. Kandasamy, Dr. N. Xavier and Dr. N. Mathiyalagan, for their wonderful teachings, encouragement and affection.

I also thank all the non-teaching staff of the school. Mr. Shetty for timely supply of chemicals, Mr. Vara Prasad for all his art with glass blowing, Mr. Satyanarayana and Mr. Bhasker Rao for their excellent job with NMR machine, Ms. Asia for her tireless effort for collecting IR spectra and Mr. Raghavaiah for mounting our crystals are acknowledged. The assistance of Dr. Manjunadh, Mr. Prasad and Mr. Suresh are gratefully appreciated.

It is a great pleasure to thank my seniors Dr. Palas Gangopadhyay and Dr. Sonika Sharma for their help and cooperation. My special thanks to Dr. Jayanty Subbalakshmi

and Mr. Siva Kumar for their support and timely help. I especially thank Sharat and Joseph for extending their cooperation and help during my thesis work. Thanks to Prakash, Shatabdi, Abhijit, Rajesh, Dr. Prem, Srinivas, Manoj and other laser labmates for their cooperation. I am extremely thankful to Dr. Ramanathan, Dr. Muthiah, Dr. Doss, Dr. Loganathan and Dr. Kamaraj for their help and encouragement. I thank Mr. Suresh Kumar, Dr. Suresh Kumar, Dr. Benedict, Dr. James, Dr Edwin and Mr. Jeba singh for their support and affection. Special thanks to Bharathi for his help in recording powder x-ray diffractogram and SEM images. I thank all research scholars and friends for the cheerful and enlivening atmosphere they maintained and for making my stay in the campus unforgettable.

I am at a loss of words to thank my parents, for their love, affection, care and unstinting support. I also thank my sister, brother-in-law, brother and sister-in-law for their constant support.

Once and for all I thank everybody directly or indirectly connected to this thesis.

S. Philip Anthony

COMMON ABBREVIATIONS

AM1	Austin Model 1
BABDC	N,N'-Bis(4-aminobenzoyl)-(1*R*,2*R*)-diaminocyclohexane
BBDC	N,N'-Bis(benzoyl)-(1*R*,2*R*)-diaminocyclohexane
BCDC	N,N'-Bis(4-cyanophenyl)-(1*R*,2*R*)-diaminocyclohexane
BFBDC	N,N'-Bis(4-flurobenzoyl)-(1*R*,2*R*)-diaminocyclohexane
BINDC	N,N'-Bis(4-isonicotinoyl)-(1*R*,2*R*)-diaminocyclohexane
BMBDC	N,N'-Bis(4-methoxybenzoyl)-(1*R*,2*R*)-diaminocyclohexane
BNBDC	N,N'-Bis(4-nitrobenzoyl)-(1*R*,2*R*)-diaminocyclohexane
CBP	(N,N'-Bis(4-cyanophenyl)-(1*R*,2*R*)-diaminocyclohexane) copper(I) hexaflurophosphate
CBPT	(N,N'-Bis(4-cyanophenyl)-(1*R*,2*R*)-diaminocyclohexane) (tetrahydrofuran)copper(I) hexaflurophosphate
CD	circular dichroism
COSMO	conductor-like screening model
d	doublet
D, A	donor, acceptor
dec	decomposition
LB	Langmuir-Blodgett
m	multiplet
M.P.	melting point
NLO	nonlinear optical
s	singlet
SBP	(N,N'-Bis(4-cyanophenyl)-(1*R*,2*R*)-diaminocyclohexane) silver(I) perchlorate
SHG	second harmonic generation
t	triplet
THF	tetrahydrofuran
ZNDA	(4-Dimethylaminopyridyl)bis(acetylacetonato)Zn(II)
ZNMPA	(4-Morpholinopyridyl)bis(acetylacetonato)Zn(II)
ZNPPA	(4-Pyrrolidinopyridyl)bis(acetylacetonato)Zn(II)

CHAPTER 1

Introduction

1.1 MOLECULAR MATERIALS

Materials have played a key role in the evolution of human civilization. The kind of materials developed and used through the course of history, serve as excellent indicators of the progress of science and technology and civilization at large; the stone age followed by the copper, bronze and iron ages have led to the present 'plastic age'. The early utilization of materials was based on their structural, mechanical, optical or thermal properties. Metals and their alloys, metal-based compounds and finally plastics were the forerunners of modern materials. The application of these materials was based primarily on their electrical, magnetic, optical and mechanical properties. Revolutionary developments such as the discovery of superconductivity and the fabrication of the first transistor marked the dawn of a new era in the field of materials. The pace at which the physical and chemical sciences grew was reflected in the appearance of new materials and materials fabrication. Starting with simple mechanical approaches to materials structuring, more sophisticated thermal, electrical, chemical and electrochemical techniques have evolved. Assembly of materials at the atomic and molecular level we witness today is the next link in the logical evolution of materials fabrication.

Molecular materials[1] made up of molecules or molecular ions as their building blocks as opposed to atoms and ions in the traditional solid state materials, form a major class of materials developed over the past five decades. They have attracted considerable attention because of the wide range of properties that can be realized and their potential utility in many technological applications. Because of the relatively weak nature of intermolecular interactions, the properties of molecular materials are generally based on additive contributions from the constituent molecular units. It often occurs that the properties that the molecules exhibit in the materials state are retained in the individual isolated state as well; significant exceptions do however exist. Traditional solids like inorganic salts, metal oxides, covalent solids, metals and alloys, on the other hand, exhibit vastly different characteristics in the bulk state compared to their constituent atoms or ions. Nanoscale materials[2] which are at the focus of extensive scientific and technological research today, show stark differences from the atomic and bulk limits in the case of metals and semiconductors, whereas in the case molecular materials, the supramolecular clusters[3] represent a smooth transition from the molecular to the bulk

materials. The properties of molecular materials are sensitive to the orientations and mutual dispositions of the molecules in the assembly. Molecular materials utilize ionic, covalent and coordinate bonding interactions and in addition, a wide variety of relatively weaker interactions, to organize the molecules in the solid state.[1,4] Polymeric materials built from macromolecules or metal complexes with extended coordination can also be classified as belonging to the general family of molecular materials. Several classes of molecular materials have been designed and developed over the years to achieve properties such as magnetism, conductivity and optical and nonlinear optical effects. Of late, there is considerable interest in the use of single molecules functioning as active devices for optical, electrical and mechanical functions. Functional molecular scale devices that have been developed include rectifiers,[5] switches,[6] gates,[7] wires,[8] shuttles,[9] brakes,[10] ratchets [11] and gears.[12]

The design and fabrication of molecular materials effectively exploits the enormous power and flexibility of synthetic chemistry to tailor specific molecular structures. The fundamental distinction between the route to molecular materials and the conventional approach to materials is shown in Fig. 1.1. Traditionally, materials are fabricated from suitable precursors, employing techniques such as ceramic methods, melt-quench processes, vapor deposition or sol-gel.[2,13] In the case of molecular materials, a well defined intermediate stage - the molecule or molecular ion – is involved. The intermediate stage effectively separates the molecule synthesis from the materials fabrication. The property of the molecule is determined by its structure while the property of the fabricated materials depends on the molecules and the way they are organized in the bulk. While the synthetic approach can be fine-tuned to achieve desired molecular structure, the control of organization of the molecules in the bulk state is a considerably more complex problem. Thus, the fabrication of molecular materials with specific organizational motifs is a challenging task that needs to be tackled to realize preferred materials properties. The possibility of dissociating the molecular materials into their constituent units in most instances, facilitates an iterative way of realizing tailored materials (Fig. 1.1) providing a unique handle to control the materials attributes.

Several techniques have been developed for the fabrication of molecular materials. Crystallization from organic or aqueous solvent medium is perhaps the most

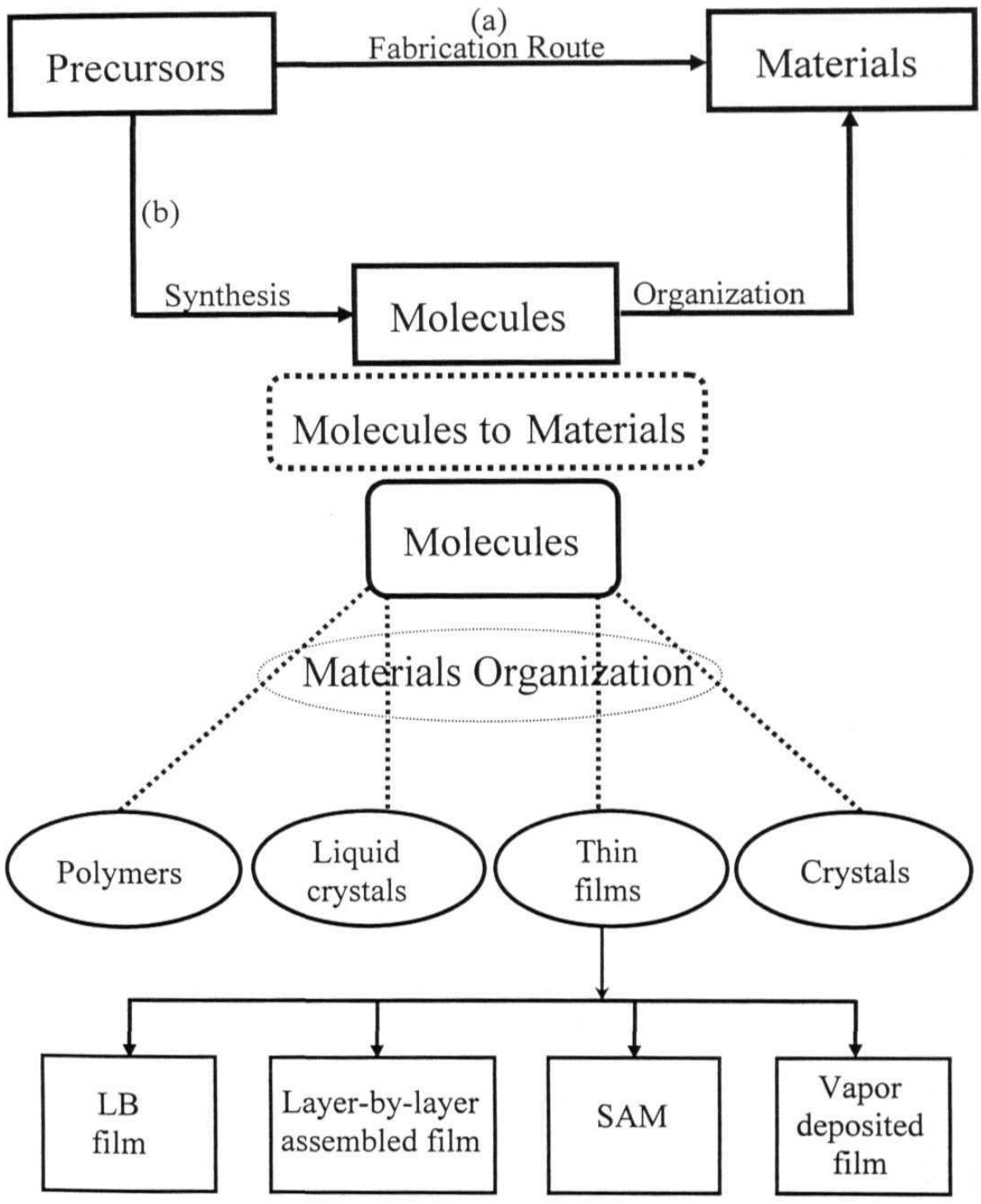

Figure 1.1 *Schematic representation of the* ***(a)*** *traditional approach to materials fabrication compared to the* ***(b)*** *two-stage synthesis of molecular materials.*

common technique.[14] Electrocrystallization is popular in the case of conductors and superconductors.[15] In this technique the molecule is oxidized or reduced in the presence of appropriate counterions. Since simple crystallization does not provide facile control on the final bulk organization, alternative techniques which involve directed assembly of molecular materials, are often adopted. They include methods such as electric field poling,[16] Langmuir-Blodgett technique[17] and layer-by-layer assembly.[18,19] Spin and dip coating, sol-gel processing[13] and chemical or physical vapor deposition[20] are other approaches resorted to.

Molecular magnetic materials

Molecular magnetic materials are potential candidates to develop magnetic, electromagnetic and magneto-optic devices. For centuries after the discovery of the naturally occurring magnet, Fe_3O_4, most of the magnets that were fabricated and used were based on the compounds and alloys of elements such as iron, cobalt, nickel and gadolinium, which are themselves ferromagnetic in their pure state. The charge transfer complex of decamethylferrocene and tetracyanoethylene was the first molecular material involving an organic ion radical that showed ferromagnetic phase transition with a $T_C \sim$ 4.8 K. Several magnetic materials based on coordination polymers and molecular systems in which metal ion serves as the source of magnetic moment have been developed. The design and fabrication of ferromagnetic solids from simple paramagnetic units and controlling the magnetism using synthetic manipulations is a fascinating problem. The basic idea is to build chains or sheets of paramagnetic metal ions with appropriate bridging ligands so that the desired magnetic interactions between the ions can be achieved. The distance between the ions and their three-dimensional interactions are of profound significance, and optimal design can lead to spontaneous magnetization at ambient temperature.[21,22] In order to achieve a strong coupling between the metal centers with their unpaired electrons, short bridging ligands such as oxo, cyano, azido, pyrazolate or triazolate have been investigated. The metalloligands are good candidates for the construction of novel bimetallic coordination polymers with spontaneous magnetization.[23]

Another approach to molecular magnetic materials is to utilize an organic radical ligand which serves as the spin carrier as well as linker to magnetically active metal ions.[24] Different methods have been used to construct coordination polymer based magnetic materials containing organic radical ligands - utilization of an organic radical ligand for a direct linker, generation of a radical on a linking ligand as a result of the formation of the coordination polymer and production of a radical by light irradiation following the construction of the coordination polymer. A strategy using π-conjugated polynitroxide radicals with high spin ground states as bridging ligands for magnetic metal ions was applied to assemble and align spins on a macroscopic scale.[25] Molecular compounds containing rare earth metal ions coupled with transition metal ions and radical ligands have also been extensively studied.[26]

Even though many organic radical systems are known, obtaining a ferromagnetic coupling in the solid state is a difficult task. Unlike in metal-based systems where the unpaired electron spin are largely confined to the metal center, in organic molecular spin systems the unpaired electron is delocalized over the various atoms that constitute the molecule. Generally, bonding tendencies between orbitals lead to preferential antiferromagnetic coupling of spins. One of the ideas proposed to obtain ferromagnetic spin coupling between molecular spin systems was to achieve a packing of the molecules in such a way that the regions of positive spin densities on one molecule would be in close contact with regions of negative spin densities on the neighboring and vice versa. The ferromagnetic coupling between the unpaired electrons of the γ-phase crystals of p-nitrophenylnitronylnitroxide (p-NPNN) radicals have been extensively studied in the recent past.[27] Combination of structural analysis and specific modification by molecular engineering have led to the preparation of molecular solids that show short range organic ferromagnetism.[28] Molecular magnetic compounds are well developed, and strategies have been worked out to obtain new materials with designed properties, molecular ferro- and ferri-magnets, organic magnets, single molecule magnets and high-spin molecules.[29,30] Though molecular magnets[30] based on organic polymers and charge transfer complexes continues to attract materials chemists, a well-characterized ambient temperature organic polymer ferromagnet is yet to be realized.

Molecular conducting materials

Most organic solids and polymers are insulators: polymers such as teflon or bakelite are some of the best electrical insulators. However several molecular materials based on charge transfer complexes and doped π-conjugated polymers show appreciable conductivity. They are called synthetic metals,[31] as they are prepared through normal organic synthesis protocols. Many molecular crystals and π-conjugated polymers show conductivity similar to semiconductors.

The first molecular conductor was synthesized in 1842 by Knop by oxidizing the metal complex $K_2(Pt(CN)_4)$[32] with bromine, though the conducting property of these materials was perhaps not realized at that time. In the early 1950's Japanese researchers observed that perylene-bromine complex[33] showed a low electrical resistivity of about 8 Ω cm, a rather unexpected property for an organic solid. The synthesis of strong π-electron donor/accepter organic molecules such as tetracyanoquinodimethane (TCNQ) in 1962[34] and tetrathiafulvalene (TTF) in 1970,[35] marked the development of a large number of conducting or semiconducting charge transfer complexes. The conducting bands in molecular charge transfer complexes are expected to be generally narrow and best visualized as an intermediate regime between band and molecular orbital limits.[36] The most popular example of an 'organic metal' is the complex between TTF and TCNQ first prepared in 1973. TTF-TCNQ exhibits a room temperature conductivity of ~10^3 S/cm. Advances related to TCNQ based acceptor molecules and other cyano compounds have been reviewed recently.[37] TTF and related molecules have been the prime focus of a majority of organic conductors and superconductors research.[38] Several molecular conductors based on metal complexes have been developed. The halogen-bridged binuclear metal mixed-valence complexes exhibit metallic conduction above room temperature.[39] One-dimensional coordination polymers constructed from stacked porphyrin and phthalocyanine complexes have been studied extensively because of their electrical conductivity.[40]

Molecular optical materials

Over the past several decades, various classes of optical materials including dyes, pigments, luminescent and electroluminescent (EL) materials have been developed. Molecules with delocalized π-electron systems, often with donor-acceptor (push-pull) structure, possess interesting optical and nonlinear optical characteristics. Organic dyes have attracted considerable attention in the field of diodes and laser optical storage devices. The use of cyanine and phthalocyanine dyes in commercial recordable compact discs (CD-R) have facilitated the use of shorter wavelength (635-650 nm) laser beams in place of traditional 780 nm lasers. Dye lasers have contributed greatly to the progress in laser spectroscopy and laser chemistry. A wide variety of organic compounds with complex chemical structures are used as the active medium in current dye lasers.[41] Quinacridine, coumarins and polypyrroles are some of the famous industrial pigments.

Luminescent molecules and materials are potential candidates for display devices and sensor applications. Molecular recognition events that trigger fluorescence response are effectively exploited in chemical and biological applications. Families of molecules which exhibit efficient fluorescence include aromatic hydrocarbons and their derivatives, azomethines, azines, several five and six membered heterocyclic derivatives, carbonyl compounds and metal complexes with a wide range of organic ligands.[42] Several strongly intercalating metal complexes of platinum and ruthenium can act as luminescent markers for DNA[43] and foot print applications. A variety of nanomaterials, polymers and sol-gel systems also display strong fluorescence.[2,44] Molecular materials which display electroluminescence could be (i) organic dyes (ii) chelate metal complexes[45] or (iii) conjugated polymers. The most widely used metal complexes for electron transport and emitting materials are hydroxyquinoline based compounds. The conjugated polymer,[46] poly (p-phenylenevinylene) (PPV) shows high fluorescence and can be used as the active material in single layer organic light emitting diodes. The potential of molecular and polymeric EL devices for extensive commercial application is bright indeed. Coordination polymers have also been studied for luminescence applications owing to their higher thermal stability compared to pure organic materials and the facility of tuning the emission wavelength of the ligand moiety by metal coordination. The combination of organic spacers and transition metal centers in coordination polymers is seen as an

efficient method for obtaining new types of EL materials for potential applications as light emitting diodes.[47] Recently, the observation of polarized photoluminescence from molecular materials have suggested the possibility of using them in flat panel displays and other optoelectronic applications.[48]

Molecular nonlinear optical materials

Considerable progress has been made in recent times in using light (photons) as carriers of information. Optical telecommunication using optical fibers and optical displays using liquid crystals or polymeric light emitting materials are significant developments in these fast growing areas. It is expected that optical information technology will expand rapidly at a rate that roughly doubles transport, processing and storage capacity in every three years.[49] It is believed that a large fraction of the elements for these technologies will use light as the information carrier. Nonlinear optical (NLO) materials interact with the intense electromagnetic fields of laser beams and produce alterations in the properties of light such as the phase, frequency, amplitude, polarization and other propagation characteristics.[50] NLO materials are the key agents for the fast processing of information and for dynamic or permanent storage applications. The field of research and development of nonlinear optical materials has progressed impressively since the invention of laser in the late 1960's. Demonstration of the nonlinear optical phenomenon of second harmonic generation (SHG) in single crystal quartz by Franken and coworkers,[51] and phase matched SHG in KDP crystal by Geordamine[52] and Maker and coworkers laid the basis for modern nonlinear optics. Parametric oscillation[53,54] in KDP single crystal and lithium niobate ($LiNbO_3$) crystal were discovered in 1965. Rentzepis and Pao[55] in 1964 observed SHG in benzopyrene, the first instance in a molecular system. The potential of organics was revealed by studies on hexamethylenetetramine,[56] hippuric acid, benzil[57] and urea.[58,59] In 1968 a systematic approach was developed to quantify and classify SHG in organic and inorganic compounds by Kurtz and Perry.[58]

In the 1970's the analysis of nonlinear interference pattern in crystals was developed by Jerphagnon and Kurtz[60] and electric field induced second harmonic

generation in solution was demonstrated by Hauchecorne and coworkers[61] which showed the possibility of measuring individual molecular nonlinearities in solution phase.[54] Several books and reviews have appeared which deal with the theory and structural characteristics and applications of nonlinear optical molecules and materials.[62-65] Organic molecules and polymers are of great importance in the area of optoelectronics and photonics.[65,66] It is believed that future information technology will be largely based on photonics, wherein photons instead of electrons will be used to acquire, transmit and store information. Photorefractive[67] and photoconductive[68] materials are actively being explored for various applications in information processing and technology.

The efficiency with which materials can carry out nonlinear optical processes is controlled primarily by its nonlinear electric susceptibility. In the traditional semiconductors and other inorganic materials, nonlinear responses are related to individual nuclei or bond polarizabilities. Nonlinearity in molecular materials arises primarily due to electronic polarization effects controlled by the molecular electronic structure. The nonlinearity is highly dependent on the geometrical arrangement of the molecules in the condensed medium in the case of second order nonlinear processes, but much less so for third order nonlinearities. Molecular materials are increasingly being recognized as the materials of the future because of their fast and strong nonlinear responses and the versatility of synthetic chemistry which can be used to alter and optimize molecular structure to maximize the nonlinear responses.

1.2 NONLINEAR OPTICS

Basic concepts

Nonlinear optics is the study of phenomena that occur as a consequence of the interaction of the strong electromagnetic field of intense light such as laser beams with materials and the resulting modification of the optical properties of the materials. The strong oscillating electric field of the laser beam creates a polarization response in the material that is nonlinear with respect to the electric field. The electric field of an electromagnetic radiation typically in the range of optical frequencies induces electronic

polarization in a molecule or material, with which it interacts. The dipole moment induced per unit volume is called polarization. At low electric fields, the polarization, P is linearly related to the field E by the proportionality constant $\chi^{(1)}$, the linear electric susceptibility tensor (Fig.1.2). At high fields typically those associated with lasers, contribution of the nonlinear (second and higher order) terms become significant and P varies nonlinearly with E.[64] Higher order susceptibilities $\chi^{(n)}$ (n >1) are inherently smaller than $\chi^{(1)}$ and their magnitudes get smaller with increasing n. The polarization in a bulk material along the direction *i* can be represented as:

$$P_i = \chi_{ij}^{(1)} E_j + \chi_{ijk}^{(2)} E_j E_k + \chi_{ijkl}^{(3)} E_j E_k E_l + \ldots\ldots \quad (1.1)$$

In Eqn. 1.1 the indices *i*, *j*, *k* and *l* refer to the coordinates of the bulk material. The polarization at the molecular level, ρ_i similarly depends on the molecular polarizability, α and hyperpolarizabilities, β, γ etc as given in Eqn. 1.2.

$$\rho_i = \alpha_{ij} E_j + \beta_{ijk} E_j E_k + \gamma_{ijkl} E_j E_k E_l + \ldots\ldots \quad (1.2)$$

The coefficients $\chi^{(n)}$ in Eqn.1.1 as well as α, β, γ etc in Eqn.1.2 are tensorial quantities. The phenomenon of frequency doubling or second harmonic generation, a quadratic nonlinear optical (NLO) effect can be visualized as follows. If the applied electric field has frequency, ω and is represented as $\sin(\omega t)$, the quadratic term will have a 2ω dependence as seen in Eqn.1.3.

$$E \propto \sin \omega t$$
$$E^2 \propto \sin^2 \omega t \; (= \frac{1}{2}(1 - \cos 2\omega t)) \quad (1.3)$$

Eqns. 1.1 and 1.2 show that there is an important symmetry constraint for observing second harmonic generation or any other even order NLO effect. In systems having a center of inversion symmetry, reversal of the electric field would exactly reverse the polarization, *ie*, P(-E) = -P(E). From Eqn. 1.1 it can be seen that this is possible if and only if all terms with even powers of E become zero. This implies that the even order coefficients such as β, δ etc and $\chi^{(2)}$, $\chi^{(4)}$ etc. are strictly zero. In a noncentric system, no

such equality exists and generally, $P(-E) \neq -P(E)$. This implies that quadratic or any other even order effects are possible only in noncentrosymmetric molecules or materials.

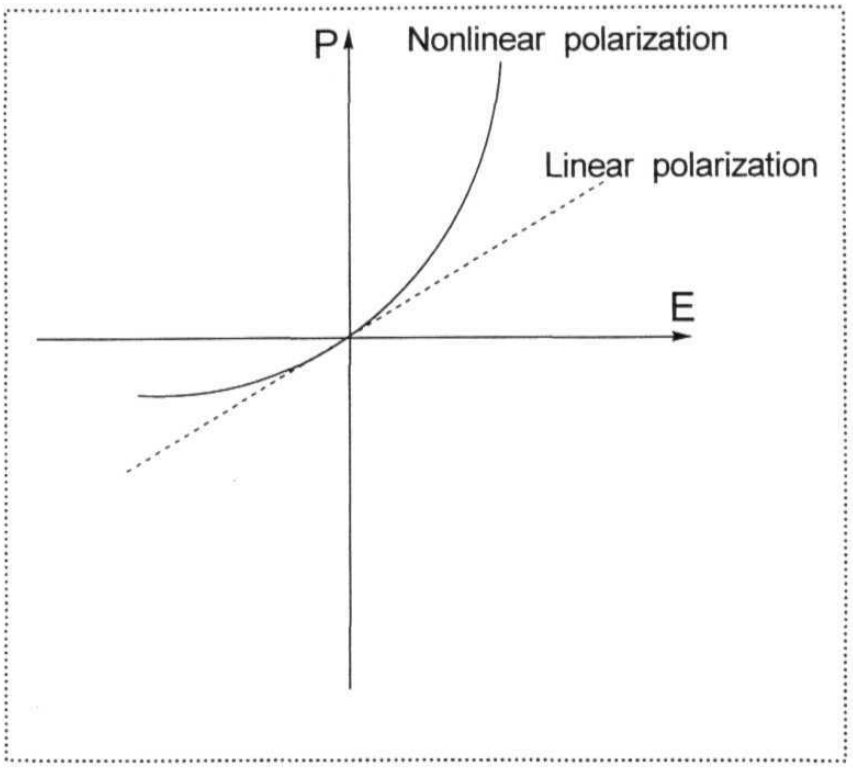

Figure 1.2 *Nonlinear polarization at high electric fields; the linearity at low fields is shown using the dashed line.*

Materials for second harmonic generation (SHG)

Materials developed initially for NLO applications were based on inorganic systems. Ferroelectric materials lacking center of symmetry were prime candidates for observing quadratic effects. Materials extensively used for second order NLO applications are inorganic crystals such as potassium dihydrogen phosphate (KDP),[69] lithium niobate ($LiNbO_3$)[70] and β-barium borate (BBO).[71] NLO effects in inorganic materials based on ionic solids arise primarily due to the ionic polarization and hence are relatively slow. Since the responses are due to bulk effects, decomposition of the NLO coefficients in terms of atomic/ionic contributions is not straightforward. Molecular

materials on the other hand with their relatively low refractive indices, exhibit faster NLO responses. Further, the NLO effects can be conveniently analyzed in terms of the molecular contributions and the impact of the molecular organization. If molecules, with large hyperpolarizabilities values are aligned so that their hyperpolarizabilities add up constructively, the assembly leads to noncentric materials with appreciable NLO response.

Organic π-conjugated molecules and polymers have been extensively studied for the past two decades and continue to be an active field in second order nonlinear optics. There is increasing activity in the area of metal-organic systems like coordination complexes and coordination polymers which show many advantages over the pure organic as well as inorganic systems for NLO applications.[72,73] Considerable effort is being made to develop materials with good thermal and mechanical stability, so that they can compete with traditional inorganic materials which at present dominate the area of technological applications. The physical mechanism of charge transfer that leads to the nonlinear optical effect in a 'donor - conjugating unit - accepter' (D-π-A) framework, can be understood in terms of Mulliken resonance structures illustrated in Fig.1.3. When a molecule is subjected to an applied field parallel to the dipole axis, the electronic polarization response will be unsymmetric as a result of the cooperative influence of the donor and accepter groups; this can be contrasted with the symmetric response of an unsubstituted structure (broken line). The asymmetry in the polarization gives rise to the harmonic frequencies of the field radiated by the molecular dipole oscillations. These simple considerations have led to the developments of a vast number of molecular crystals and polymers as candidates for NLO applications.

Various classes of quadratic NLO molecules have been developed based mostly on donor-acceptor substituted aromatics. Some of the extensively studied classes of NLO chromophores of this type are 1,4-substituted benzenes and stilbenes,[74,75] 4-nitroanilines and 4-(N,N-dimethylamino)-4'-nitrostilbene (DANS).[76] Dulcic and Sauteret[77] were the first to study the substituent effect in *para* disubstituted benzene derivatives and Oudar and Leperson reported on the effect of conjugation length by using stilbene in the place of the benzene system.[78] Since then several systematic investigations have been carried out on the structure-property relationship of NLO chromophores. Compounds with

conjugating bridges such as tolans,[75] diazostilbenes,[79] polyenes,[80,81] polyphenylenes,[82] as well as heteroaromatic 5- or 6- membered rings like thiophenes and azoles[83] have been investigated. In order to overcome the problem of absorption in the organic compounds, Mignani and coworkers have developed an interesting approach of linking donor and acceptor groups through s-p conjugative units, such as silanes, oligo-silanes and poly-silanes.[84] A variety of salts especially with pyridinium and stilbazolium cations have been studied for their second order NLO properties. Organometallic and coordination complexes form another class of materials that have been studied for the quadratic NLO properties.[85] Extensive investigations have been carried out to understand the role of metal ions, oxidation state of the metal, donor/acceptor substituents on the ligand, and length of conjugation in the ligand on the quadratic NLO properties of the metal complexes. The metal complexes generally show an enhancement of molecular hyperpolarizability compared to the free ligand. The transparency - nonlinear response trade-off problem in the metal-organic materials could be overcome by using d^{10} metal ions.[73] In several instances, octupolar metal complexes have shown better nonlinearity

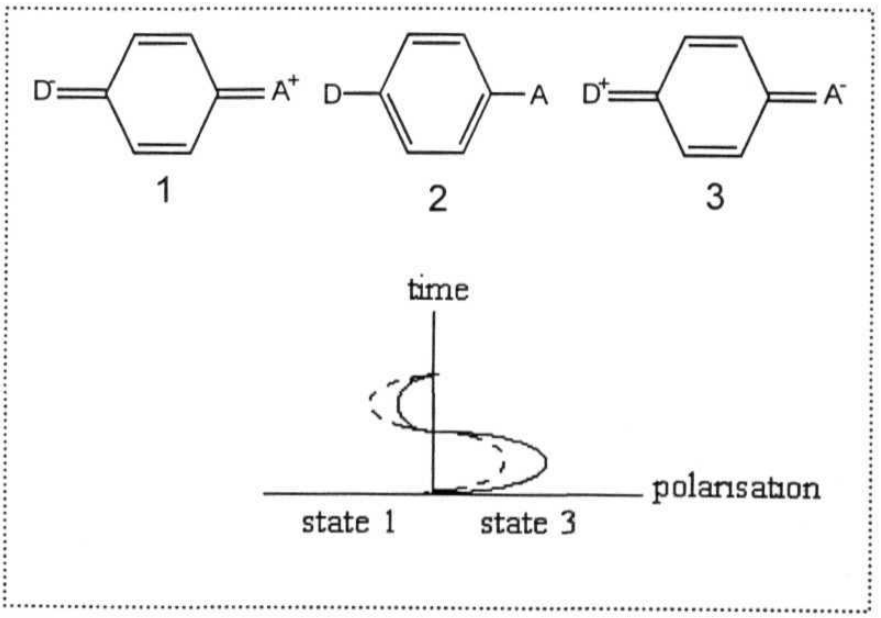

Figure 1.3 *Origin of nonlinear polarization in a 'donor – conjugating unit – acceptor' system. The broken line represents the response of unsubstituted system.*

and transparency compared to the dipolar counterparts.[86] Other systems studied include ferrocene, metallocene compounds[72,87] and calixarenes.[88] We discuss more about metal-organic systems in Sec. 1.5.

Since D-π-A type systems often tend to prefer centrosymmetric organization in the bulk, there has been considerable interest in exploring octupolar molecules.[89,90,91] Recently there have also been reports on novel NLO chromophores with through space or through σ-bond (as opposed to π conjugative) interactions between the donor and acceptor groups which show improved absorption characteristics.[92] There is also growing interest in chromophores organized as mesoscopic and crystalline superstructures; the significance of helical organization for enhanced nonlinearity has been investigated.[93]

Molecular hyperpolarizability

The first hyperpolarizability, β quantifies the second order NLO response at the molecular level. The simplest model to take into account the contribution of charge transfer within a molecule to the first hyperpolarizability is the two-level model proposed by Oudar and Chemla.[76,94] Red shift in the absorption spectrum due to an increase in the conjugation length or lower energy charge transfer between the donor and acceptor substituents leads to increased β.[95] Several theoretical methodologies are available to compute molecular hyperpolarizabilities. Two general approaches[96] are often employed: (i) methods in which the perturbation due to the field is explicitly included in the Hamiltonian (the finite field (FF) and coupled perturbed Hartree-Fock (CPHF) method) and (ii) perturbative schemes in which the calculations are carried out on the free (independent of field) molecules and the response involves the coupling of excited states (the sum-over-states (SOS) method). The CPHF method is equivalent to the time dependent Hartree-Fock approximation (TDHF) for static calculations. The semiempirical AM1/TDHF method incorporated in the MOPAC93 programme package provides a convenient means for the prediction of β of organic molecules.

Experimental determination of molecular hyperpolarizability is often carried out in the solution phase. Since molecular motion in solution leads to an average center of inversion symmetry, high electric fields are applied to break the symmetry of the isotropic solution in the approach called electric field induced second harmonic generation (EFISHG).[97] In another technique called the harmonic light scattering or hyper-Rayleigh scattering (HRS),[98] local anisotropy within the solution is used to produce incoherent harmonic scattering which allows determination of the β. The latter technique is applicable to charged and octupolar compounds that are not amenable to EFISHG studies. Molecular β values can be related to the bulk crystal NLO coefficients through the oriented gas model.[99]

Organization of molecules in materials for SHG

Noncentrosymmetric arrangement of molecular chromophores in the crystalline state is a prerequisite condition to have a nonvanishing macroscopic second order nonlinear optical response from the materials. Even though ground state dipole moment of the dipolar molecules are not having direct correlation to the formation of centrosymmetric lattices,[100] dipole-dipole interactions between dipolar molecule generally promotes centrosymmetric organization in the bulk. Search of the Cambridge crystallographic database shows that typically 70-80% of the molecular crystals belong to centrosymmetric space groups. Different strategies have been developed to obtain noncentrosymmetric organizations, (i) inclusion of chirality,[80,101] (ii) exploitation of weak as well as strong intermolecular forces[102] and (iii) incorporation of alkyl chains of appropriate length[103] are some of the approaches developed for molecular crystals. Other strategies include, (i) electric field poling of polymer films containing the NLO-phores,[16] (ii) fabrication of X and Z type LB films,[17] (iii) formation of host–guest systems,[104] (iv) sol-gel synthesis[13] and (v) salt formation.[105] Crystal engineering strategies have also been utilized to generate acentric metal-organic polymers based on asymmetric bridging ligands.[73] Recently remote functionality and complexation strategy was explored to obtain noncentrosymmetric organization.[106] Even though noncentrosymmetry is an essential condition for quadratic NLO materials, optimum molecular organization required for efficient SHG is not guaranteed by the noncentrosymmetric assembly alone.

Very often noncentrosymmtric structures depart only slightly from the centrosymmetric one. The oriented gas model developed by Zyss and Oudar provides a basis to determine the optimal molecular orientation of dipolar chromophores which can give rise to efficient SHG.[99]

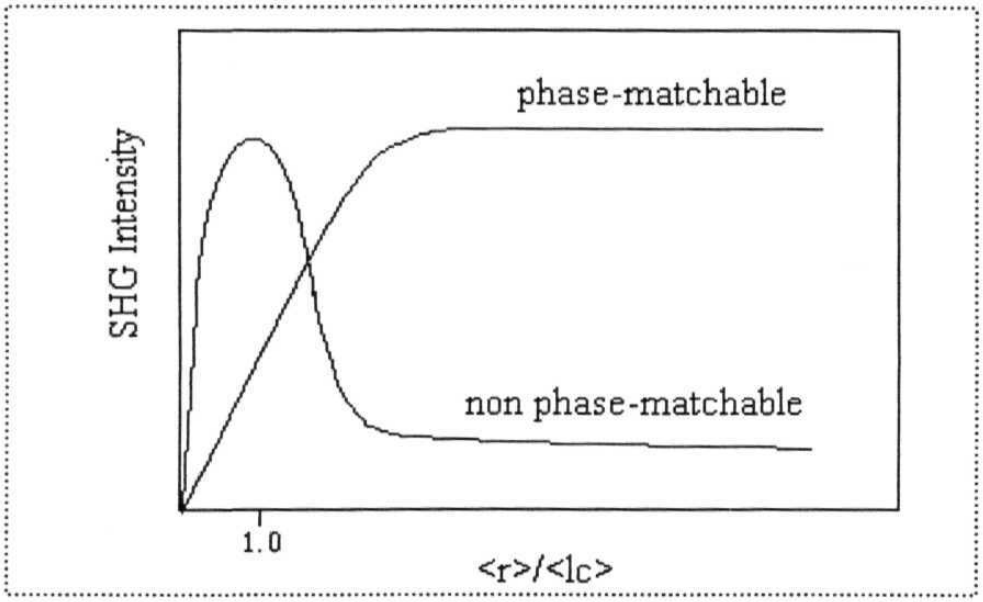

Figure 1.4 *The dependence of SHG intensity on the average particle size, <r> for phase-matchable and non phase-matchable materials; $<l_c>$ is the average coherence length.*

The Kurtz-Perry powder technique[55] is a convenient and simple method for screening large sets of microcrystalline materials for SHG activity. It involves the determination of the variation of SHG intensity with the average particle size of the microcrystalline powder as illustrated in Fig. 1.4 for phase-matchable and non phase-matchable materials. The salient feature to be noted here is that for particle sizes much greater than the average coherence length (*ie.* to the right of $<r> = <l_c>$), the SHG intensity, $I_{2\omega}$ for phase-matchable materials reaches a saturation value and is independent of the particle size whereas $I_{2\omega}$ for non phase-matchable materials decreases with increasing particle size and becomes negligible or undetectable at large sizes. Materials that are phase-matchable include $LiNbO_3$, urea, 4-nitrophenyl-*S*-prolinol (NPP) and 2-

methyl-4-nitroaniline (MNA). The powder technique is often employed as a simple tool to probe for the presence or absence of center of inversion symmetry in the crystal lattice. However one should exercise caution in using this technique, since factors such as changes of chemical composition on powdering the crystals (for example by loss of solvate molecules[98]) and modification of surface features are known to cause artifacts. Detailed characterization of the SHG coefficient of crystals and their correlation to the molecular hyperpolarizability tensor components is possible by measurements on large size single crystals. Such measurements are essential to investigate the phase-matching direction in the crystals.

Fabrication of molecular materials for SHG

The main approaches to the fabrication of materials for second order nonlinear optical studies are: (i) crystal growth, including inclusion and host-guest complexes, (ii) growth in confined structures such as wave guides and fibres, (iii) poled polymer systems and polymer crystal composites, and (iv) thin films formed by the Langmuir-Blodgett (LB), self-assembly (SAM) and vapor phase deposition techniques.

Crystallization is the most common technique for the purification and fabrication of molecular materials.[14] Different kinds of approaches have been developed to grow good quality crystals. The advantages of crystals lie in the highly specific arrangement of molecules and the improved density of packing in the crystalline state. The specific arrangement of molecules leads to high levels of bulk nonlinearity, provided that optimal geometrical arrangements and crystal symmetries are achieved.[99] The high packing density also contributes to the magnitude since bulk nonlinearity depends on the chromophore density. In favorable cases, crystals can be cut, polished and shaped into devices for various applications. In poled polymers,[16] considerable flexibility exists in the choice of molecular and polymeric constituents, allowing for systematic design and optimization. Polymer films deposited from solutions lend themselves well to planar fabrication approaches so that waveguide and integrated optical devices can be fabricated.

In general, thin films can be grown from solution or deposited from the gas phase. The solution-based techniques are easy to setup and are extensively used. Langmuir-Blodgett (LB)[17] and self-assembled monolayer[18,19] techniques are capable of forming noncentrosymmetric films with molecular alignment perpendicular to the surface with well-defined thickness. Rational design through synthesis of suitable chromophores and the use of appropriate templates, have resulted in considerable progress towards increasing the quality and stability of the films. Vapor phase deposition[20] technique offers the advantages of layer thickness control of the thin films with very high chemical purity, *in-situ* growth monitoring and high growth rates. The materials should be stable to sublimation processes and temperatures. Noncentrosymmetric thin films were prepared by vapor deposition on to lattice-matched inorganic crystals or oriented substrates. Recently hydrogen-bonding approach was utilized in the preparation of noncentrosymmetric thin films by organic molecular beam deposition technique.[107] We discuss more about thin films for SHG in the next section.

1.3 THIN FILMS FOR OPTICAL SECOND HARMONIC GENERATION

Thin films and nanostructures have attracted increasing interest because of their potential applications in a variety of advanced technologies, including nonlinear optics, microelectronics, nanotechnology, light emitting devices, field-effect transistors, liquid crystals, sensors, and solar cells.[18,19,44,108] For many of these applications, the device performance is crucially dependent on the orientation of the functional molecules in the film or the nanostructures.[109] Therefore, methods for alignment of molecules in the structures are of great technological interest. The alignment can be centrosymmetric or noncentrosymmetric. Thin films with noncentrosymmetric ordering of molecular dipoles are attractive for a multitude of information processing and photonics applications, such as high speed electro-optic modulation, optical switches, terahertz wave generation, holographic storage, anisotropic charge transport, self-assembled molecular nanowires, or NLO wave guides for integrated frequency conversion using low-power semiconductor lasers.[42,108,109]

Several techniques have been developed for the growth of anisotropic thin films, including electric field poling,[16] Langmuir-Blodgett transfer,[17] self-assembling monolayer[18,19] and vapor phase deposition[20] techniques. The classical poling method consists of heating the polymer close to its glass transition temperature (T_g), so as to increase the molecular mobility in the polymer matrix and application of a DC electric field which results in statistical polar orientation of the molecular dipoles along the field direction. Cooling to room temperature while keeping the orienting field on, freezes the chromophores in the polar orientation. Adjustment of the electrode configuration, can in principle, be used to obtain any desired direction of the orientation axis imprinted inside the materials.[110] Even though the poled polymers offer many advantages as materials for second order nonlinear optical applications, the dilution of the NLO chromophore in the matrix, the broad orientational distribution and the temporal instability of the dipole orientational ordering often limit their utility.

The LB technique is the first technique that provided the chemist with the capability to construct ordered molecular assemblies. This technique in the most general form, consists of forming monolayer of amphiphilic molecules (composed of a hydrophobic tail and a hydrophilic head group) at the air/water interface and transferring them onto a suitable substrate, preserving the monolayer organization to a large extent. Repeating the process allows the growth of multilayers. The advantages provided by the LB technique for the growth anisotropic thin films include, the possibility of easily modifying the environmental parameters of a monolayer, the flexibility and range of strategies available in the design of NLO chromophores and the homogeneity of the film thickness that can be achieved. In most of the cases, the multilayer films adopt a centrosymmetric head-to-head or tail-to-tail arrangement, the so-called Y-layer deposition. However, the technique has been used to obtain noncentrosymmetric thin films displaying a herringbone arrangement,[111] with the direction of the herringbone structure parallel to the dipping direction. The X and Z-type depositions lead to noncentrosymmetric organization of the multilayers. The second harmonic intensity varies linearly with the square of the film thickness, when the multilayers are well-ordered, and NLO waveguides using such films have been successfully demonstrated.[112] While the LB technique is relatively successful in obtaining noncentrosymmetric thin films consisting of up to ~100 monolayers, it has the disadvantage that it is very time

consuming. In many cases, the structures are also thermally unstable; the thermal instability has been attributed to the weak nature of the intermolecular forces within the layers.

Self-assembled monolayers (SAM) and molecular self-assembly provide an attractive alternative approach to second order NLO materials. One of the successful methods is based on the construction of covalently linked, intrinsically acentric super-lattices containing molecular chromophoric subunits. SAMs are molecular assemblies that form spontaneously by the immersion of an appropriate substrate into a solution of an active surfactant in an organic solvent.[19] One obtains films consisting of densely packed long chain organic molecules which are chemisorbed, usually on inorganic substrates, through a head group which has specific affinity for the substrate. These materials offer higher net chromophoric alignment, larger number densities and greater stability and structural control than LB films. In the first step, the substrate is thoroughly cleaned, washed and dried to produce a well-defined surface. In the second step the coupling layer is formed. This layer will provide the binding specificity of the NLO chromophore. The next step involves the introduction of the chromophore layer. In the last step a capping layer is added to promote structural stability. Recently the method has been used to produce robust, densely packed thin films and further extended to produce multilayered films with strong NLO properties.[113] The major disadvantage afflicting this technique comes from it being a solution based technique were side reactions and several intermolecular interactions can interfere with the deposition processes. In addition, the rates at which films can be grown with this technique are not sufficient for practical purposes.

In the vapor-phase deposition method, two kinds of method such as organic molecular beam epitaxy (OMBE) and organic molecular beam deposition (OMBD) have been developed to fabricate thin films. Organic thin films can in principle be grown by epitaxy on a lattice-matched substrate. Such an OMBE procedure needs good film-substrate interactions for the achievement of single domain crystalline organic thin films that are required for NLO applications. This is a major limitation of the technique. Epitaxial growth of a specific class of organic compounds have been demonstrated,[114] but ordered growth on inorganic substrates could not be achieved due to incompatibility of

lattice parameters and the weak forces between the substrates and the organic films. In order to overcome the problems of lattice-matching of the substrate and epitaxial growth, another approach called OMBD has been developed. In this technique, thin films are fabricated by the evaporation of molecules onto a thermally stabilized substrate under high or ultra high vacuum conditions. OMBD technique is interesting because it has many advantages over the solution-based techniques, such as greatly reduced contamination in the ultra-high vacuum condition, a solvent free environment, superior control over growth parameters, and reasonably high growth rates. In addition, mask-designed microstructures, such as strip waveguides and integrated hetero-layered structures, can be easily fabricated using this technique. Günter *et al* have demonstrated the utility of the OMBD technique to fabricate organic thin films with hydrogen bond directed preferred orientation of molecular dipoles on amorphous glass substrate.[115] Other methods like rubbing[116] and dragging[117] techniques have also used to fabricate oriented thin films. Kim *et al*[118] have demonstrated a new strategy using a supramolecular device technique, for the spontaneous self-assembly of NLO chromophores with directional order and enhanced polar stability. In this approach, the chromophore is uniaxially included in the helical cavity of amylose as receptor, which preferentially accommodates hydrophobic guests, forming a helical rigid-rod supramolecular complex. The various thin film techniques allow the fabrication of large area NLO materials and devices and hence hold great promise from the point of view of practical application. The small dimensions perpendicular to the film plane also facilitates the utilization of small voltage to achieve large electric fields when required.

1.4 POLAR ASSEMBLY OF DIPOLAR MOLECULES IN CRYSTALS

The bulk properties of molecular materials are intimately linked to the relative orientation and organization of the constituent molecules. For example, the electrical transport in organic molecular conductors based on charge transfer complexes critically depends on the interplanar distances and π-orbital overlaps of the donor/acceptor molecules.[36] Magnetic interactions and hence the cooperative magnetism in molecular magnets can change drastically when the mutual disposition of the molecular radicals is altered.[27,28,119] Molecular materials that crystallizes in acentric space groups are of

general interest to studies of solid state properties such as pyroelectricity, piezoelectricity and second order nonlinear optical responses such as SHG, frequency mixing, linear electro-optic effect and photorefractive effects.[62,66] Polar solids in particular, are an important class of materials for pyrroelectric, piezoelectric and second order NLO applications, especially for the linear electro-optic (EO) effects. Parallel alignment of dipolar molecule with large β leads to high values of bulk nonlinearity. The linear electro-optic (EO) effect, the electric field induced change of the refractive index, of several organic and inorganic materials have been extensively investigated and is a technologically important phenomenon which is currently employed in electro-optic modulators. Therefore, developing acentric materials wherein the chromophores are aligned in a parallel fashion, is an interesting as well as challenging problem.[120] Parallel orientation of the molecular dipoles can be achieved by electric field poling technique in doped polymer films; however as discussed in Sec. 1.3, the temporal instability and the dilution of the nonlinear chromophores in the polymer matrix are major handicaps for device applications.[16]

The crystalline state is, in principle, the best medium for generating NLO phenomena because of the high packing density of the active components. In the past, several design strategies have been attempted to achieve parallel molecular dipole orientations in NLO crystal (Table 1.1). Marder *et al*[105,121] have developed a 'salt methodology' wherein the anion sheets provide the shielding required to achieve net polar alignment of the NLO-phore cations and lead to materials with large SHG capability. Bosshard *et al* demonstrated a cocrystal approach, in which careful selection of the molecular units, led to one of the first examples of a geometrically and electronically optimized electro-optic crystal.[122] Crystal engineering strategies have also been used in the development polar supramolecular assemblies of molecular dipoles.[123,124] Approaches to obtain polar supramolecular host-guest systems by incorporating NLO molecules in a parallel fashion is an interesting strategy and are relatively more successful compared to the other approaches. Starting with β-cyclodextrin[125] a number of clathrate-forming compounds[126] such as urea and thiourea, cyclophosphazen, deoxycholic acid and perhydrotriphenyllene (PHTP)[127] were examined with respect to the formation of inclusion compounds with small organic as well as

Table 1.1 *Routes developed in earlier work towards parallel molecular dipole alignment in NLO crystals*

Design Principle	Examples	Comments
Probability (ca. 25% crystal structures in CSD are acentric)	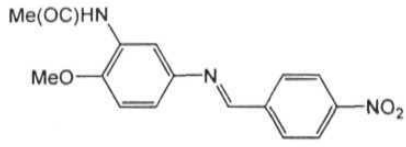	High density of NLO active component; parallel alignment rare
Minimum ground state dipole moment	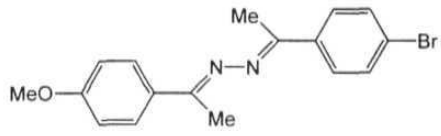	Large β values possible Examples rare
Co-crystallization or salt formation	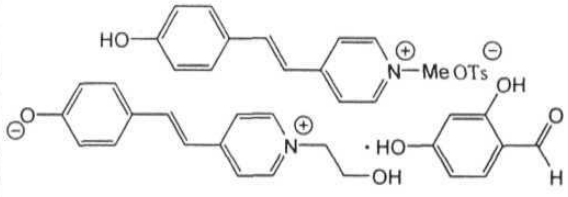	Greater synthetic flexibility, Dilution of NLO component
Supramolecular synthons (strong, directional interaction)	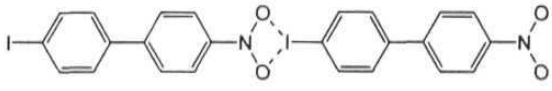	Parallel alignment of polar molecular 'strings'. Antiparallel alignment possible
Inclusion in inorganic zeolites	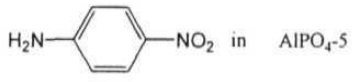	Small guests preferable small crystal, dilution
Inclusion in α- or β-cyclodextrins	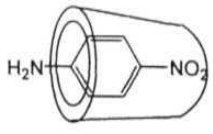	Limited to few guests, Dilution effect
Inclusion in organic, channel-forming host molecules	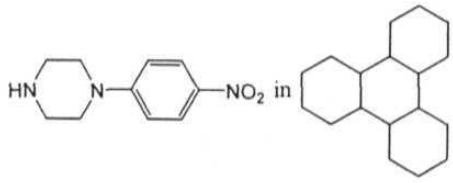	Applicable to many rod-like NLO active guests, Dilution
Inclusion in organic open frameworks	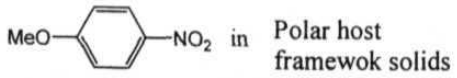	Applicable to few NLO guests, Dilution

organometallic species. The host-guest systems provided a high proportion of polar structures for the inclusion compounds.[128] Zeolite channels have also been utilized to include the NLO chromophore in a parallel arrangement.[129] Hulliger *et al* successfully demonstrated the inclusion of polar guest molecules into the PHTP host channels with parallel alignment of the dipoles.[130] They have developed a model based on the Markov's theory of stochastic processes to understand the mechanism of spontaneous polarity evolution of the guest molecules in the PHTP channels.[131] They have concluded that the polarity in supramolecular materials is a tunable property and that the polar structure formation in three-dimensions results from a subtle balance of intermolecular interactions, between donor/acceptor groups of the push-pull molecules and along/perpendicular to the molecular dipole axis. In the open framework strategy, the polar host frameworks enforce the alignment of guest molecules into a polar organization.[132]

Most of the strategies developed so far, to obtain parallel alignment of the molecular dipoles in the crystals require the involvement of a supporting structure based on host polymer or framework lattice, counterion or cocrystallization partner. This invariably leads to a lower density of the NLO active component in the bulk materials (dilution effect mentioned in Table 1.1) and hence reduces the effective utilization of the materials to achieve desired solid state effects. Further, multicomponent systems in many cases pose difficulties with crystallization. It is therefore desirable to develop single component crystals with a perfectly polar alignment of the constituent molecular dipoles. Hulliger *et al* proposed a theoretical concept for designing geometrically optimized, single component crystals for electro-optic effects.[133] The idea relies on the mechanism responsible for the spontaneous evolution of polarity in channel-type inclusion compounds consisting of non-polar hosts. They envisaged that elongated, rod-like molecular chromophoric structures, which incorporate both a strongly hyperpolarizable core and peripheral, non-polarizable groups and carefully optimized intermolecular interactions have a high probability to form polar single component NLO crystals. Some of the single component polar supramolecular systems that have been reported recently are the following. Weak intermolecular interactions in 2,6-diethynylpyridine lead to the parallel arrangements of the molecular dipoles in the supramolecular assembly and a chiral, parallel alignment of one-dimensional coordination polymer using the chiral

system, the molecule assembled in a noncentrosymmetric parallel alignment in the three-dimensional lattice. Parallel arrangement of molecules have been observed in the crystal lattice of tetrahedral and square pyramidal zinc coordination compounds.[135] Azines were shown to form parallel alignment of molecular dipoles in crystal.[136] Recently, a new strategy for the design of polar organic solids have been demonstrated on the basis of intermolecular interactions in the crystal lattice.[137] Hydrogen-bonded sulfamide sheets lead to the formation of polar assembly of molecules in the crystals of N,N'-Bis(4-substituted benzyl)sulfamides.[138] The single component perfectly polar crystals we have developed will be discussed in Sec. 2.3 and 2.4.

1.5 METAL-ORGANIC SYSTEMS AS SECOND ORDER NLO MATERIALS

Ever-expanding areas such as information technology, image processing and data transmission and storage as well as the advances in applications like optical switching, optical frequency conversion and optoelectronics lay heavy demands on new and more efficient materials. Several classes of materials have been developed based on inorganic crystals and semiconductors, organic crystalline materials, metal-organic systems and polymers with delocalized π-electrons. However, each type of materials is superior in one aspect but of limited merits in another. Inorganic materials generally show relatively weaker and slower nonlinear optical responses than π-conjugated organic molecules, but posses superior crystal attributes. Organic materials with strong optical nonlinearities often suffer from poor thermal and mechanical stability.[139,140] In spite of these drawbacks, however, the correlation between the molecular structure and materials properties for molecular second order NLO materials is well developed. Therefore, the synthesis of optimized molecules and fabrication of the molecular materials with appropriate arrangement of the building blocks to achieve efficient second order NLO materials, continues to be an active field of research.

Investigations were initially focused on purely inorganic systems, and some of the first solids to demonstrate second order NLO properties were inorganic crystals (e.g. quartz, lithium niobate and potassium dihydrogen phosphate),[51,52,55] in which photo-induced change in refractive index and later, photorefractive effect were observed.

Inorganic semiconductors followed, such as gallium arsenide and indium antimonide which displayed large optical nonlinearities. Multilayer semiconductor materials that were synthesized using new crystal growth techniques[141] exhibited special optical properties not apparent in the bulk materials[6]. These materials are commercially being used as frequency converters, electro-optic modulators and optical switches.[142] However problems such as 'trade-off' between response time and magnitude of optical nonlinearity and cost of fabrication persist with these materials.

In later years, organic systems were investigated as an alternative to inorganic materials because of their low cost, fast and large nonlinear response over a broad frequency range, inherent synthetic flexibility and intrinsic tailorability.[62,64,66] Particular attention has been paid to the development of discrete organic molecular NLO chromophores.[139,140] In such molecule-based NLO materials, the optical properties can be readily fine-tuned through subtle changes in the molecular structure using the tools of synthetic organic chemistry. However, in spite of extensive investigations, organic materials are yet to find practical NLO applications. Molecular materials in general are fragile and brittle, and have relatively low thermal stability and low damage thresholds under laser irradiation. Large, optically clear crystals are difficult to grow; for specialized applications, the crystals must be large enough to cut and polish. Good transparency of the materials at the operating frequencies is essential and several organic compounds with large β absorb visible light making NLO applications at these wavelengths inefficient. Recently, investigations of coordination complexes and organometallic systems have intensified considerably. Incorporation of metals into NLO systems gives a new dimension of study and introduces several new variables that can be optimized.

Metal-organic Materials

We use the general term metal-organic systems to denote the class of materials including coordination complexes of metal ions, organometallics and coordination polymers. Metal-organic systems are of special interest because of the relatively higher thermal and mechanical stability they posses and the utility of metal centers in the

construction of various one, two and three-dimensional architectures for NLO application. The metals can have a large diversity of oxidation states and ligand environments, and due to the polarizable d-electrons, a number of interesting effects and greater nonlinear optical effects are likely to be observed. Molecular configuration also plays a significant role on second order NLO properties of coordination compounds.[143] The reasons for studying the NLO properties of metal complexes have been expounded in several reviews.[22,22,64,87,89,90,144-147] The salient features of metal-organic systems as NLO materials are the following.

a) Metal-organic systems often exhibit metal-ligand or ligand-metal charge transfer bands in the visible region of the spectrum. These optical absorption bands are usually associated with large β, although they can lead to transparency problem.

b) Transition metal centers can undergo redox changes, which can lead to electron-poor or electron-rich situations depending on the oxidation state and ligand environment. Facile redox ability can be envisaged as leading to large β, in view of the metal center being stronger donor or acceptor in comparison to conventional organic systems.

c) Chromophores, such as porphyrins and phthalocyanines, containing metal ions are amongst the more intensely colored materials known. The strength of the optical absorption band is also associated with large optical nonlinearities.

d) Many metal-organic compounds have low-energy excited states with excited-state dipole moment significantly different from the ground-state dipole moment. Many of the excited states involve transfer of electron density between the central metal and one or more of the associated ligands. Such excited states usually provide a substantial contribution to β.

e) Metal-organic compounds also have important advantages in the range of non-aromatic ligands that can be attached to the metals. These ligands can shift the occupied and unoccupied metal d-orbitals that interact with the π-electron of the conjugated ligand system. This provides a mechanism for fine-tuning and optimizing β or the crystallographic arrangements that control the bulk nonlinear susceptibility.

f) Additionally, the metal centers in these molecules can be used to generate chiral species so that if resolvable, they can crystallize as noncentrosymmetric lattices, essential to observe quadratic NLO effects.

A general problem is the low energy d-d transitions present in most of the coordination compounds, normally observed in the visible region. This gives rise to what is termed as the nonlinearity/transparency trade-off. If a material is to be used for frequency doubling, then obviously, the absorption of the second harmonic light that is produced will limit the usefulness of the material. Depending on the location of these bands, the 'transparency window' can be large or small; larger a materials' transparency range the greater its potential applications. These considerations suggest that d^{10} metal ions such as Zn(II), Cd(II), Cu(I) and Ag(I) are potentially important candidates for the fabrication of metal-organic materials for NLO applications.

Coordination complexes with second order NLO properties

Several classes of coordination complexes have been investigated for second order nonlinear optical properties. The materials that have been extensively studied are those based on pyridyl, Schiff base and thiocyanate ligands. Even though there are some reports on quadratic NLO properties of porphyrin and phthalocyanine complexes, they are better known for their third order NLO effects, which stem from the extended delocalized π-systems and strong absorption. Recently, an excellent review of the NLO properties of coordination complexes has appeared.[85]

Complexes of pyridyl ligands

One of the earliest NLO studies involving metal pyridyl complexes was reported by Frazier et al. in 1986 who investigated the SHG from various Group 6 metal pyridyl carbonyls. SHG was observed in a Re(I) complex and inclusion compounds of various metal complexes with thiourea or tris-ortho-thymotide.[148] Following these early solid state investigations, electric field induced second harmonic generation (EFISHG) and theoretical calculations were carried out on several pyridyl complexes; the β values similar to that of 4-nitroaniline were observed in several cases and the values are sensitive to the nature of the pyridyl substituent.[87,142] Kanis *et al* carried out detailed computational studies on pyridyl complexes that showed excellent agreement with EFISHG data, it was concluded that the β is greatly influenced by the substituents in the

4-position of the pyridyl systems than the phenylene 4-substituents in the stilbazole systems.[149] The extension of the conjugation length does not lead to sharp increase in β, in marked contrast to the behavior of purely organic NLO-phores. Generally, pyridine and stilbazole ligands show appreciable enhancement in the β upon complexation with the metal centers. Molecular hyperpolarizability enhancements of the metal complexes depend on the σ-electron withdrawing capability of the metal centers as well as the donor/acceptor substituents on the ligand.

Coe and coworkers have investigated the NLO properties of ruthenium amine complex salts of pyridyl ligands, focusing on the establishment of structure-activity correlations for β values derived from hyper Rayleigh scattering (HRS) measurements.[150] Perhaps the most interesting result to emerge from these studies is the observation that the MLCT absorptions and β_0 responses of certain complexes can be reversibly and effectively attenuated by $Ru^{III/II}$ redox changes using chemical reagents.[150] This demonstration of redox-induced switching of NLO responses provides a novel justification for incorporating transition metal centers in molecules with large β_0 values. The donor ability of the $\{Ru(NH_3)_5\}^{2+}$ has been demonstrated in 4,4'-bipyridine based coordination complex and shows better ability than dimethylamino group as a π-electron donor. Bimetallic complexes containing pyridyl carbonyl centers with ruthenium σ-acetylide[87] or ferrocenyl[87,147] electron donor groups have also been investigated. Fabrication of ruthenium coordination complexes into thin films by the LB technique and their second order NLO properties have been investigated.[85] Rapid photoinduced modulation of the SHG from LB films have also been studied.[151]

Attention has been drawn to octupolar chelate complexes by the work of Zyss *et al.*[152] Octupolar molecules are non-dipolar species based on two-dimensional or three-dimensional chromophore structures. Metal ions are well suited for building coordination molecules with two-fold (D_2) or three-fold (D_3) symmetries around the metal center (e.g. tetrahedral, octahedral, or trigonal bipyramidal geometries). NLO systems based on octupolar metal complexes, mainly of bipyridine ligands, have been reported and recently reviewed.[91] Le Bozec *et al* have incorporated octupolar chromophoric unit into macromolecular structures and measured their β by the HRS method.[153] The enhancement of β without significant loss of transparency in octupolar molecules

compared to dipolar molecules makes them attractive candidates for nonlinear optical applications.

Complexes of Schiff base ligands

The first observation of SHG in metal Schiff base complexes was reported in 1991.[154] The metal-ligand core was used to enhance the NLO response of an apically substituted pyridine ligand. Thami *et al* reported[155] Co(II) complexes of electron donor/accepter substituted Schiff base ligands with approximate C_2 symmetry. Di Bella *et al* have studied the quadratic NLO properties of various types of Schiff base complexes.[156] The metal center in such complexes behaves like a template in the formation of noncentrosymmetric molecular structures; the thermal stability of the chelate ring structure is enhanced and metal helps to 'switch on' and enhance the nonlinear response. A review of these studies including a brief discussion of the complexes incorporated into main chain polymer, has appeared.[157] Recently, a combination of HRS experiments and theoretical calculations have been used to investigate the three-dimensional character of the β of Schiff base complexes. Lacroix *et al* investigated[157] the quadratic NLO properties of Schiff base complexes by substituent modification, doping the complexes in polystyrene thin films followed by poling and by incorporating chirality in the Schiff base ligand. Colorless, tetrahedral complexes based on Zn(II) and Cd(II) metal centers have been prepared and the SHG capabilities of the complexes investigated.[71] A series of octahedral complexes have been reported to show weak SHG, the most active one adopting a helical structure.[158] EFISHG and solid state SHG studies have also been carried out on binuclear square planar and square pyramidal Schiff base complexes. Tetrahedral Zn^{II} complexes of chiral ligands substituted with electron donating groups show strong SHG, combined with good transparency in the visible range.[146,159]

Complexes of thiocyanate ligands

The first coordination complexes to be studied for their NLO properties were the colorless thiocyanate bimetallic single crystals, which exhibited efficient and phase-matchable SHG.[160] This early discovery stimulated considerable research into these and

related types of materials. Easy growth of large, high quality single crystals, combination of good thermal stability with relatively high optical damage threshold and efficient SHG at wavelengths such as 380 nm and 404 nm make $[Zn^{II}Cd^{II}(SCN)_4]$, promising candidates for ultra-violet SHG and related NLO device applications.[161] The second order NLO properties of several other thiocyanate complexes have also been reported.[85]

Coordination polymers for SHG

Coordination polymers, in some cases referred to as metal-organic coordination networks (MOCN) or metal-organic frameworks (MOF), are metal-ligand compounds which form structures extending in one, two or three dimensions via coordinate metal-ligand bonding.[162] The use of metal atoms in coordination polymers offers several advantages over purely organic chains, grids or frameworks which are organized by non-covalent interactions.[4] Coordinate metal-ligand bonds are stronger and in many instances show more directionality than several other weak interactions, such as hydrogen bonding or π-π stacking.[163] Differences in the size, hardness/softness, ligand field stabilization of the metal ions and the various coordination modes (octahedral, tetrahedral, square planar etc) facilitate a wide range of construction possibilities. The metal atoms in coordination polymers can act as assembling and templating joints for the organic bridging ligands. More interestingly, metal-ligand combination can give rise to two or more different structures, even with the same stoichiometry of all the components. This has been termed as polymorphism or supramolecular isomerism in the context of coordination networks.[162,164] Subtle factors of crystallization conditions such as solvents, temperature, time, concentration, anions and pH play significant role in the formation of specific strucutres.[164] Considerable research work has been dedicated towards understanding the self-assembly process between metal ions or secondary building units derived from them and the multidentate ligands.[162,164,165] The design and properties of the ligand itself is an active area of research, because the ligand can play a crucial role in the construction of novel structure as well as in the properties of the coordination polymers. The synthesis or self-organization of coordination polymers is often achieved by combining the appropriate metal salt and ligand in a suitable solvent under mild or at most hydrothermal conditions. Even though much effort is still devoted to the preparation and structure

determination of crystalline materials, the final goal is to design properties of the polymeric assemblies of metal complexes with applications in catalysis and conducting, luminescent, magnetic, spin-transition, nonlinear optical or porous materials.[21]

NLO materials based on coordination polymers can be designed so as to contain organic ligands with large hyperpolarizabilities, and possessing noncentrosymmetric structures.[21,159,166] Molecular hyperpolarizabilities are frequently larger for the metal complex than for the free ligand chromophore, because of the metal-to-ligand or ligand-to-metal charge transfer and due to the involvement of the metal orbitals.[155,166,167] Another appealing aspect for the design of NLO properties is that metal centers can serve as pivotal points in the engineering of three dimensional tetrahedral and octahedral structures, giving rise to octupolar molecules.[90,168] The recent success in the design and synthesis of novel materials based on metal-organic coordination networks has stimulated much interest in the developments of noncentrosymmetric solids for NLO effects by exploiting the strong and highly directional metal-organic coordination bonds. Examples of some systems and direction of research in this area are described below.

The polynitrile lanthanide complex which crystallized in acentric network structures was found to exhibit solid state SHG, 16.8 times that of urea.[169] Lin *et al* have demonstrated that noncentrosymmetric solids based on infinite networks can be rationally synthesized by combining unsymmetrical bridging ligands and metal centers with well defined coordination geometries.[73] Several noncentrosymmetric coordination polymer assemblies with different network topology have been successfully synthesized and their SHG capabilities were explored. An obvious choice of three-dimensional network for realizing noncentrosymmetric solids is the diamondoid network. The connecting points in the diamondoid networks are tetrahedral or pseudotetrahedral.[170] In fact, the prototypical NLO material, KDP crystallizes as a diamondoid network.[171] Metal-organic diamondoid structures have a high propensity to interpenetrate in order to fill void space in the network.[172] Despite the inherent noncentrosymmetric nature of the diamondoid net, an even number of interpenetrations could potentially lead to inversion centers relating pairs of mutually independent nets. On the other hand, an odd number of diamondoid net interpenetrations synthesized from unsymmetrical bridging ligands will lead to the formation of a noncentrosymmetric lattice. Another approach that is

employed to generate acentric diamondoid nets involves the use of low symmetry bridging ligands to link four connecting centers.[173]

Acentric metal-organic coordination polymers based on two-dimensional network structures have also been synthesized and their solid state SHG investigated.[174] Octupolar metal-organic NLO materials based on a chiral two-dimensional coordination network has also been reported.[175] Even though the design of noncentrosymmetric one-dimensional chains can be readily achieved, the construction of a noncentrosymmetric solid based on one-dimensional chains is a more difficult task, owing to the lack of control in the assembly of chains. Teo *et al* have demonstrated a novel approach, in which tetrahedrally coordinated tetraalkylammonium ions control the arrangement and alignment of the cadmium thiocyanate anion chains and leads to the formation noncentrosymmetric structures.[176] *In situ* synthesis of ligands and the formation novel, acentric metal-organic coordination polymers under hydrothermal conditions have been reported by Xion *et al.*[177] Metal-organophosphate hybrid frameworks have also been explored for optical SHG.[178] Helical coordination polymers have been generated using chiral as well as achiral ligands and enhancement of solid state SHG compared to the free ligand and the role of helical chains in the formation of noncentrosymmetric solid have been studied.[179]

1.6 LAYOUT OF THE THESIS

This thesis describes the development of novel metal-organic systems and the investigation of optical second harmonic generation from them. Observation of perfectly polar organization of molecular dipoles as well as extreme molecular orientation of dipoles in dimorphic structures of new zinc coordination complexes that we have synthesized, are highlighted; the unusual molecular assembly is analyzed and SHG capability of these materials are presented. Thin films of these polar molecular materials fabricated by physical vapor deposition on amorphous glass substrates show uniaxial ordering of crystallites and are of potential interest in electro-optic applications. In addition to being the acceptor moiety in the molecular unit, the metal center is used to assemble C_2-symmetric chiral 'push-pull' ligand into hierarchical network coordination

polymer structures; one-dimensional helical polymers showed the highest second harmonic generation capability among the hierarchical structures. The strong hydrogen bonding capability of some of the ligand molecules was exploited to develop thermally stable organic materials as well as of coordination polymers for SHG applications. A schematic representation of the research work presented in this thesis is shown in Fig.1.5. The thesis is divided into five chapters. Development of molecular materials and its importance as magnetic, conducting, optical and nonlinear optical materials are already discussed in the previous sections of this chapter. We describe below, the salient feature of the remaining chapters.

Chapter 2

After introductory remarks in Sec. 2.1 and synthesis details in Sec. 2.2, we present in Sec. 2.3, the discovery of single component perfectly polar crystals of a family of zinc complexes. The formation of such structures is analyzed on the basis of the molecular structure and the hierarchy of non-bonding interactions in the crystal lattice. The investigation of the effect of solvent polarity and rate of crystallization on the formation of dimorphic structures of a complex, with extreme molecular orientation of dipoles is discussed in Sec. 2.4. Cogrowth of the polar/centric and polar/polar structures as well as the formation of twin polar domains in monolithic crystals are also presented. Semiemprical computational investigations indicate the delicate balance between the solvent polarity control of parallel and antiparallel molecular organizations. Uniaxial ordering of the perfectly polar crystallites in physical vapor deposited thin films, structural and morphological investigations and optical second harmonic generation measurements are discussed in Sec. 2.6.

Chapter 3

We have developed a new C_2-symmetric 'push-pull' ligand with multi-dentate coordination capability and its coordination polymers with Ag(I) and Cu(I) metal ions.

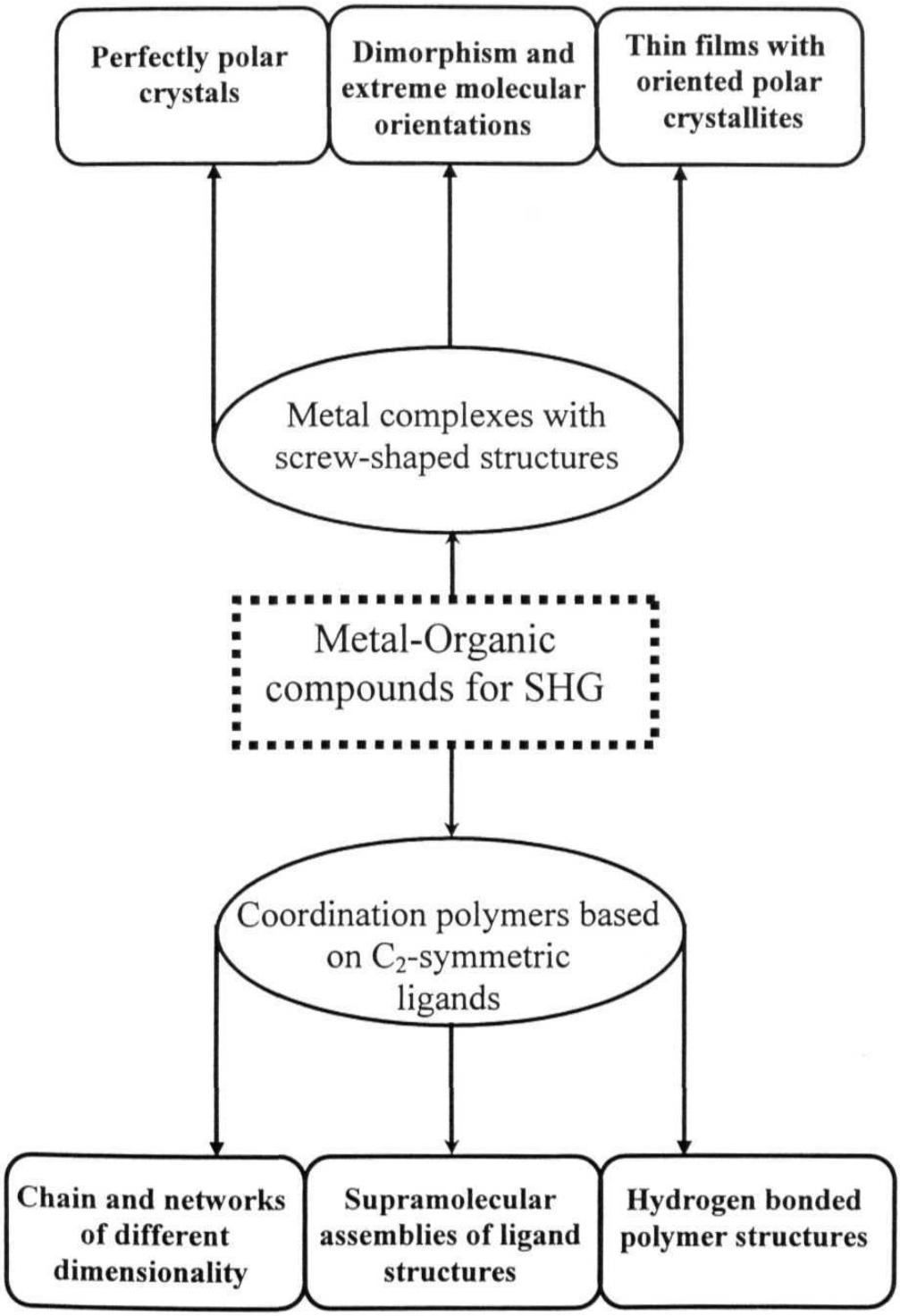

Figure 1.5 *Overview of the work presented in the thesis*

They show hierarchical structures including helical chain. In Sec. 3.3, we discuss the role of ligand conformations and the mode of ligation on the formation of helical and network structures. Solvent influences on the formation of coordination polymers with different ligand conformations are also presented. Impact of the structural motifs on the optical second harmonic generation capability of these coordination polymers is presented in Sec. 3.4. A simple computational approach that can be used to understand the influence of the ligand conformation and coordination of metal ions on the molecular hyperpolarizability is discussed in Sec. 3.5.

Chapter 4

This chapter presents C_2-symmetric molecules possessing bis(amide) functionality and coordination polymers developed based on them. In Secs. 4.3 and 4.4, we present the crystal structure investigations of different derivatives, a variety of extended H-bonded structures including polar ones are observed. The unusual occurrence of the *syn* conformer of the bis(amide) group and interesting helical assemblies through various H-bonding interactions in crystals are presented. Role of the substituents in the bis(amide) derivatives on the solid state second harmonic generation capability of these organic materials are discussed. Influence of the strong complementary amide hydrogen bonds on the assembly of coordination polymer network structures and their high thermal stability as well as the second harmonic generation capability of these materials are highlighted in Sec. 4.5 and 4.6.

Chapter 5

In Sec. 5.1 we provide an overview of the various investigations presented in the thesis. The highlights of the work include: (i) the development of a class of zinc complexes, which exhibit single component perfectly polar molecular assemblies in crystals, (ii) fabrication of these materials into thin films with acentric uniaxial ordering of the polar crystallites, (iii) utilization of a C_2-symmetric 'push-pull' ligand in the formation of a range of coordination polymer topologies and the correlation of the

network structure with optical second harmonic generation capability and (iv) structural and solid state second harmonic generation investigations of strongly hydrogen bonded, thermally stable bis(amide) derivatives and hydrogen bond directed coordination polymeric network structures. Directions for further explorations in this area of research are outlined in Sec. 5.2.

REFERENCES

1. Simon, J; Bassoul, P. *Design of Molecular Materials : Supramolecular Engineering*, John Wiley: Chichester, 2000.
2. (a) Klabunde, K. J. *Nanoscale Materials in Chemistry*, John Wiley: New York, 2001; (b) Rao, C. N. R.; Cheetham, A. K. *J. Mater. Chem.* **2001**, *11*, 2887; (c) Nalwa, H. S. (Ed.) *Handbook of Nanostructured Materials and Nanotechnology*, Vols. 1-5, Academic Press, New york, 2000.
3. (a) Lehn, J.–M. *Supramolecular Chemistry : Concepts and Perspectives*, VCH: Weinheim, 1995; (b) Steed, J. W.; Atwood, J. L. *Supramolecular Chemistry*, John Wiley: Chichester, 2000.
4. Desiraju, G. R. *Crystal Engineering: The Design of Organic Soilds*, Elsevier, Amsterdam, 1989.
5. (a) Metzger, R. M. *Acc. Chem. Res.* **1999**, *32*, 950; (b) Ashwell,G. J.; Gandolfo, D. S. *J. Mater. Chem.* **2002**, *12*, 411; (c) Ashwell,G. J.; Gandolfo, D. S.; Hamilton, R. *J. Mater. Chem.* **2002**, *12*, 416; (d) Martin, A. S.; Sambles, J. R.; Ashwell, G. J. *Phy. Rev. Lett.* **1993**, *70*, 218.
6. (a) Fabbrizzi, L.; Licchelli, M.; Pallavicini, P. *Acc. Chem. Res.* **1999**, *32*, 846; (b) Pease, A. R.; Jeppesen, J. O.; Stoddart, J. F.; Lou, Y.; Collier, C. P.; Heath, J. R. *Acc. Chem. Res.* **2001**, *34*, 433.
7. (a) De Silva, A. P.; Gunaratne, H. Q. N.; McCoy, C. P. *Nature* **1993**, *364*, 42; (b) Credi, A; Balzani, V.; Langford, S. J.; Stoddart, J. F. *J. Am. Chem. Soc.* **1997**, *119*, 2679; (c) De Silva. A P.; McClenagham, N. D. *J. Am. Chem. Soc.* **2000**, *122*, 3965; (d) Gunnlaugsson, T.; Dánail, D. A. M.; Parker, D. *Chem. Commun.* **2000**, 93; (e) Rong, D.; Mallouk, T. E. *Inorg. Chem.* **1993**, *32*, 1454.
8. (a) Davis, W. B.; Svec, W. A.; Ratner, M. A.; Wasielewski, M. R. *Nature* **1998**, *396*, 60; (b) Bumm, L. A.; Arnold, J. J.; Cygan, M. T.; Dunbar, T. D.; Burgin, T. P.; Jones, L.; Allara, D. L.; Tour, J. M.; Weiss, P. S. *Science* **1996**, *271*, 1705; (c) Barigelletti, F.; Flamigni, L. *Chem. Soc. Rev.* **2000**, *29*, 1.
9. Bissell, R. A.; Cordova, E.; Kaifer, A. E.; Stoddart, J. F. *Nature* **1994**, *369*, 133.
10. Kelly, T. R.; Bowyer, M. C.; Bhaskar, K. V.; Bebbington, D.; Garcia, A.; Lang, F.; Kim,M. H.; Jette, M. P. *J. Am. Chem. Soc.* **1994**, *116*, 3657.
11. Kelly, T. R.; Tellitu, I.; Sestelo, J. P. *Angew. Chem. Int. Ed. Engl.* **1997**, *36*, 1866.

12. Clayden, J.; Pink, J. H. *Angew. Chem. Int. Ed. Engl.* **1998**, *37*, 1937.
13. (a) Hench, L. L.; West, J. K. *Chem. Rev.* **1990**, *90*, 33; (b) Gesser, H. D.; Goswami, P. C. *Chem. Rev.* **1989**, *89*, 765; (c)) Rao, C. N. R.; Gopalakrishnan, J. *New Directions in Solid State Materials*, Cambridge Univeristy Press, Cambridge, 1986.
14. Hulliger, J. *Angew. Chem. Int. Ed. Engl.* **1994**, *33*, 143.
15. Han, Y,-K.; Seo, D,-K.; Kang, H.; Kang, W.; Noh, D,-Y. *Inorg. Chem.* **2004**, *43*, 7294.
16. (a) Burland, D. M.; Miller, R.D.; Walsh, C.A. *Chem. Rev.* **1994**, *94*, 31; (b) Miyata, S.; Sasabe, H. (Eds.), *Poled Polymers and their Applications to SHG and EO Devices*, Gorden and Breach Science Publishers: Amsterdam, 1997.
17. (a) Ashwell, G. J.; Jackson, D. P.; Crossland, W. A. *Nature* **1994**, *368*, 438; (b) Ashwell, G. J.; Jefferies, G, George, C. D.; Ranjan, R.; Charters, R. B.; Tatam, R. P. *J. Mater. Chem.* **1996**, *6*, 131.
18. (a) Lvov, Y.; Ariga, K.; Onda, M.; Ichinose, I.; Kunitake, T. *Colloids and surfaces A* **1999**, *146*, 337; (b) Cui, X.; Pei, R.; Wang, Z.; Yang, F.; Ma, Y.; Dong, S.; Yang, X. *Biosensors & Bioelectronics* **2003**, *18*, 59; (c) Park, S. Y.; Rubner, M. F.; Mayes, A. M. *Langmuir* **2002**, *18*, 9600.
19. Ulman, A. *Chem. Rev.* **1996**, *96*, 1533.
20. Forrest, S. R. *Chem. Rev.* **1997**, *97*, 1793.
21. Chen, C. –T.; Suslick, K. S. *Coord. Chem. Rev.* **1993**, *128*, 293.
22 Kahn, O. *Molecular Magnetism*, VCH, Weinheim, 1993.
23. (a) Pei, Y.; Kahn, O.; Sletten, J.; Renard, J. –P.; Georges, R.; Gianduzzo, J. –C.; Curely, J.; Xu, Q. *Inorg. Chem.* **1998**, *27*, 47; (b) Baron, V.; Gillon, B.; Cousson, A.; Mathoniere, C.; Kahn, O.; Grand, A.; Ohrstrom, L.; Delley, B.; Bonnet, M.; Boucherle, J. –X. J. *Am. Chem. Soc.* **1997**, *119*, 3500; (c) Stumpf, H. O.; Ouahab, L.; Pei, Y.; Bergerat, P.; Kahn, O. *J. Am. Chem. Soc.* **1994**, *116*, 3866.
24. Caneschi, A.; Gatteschi, D.; Rey, P.; Sessoli, A. *Acc. Chem. Res.* **1989**, *22*, 392.
25. Kumagai, H.; Inoue, K. *Angew. Chem., Int. Ed. Engl.* **1999**, *38*, 1601.
26. Benelli, C.; Gatteschi, D. *Chem. Rev.* **2002**, *102*, 2369.
27. Takahashi, M.; Turek, P.; Nakazawa, Y.; Tamura, M.; Nozawa, K.; Shiomi, D.; Ishikawa, M.; Kinoshita, M. *Phys. Rev. Lett.* **1991**, *67*, 746.
28. Allemand, P.-M.; Srdanov, G.; Wudi, F. *J. Am. Chem. Soc.* **1990**, *112*, 9391.

29. (a) Gatteschi, D.; Kahn, O.; Miller, J. S.; Palacio, F. (Eds.) *Magnetic Molecular Materials*, NATO Series Vol. 198, Kluwer Academic Publishers, Dordrecht, 1991; (b) Miller, J. S.; Drillon, M. *Magnetism: Molecules to Materials*, Wiley-VCH: Weinheim, 2001.

30. (a) Christou, G.; Gatteschi, D.; Hendrickson, D. N.; Sessoli, R. *MRS Bull.* **2000**, *25*, 66; (b) Miller, J. S.; Drillon, M. Magnetism: *Molecules to materials I*, Wiley-VCH: Weinheim, 2001; (c) Miller, J. S.; Drillon, M. *Magnetism: Molecules to materials II*, Wiley- VCH: Weinheim, 2001; (d) Miller, J. S.; Drillon, M. *Magnetism: Molecules to materials III*, Wiley- VCH: Weinheim, 2002.

31. Bernier, P.; Lerant , S.; Bidan, G. *Advances in synthetic metals*: *Twenty Years of Progress in Science and Technology,* Elsevier Science, Amsterdam, 1999.

32. (a) Bruce, D.W.; O'Hare, D. (Eds.) *Inorganic Materials,* John Wiley: Chichester, 1992; (b) Knop, W. *Justus Leibigs. Ann. Chem.* **1842**, *43*, 111.

33. Akamatu, H.; Inokuchi, H.; Matsunaga, Y. *Nature* **1954**, *173*, 168.

34. (a) Wudl, F. *Acc. Chem. Res.* **1984**, *17*, 227; (b)Williams, J. M.; Beno, M. A.; Wang, H. H.; Leung, P. C. W.; Emge, T. J.; Geiser, U.; Carlson, K. D. *Acc. Chem. Res*. **1985**, *18*, 261; (c) Kristenmacher, T. J.; Philips, T. E.; Cowan, D. O. *Acta Crystallogr. B* **1974**, *30*, 763.

35. Wudl, F.; Smith, G. M.; Hufnagel, E. J. *J. Chem. Soc. Chem. Commun.* **1970**, 1453.

36. Torrance, J. B. *Acc. Chem. Res.* **1979**, *12*, 79.

37. (a) Martín. N.; Segura, J. L.; Seoane, C. *J. Mater. Chem.* **1997**, *7*, 1661; (b) Yamashita, Y.; Tomura, M. *J. Mater. Chem.***1998**, *8*, 1933.

38. (a) Bernier, P.; Lerant , S.; Bidan, G. *Advances in synthetic metals*: *Twenty Years of Progress in Science and Technology,* Elsevier Science, Amsterdam, 1999; (b) Metzger, R. M.; Day, P.; Papavassiliou, G. C. (Eds.) *Low Dimensional Systems and Molecular Electronics.* NATO Series Vol. 128, Plenum Press, New York, 1990; (c) Papavassiliou, G. C.; Terzis, A.; Delhaes, P. in *HandBook of Organic Conductive Molecules and Polymers*, Nalwa, H. S. (Ed.) Vol. 1, p.151, John Wiley: Chichester, 1997.

39. Kitagawa, H.; Onodera, N.; Sonoyama, T.; Yamamoto, M.; Fukawa, T.; Mitani, T.; Seto, M.; Maeda, Y. *J. Am. Chem. Soc.* **1999**, *121*, 10068.

40. Hanack, M.; Deger, S.; Lange, A. *Coord. Chem. Rev.* **1988**, *83*, 115.

41. Schäfer, E. P.; Maeda, M. *Dye Lasers*, Springer-Verlag, Berlin, 1990.
42. (a) Šulcová, P.; Trojan, M. *Dyes and Pigments* **1998**, *4*, 83; (b) Šulcová, P.; Trojan, M. *Dyes and Pigments* **1998**, *36*, 287.
43. Friedman, A. E.; Chambron, J. C.; Sauvage, J. P.; Turro, N. J.; Barton, J. K. *J. Am. Chem. Soc.* **1990**, *112*, 4960.
44. (a) Krasovitskii, B. M.; Bolotin, B. M. *Organic Luminescent Materials*, VCH: Weiheim, 1988; (b) Miyata, S.; Nalwa, H. S. (Eds.) *Organic Electroluminescent Materials and Devices,* Gordon and Breach: Amsterdam, 1997.
45. Hamada, Y. *IEEE Trans. Electron. Dev.* **1997**, *44*, 1208.
46. (a) Sheats, J. R.; Chang, Y. L.; Roitman, D. B.; Stocking, A. *Acc. Chem. Res.* **1999**, *32*, 193; (b) Friend, R. H.; Gymer, R. W.; Holmes, A. B.; Burroughes, J. H.; Marks, R. N.; Taliani, C.; Bradley, D. D. C.; Santos, D. A. D.; Brédas, J. L.; Lögdlund, M.; Salaneck, W. R. *Nature* **1999**, *397*, 121.
47. Dong, Y. –B.; Jin, G. –X.; Smith, M. D.; Huang, R. –Q.; Tang, B.; zur Loye, H. –C. *Inorg. Chem.* **2002**, *41*, 4909.
48. (a) Grell, M.; Bradly, D. D. C. *Adv. Mater.* **1999**, *11*, 895; (b) Carson, T. D.; Seo, W.; Tam-chang, S-W.; Casey, S. M. *Chem. Mater.* **2003**, *15*, 2292
49. National Research Council, *Harnessing Light : Optical Science and Engineering for the 21st century National*, Academic Press, Washington, DC 1998.
50. (a) Yariv, A. *Quantum Electronics*, John Wiley & Sons, New York, 1988; (b) Butcher, P. N.; Cotter, D. *The Elements of Nonlinear Optics*, Cambridge University Press, Cambridge, 1990; (c) Boyd, R. W. *Nonlinear Optics*, Academic Press, New York, 1992.
51. Franken, P. A.; Hill, A.E.; Peters, C.W.; Weinreich, G. *Phys. Rev. Lett.* **1961**, *6*, 118.
52. Giordmaine, J. A. *Phys. Rev. Lett.* **1962**, *8*, 19.
53. Maeda, M. *Laser Dyes: Properties of Organic Compounds for Dye Lasers*, Academic Press Inc, New York, 1984.
54. Levine, B. F. *Chem. Phys. Lett.* **1976**, *37*, 516.
55. Rentzepis, P. M.; Pao, Y. H. *Appl. Phys. Lett.* **1964**, *5*, 156.
56. Heilmeier, G. H.; Ockman, N.; Braunstein, R.; Kramer, D. A. *Appl. Phys. Lett.* **1964**, *5*, 228.
57. Gott. J. R. *J. Phys. B* **1971**, *4*, 116.

58. Kurtz, S. K.; Perry, T. T. *J. Appl. Phys.* **1968**, *39*, 3798.
59. Zyss, J.; Berthier, G. *J. Chem. Phys.* **1982**, *77*, 3635.
60. (a) Jerphagnon, J.; Kurtz, S. K. J. *Appl. Phys.* **1970**, *41*, 1667; (b) Jerphagnon, J.; Kurtz, S. K. *Phys. Rev. B* **1970**, *1*, 1739.
61. Hauchecorne, G.; Kerherve, F.; Mayer, G. *J. Phys.* **1971**, *32*, 47.
62. (a) Chemla, D. S.; Zyss, J. (Eds.) *Nonlinear Optical Properties of Organic Molecules and Crystals,* Vols. 1-2, Academic Press, Orlando, 1987; (b) Günter, P. *Nonlinear Optical Effects and Materials, Springer Series in Optical Sciences, Vol. 72*, Springer-Verlag, Heidelberg, 2000.
63. Williams, D. J. *Angew. Chem. Int. Ed. Engl.* **1984**, *23*, 690.
64. Kanis, D. R.; Ratner, M. A.; Marks, T. J. *Chem. Rev.* **1994**, *94*, 195.
65. (a) Messier, J.; Kajzar, F.; Prasad, P. (Eds.) *Organic Molecules for Nonlinear Optics and Photonics,* Vol. 194, Kluwer Academic Publishers, Nato ASI Series, Dordrecht, 1991; (b) Wolff, J. J.; Wortmann, R. *Adv. Phys. Org. Chem.* **1999**, *32*, 121.
66. (a)Wang, C.P. *Polymers for Photonic and Electronic Applications*, Academic Press, London, 1993; (b) Prasad, P. N.; Williams, D. J. *Introduction to Nonlinear Optical Effects in Molecules and Polymers*, John Wiley: New York, 1991.
67. (a) Moerner, W. E.; Silence, S .M. *Chem. Rev.* **1994**, *94*, 127; (b) Zhang, Y.; Wada, T.; Sasabe, H. *J. Mater. Chem.* **1998**, *8*, 809.
68. Law, K.Y. *Chem. Rev.* **1993**, *93*, 449.
69. Shen, H. Y.; Zhou, Y. P.; Lin, W. X.; Zeng, Z. D.; Zeng, R. R.; Yu, G. F.; Huang, C. H.; Jiang, A. D.; Jia, S. Q.; Shen, D. Z. *IEEE J. Quant. Electron.* **1992**, *28*, 48.
70. Smith, R. G.; Geusic, J. E.; Levinstein, H. J.; Rubin, J. J.; Singh, S.; Uitert, L. G. V. *Appl. Phys. Lett.* **1968**, *12*, 308.
71. Lin, S.; Wu, B.; Xie, F.; Chen, C. *Appl. Phys. Lett.* **1991**, *59*, 1541.
72. Long, N. J. *Angew. Chem., Int. Ed. Engl.* **1995**, *34*, 21.
73. Evans, O. R.; Lin, W. *Acc. Chem. Res.* **2002**, *35*, 511.
74. Cheng, L. -T.; Tam, W.; Stevenson,S. H.; Meredith G .R,.;Rikken, G.; Marder, S. R. *J. Chem. Phys.* **1991**, *95* ,10631.
75. Cheng, L. -T.; Tam, W.; Marder, S. R.; Steigman, A. E.; Rikken, G.; Spangler, C. W. *J. Chem. Phys.* **1991**, *95* ,10643.

76. (a) Oudar, J. L. *J. Chem. Phys.* **1977**, *67*, 446; (b) Levine, B. F. *J. Chem. Phys.* **1975**, *63*, 115.
77. Dulcic, A.; Sauteret, C. *J. Chem. Phys.* **1978**, *69*, 3453.
78. Oudar, J. L.; Leperson, H. *Opt. Commun.* **1975**, *15*, 258.
79. (a) Katz, H. E.; Singer, K. D.; Sohn, J. E.; Dirk, C. W.; King, L. A.; Gordon, H. M. *J. Am. Chem. Soc.* **1987**, *109*, 6561; (b) Singer, K. D.; Sohn, J. E.; King, L. A.; Gordon, H. M.; Katz, H. E.; Dirk, C. W. *J. Opt. Soc. Am. B* **1989**, *6*, 1339.
80. Eaton, D. F. *Science* **1991**, *253*, 281.
81. (a) Blanchard-Desce, M.; Wortmann, R.; Lebus, S.; Lehn, J. M.; Krämer, P. *Chem. Phys. Lett.* **1995**, *243*, 526; (b) Marder, S. R.; Cheng, L. T.; Tiemann, B. G.; Friedli, A. C.; Blanchard-Desce, M.; Perry, J. W.; Skindhøj, J. *Science* **1994**, *263*, 511.
82. Morley, J. O.; Docherty, V.J.; Pugh, D. *J. Chem. Soc. Perkin. Trans. 2* **1987**, 1351.
83. (a) Miller, R. D.; Lee, V. Y.; Moylan, C. R. *Chem. Mater.* **1994**, *6*, 1023; (b) Dirk, C. W.; Katz, H. E.; Schilling, M. L.; King, L. A. *Chem. Mater.* **1990**, *2*, 700.
84. (a) Mignani, G.; Barzoukas, M.; Zyss, J.; Soula, G.; Balegroune, F.; Grandjean, D.; Josse, D. *Organometallics*. **1991**, *10*, 3660; (b) Mignani, G.; Krämer, A.; Puccetti, G.; Ledoux, I.; Soula, G.; Zyss, J.; Meyrueix, R. *Organometallics*. **1990**, *9*, 2640.
85. Coe, B, J. *Comprehensive Coord. Chem. II* **2004**, 9, 612.
86. Sénéchal, K.; Maury, O,; Le Bozec, H.; Ledoux, I.; Zyss, J. *J. Am. Chem. Soc.* **2002**, *124*, 4560.
87. Marder, S, R. *Metal containing Materials for Nonlinear optics. In Inorganic Materials,* 2nd ed. Bruce D. W.; O'Hare, D. (Eds.). Wiley: Chichester, 1992, 195.
88. (a) Kelderman, E.; Starmans, W. A. J.; van Duynhoven. J. P. M ; Verboom, W.; Engbersen, J. F. J.; Reinhoudt, D. N.; Derhaeg, L.; Verbiest, T.; Clays, K.; Persoons, A. *Chem. Mater.* **1994**, *6*, 412; (b) Kelderman, E; Derhaeg, L.; Heesink, G. J. T.; Verboom, W.; Engbersen, J. F. J.; van Hulst, N. F. Persoons, A.; Reinhoudt, D. N. *Angew. Chem. Int. Ed. Engl.* **1992**, *31*, 1075.
89. (a) Verbiest, T.; Clays, K.; Samyn, C.; Wolff, J.; Reinhoudt, D.; Persoons, A. *J. Am. Chem. Soc.* **1994**, *116*, 9320; (b) Ray, P. C.; Das, P. K. *Chem. Phys. Lett.* **1995**, *244*, 153.

90. Zyss. J.; Ledoux, I. *Chem. Rev.* **1994**, *94*, 77.
91. Le Bozec, H.; Renourd T. *Eur. J. Inorg. Chem.* **2000**, 229.
92. Bahl, A.; Grahn, W.; Stadler, S.; Feiner, F.; Bourhill, G.; Bräuchle.; Reisner, A.; Jones, P. G. *Angew. Chem. Int. Ed. Engl.* **1995**, *34*, 1485.
93. (a) Verbiest, T.; van Elshocht, S.; Kauranen, M.; Hellemans, L.; Snauwaert, J.; Nuckolls, C.; Katz, J. T.; Persoons, A. *Science* **1998**, *282*, 913; (b) Gangopadhyay, P.; Radhakrishnan, T. P. *Angew. Chem. Int. Ed.* **2001**, *40*, 2451.
94. Oudar, J. L.; Chemla, J. S. *J. Chem. Phys.* **1977**, *66*, 2664.
95. Verbiest, T.; Houbrechts, S.; Kauranen, M.; Clays, K.; Persoons, A. *J. Mater. Chem.* **1997**, *7*, 2175.
96. (a) Kurtz, H. A.; Stewart, J. J.; Dieter, K. M. *J. Comput. Chem.* **1990**, *11*, 82; (b) Jain, M.; Chandrasekhar, J. *J. Phys. Chem.* **1993**, *97*, 4044.
97. (a) Levine, B. F.; Bethea, C. G. *J. Chem. Phys.* **1975**, *63*, 2666; (b) Singer, K. D.; Sohn, J. E.; King, L. A.; Gordon, H. M.; Katz, H. E.; Dirk, C. W. *J. Opt. Soc. Am. B* **1989**, *6*, 1339.
98. (a) Kielich, S.; Lalane, J. R.; Martin, F. B. *Phys. Rev. Lett.* **1971**, *26*, 1295; (b) Clays, K.; Persoons, A. *Phys. Rev. Lett.* **1991**, *66*, 2980.
99. Zyss, J.; Oudar, J. L.; *Phys. Rev. A* **1982**, *26*, 2028.
100. Whitesell, J. K.; Davis, R. E.; Saunders, L. L.; Wilson, R. J.; Feagins, J. P. *J. Am. Chem. Soc.* **1991**, *113*, 3267.
101. (a) Reichoff. K.; Peticolas. W. F. *Science* **1965**, *147*, 611; (b) Ukachi, T.; Shigemoto, T.; Komatsu, H.; Sugiyama, T. *J. Opt. Soc. Am. B* **1993**, *10*, 1372.
102. (a) Etter, M. C. *Acc. Chem. Res.* **1990**, *23*, 120; (b) Russell, V. A.; Ward, M. D. *Chem. Mater.* **1996**, *8*, 1654; (c) Lipscomb, G. F.; Garito, A. F.; Narang, R. S. *J. Chem. Phys.* **1981**, *75*, 1509; (d) Lipscomb, G. F.; Garito, A. F.; Narang, R. S. *Appl. Phys. Lett.* **1981**, *38*, 663; (e) Twieg, R.; Azema, A.; Jain, K.; Cheng, Y. Y. *Chem. Phys. Lett.* **1982**, *92*, 208; (f) Levine, B. F.; Bethea, C. G.; Thurmond, C. D.; Lynch, R. T.; Bernstein, J. *J. Appl. Phys.* **1979**, *50*, 2523; (g) Zerkowski, J. A.; MacDonald, J. C.; Whitesides, G. M. *Chem. Mater.* **1994**, *6*, 1250; (h) Sarma, J. A. R. P.; Rao, J. L.; Bhanuprakash, K. *Chem. Mater.* **1995**, *7*, 1843; (i) Bernstein, J.; Davis, R. E.; Shimoni, L.; Chang, N. L. *Angew. Chem. Int. Ed. Engl.* **1995**, *34*, 1555; (j) Sarma, J. A. R. P.; Allen, F. H.; Hoy, V. J.; Howard, J. A. K.; Thaimattam, R.; Biradha, K.; Desiraju, G. R. *Chem. Commun.* **1997**, 101.

103. (a) Gangopadyay, P.; Rao, S. V.; Rao, D. N.; Radhakrishnan, T. P.; *J. Mater. Chem.* **1999**, *9*, 1699; (b) Gangopadyay, P.; Sharma, S.; Rao, A. J.; Rao, D. N, Cohen, S.; Agranat, I.; Radhakrishnan, T. P. *Chem. Mater.* **1999**, *11*, 466; (c) Sharma, S.; Radhakrishnan, T. P. *Mol. Cryst. Liq. Cryst.* **1999**, *338*, 257; (d) Gangopadyay, P.; Radhakrishnan, T. P. *Chem. Mater.* **2000**, *12* , 3362.

104. (a) Ramamurty, V.; Eaton, D. F. *Chem. Mater.* **1994**, *6*, 1128; (b) Weissbuch, I.; Lahav, M.; Leiserowitz, L.; Meredith, G. R.; Vanherzeele, H. *Chem. Mater.* **1989**, *1*, 114; (c) Cox, S. D.; Gier, T. E.; Stucky, G. D. *Chem. Mater.* **1990**, *2*, 609.

105. Marder, S. R.; Perry, J. W.; Yakymyshyn, C. P. *Chem. Mater.* **1994**, *6*, 1137.

106. Jayanty, S.; Gangopadhyay, P.; Radhkarishnan, T. P. *J. Mater. Chem.* **2002**, *12*, 2792.

107. Rasid, A. N.; Erny, C.; Gunter, P. *Adv. Mater.* **2003**, *15*, 2024.

108. (a) Bosshard, C.; Sutter, K.; Prêtre, P.; Hulliger, H.; Flörsheimer, M.; Kaatz, P.; Günter, P. *Organic Nonlinear Optical Materials*, Gorden & Breach, Amsterdam, 1995; (b) Kajzar, F.; Swalen, J. D. (Eds.), *Organic Thin Films for Waveguiding Nonlinear Optics*, Gorden & Breach, Amsterdam, 1996; (c) Tregold, R. H. *Order in Thin Organic Films*, Cambridge Univ. Press, Cambridge, 1994; (d) Reed, M. A. *Proceedings of the IEEE* **1999**, *87*, 652.

109. (a) Whitsides, G. M.; Mathias, J. P.; Seto, C. T. *Science* **1991**, *254*, 1312; (b) Interrante, L. V.; Casper, L. A.; Ellis, A. B. *Materials Chemistry of Organic Monolayer and Multilayer Thin Films*, American Chemical Society, Washington, DC 1995.

110. Oh, M. C.; Shin, S. Y. *IEEE Phot. Tech. Lett.* **1996**, *8*, 1483.

111. (a) Decher, G.; Tieke, B.; Bosshard, C.; Günter, P. *Chem. Commun.* **1988**, 933; (b) Bosshard, C.; Decher, G.; Tieke, B.; Günter, P. *Proc. SPIE-Int. Soc. Opt. Eng.* **1988**, *141*, 1017; (c) Decher, G.; Tieke, B.; Bosshard, C.; Günter, P. *Ferroelectrics* **1989**, *91*, 193; (d) Nakahara, H.; Liang, W.; Kimura, H.; Wada, T.; Sasabe, H. *J. Opt. Soc. Am. B* **1999**, *15*, 458; (e) Liang, W.; Nakahara, H.; Kimura, H.; Wada, T.; Sasabe, H. *Thin Solid Films* **1998**, *423*, 327.

112. Bosshard, C.; Florsheimer, M.; Küpfer, M.; Günter, P. *Opt. Commun.* **1991**, *85*, 247.

113. (a) Li, D.; Ratner, M. A.; Marks, T. J.; Zhang, C.; Yang, J.; Wong, G. K. *J. Am. Chem. Soc.* **1990**, *112*, 7389; (b) Facchetti, A.; van der Boom, M. E.; Abbotto,

A.; Beverina, L.; Marks, T. J.; Pagani, G. A. *Langmuir*, **2001**, *17*, 5939; (c) van der Boom, M. E.; Richter, A. G.; Malinsky, J. E.; Lee, P. A.; Armstrong, N. R.; Dutta, P.; Marks, T. J. *Chem. Mater*. **2001**, *13*, 15.

114. (a) Mobus, M.; Karl, N.; Kobayashi, T. *J. Cryst. Growth* **1992**, *116*, 495; (b) Englund, C. D.; Collins, G. E.; Schuerlein, T. J.; Armstrong, N. R. *Langmuir* **1994**, *10*, 2748; (c) Haskal, E. J.; So, F. F.; Burrows, P. E.; Forrest, S. R. *Appl. Phy. Lett*. **1992**, *60*, 3223; (d) Ito, Y.; Hikito, M.; Kimura, T. *Jpn. J. Appl. Phys*. **1990**, *29*, 1128; (e) Ehara, T.; Hirose, H.; Kobayashi, H.; Kotani, M. *Synthetic Metals* **2000**, *109*, 43.
115. (a) Cai, C.; Bösch, M. M.; Tao, Y.; Mülleer, B.; Gan, Z.; Kündig, A.; Bosshard, C.; Liakatas, I.; Jäger, M.; Günter, P. *J. Am. Chem. Soc*. **1998**, *120*, 8563; (b) Rashid, A. N.; Erny, C.; Günter, P. *Adv. Mater*. **2003**, *15*, 2024.
116. Ge, J. J.; Li, C. Y.; Xue, G.; Mann, I. K.; Zhang, D.; Wang, S. Y.; Harris, F. W.; Cheng, S. Z. D.; Hong, S. C.; Zhuang, X.; Shen, Y. R. *J. Am. Chem. Soc*. **2001**, *123*, 5768.
117. Komatsu, K.; Nanjo, H.; Yamagishi, Y.; Kaino, T. *Thin Solid Films* **2001**, *393*, 1.
118. (a) Kim, O. K.; Choi, L.-S.; Zhang, H.-Y.; He, X.-H.; Shih, Y.-H. *J. Am. Chem. Soc.* **1996**, *118*, 12220; (b)) Kim, O. K.; Choi, L.-S.; Zhang, H.-Y.; He, X.-H.; Shih, Y.-H. *Thin Solid Films* **1998**, *327-329*, 172.
119. McConnell, H. M. *J. Chem. Phys*. **1963**, *39*, 1910.
120. (a) Curtin, D. Y.; Paul, I. C. *Chem. Rev*. **1981**, *81*, 525; (b) Etter, M. C.; Huang, K. S. *Chem. Mater*. **1992**, *4*, 824; (c) Gong, B.; Zheng, C.; Zheng, H.; Zhu, J. *J. Am. Chem. Soc.* **1999**, *121*, 9766;
121. Marder, S. R.; Perry, J. W.; Schaefer, W. P. *Science* **1989**, *245*, 626.
122. (a) Wong, M. S.; Pan, F.; Bosch, M.; Spreiter, R.; Bosshard, C.; Günter, P.; Gramlich, V. *J. Opt. Soc. Am. B* **1998**, *15*, 426; (b) Pan, F.; Wong, M. S.; Gramlich, V.; Bosshard, C.; Günter, P. *J. Am. Chem. Soc*. **1996**, *118*, 6315.
123. (a) Wong, M. S.; Bosshard, C.; Günter, P. Adv. Mater. 1997, *9*, 837; (b) Burgi, H.- B.; Hulliger, H.; Langely, P. J. *Curr. Opin. Solid State Mater. Sci*. **1998**, *3*, 425.
124. (a) Desiraju, G. R. *Angew. Chem. Int. Ed. Engl*. **1996**, *34*, 2328; (b) Sarma, J. A. R. P.; Allen, F. H.; Hoy, V. J.; Howard, J. O. K.; Thaimattam, R.; Biradha, K.; Desiraju, G. R. *Chem. Commun*. **1997**, 101; (c) Masciocchi, N.; Bergamo, M.;

Sironi, A. *Chem. Commun*, **1998**, 1347; (d) Thallapally, P. K.; Desiraju, G. R.; Bagieu-Beucher, M.; Masse, R.; Bourgogne, C.; Nicoud, J. –F. *Chem. Commun.* **2001**, 1052.

125. Tomaru, S.; Zembutstu, S.; Kawachi, M.; Kobayachi, M. *Chem. Commun.* **1984**, 1207.
126. (a)Weber, E. *Top. Curr. Chem.* **1987**, *140*, 3; (b) Davies, J. E. D.; Kemula, W.; Powell, H. M.; Smith, N. O. *J. Inclusion Phenom. Mol. Recognit. Chem.* **1983**, *1*, 3.
127. (a) Farina, M. *Inclusion Compd.* **1984**, 69; (b) Allegra, G.; Farina, M.; Immirzi, A.; Colombo, A.; Rossi, U.; Broggi, R.; Natta, G. *J. Chem. Soc. B* **1967**, 1020; (c) Farina, M.; de Silvestro, G.; Sozzani, P. *Comp. Supramol. Chem. Vol. 6, Solid State Supramolecular Chemistry: Crystal Engineering,* MacNicol, D. D.; Toda, F.; Bishop, F. (Eds.), Pergamon.
128. (a) Eaton, D. F.; Anderson, A. G.; Tam, W.; Wang, Y. *J. Am. Chem. Soc.* **1987**, *109*, 1886; (b) Tam, W.; Eaton, D. F.; Calabrese, J.; Williams, I.; Wang, Y.; Anderson, A. G. *Chem. Mater.* **1989**, *1*, 128.
129. (a) Cox, S. D.; Gier, T. E.; Stucky, G. D.; Bierlein, J. D. *J. Am. Chem. Soc.* **1988**, *110*, 2986; (b) Girnus, I.; Pohl, M. –M.; Richter-Mendau, J.; Schneider, M.; Noack, M.; Venzke, D.; Caro, J. *Adv. Mater.* **1995**, *7*, 711.
130. (a) Höss, R.; König, O.; Kramer-Hoss, V.; Berger, U.; Rogin, P.; Hulliger, J. *Angew, Chem., Int Ed. Engl.* **1996**, *35*, 1664; (b) König, O.; Bürgi, H.-B.; Armbruster, T.; Hulliger, J.; Weber, T. *J. Am. Chem. Soc.* **1997**, *119*, 10632; (c) Hulliger, J.; Rogin, P.; Quintel, A.; Rechsteiner, P.; König, O.; Wübbenhorst, W. *Adv. Mater.* **1997**, *9*, 677; (d) Hulliger, J.; Langly, P. J.; König, O.; Roth, S. W.; Quintel, A.; Rechsteiner, P. *Pure Appl. Opt.* **1998**, *7*, 221;
131. (a) Hulliger, J.; Langly, P. J.; Quintel, A.; Rechsteiner, P.; Roth, S. W. *Supramolecular Engineering of Synthetic Metallic Materials*, Veciana, J.; Rovira, C.; Amabilino, D. B. (Eds.), Kluwer, Dordrecht, **1999**, 67; (b) Hulliger, J.; Roth, S. W.; Quintel, A.; Bebie, H. *J. Solid State Chem.* **2000**, *152*, 49.
132. Holman, K. T.; Pivovar, A. M.; Ward, M. D. *Science* **2001**, *294*, 1907.
133. Hulliger, J.; Langly, P. J.; Roth, S. W. *Cryst. Engg.* **1998**, *1*, 177.
134. (a) Ohkita, M.; Suzuki, T.; Nakatani, K.; Tsuji, T. *Chem. Lett.* **2001**, 988; (b) Jouaiti, A.; Hosseini, M. W.; Kyritsakas, N. *Chem. Commun.* **2002**, 1896.

135. (a) Qin, J.; Su, N.; Dai, C.; Yang, C.; Liu, D.; Day, M. W.; Wu, B.; Chen, C. *Polyhedron* **1999**, *18*, 3461; (b) Qin, J.; Dai, C.; Zhang, J.; Su, N.; Yang, C.; Luo, B.; Liu, D.; Wu, B.; Chen, C.; Day, M. W. *Progress in Crystal Growth and Characterization of Materials* **2000**, 115.
136. Chen, G. S.; Wilbur, J. K.; Barnes, C. L.; Rainer, G. *J. Chem. Soc. Perkin Trans.* **1995**, 2311.
137. Rainer, G.; Nathan, K.; Hong, W. *Chemstrcts* **2003**, *16*, 643.
138. Gong, B.; Zheng, C.; Zeng, H.; Zhu, J. *J. Am. Chem. Soc.* **1999**, *121*, 9766.
139. (a) Moerner, W. E.; Silence, S. M. *Chem. Rev.* **1994**, *94*, 127; (b) Burland, D. M.; Miller, R. D.; Walsh, C. A. *Chem. Rev.* **1994**, *94*, 31.
140. Marks, T. J.; Ratner, M. A. *Angew. Chem. Int. Ed. Engl.* **1995**, *34*, 155.
141. Ashkin, A.; Boyd, G. D.; Dziezik, J. M.; Smith, R. G.; Ballman, A. A.; Nassan, K. *Appl. Phys. Lett.* **1966**, *9*, 72.
142. (a) Glass, A. M. *MRS Bull.* **1988**, *13*, 16; (b) Fan, Y, X.; Eckhardt, R. C.; Byer, R. L.; Route, R. K.; Fiegelson, R. S. *Appl. Phys. Lett.* **1984**, *45*, 313.
143. Qin, J.; Liu, D.; Dai, C.; Chen, C.; Wu, B.; Yang, C.; Zhan, C. *Coord. Chem. Rev.* **1999**, *188*, 23.
144. (a) Nalwa, H. S. *Appl. Organomet. Chem.* **1991**, *5*, 349; (b) Whittall, I. R.; McDonagh, A. M.; Humphery, M. G.; Samoc, M. *Adv. Organomet. Chem*, **1998**, *42*, 291; (c) Whittall, I. R.; McDonagh, A. M.; Humphery, M. G.; Samoc, M. *Adv. Organomet. Chem*, **1998**, *43*, 349.
145. Heck, J.; Dabek, S.; Meyer-Friedrichsen, T.; Wong, H. *Coord. Chem. Rev.* **1999**, *190-192*, 1217; (c) Shi, S. *Optoelectronic Properties of Inorganic Compounds*, Roundhill, D. M.; Fackler, J. P. (Eds.), Plenum, New York, **1999**, 55.
146. Barlow, S.; Marder, S. R. *Chem. Commun.* **2000**, 1555.
147. Bella, S. D. *Chem. Soc. Rev.* **2001**, *30*, 355.
148. (a) Eaton, D. F.; Anderson, A. G.; Tam, W.; Wang, Y. *J. Am. Chem. Soc.* **1987**, *109*, 1886; (b) Tam, W.; Eaton, D. F.; Calabrese, J. C.; Williams, I. D. Wang, Y.; Anderson, A. G. *Chem. Mater.* **1989**, *1*, 128.
149. Kanis, D. R.; Lacroix, P. G.; Ratner, M. A.; Marks, T. J. *J. Am. Chem. Soc.* **1994**, *116*, 10089.
150. (a) Coe, B. J.; Houbrechts, S.; Asselbeghs, I.; Persoons, A. *Angew. Chem. Int. Ed. Engl.* **1999**, *38*, 366; (b) Coe, B. J.; Essex-Lopresti, J. P.; Harris, J. A.;

Houbrechts, S, Persoons, A. *Chem. Commun.* **1997**, 1645; (c) Coe, B. J. *Chem. Eur. J.* **1999**, *5*, 2464.

151. Umemura, Y.; Yamagishi, A.; Schoonheydt, R.; Persoons, A. J. *Am. Chem. Soc.* **2002**, *124*, 992.
152. Zyss, J.; Dhenaut, C.; Chauvan, T.; Ledoux, I. *Chem. Phys. Lett.* **1993**, *206*, 409.
153. Le Bozec, H.; Le Bouder, T.; Maury, O.; Bondon, A.; Ledoux, I.; Deveau, S.; Zyss, J. *Adv. Mater.* **2001**, *13*, 1677.
154. Chiang, W.; Thompson, M. E.; VanEngen, D.; Perry, J. W. *Spec. Publ. R. Soc. Chem.* **1991**, *91*, 210.
155. Thami, T.; Bassoul, P.; Petit, M. A.; Simon, J.; Gort, A.; Barzoukas, M.; Villaeys, A. *J. Am. Chem. Soc.* **1992**, *114*, 915;
156. Bella, S. D.; Fragala, I.; Ledoux, I.; Diaz-Garcia, M. A.; Lacroix, P. G.; Marks, T. J. *Chem. Mater.* **1994**, *6*, 881.
157. Lacroix, P. G. *Eur. J. Inorg. Chem*, **2001**, 339.
158. Chiang, W.; Van Engen, D.; Thompson, M. E. *Polyhedron* **1996**, *15*, 2369.
159. Evans, C.; Luneau, D. *Dalton Trans.* **2002**, 83.
160. Bergman, J. G. Jr.; McFee, J. H.; Crane, G. R. *Mater. Res. Bull.* **1970**, *5*, 913.
161. Wang, X.-Q.; Xu, D.; Lu, M.-K.; Yuan, D.-R.; Zhang, G.-H.; Meng, F.-Q.; Guo, S.-Y.; Zhou, M.; Liu, J.-R.; Li, X.-R. *Cryst. Res. Technol.* **2001**, *36*, 73.
162. Moulton, B.; Zaworotko, M. J. *Chem. Rev.* **2001**, *101*, 1629.
163. Janiak, C. *J. Chem. Soc., Dalton Trans.* **2000**, 3885.
164. (a) Zaworotko, M. J. *Chem. Commun.* **2001**, 1; (b) Batten, S. R.; Murray, K. S. *Aust. J. Chem.* **2001**, *54*, 605.
165. (a) Batten, S. R.; Robson, R. *Angew. Chem. Int. Ed. Engl.* **1998**, *37*, 1460; (b) Batten, S. R.; Robson, R. *Molecular Catenanes, Rotaxanes and Knots,* Sauvage, J. P.; Dietrich-Buchecker, C. (Eds.), Wiley-VCH, Weinheim, **1999**, 77; (c) Robson, R.; Abrahams, B. F. Batten, S. R.; Gable, R. W.; Hoskins, B. F.; Liu, J. *Supramolecular Architecture,* Bein, T. (Ed.), ACS, Washington DC, 1992, 19.
166. (b) Zhang, H.; Wang, X..; Zhang, K.; Teo, B. K. *J. Solid State Chem.* **2000**, *152*, 191.
167. (a) Bourgault, M.; Mountassir, C.; Le Bozec, H.; Ledoux, I.; Pucetti, G.; Zyss, J. *Chem. Commun.* **1998**, 517; (b) Bella, S. D.; Fragala, L.; Ledoux, I.; Marks, T. J.

J. Am. Chem. Soc. **1995**, *117*, 9481; (d) Lacroix, P. G.; Bella, S. D.; Ledoux, I. *Chem. Mater.* **1996**, *8*, 541.

168. Dhenaut, C.; Ledoux, I.; Samuel, I.; Zyss, J.; Bourgault, M.; Le Bozec, H. *Nature* **1999**, 871.
169. Shi, J.-M.; Xu, W.; Liu, Q.-Y.; Liu, F.-L.; Huang, Z.-L.; Lei, H.; Yu, W.-T.; Fang, Q. *Chem. Commun.* **2002**, 756.
170. (a) Evans, O. R.; Xiong, R.-G.; Wang, Z.; Wong, G. K.; Lin, W. *Angew. Chem. Int. Ed. Engl.* **1999**, *38*, 536; (b) Evans, O. R.; Wang, Z.; .; Xiong, R.-G.; Foxman, B. M.; Lin, W. *Inorg. Chem.* **1999**, *38*, 2969; (c) Evans, O. R.; Lin, W. *Chem. Mater.* **2001**, *13*, 2705; (d) Lin, W.; Ma, L.; Evans, O. R. *Chem. Commun.* **2000**, 2263; (e) Zhang, J.; Lin, W.; Chen, Z.-F.; Xiong, R.-G.; Abrahams, B. F.; Fun, H.-K. *Dalton Trans.* **2001**, 1806; (f) Qu, Z.-R.; Zhao, H.; Wang, Y.-P.; Wang, X.-S.; Ye, Q.; Li, Y.-H.; Xiong, R.-G.; Abrahams, B. H.; Liu, Z.-G.; Xue, Z.-L.; You, X.-Z. *Chem. Eur. J.* **2004**, *10*, 53.
171. Endo, S.; Chino, T.; Tsuboi, S.; Koto, K. *Nature* **1989**, *340*, 452.
172. Prosperio, D. M.; Hoffman, R.; Preuss, P. *J. Am. Chem. Soc.* **1994**, *116*, 9364; (b) Zaworotka, M. *Chem. Soc. Rev.* **1994**, 283; (c) Hirsch, K. A.; Wilson, S. R.; Moore, J. S. *Chem. Eur. J.* **1997**, *3*, 765.
173. Chen, Z.-F.; Xiong, R.-G.; Abrahams, B. F.; You, X.-Z.; Che, C.-M. *Dalton Trans.* **2001**, 2453.
174. (a) Janiak, J.; Scharmann, T. G.; Albrecht, P.; Marlow, F.; Macdonald, R. J. *Am. Chem. Soc.* **1996**, *118*, 6307; (b) Lin, W.; Evans, O. R.; Xiong, R.-G.; Wang, Z. *J. Am. Chem. Soc.* **1998**, *120*, 13272; (c) Evans, O. R.; Lin, W. *Chem. Mater.* **2001**, 13, 3009; (d) Xie, Y.-R.; Zhao, H.; Wang, X.-S.; Qu, Z.-R.; Xiong, R.-G.; Xue, X.; Xue, Z.; You, X.-Z. Eur. J. *Inorg. Chem.* **2003**, 3712.
175. Lin, W.; Wang, Z Ma, L. J. *Am. Chem. Soc.* **1999**, *121*, 11249.
176. (a) Zhang, H.; Wang, X.; Zhang, K.; Teo, B. K. *Coord. Chem. Rev.* **1999**, 183, 157; (b) Zhang, H.; Zelmon, D. E.; Price, G. E.; Teo, B. K. *Inorg. Chem.* **2000**, *39*, 1868.
177. Xiong, R.-G,; Xue, X.; Zhao, Z.; You, Z.; Abrahams, B. F.; Xue, Z. *Angew. Chem. Int. Ed. Engl.* **2002**, *41*, 3800.
178. (a) Katz, H. E.; Schller, G.; Putvinski, T. M.; Schilling, M. L.; Wilson, W. L.; Chidsey, C. E. D. *Science* **1991**, *254*, 1485; (b) Neff, G. A.; Mahon, T. M.;

Abshere, T. A.; Page, C. *J. Mater. Res. Soc. Sym. Proc.* **1996**, *435*, 661; (c) Ayyappan, P.; Evans, O. R.; Cui, Y.; Wheeler, K. A; Lin, W. *Inorg. Chem.* **2002,** *41*, 4978.

179. (a) Han, L.; Hong, M.; Wang, R. Luo, J.; Lin, Z.; Yuan, D.; *Chem. Commun.* **2003**, 2580; (b) Xie, Y.-R.; Xiong, R.-G.; Xue, X.; Chen, X.-T.; Xue, Z, You, X.-Z; (c) Evans, O. R.; Wang, Z.; Lin, W. *Chem. Commun.* **1999**, 1903; (d) Maggard, P. A.; Stern, C. L.; Poeppelmeier, K. R. *J. Am. Chem. Soc.* **2001**, *123*, 7742.

CHAPTER 2

Polar Assembly of Dipolar Molecules in Crystals and Thin Films of Metal Complexes

Papers published

- Anthony, S. P.; Radhakrishnan, T. P. *Chem. Commun.* **2001**, 931.
  Perfectly Polar Assembly of Molecular Dipoles in Crystals of Zn(II)(DMAP)$(acac)_2$: A Case of Self-Poling.

- Anthony, S. P.; Srikanth, L.; Radhakrishnan, T. P. *Mol. Cryst. Liq. Cryst.* **2002**, *381*, 133.
  Impact of Molecular Structure Change on the Hierarchy of Intermolecular Interactions Leading to Polar/Centrosymmetric Crystals.

- Anthony, S. P.; Raghavaiah, P.; Radhakrishnan, T. P. *Cryst. Growth Des.* **2003**, *3*, 631.
  Extreme Molecular Orientations in a Dimorphic Systems: Polar/Centric and Polar/Polar Cogrowth Crystal Architectures.

- Anthony, S. P.; Naga Srinivas, N. K. M.; Rao, D. N.; Radhakrishnan, T. P. *J. Mater. Chem.* **2005**, *15*, 739.
  Thin Films of Perfectly Polar Crystallites with Uniaxial Orientational Ordering.

- Anthony, S. P.; Porel, S.; Rao, D. N.; Radhakrishnan, T. P. (Submitted).
  Thin Films of Metal-Organic Compounds and Metal Nanoparticle Embedded Polymer for Nonlinear Optical Applications.

2.1 INTRODUCTION

There has been intense research activity in recent years, in the area of molecular materials focusing on the design and systematic alteration of the structure of the constituent molecules with a view to realize specific materials properties.[1] Synthetic chemistry provides great scope for the structural modification of the molecular materials both at the molecular level and at the organization level, i.e. the level where we wish to control the assembly of molecules in the solid state.[2] Bulk properties of molecular materials are often directly related to the relative orientation and organization of the constituent molecules. Molecular materials based on dipolar molecules with a polar organization of the molecules, form an important class of materials, since many technologically useful solid state properties such as ferroelectricity, pyroelectricity, piezoelectricity and second order nonlinear optical effects could be realized in them.[3] A brief account of the relevance of molecular orientation to many solid state properties was presented in Sec. 1.4. We have developed a novel family of metal-organic compounds with a push-pull structure which forms perfectly polar assemblies in the crystal lattice. Interesting cases of polymorphism and oriented growth of crystallites in vapor deposited thin films were observed with these molecular materials. All the materials show moderate second harmonic generation.

Fabrication of polar molecular materials often requires special techniques. For example, parallel alignment of molecular dipoles in doped polymer films is achieved through electric field poling.[4] Approaches towards polar molecular assembly in crystals have relied on the use of a supporting framework structure. In Sec. 2.2, we describe the synthesis of a new class of coordination complexes of zinc which exhibit perfectly polar organization of the molecular dipoles in the crystal lattice. The polar ordering of the single component system can be described as a case of 'self-poling', and is discussed on the basis of a hierarchy of anisotropic intermolecular interactions in the three-dimensional crystal lattice. We discuss two of the new materials in Sec. 2.3.

In Sec. 2.4, we describe the polymorphism observed in another complex in this series; it forms perfectly polar as well as centrosymmetric crystal structures depending sensitively on the solvent and the rate of crystallization. A suitable choice of solvents

provides crystals exhibiting an unusual cogrowth of polar/centric as well as polar/polar domains. Semiempirical computational modeling studies of molecular clusters of the dimorphic structures gives useful insight into the delicate balance of energetics involved in the solvent polarity preference of the extreme structures. The SHG of microcrystalline powders of the different compounds are presented in Sec. 2.5.

In Sec. 2.6, we discuss the fabrication of thin films of these metal-organic systems on amorphous glass substrates by vapor deposition method. X-ray diffraction studies reveal orientational ordering of the perfectly polar crystallites in these films. Position and distance of the substrate from the sublimation boat is shown to be the critical factors controlling the crystallite orientation. Morphology of the films was studied by scanning electron microscopy. Optical second harmonic generation measurements on the thin films clarify further, the uniaxial orientational ordering of the crystallites and the random orientation within the plane. Sec. 2.7 summarizes the work presented in this chapter.

2.2 SYNTHESIS AND CHARACTERIZATION

The new zinc complexes we have developed and present in this chapter are: (4-dimethylaminopyridyl) bis(acetylacetonato) zinc(II) (ZNDA), (4-morpholinopyridyl) bis(acetylacetonato) zinc(II) (ZNMPA) and (4-pyrrolidinopyridyl) bis(acetylacetonato) zinc(II) (ZNPPA). The structures and synthesis are depicted in Scheme 2.1. Morpholinopyridine, pyrrolidinopyridine and $Zn(acac)_2.H_2O$ were synthesized following the procedures reported in the literature.[5] General procedure for the preparation of ZNDA, ZNMPA and ZNPPA is as follows. The compounds were prepared by the direct addition of the solution of 1 mmol of the appropriate pyridine ligand in 10 ml methanol to a solution of 1 mmol of $Zn(acac)_2.H_2O$ in 50 ml methanol. The mixture was stirred for 5 min at room temperature and the white microcrystalline product obtained was filtered, washed with cold methanol and vacuum dried. Characterization of each of the compounds is listed below.

(4-dimethylaminopyridyl)bis(acetylacetonato)zinc(II) (ZNDA): Yield: 90%; M. P: 237-240°C; UV-Vis (methanol): λ_{max} ($\lambda_{cut\text{-}off}$) = 282 nm (330 nm); FT-IR (KBr pellet):

$\bar{\upsilon}$/cm^{-1} : 3078.7, 2918.6 (C-H stretch), 1608.8 (aromatic C=C stretch), 1010.8 (C-H bend); ^{1}H NMR ($CDCl_3$): δ/ppm = 1.85 (s, 12H), 2.98 (s, 6H), 5.25 (s, 2H), 6.67 (d, *J*=6Hz, 2H), 8.01 (d, *J*=6Hz, 2H); ^{13}C NMR ($CDCl_3$): δ/ppm = 28.0, 46.1, 99.1, 107.1, 148.5, 153.6, 191.8.

(4-morpholinopyridyl)bis(acetylacetonato)zinc(II) (ZNMPA): Yield: 90%; M. P: 228-230°C; UV-Vis (methanol): λ_{max} ($\lambda_{cut\text{-}off}$) = 283 nm (323 nm); FT-IR (KBr pellet): $\bar{\upsilon}$/cm^{-1} : 3078.7, 2918.6 (C-H stretch), 1610.7 (aromatic C=C), 1010.8 (C-H bend); ^{1}H NMR ($CDCl_3$): δ/ppm = 1.85 (s, 12H), 3.31 (t, 4H), 3.68 (t, 4H), 5.25 (s, 2H), 6.92 (d, 2H), 8.05 (d, 2H); ^{13}C NMR ($CDCl_3$): δ/ppm = 28.0, 45.6, 65.8, 99.1, 108.3, 148.9, 155.6, 191.8.

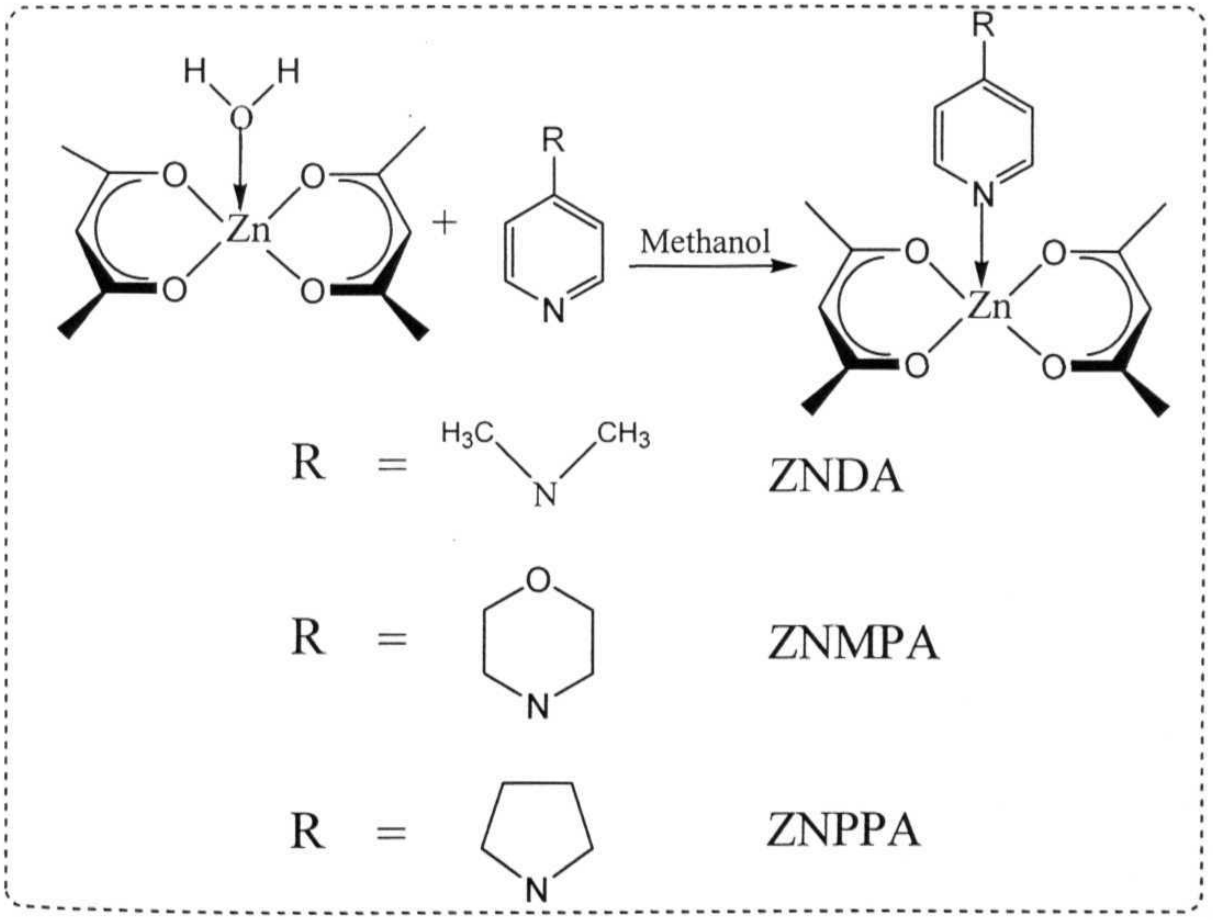

Scheme 2.1

(4-pyrrolidinopyridyl)bis(acetylacetonato)zinc(II) (ZNPPA): Yield: 90%; M. P: 245°C; UV-Vis (methanol): λ_{max} ($\lambda_{cut\text{-}off}$) = 282 nm (322 nm); FT-IR (KBr): $\bar{\upsilon}$/cm^{-1} : 3074.9, 2949.7 (C-H stretch) 1606.7 (aromatic C=C), 1009.3(C-H bend); ^{1}H NMR ($CDCl_3$): δ/ppm = 7.98 (d, 2H), 6.36 (d, 2H), 5.29 (s, 2H), 3.29 (t, 4H), 2.05 (m, 4H), 1.98 (s, 12H); ^{13}C NMR ($CDCl_3$): δ/ppm = 25.0, 28.9, 47.1, 99.4, 107.0, 148.2, 152.6, 192.9.

2.3 PERFECTLY POLAR ORGANIZATION OF DIPOLAR MOLECULES IN CRYSTALS OF ZNDA AND ZNMPA

The formation of molecular assemblies possessing a polar axis, is one of the most remarkable aspects of solid state organization. This unique solid state phenomenon has no counterpart in liquid or gas phase where molecules can undergo relatively ready reorientation. Molecular materials with a polar organization of the constituent dipoles are of interest in the development of novel electro-optic (EO) and photo-refractive devices[6] and nanoscale components such as molecular rectifiers.[7] Inclusion[8] compounds have been investigated in the past with a view to develop new strategies for designing polar solids.

It is essential that the molecular chromophores are arranged non-centrosymmetrically in the crystalline state to have a nonvanishing macroscopic second order nonlinear optical response from the material. Molecular crystals show a strong predilection towards centrosymmetric organization.[9] Special design strategies are often employed to induce noncentrosymmetricity.[10] Still rarer are highly polar molecular crystals with molecular dipoles aligned parallel to a single axis. Strategies such as cocrystallization,[11] salt formation,[12] host-guest complexation[8,13] and framework systems[14] have been developed for achieving polar molecular assembly in crystals. These approaches require a supporting structure to achieve parallel alignment of molecular dipoles, which reduces the density of the active component in the bulk and invariably leads to less effective utilization of the bulk materials to achieve desired solid state properties. Crystal engineering strategies have been utilized in the development of single component systems with polar organization of molecular dipoles.[15] Parallel alignment of

molecules has been achieved in crystals of some zinc complexes.[16] A molecular design strategy proposed by Hulliger[17] involves a dipolar backbone with an optimal decoration that dictates weak or non-bonding lateral recognition, leading to a polar crystal lattice. A potential candidate for such an approach would be a 'screw'-shaped molecule with a dipolar axis and 'head' which curtails lateral interactions without obstructing one-dimensional head-to-tail Coulombic interactions. We have developed the simple metal-organic compounds, ZNDA, ZNMPA and ZNPPA that form perfectly polar organization of molecular dipoles in the crystals.[18] In these compounds, the pyridyl-zinc combination forms the polar entity and the acetylacetonate ligands, the 'head' structure. We have analyzed the crystal structure of these compounds and the intermolecular interactions which appear to promote the parallel orientation of the molecular dipoles in the three-dimensional supramolecular assembly. We discuss the structure of ZNDA and ZNMPA in this section.

Crystal Structure Investigations

ZNDA

Colorless crystals of ZNDA could be grown by slow evaporation of methanol solution. X-ray analysis showed that the crystals belong to the orthorhombic space group Fdd2 with half a molecule in the asymmetric unit; the C_2 operation generates the other half. The basic crystallographic data are presented in Table 2.1. The molecular structure of ZNDA is shown in Fig. 2.1. Zinc and the coordinated pyridine nitrogen, the *para* carbon and dimethylamino nitrogen atoms on 4-dimethylaminopyridine (DMAP) lie on special positions on the *c*-axis. Zn(II) has distorted square-pyramidal coordination with normal bond parameters.[19] The space filling model of the molecular structure shows the 'screw'-shaped structure clearly (Fig. 2.2). More interestingly, the molecules pack into a perfectly polar lattice with the dipoles aligned along the *c* axis (Fig. 2.3) by virtue of the special position of Zn and DMAP and the space group operations. The origin of this organizational motif may be sought in the interplay of intermolecular interactions in the ZNDA lattice.

ZNDA is expected to have a sizeable dipole moment due to the push-pull nature of the DMAP-Zn(II) combination; AM1 calculation[20] on the molecular geometry taken from the crystal structure, gives a value of 8.919 D. The electrostatic interaction between the dipoles directs the head-to-tail chain formation along the *c* axis. This is augmented by weak intermolecular H-bonds[21] between the carbon atoms of the dimethylamino groups of the DMAP ligand and oxygen atoms of the *acac* ligand of neighboring

Table 2.1 *Crystallographic data for* ***ZNDA*** *and* ***ZNMPA***

Identification code	**ZNDA**	**ZNMPA**
Empirical formula	$C_{8.50}H_{12}NO_2Zn_{0.5}$	$C_{9.50}H_{13}NO_{2.50}Zn_{0.5}$
Formula weight	192.88	213.89
Crystal system	Orthorhombic	Monoclinic
Space group	Fdd2 (No. 43)	Cm (No. 8)
a / Å	28.057(4)	8.601(9)
b/ Å	11.363(2)	14.833(12)
c / Å	11.3253(17)	7.782(8)
β /°	90.00	91.57(8)
V / Å^3	3610.6(10)	992.4(17)
Z	16	4
$\rho_{calc.}$ / g cm^{-3}	1.419	1.432
μ / mm^{-1}	1.383	1.27
T_{min}, T_{max}	0.978, 0.988	0.7896, 0.9739
λ / Å	0.71073	0.71073
2θ range / deg.	2.64 – 30.92	2.74 – 27.96
Unique reflections	1496	1153
Reflection with $I \geq 2\sigma_I$	1353	1113
No. of parameters	117	159
GOF	1.064	1.001
R [for $I \geq 2\sigma_I$]	0.0257	0.0501
wR^2[for $I \geq 2\sigma_I$]	0.0626	0.1189

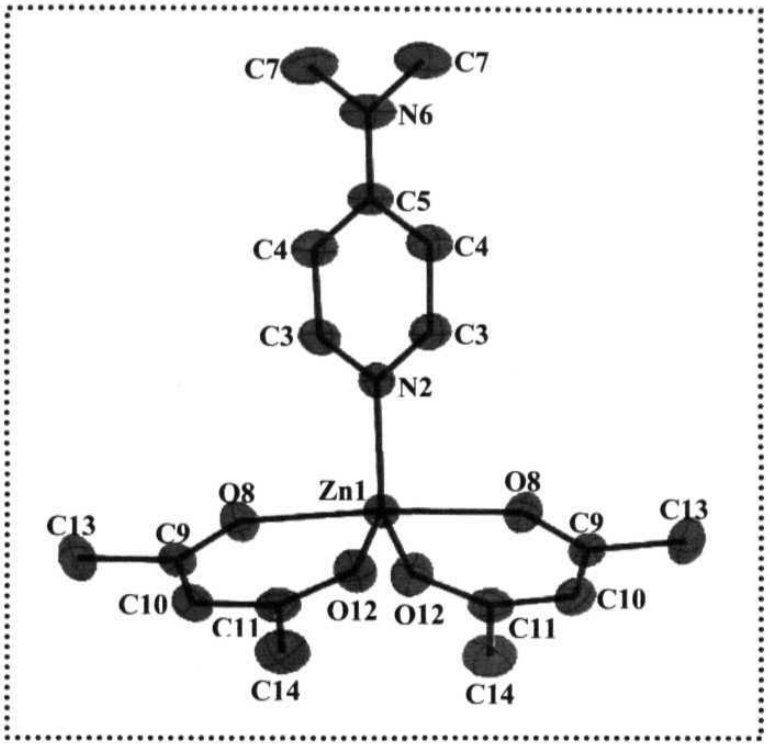

Figure 2.1 *Molecular structure of **ZNDA** from single crystal analysis. 95% probability thermal ellipsoids are indicated; H atoms are omitted for clarity.*

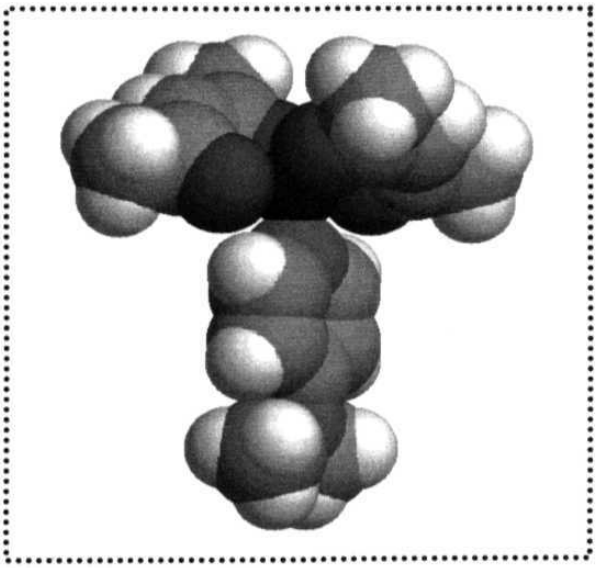

Figure 2.2 *Space-filling model of the molecular structure of **ZNDA** determined from single crystal analysis.*

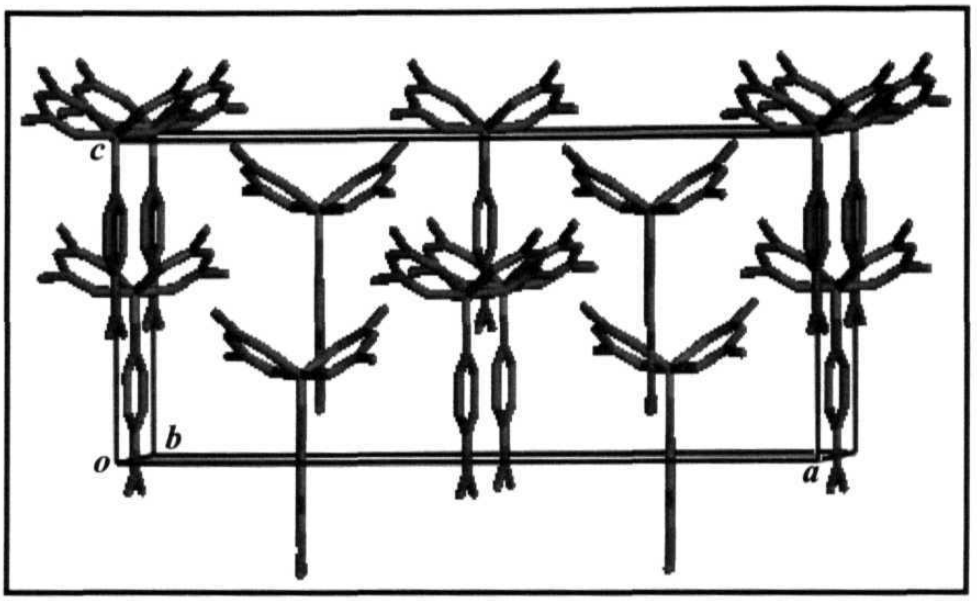

Figure 2.3 *View of the unit cell of **ZNDA** viewed along the b axis; H atoms are omitted for clarity.*

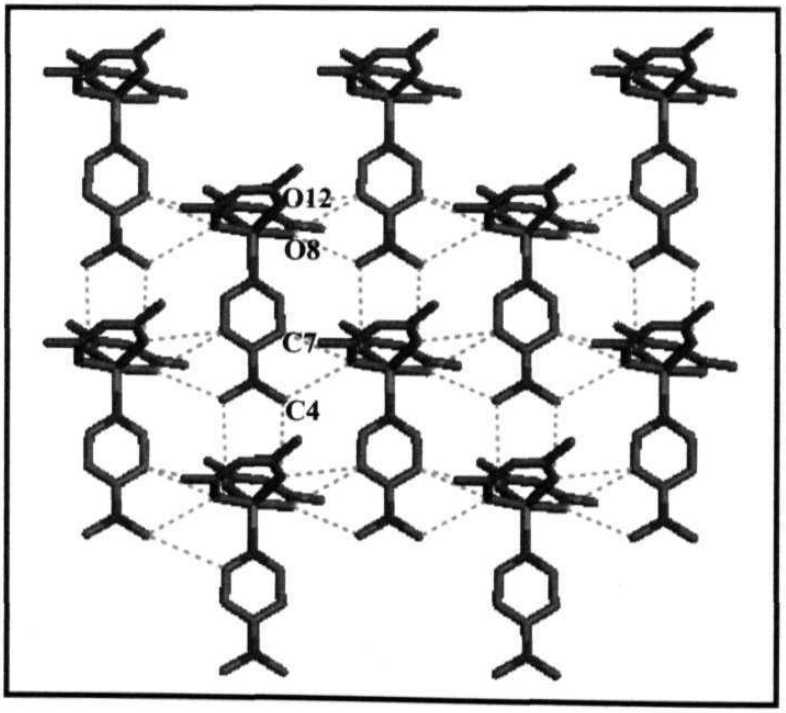

Figure 2.4 *Intermolecular close contacts (broken lines) in the sheets of **ZNDA** molecules in the bc plane; H atoms are omitted for clarity.*

molecules ($r_{C7...O12}$ = 3.679 Å; $\theta_{C7-H7B...O12}$ = 158.7°). A further network of weak intermolecular H-bonds ($r_{C4...O8}$ = 3.612 Å, $\theta_{C4-H4...O8}$ = 139.6°; $r_{C7...O8}$ = 3.526 Å, $\theta_{C7-H7A...O8}$ = 155.6°; $r_{C4...O12}$ = 3.585 Å, $\theta_{C4-H4...O12}$ = 151.0°) between DMAP and *acac* binds the ZNDA molecules into a sheet parallel to the *bc* plane (Fig. 2.4). The sheets are well separated in the *a*-direction with a distance of ~ 7 Å between adjacent DMAP planes (Fig. 2.5).

Neither strong nor even the weak bonding interactions present within the sheets are observed between the sheets. Thus the three-dimensional lattice structure of ZNDA is built from electrostatic interactions along the *c* axis and weak noncovalent interactions within the *bc* plane leading to sheet structures with no bonding recognition between the sheets in the *a* direction. This bulk organization can be viewed in terms of the Hulliger model[17] for the generation of polarity in supramolecular systems.

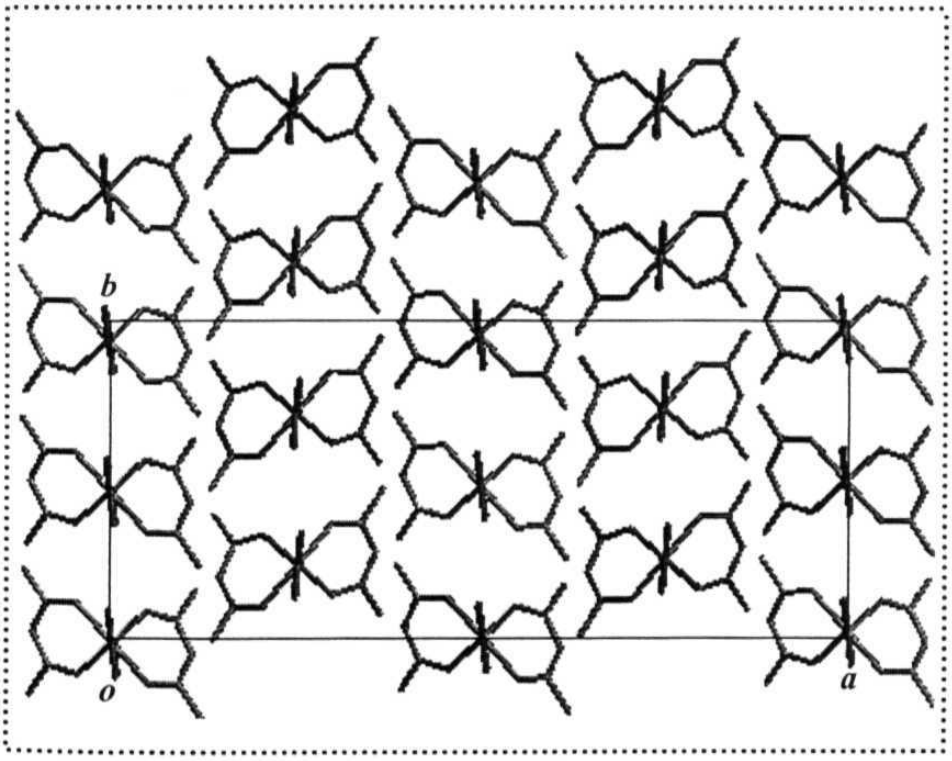

Figure 2.5 *Projection of the crystal lattice of* ***ZNDA*** *onto the ab plane; H atoms are omitted for clarity.*

ZNMPA

Crystals of ZNMPA grown from methanol are found to belong to the polar monoclinic space group, Cm with half a molecule in the asymmetric unit. The basic crystallographic data are presented in Table 2.1. The molecular structure is shown in Fig. 2.6. Zn(II) has similar distorted square-pyramidal coordination environment as found in

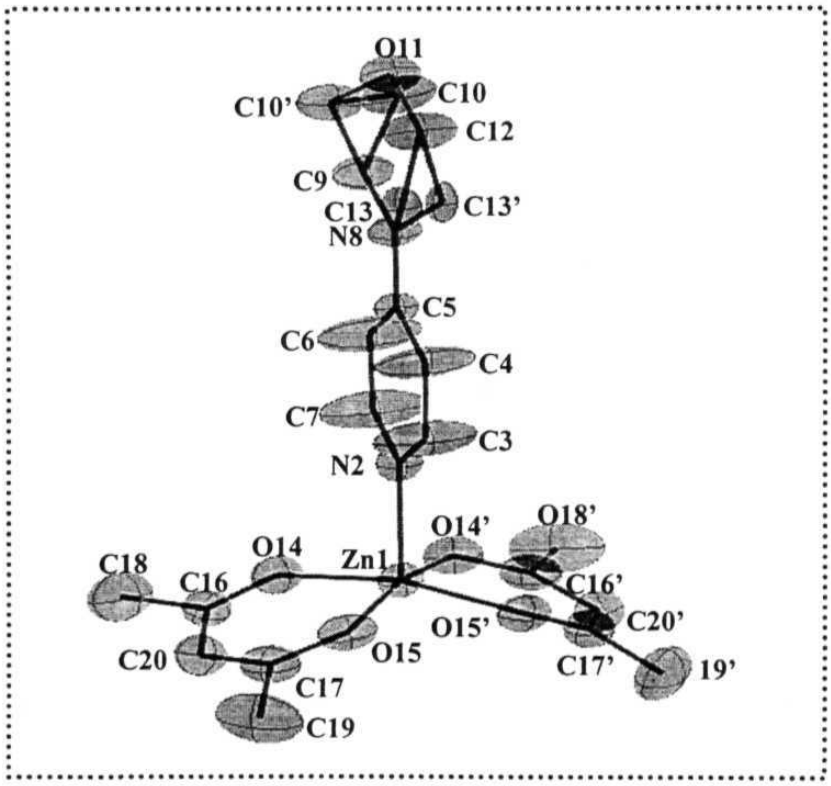

Figure 2.6 *Molecular structure of **ZNMPA** from single crystal analysis. 95% probability thermal ellipsoids are indicated. The disordered position of C10 and C13 are shown; H atoms are omitted for clarity.*

ZNDA. The space-filling model of the ZNMPA molecule clearly shows the 'screw'-shaped structure in this molecule as well (Fig. 2.7). Two carbon atoms of the morpholine ring in chair conformation show disorder due to ring flipping. The molecules assemble into a perfectly polar lattice with the molecular dipoles aligned along the [1 0 $\bar{1}$] direction (Fig. 2.8).

Similar to the situation in ZNDA, this can be analyzed in terms of the intermolecular interactions in the lattice. A weak coordinate bonding interaction between the morpholino oxygen and the zinc metal of the neighboring molecules ($r_{O11.....Zn1}$ = 2.628 Å) directs the head-to-tail chain formation. The polar chain is further supported by the weak intermolecular H-bonds between the morpholino carbon atoms and oxygen atoms of *acac* ligands ($r_{C12....O15}$, $r_{C10....O14}$ = 3.279, 3.366 Å) (Fig. 2.9). A further network of weak intermolecular H-bonds ($r_{C13....O14}$, $r_{C4....O15}$ = 3.402, 3.569 Å) between the morpholinopyridine and *acac* in the *ac* plane binds the ZNMPA molecules into a sheet structure. The lattice can be visualized in terms of the stacking of the polar sheets along the *b* direction. The mirror plane (*ac*) ensures that the sheets are oriented in the same direction. The sheets are well separated in the *b* direction with negligible interactions between ZNMPA molecules (Fig 2.10). The three-dimensional polar structure of ZNMPA is built from weak coordinate bonding as well as noncovalent interactions within the *ac* plane leading to sheet structures with no bonding recognition

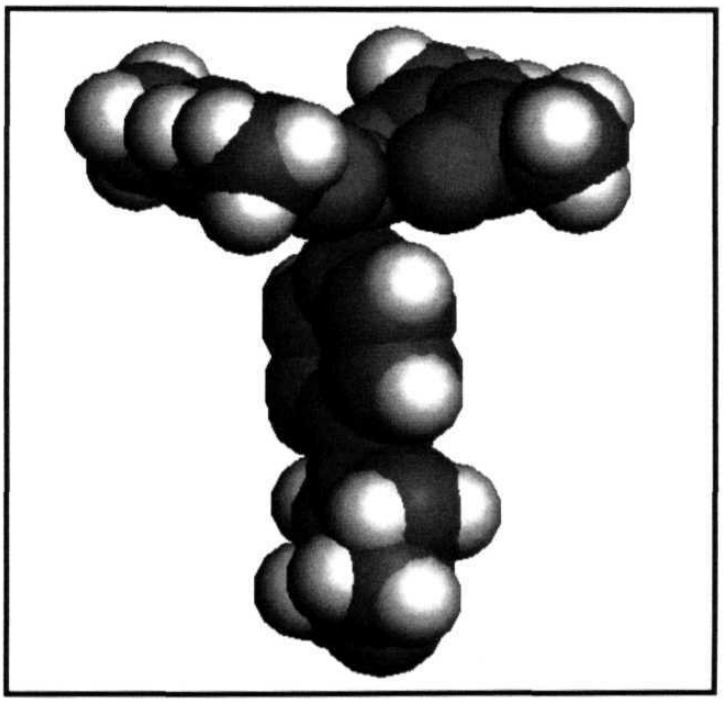

Figure 2.7 *Space-filling model of the molecular structure of* ***ZNMPA*** *determined from single crystal analysis; only one of the (disordered) conformation of cyclohexane is shown.*

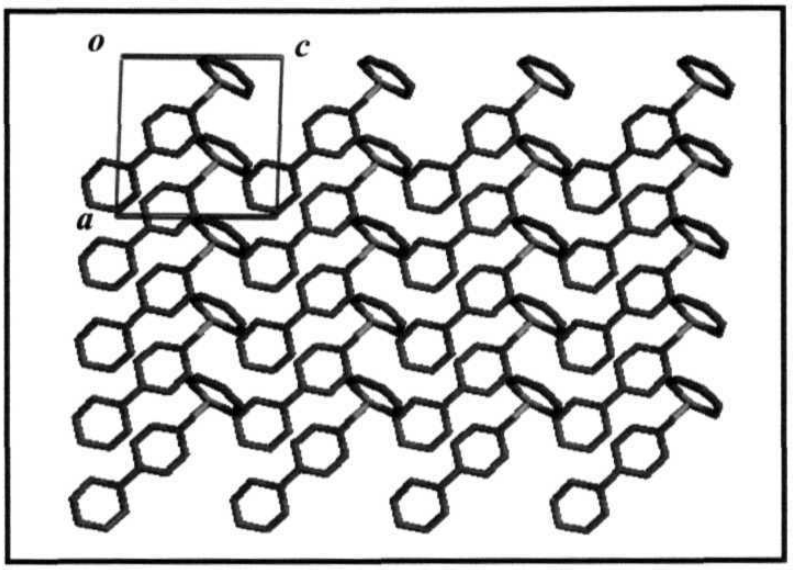

Figure 2.8 *Perfectly polar assembly of molecules in crystals of **ZNMPA** viewed along b-axis; H atoms, the methyl C atoms of the acac ligand and the disordered positions of two C atoms in the morpholine group are omitted for clarity.*

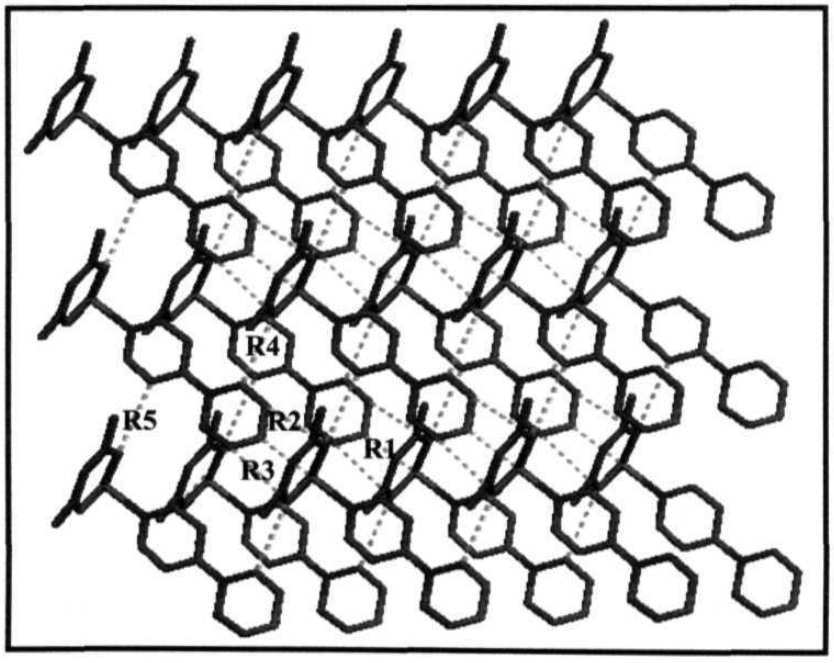

Figure 2.9 *Intermolecular close contacts (broken lines) in **ZNMPA** crystal lattice (R1 = 2.628, R2 = 3.279, R3 = 3.366, R4 = 3.402, R5 = 3.569 Å) .*

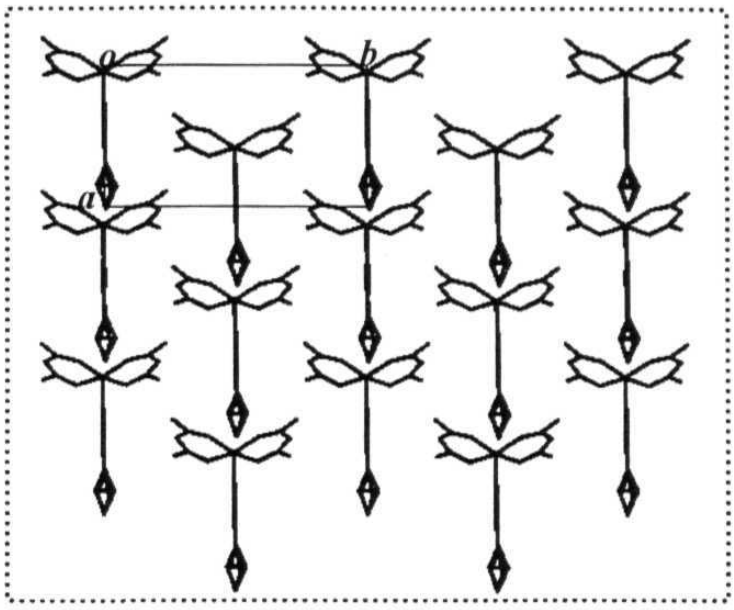

Figure 2.10 *Projection of the crystal lattice of **ZNMPA** onto the ab plane; H atoms, the methyl C atoms of the acac ligand and the disordered position of the two C atoms in the morpholine group are omitted for clarity.*

between the sheets in the *b* direction. It once again establishes the tendency of this family of molecules to form polar assemblies without the assistance of counterions, cocrystallization partners or a host lattice. As noted earlier, the model for polarity generation developed by Hulliger and coworkers[13,17] provides a basis to understand the perfectly polar assemblies of these 'screw'-shaped molecules in the crystal lattice.

2.4 EXTREME ORIENTATIONS OF DIPOLAR MOLECULES IN DIMORPHIC STRUCTURES OF ZNPPA

The process of crystallization is of great scientific and technological importance because the resulting crystal structures largely determine the solid state properties,[22] the electronic, magnetic and optical attributes of materials. Molecules often adopt different packing arrangements that are close in energy leading to polymorphic crystal structures.[23] Organization of molecules in crystals results from a complex, often subtle interplay of

intermolecular interactions, making accurate *ab initio* prediction of crystal structures, a very difficult proposition.[24] The problem is considerably compounded in the case of polymorphic structures where, even under apparently identical conditions as in concomitant polymorphs,[25] the same molecule organizes in different crystalline assemblies. Particularly intriguing would be the case of polymorphs which manifest grossly different packing motifs. Such a situation could, in principle be encountered in the context of centrosymmetric and noncentrosymmetric polymorphic structures of dipolar molecules, the latter being of potential interest in quadratic nonlinear optical applications.[26] Though several instances of such polymorphism are known,[27] noncentrosymmetric lattices often involve small deviations from a centrosymmetric organization,[28] leading to descriptions such as 'approximately centrosymmetric'.[27] Optimal molecular orientations for applications like phase-matched second harmonic generation or electro-optic effect call for specific design strategies.[29,11]

A case that merits special attention is the formation of perfectly polar molecular assemblies[30,14,15] as described in the previous section. Such a situation where the molecules make exactly 0^{o} angle with respect to a specific crystallographic direction would be the opposite extreme of the commonly encountered centrosymmetric formation,[9] which by analogy can be described as constituted of 'perfectly antiparallel' molecular dipoles with equal numbers making 0^{o} and 180^{o} angles with respect to a specific crystallographic direction. Even though, polymorphism has been extensively studied in supramolecular chemistry, cases of such extreme molecular organizations in polymorphic structures are rare. One case that we are aware of is that of the dithiadiazolyl radical.[31]

During our investigation of the perfectly polar compounds, we have observed that (4-pyrrolidinopyridyl)bis(acetylacetonato)zinc(II) (ZNPPA) shows extreme molecular orientation of dipoles in dimorphic structures.[32] ZNPPA forms perfectly polar as well as centrosymmetric crystal structures depending sensitively on the solvent and the rate of crystallization. We have carried out semiempirical computational modeling of molecular clusters, incorporating solvation effects, to understand the energies involved in the solvent polarity preference of the extreme structures. We have observed an interesting cogrowth of the dimorphic structures as well as formation of twin polar domains in

monolithic crystals of ZNPPA. This observation suggests the possibility of realizing novel multidomain crystal architectures.

Crystal Structure Investigations : Role of the solvent and rate of crystallization in the formation of the dimorphic structures and multidomain crystals

ZNPPA was synthesized by mixing methanolic solutions of 4-pyrrolidinopyridine and $Zn(acac)_2.H_2O$. The microcrystalline powder showed clear SHG, suggesting that the molecules are assembled in a noncentric lattice structure. However the crystals of ZNPPA grown by slow cooling and evaporation of methanol solution were SHG inactive and found to belong to the centrosymmetric space group, C2/c; we will refer to this structure as ZNPPA1. The basic crystallographic data are collected in Table 2.2. The molecular structure of ZNPPA1 is shown in Fig. 2.11. Zn(II) has distorted square-pyramidal coordination with normal bond parameters[19] as found in ZNDA and ZNMPA. Weak intermolecular H-bonds between the pyrrolidino carbons and *acac* of the neighboring molecules are observed in the polar chains formed along the *b*-axis. A further network of weak intermolecular H-bonds between 4-pyrrolidinopyridine and *acac* binds the ZNPPA1 molecules into a sheet parallel to the *ab* plane (Fig. 2.12). Adjacent sheets are oriented in opposite directions leading to a centrosymmetric structure (Fig. 2.13).

The structure of ZNPPA1 was surprising since the perfectly polar crystals of the similar molecules, ZNDA and ZNMPA were grown from methanol and microcrystals of ZNPPA precipitated from methanol showed SHG. Semiemprical AM1 calculation[20] on the molecular geometry taken from the respective crystal structures indicated that the dipole moment of ZNPPA (9.53 D) is higher than that of ZNDA (8.92 D). This suggested that the stronger dipole-dipole interactions in the case of ZNPPA might be screened more effectively in a solvent more polar than methanol. Slow evaporation of methanol-water (80:20) solutions of ZNPPA yielded crystals with two morphologies - nearly square plates and prismatic blocks in approximately 2:1 weight ratio. X-ray analysis of the square plates showed that they were ZNPPA1 crystals. Single crystal

studies of the prismatic blocks showed that they posses a new crystal structure belonging to the noncentrosymmetric space group, Fdd2; we refer to this polymorph as ZNPPA2. The basic crystallographic data are collected in Table 2.2. The molecular structure is

Table 2.2 *Crystallographic data for **ZNPPA1** and **ZNPPA2***

Identification code	**ZNPPA1**	**ZNPPA2**
Empirical formula	$C_{9.5}H_{13}NO_2Zn_{0.5}$	$C_{9.5}H_{13}NO_2Zn_{0.5}$
Formula weight	205.89	205.89
Crystal system	Monoclinic	Orthorhombic
space group	C2/c (No.15)	Fdd2 (No.43)
a / Å	10.994(6)	11.1810(8)
b/ Å	12.322(12)	28.583(3)
c / Å	15.365(15)	12.3090(10)
β / deg.	104.93(6)	90.0
V / Å^3	2011.0(3)	3933.8(6)
Z	8	16
$\rho_{calc.}$ / g cm^{-3}	1.360	1.391
μ, cm^{-1}	1.24	1.27
T_{min}, T_{max}	0.841, 0.999	0.929, 0.999
λ / Å	0.71703	0.71703
2θ range / deg.	2.53 - 25.97	2.56 - 24.96
No. of unique reflections	1971	905
No. of reflections with $I \geq 2\sigma_I$	1753	839
No. of parameters	120	120
GOF	1.125	0.963
R [for $I \geq 2\sigma_I$]	0.0329	0.0300
wR^2[for $I \geq 2\sigma_I$]	0.1106	0.0993

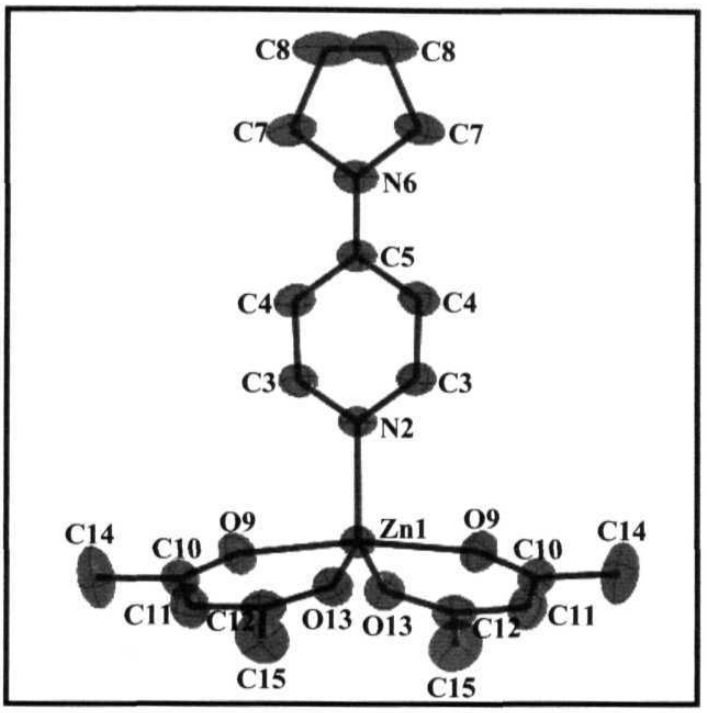

Figure 2.11 *Molecular structure of **ZNPPA** from single crystal analysis. 95% probability thermal ellipsoids are indicated; H atoms are omitted for clarity.*

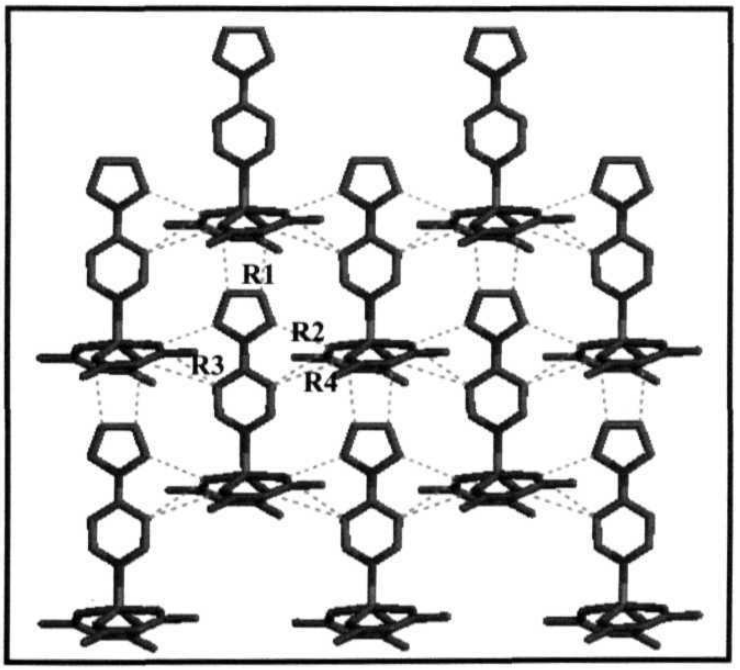

Figure 2.12 *Intermolecular close contacts (broken lines) leading to polar sheets in the ab plane of **ZNPPA1** crystal (R1 = 3.580, R2 = 3.356, R3 = 3.670, R4 = 3.610 Å) .*

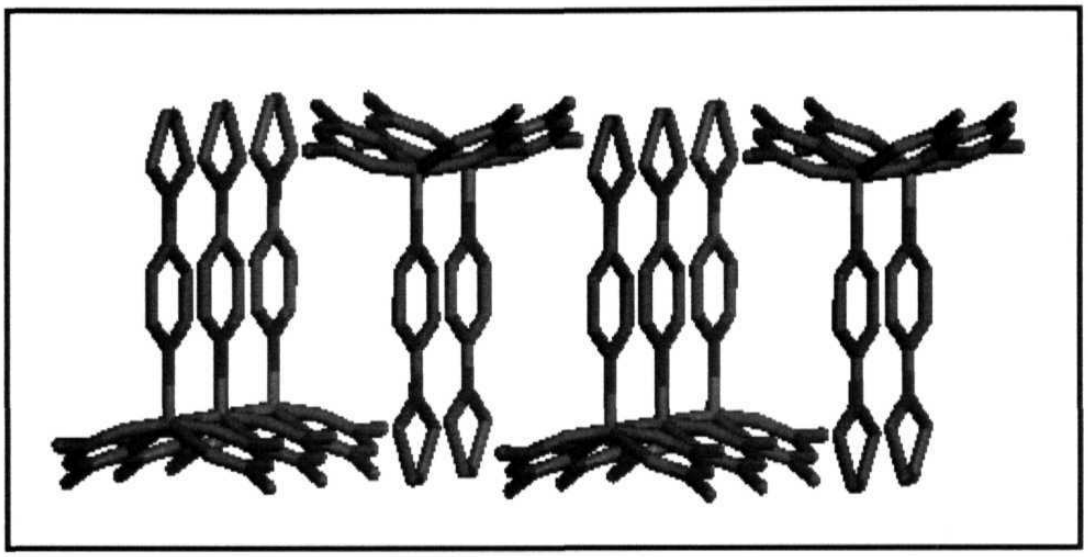

Figure 2.13 *Centrosymmetric assembly of molecules in **ZNPPA1**; H atoms are omitted for clarity.*

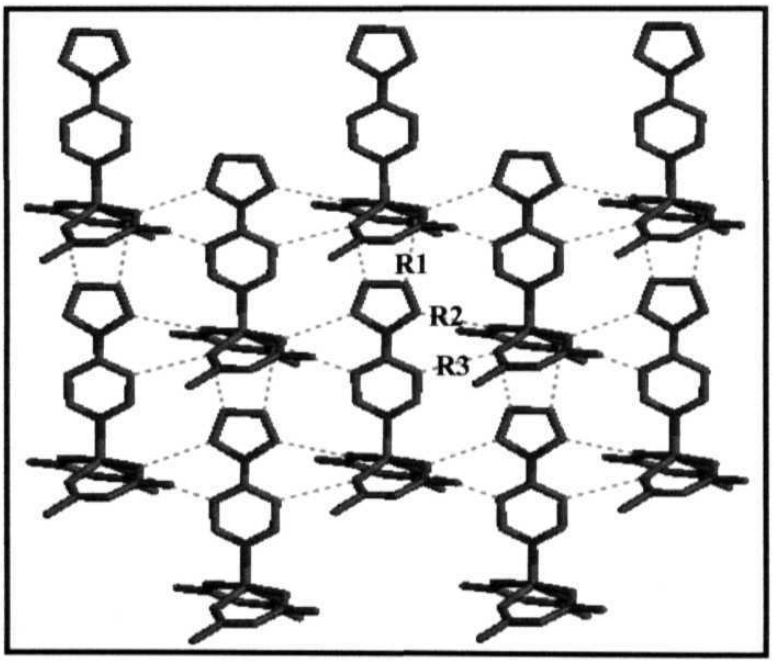

Figure 2.14 *Intermolecular close contacts (broken lines) leading to polar sheets in the ac plane of **ZNPPA2** crystal lattice (R1 = 3.463, R2 = 3.400, R3 = 3.551 Å) .*

nearly identical to that observed in ZNPPA1. Weak intermolecular H-bonding networks between the pyrrolidinopyridine and *acac* ligand of the neighboring molecules leads to the polar sheet parallel to the *ac* plane (Fig 2.14). The sheets are well separated along the *b* axis. More significantly, the adjacent sheets assemble in a parallel fashion along the *b* direction and lead to the perfectly polar organization with all molecular dipoles aligned along the *c* axis (Fig. 2.15).

Crystals of ZNPPA1 and ZNPPA2 possess very similar two-dimensional formations of ZNPPA molecules in the *ab* and *ac* planes, respectively, bound through weak intermolecular interactions; the molecular dipoles are aligned parallel within the sheets. The critical differentiation between the two crystal packings arises at the level of organization of these molecular sheets, with net macroscopic dipole of adjacent sheets antiparallel in ZNPPA1 and parallel in ZNPPA2. The extreme molecular orientation of dipoles exhibited by the dimorphic structures (Fig. 2.16a) is illustrated by the linear array of molecules that may be envisioned using one from each sheet (Fig. 2.16b). ZNPPA2 is one more entry to the series of perfectly polar structures.

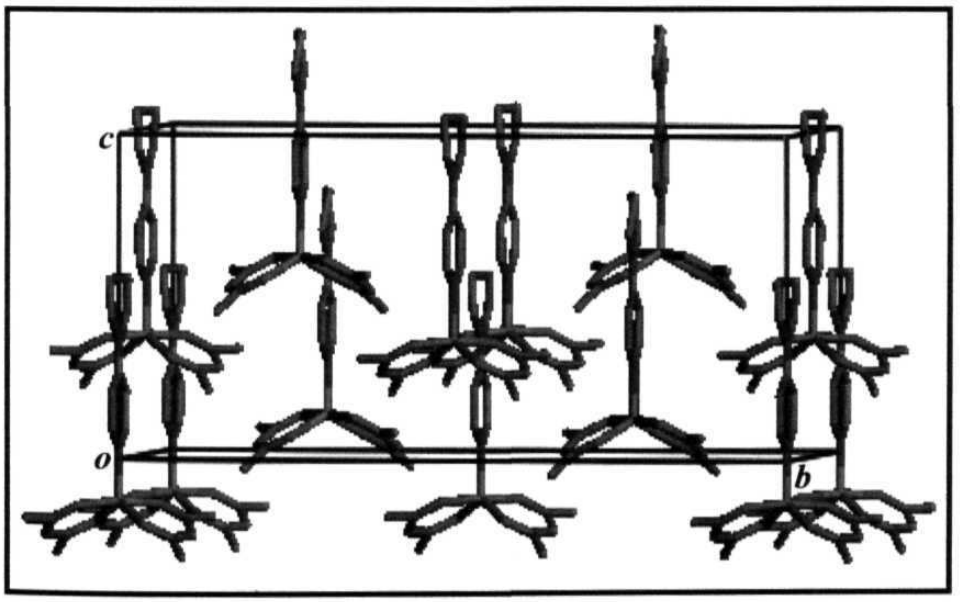

Figure 2.15 *Unit cell of **ZNPPA2** viewed approximately along the a axis; H atoms are omitted for clarity.*

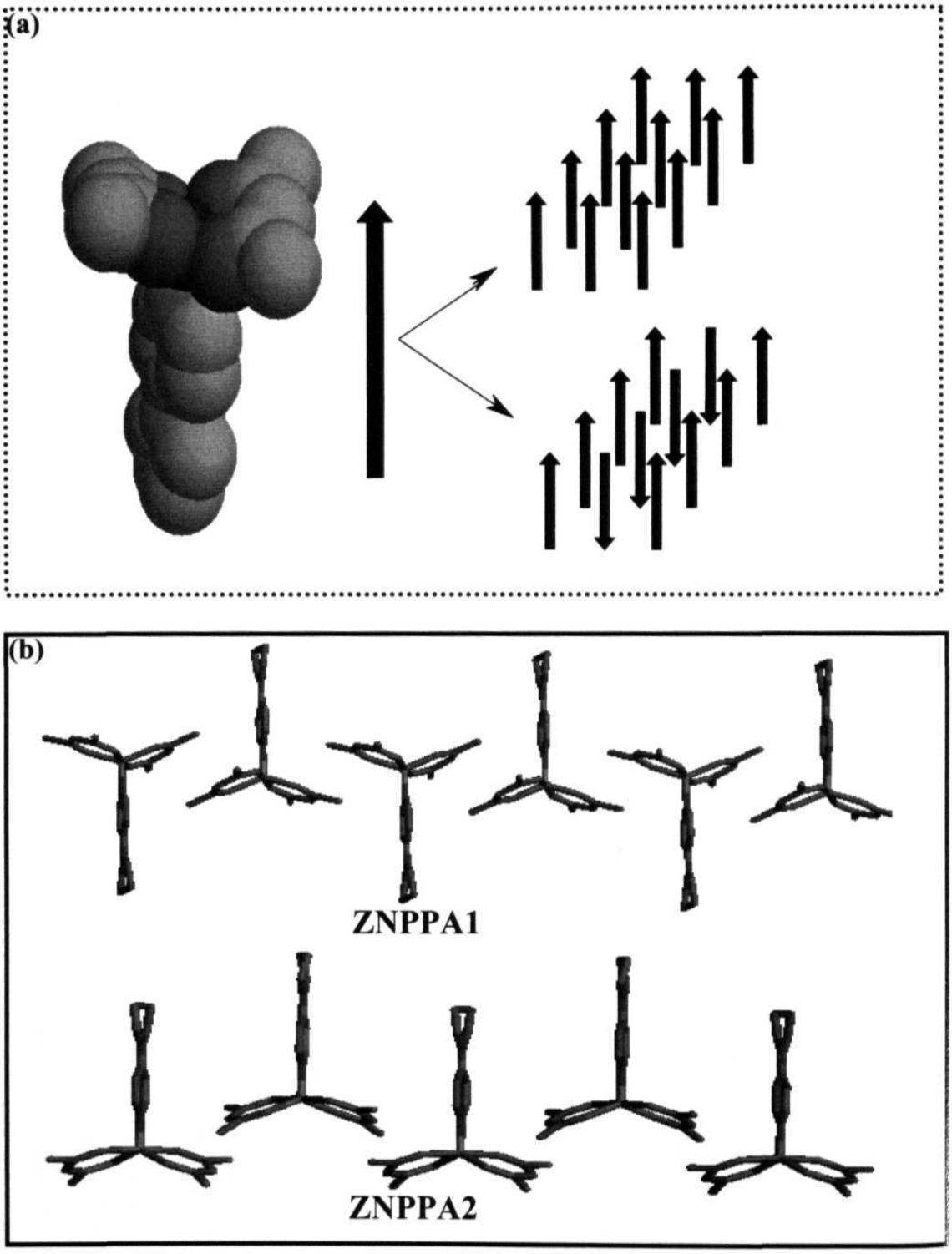

Figure 2.16 *Extreme orientations of molecular dipoles in **ZNPPA1** and **ZNPPA2** lattices (a) schematic view; (b) view from crystal structure analysis.*

We have systematically explored the conditions promoting the formation of ZNPPA1 and ZNPPA2 in different solvent polarity environment. ZNPPA obtained by the direct addition of its components in methanol is inferred to be ZNPPA2, based on the SHG observed as well as the comparison of the powder x-ray diffractogram of the microcrystalline sample with the pattern simulated using the ZNPPA2 crystal structure (Fig. 2.17). However, as noted earlier, slow crystallization of ZNPPA2 from methanol yielded exclusively ZNPPA1; these crystals have nearly square plate morphology. The

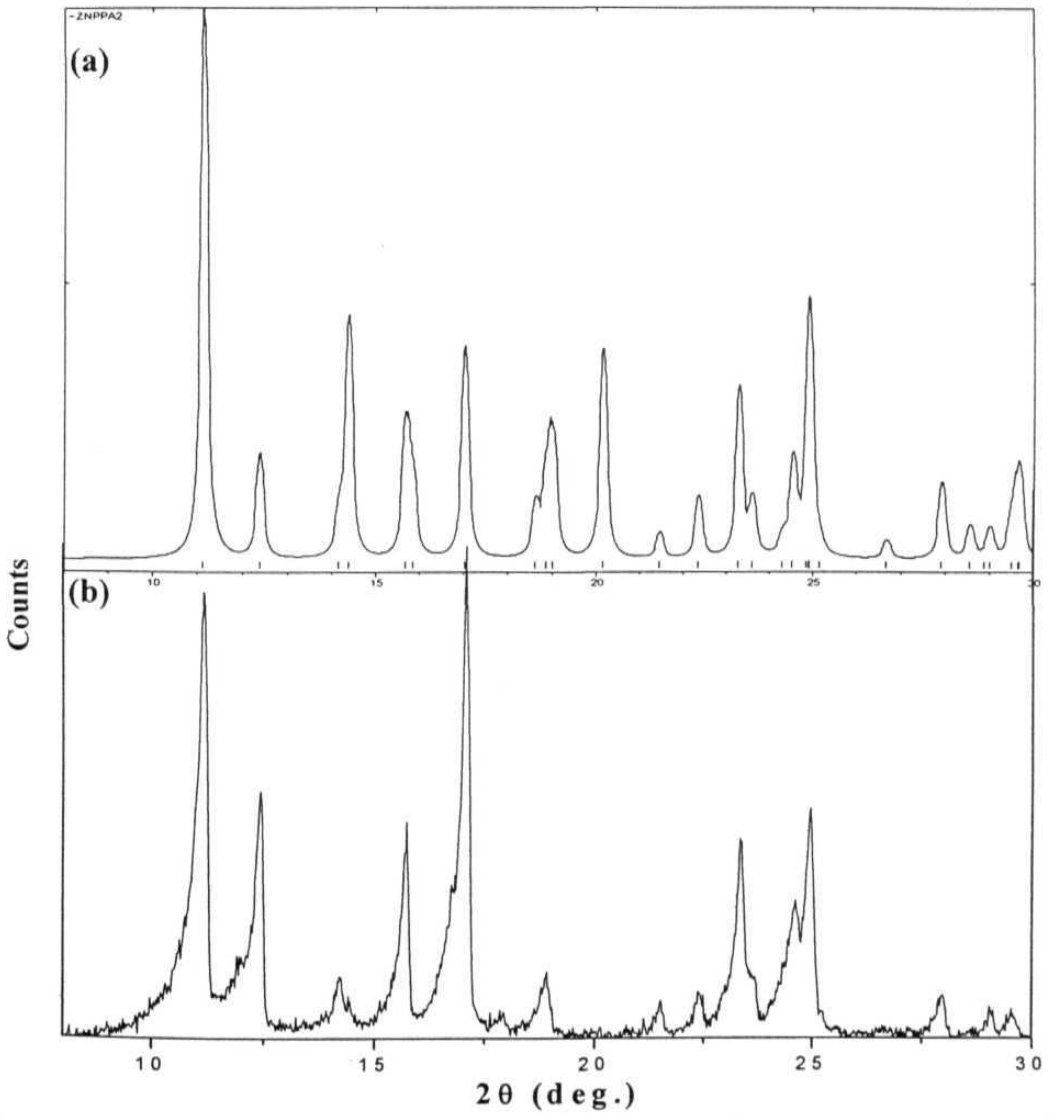

Figure 2.17. *Powder x-ray diffractogram of **ZNPPA2** (a) simulated from single crystal structure (b) recorded for microcrystalline sample obtained by direct addition of 4-pyrrolidinopyridine and $Zn(acac)_2.H_2O$ in methanol.*

exclusive formation of ZNPPA1 polymorph from methanol was also confirmed by the comparison of powder x-ray diffractogram with the pattern simulated using ZNPPA1 crystal structure (Fig. 2.18). Crystals grown from chloroform-toluene were also found to be ZNPPA1. This suggests that the formation of ZNPPA2 is promoted in more polar solvents. Since water-methanol mixture yields a mixture of the dimorphs as stated

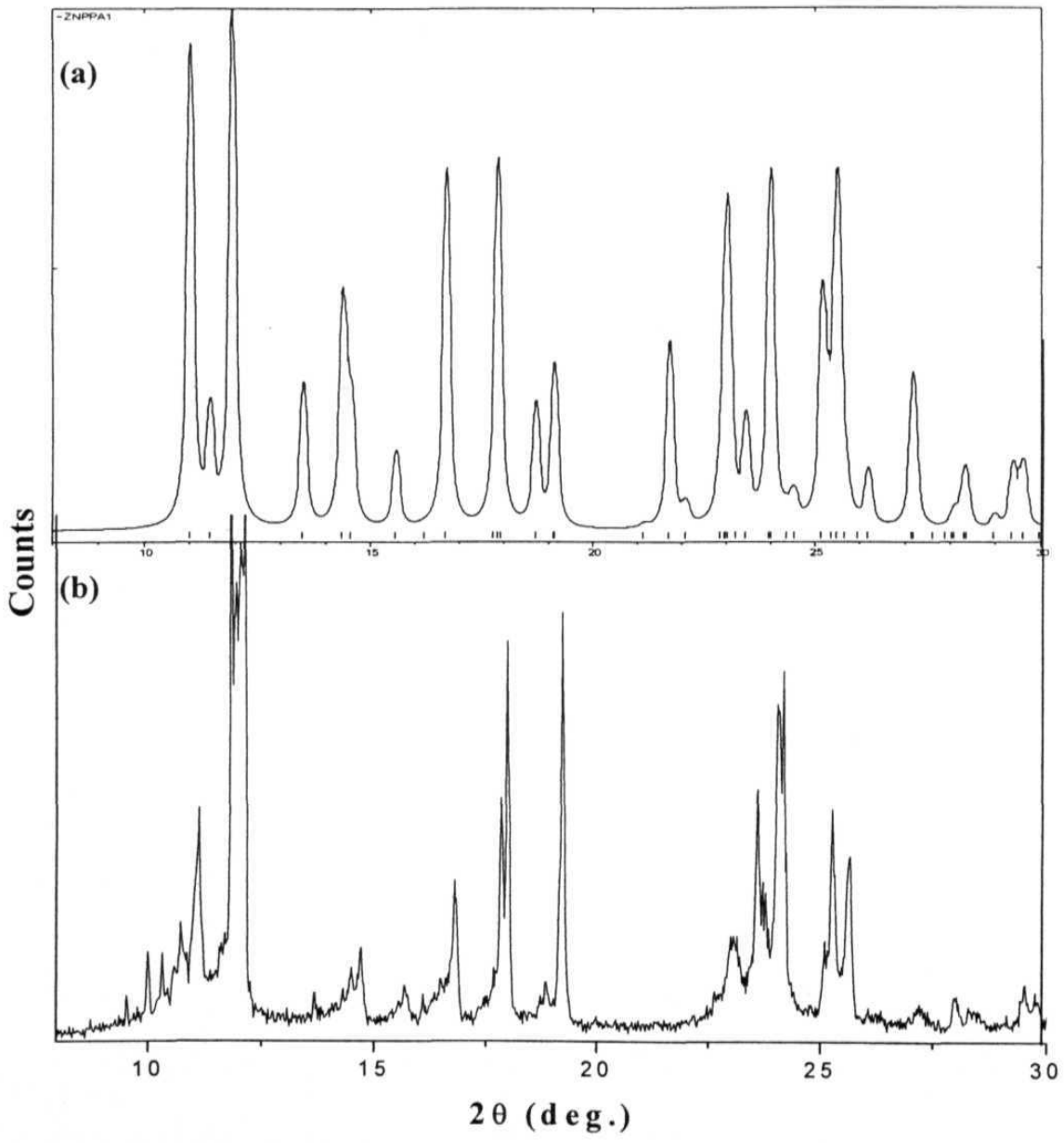

Figure 2.18. *Powder x-ray diffractogram of **ZNPPA1** (a) simulated from single crystal structure (b) recorded for microcrystals sample of ZNPPA1 obtained by recrystallization from methanol.*

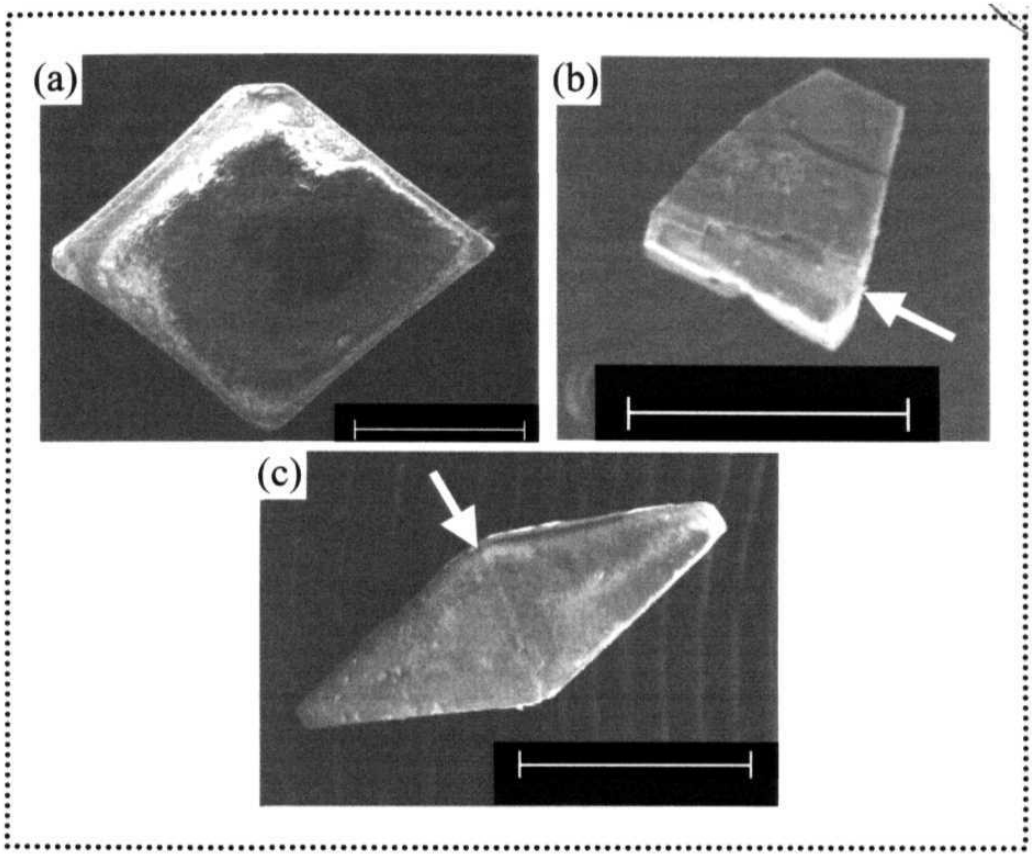

Figure 2.19 *Morphology of ZNPPA crystals : **(a)** centric (ZNPPA1) from methanol, **(b)** polar/centric from DMSO and **(c)** polar/polar from chloroform-DMSO. The scales indicate 500 μm and the arrows, the boundary between the domains.*

earlier, and ZNPPA has negligible solubility in pure water, we have investigated the use of DMSO as the solvent for crystallization. Fast precipitation by cooling produces SHG inactive material suggesting that ZNPPA1 is obtained. However, slow evaporation of dilute solutions yielded crystals of ZNPPA1 as well as new crystals of an unusual morphology (Fig. 2.19), which could not be indexed satisfactorily (the latter was approximately 25% by weight). However, this crystal can be smoothly cleaved to separate the cuboid and truncated pyramidal halves. Interestingly, the two domains could be independently indexed to the unit cells of ZNPPA1 and ZNPPA2 respectively, proving that the crystals from DMSO are indeed composite monoliths comprising of the extreme dimorphs. The cleavage plane corresponds to the (001) and (010) planes of the two

Table 2.3 *Crystallization condition and the polymorph of* ***ZNPPA*** *obtained; multidomain crystals are indicated with a slash.*

Crystallization condition		Polymorph
Solvent	**Rate**	
Methanol*	Fast / Slow	ZNPPA1
$CHCl_3$-Toluene	Slow	ZNPPA1
Methanol-Water	Slow	ZNPPA1, ZNPPA2
DMSO	Fast	ZNPPA1
DMSO	Slow	ZNPPA1, ZNPPA1 / ZNPPA2
$CHCl_3$-DMSO	Slow	ZNPPA2 / ZNPPA2
$CHCl_3$-NMP	Slow	ZNPPA1, ZNPPA2 / ZNPPA2

*Direct synthesis of ZNPPA in methanol provides ZNPPA2, but only as microcrystals

crystals respectively which have a close registry as seen from the unit cell lengths (Table 2.2). When crystals of ZNPPA are grown from chloroform-DMSO mixture, a still different morphology is obtained. The different morphologies of the crystals are shown in Fig. 2.19. The bipyramidal crystal again could not be indexed as a whole, but when cleaved at the middle, the two parts could be indexed to ZNPPA2 crystal with the cleavage plane corresponding to (010). Crystals grown from chloroform-NMP mixture gives square plate (ZNPPA1) as well as bipyramidal (ZNPPA2) morphologies. The different crystallization conditions and the types of polymorphs formed are summarized in Table 2.3. It may be noted that the cogrowth of centric/polar domains exhibited by ZNPPA is different from situations such as statistical twinning[33] where the demarcation of the polymorphic domains is not well defined and lamellar twinning involving mirror image domains of enantiomorphic molecules,[34] where the molecular packing in the two domains are identical.

Semiempirical Computational Modeling of Molecular Clusters of ZNPPA1 and ZNPPA2

It is important to note that neither of the structures, ZNPPA1 and ZNPPA2, includes solvent molecules in the lattice. This has enabled us to compare the energetics of supramolecular assembly at the level of small clusters, which lead to the extreme cases of three-dimensional organization. The utility of such an approach in modeling the polymorphism of some nitroaniline derivatives have been demonstrated earlier.[35] AM1 computations were carried out on molecular clusters (dimers to octamers) extracted from the crystal structures; H atom positions alone were optimized. The solvent environment during the crystallization was mimicked[35,36] using the COSMO option;[37] calculations employed dielectric constants of methanol and water representing environments with

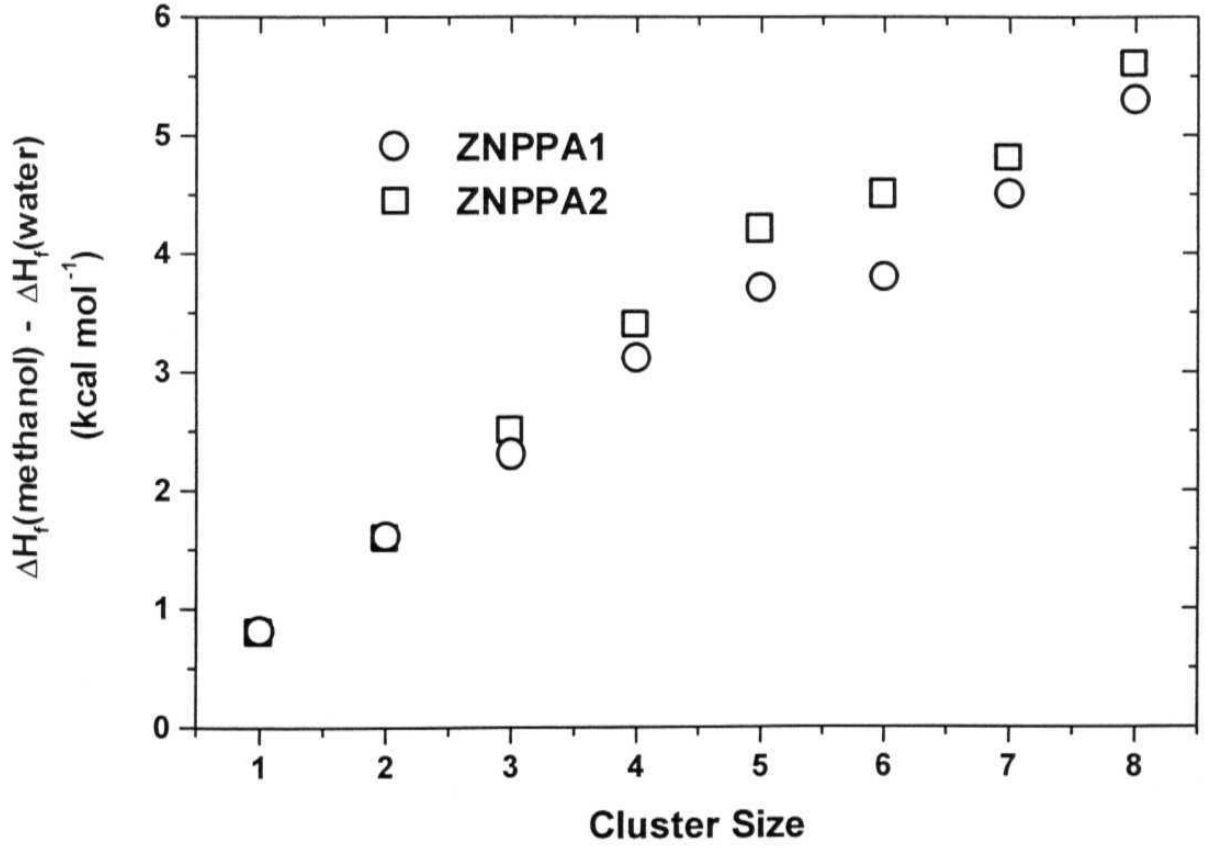

Figure 2.20 *AM1/COSMO computed enthalpies of formation (in water vs. methanol) of various molecular clusters of* ***ZNPPA1*** *and* ***ZNPPA2****.*

different polarities. The clusters from both the structures show higher stabilization in the more polar environment; however, the relative stabilization is slightly enhanced for ZNPPA2 compared to ZNPPA1 (Fig. 2.20). This suggests that even though the higher polarity preference of ZNPPA2 clusters is marginally more, solvent polarity control of the formation of the apparently extreme motifs in ZNPPA1 and ZNPPA2 are very closely balanced. Comparison of the enthalpies of formation of similar size clusters from the dimorphic structures in either solvent indicates that ZNPPA1 is always stabilized over ZNPPA2. The formation of both structures in water-methanol as well as DMSO, therefore suggests that thermodynamic factors alone do not determine the dimorph formation. It is interesting however, that ZNPPA1 is the major product in most of the cases (Table 2.3).

2.5 SHG STUDIES ON MICROCRYSTALLINE POWDERS OF ZNDA, ZNMPA AND ZNPPA2

ZNDA, ZNMPA and ZNPPA molecules possess a 'push-pull' electronic system with the amino group as the donor and the pyridinium unit involving the electropositive metal as the acceptor. AM1/TDHF[38] calculations using the molecular geometry from crystal structures show a static hyperpolarizability of $\sim 4 \times 10^{-30}$ esu for these molecules. Even though the hyperpolarizabilities are small and the polar organization is not the optimal arrangement[39] for SHG, the noncentrosymmetric organization of molecules in the crystal lattice of ZNDA, ZNMPA and ZNPPA2 is expected to lead to solid state SHG in these materials. These compounds are found to have good thermal stability and stability towards laser radiation (at a power of $\sim$ 1 GW cm^{-2}). SHG from microcrystalline powders was examined using the Kurtz-Perry[40] technique. Details of the experiment are provided in Appendix C. Table 2.4 presents the powder SHG of ZNDA, ZNMPA and ZNPPA2 at various particle sizes. The particle size dependence of SHG indicates phase-matchable behavior of these materials.

Table 2.4 *SHG of microcrystalline powders of* ***ZNDA, ZNMPA*** *and* ***ZNPPA2*** *at different particle sizes. 1 U = SHG of urea having particle size > 150 μm.*

Compound	SHG (U)				
	Particle size (μm)				Average value at saturation
	100-150	150-200	200-250	250-300	
ZNDA	0.92	0.91	1.02	1.26	1.00
ZNMPA	0.93	1.21	1.30	1.26	1.12
ZNPPA2	0.86	0.89	0.95	1.19	0.96

2.6 FABRICATION OF THIN FILMS WITH UNIAXIALLY ORIENTED MICROCRYSTALLITES AND OPTICAL SHG STUDIES

Acentric supramolecular assemblies of dipolar molecules are potential candidates for a multitude of information-processing and photonic applications, such as high speed electro-optic modulation, optical switches, and nonlinear optical waveguides for integrated frequency conversion.[41] The desirable characteristics of thin films for frequency conversion and telecommunication applications are the following. (i) They must be noncentrosymmetric showing strong second order NLO effects, (ii) their thickness must be of the order of one micrometer, able to support waveguiding, (iii) they must be homogenous and of good optical quality over large areas of the order of square centimeters, and iv) they must have good photostability.

Thin films of dipolar molecules with noncentrosymmetric ordering have been grown using techniques such as LB[42] and self-assembled monolayer[43] method. The drawbacks of these approaches are that they are time consuming processes and the final material is usually fragile since the assembly is principally by van der Waals interactions.[42] Vapor phase depositions techniques offer the advantages of high growth

rates, good chemical purity due to vacuum conditions, *in-situ* growth monitoring, and layer thickness control.[44] Thin films with oriented crystallites have been fabricated by sublimation onto oriented PTFE[45] and cleaved single crystals[46] and by mechanical dragging procedures.[47] Günter and coworkers have used organic molecular beam deposition process to grow films of H-bonded molecules with preferred orientations.[48] Oriented crystallites and thin films of NLO-phores have been fabricated through vapor phase assembly on functionalized substrates.[49]

In the previous sections we have described the novel, single component perfectly polar supramolecular organization of simple metal-organic compounds in crystals. In addition to possessing good optical transparency ($\lambda_{cut\text{-}off} < 330$ nm), these materials have good thermal stability and can be sublimed without decomposition. We envisaged that they would be ideal candidates for thin film assembly through vapor deposition on glass substrates. Examination of ZNDA, ZNPPA and ZNMPA showed that, not only is the perfectly polar crystal structure maintained in the thin films, but additionally the crystallites in the film show orientational ordering with respect to the substrate normal. Oriented crystallite growth through the vapor phase assembly on amorphous substrates is driven by intermolecular interactions rather than substrate control and hence is especially interesting from a molecular materials perspective. Distance of the substrate from the sublimation boat plays a critical role in effecting the crystallite orientation. Interestingly, ZNPPA films show the presence of both the dimorphic forms, ZNPPA1 and ZNPPA2. Morphology of the thin films were investigated by scanning electron microscopy (SEM). Polarization dependence of SHG is in agreement with the uniaxial orientational ordering of the crystallites in the films.[45]

Thin Film Fabrication and X-ray Diffraction Studies

Microcrystalline powder of the compound to be sublimed was taken in a molybdenum boat. The glass substrate for deposition was cleaned by sonication in methanol followed by acetone and dried in oven at 100 °C for 1 h. Pressure inside the vacuum chamber was maintained at ~ 10^{-6} mbar. Sublimation was achieved using typically 25 A current. The schematic diagram of sublimation set up is shown in Fig.

2.21. Different positions of the substrate, on and away from the normal to the sublimation boat were explored;[48] the position directly above the boat was found to be the most suitable for obtaining oriented crystallites. Distance of the substrate from the sublimation boat was found to be the critical factor for effecting the crystallite orientation. We have checked the films for any signs of decomposition. The microcrystalline powders obtained by scratching the films off the substrate show the full diffraction pattern expected from the crystal structure of the material indicating that no chemical or crystallographic alterations occur during the fabrication process. The ir spectrum of the sublimed material also was consistent with that of the original compound.

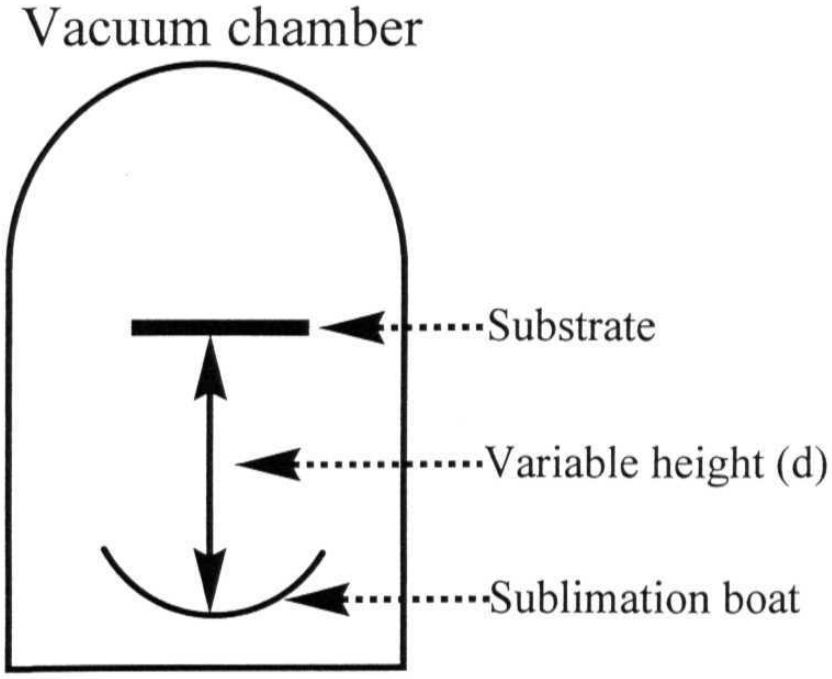

Figure 2.21 *Schematic diagram of the sublimation setup*

Thin films were fabricated by placing the substrate at different distances directly above the sample and its structural ordering was probed by x-ray diffraction. X-ray diffractogram of ZNDA film grown at different distances is shown in Fig. 2.22a. Comparison of the diffractogram to the pattern simulated using the single crystal structure of ZNDA (Fig. 2.22c) shows that the films show a high degree of crystallite orientational ordering. When the substrate is at the optimal distance of 5 cm, the film

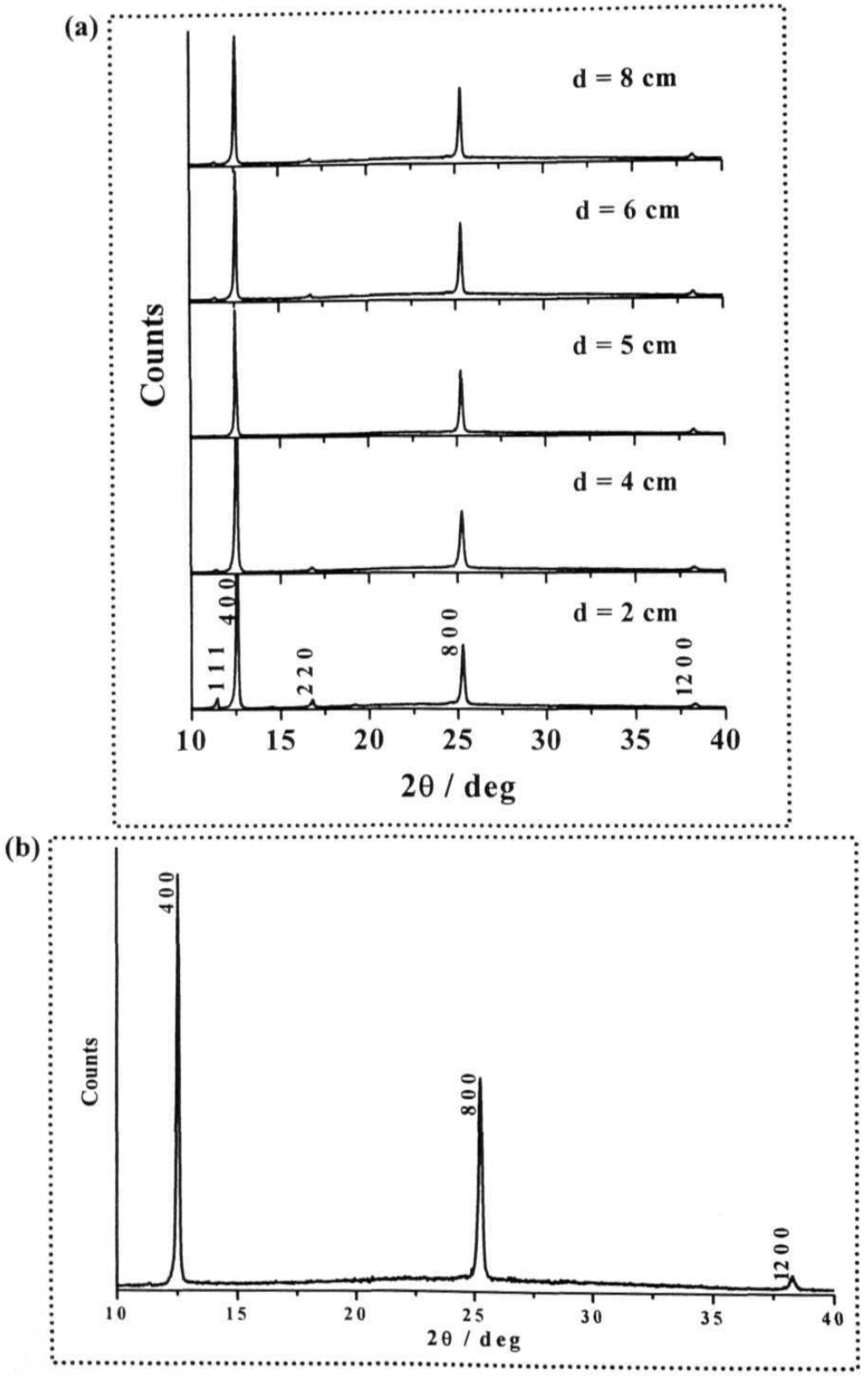

Figure 2.22 *X-ray diffractograms of **ZNDA** thin film fabricated at (a) different boat-substrate distances, d and (b) at d = 5 cm (enlarged).*

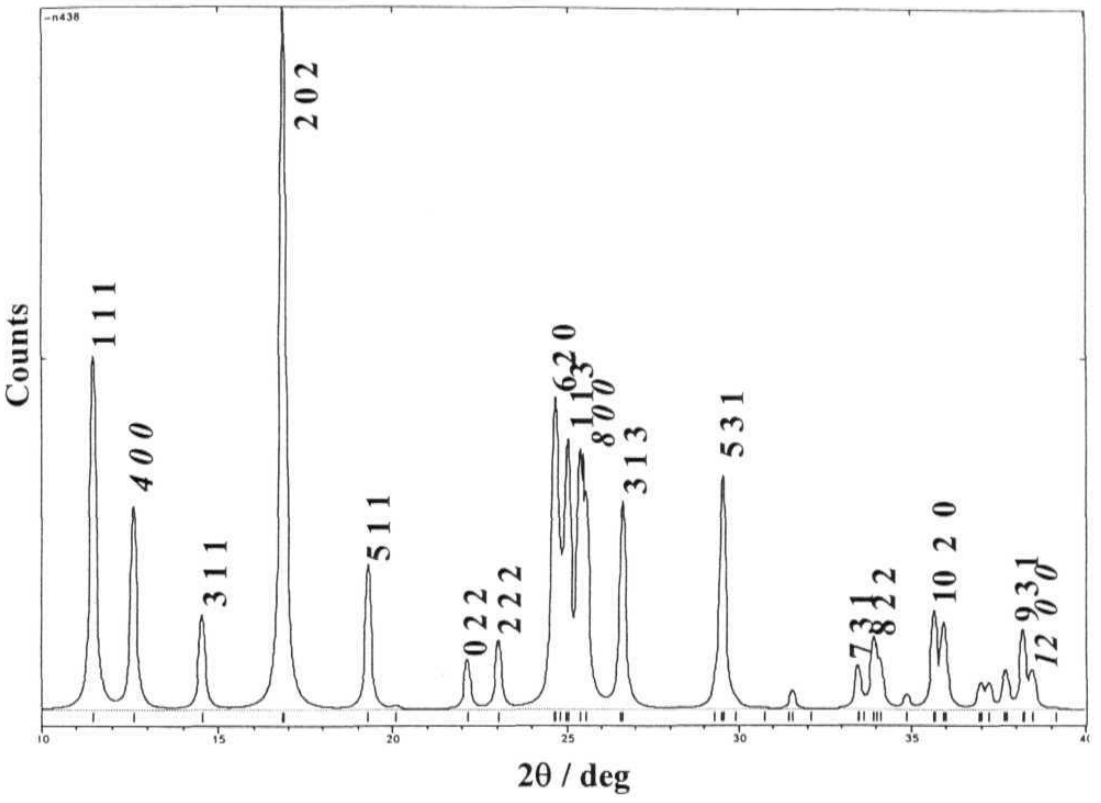

Figure 2.22c *Powder x-ray diffraction pattern simulated using **ZNDA** crystal structure with peak indexing.*

shows exclusively (h 0 0) peaks (Fig. 2.22b) suggesting a preferential *a* axis orientation normal to the substrate (h = 4n is imposed by the Fdd2 space group); at other distances, (1 1 1) and (2 2 0) peaks are also observed. From the x-ray diffraction data on the films and the single crystal structure it can be inferred that the molecular dipoles which point along the crystallographic *c* axis are oriented parallel to the substrate plane in the thin films of ZNDA.

The diffractogram of the films of ZNMPA grown at different distances are collected in Fig. 2. 23a. ZNMPA grown at the optimal distance of 7 cm show exclusively (h k 0) reflections (h = k), suggesting crystallite orientation with the [1 1 0] axis normal to the substrate (Fig. 2.23b). The x-ray pattern simulated using the single crystal structure of ZNMPA is shown in Fig. 2.23c. From the x-ray diffraction of the film and

the single crystal structure, it can be shown that the molecular dipoles are oriented at an angle of 50.8° with respect to the substrate in the thin films of ZNMPA.

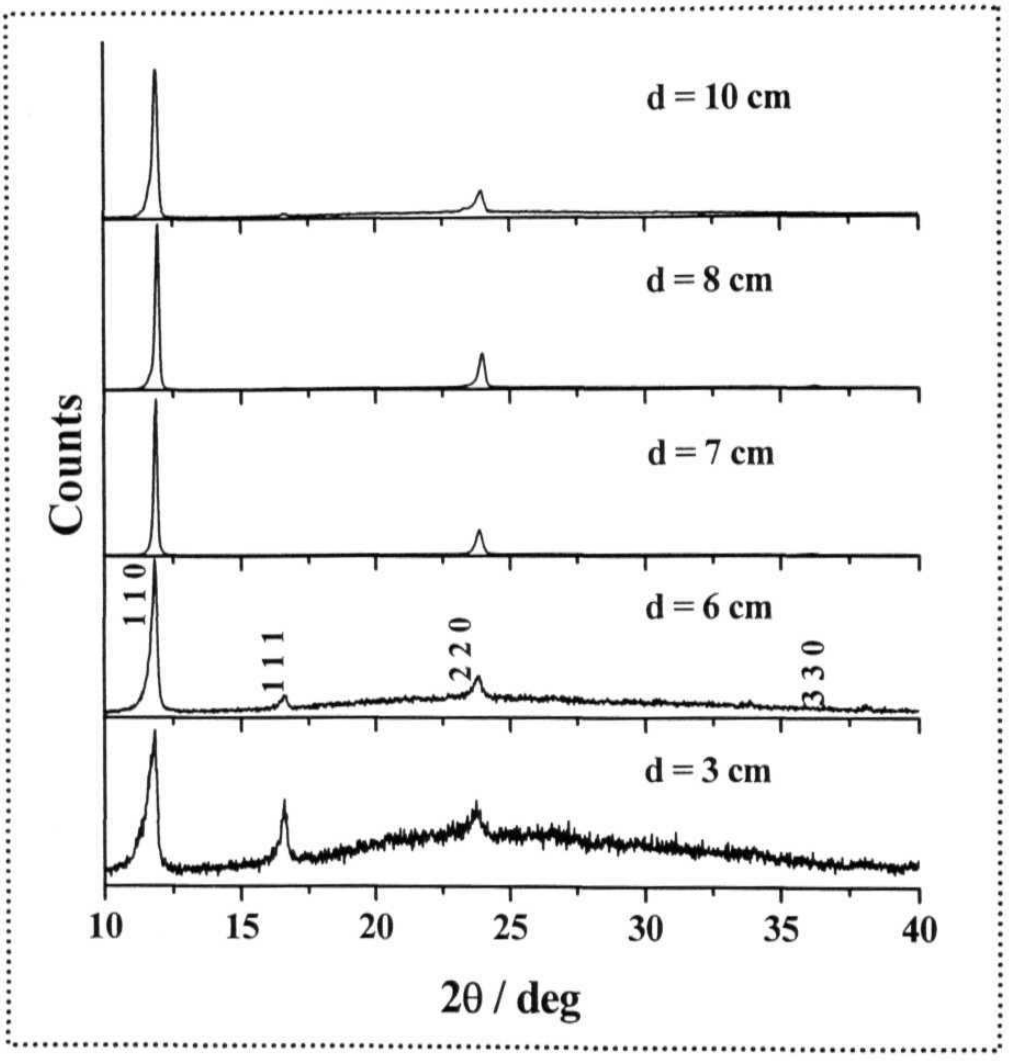

Figure 2.23a *X-ray diffractograms of **ZNMPA** films formed at different boat-substrate distances, d.*

In the previous section we have shown that crystals of ZNPPA form dimorphic structures with extreme dipole orientations.[35] Interestingly, ZNPPA forms the dimorphic structures in the thin films as well. At nonoptimal distances, both centrosymmetric and noncentrosymmetric structures are obtained in the films as well (Fig. 2.24a); interestingly, both show preferred orientations. When the substrate is at 5 cm, the

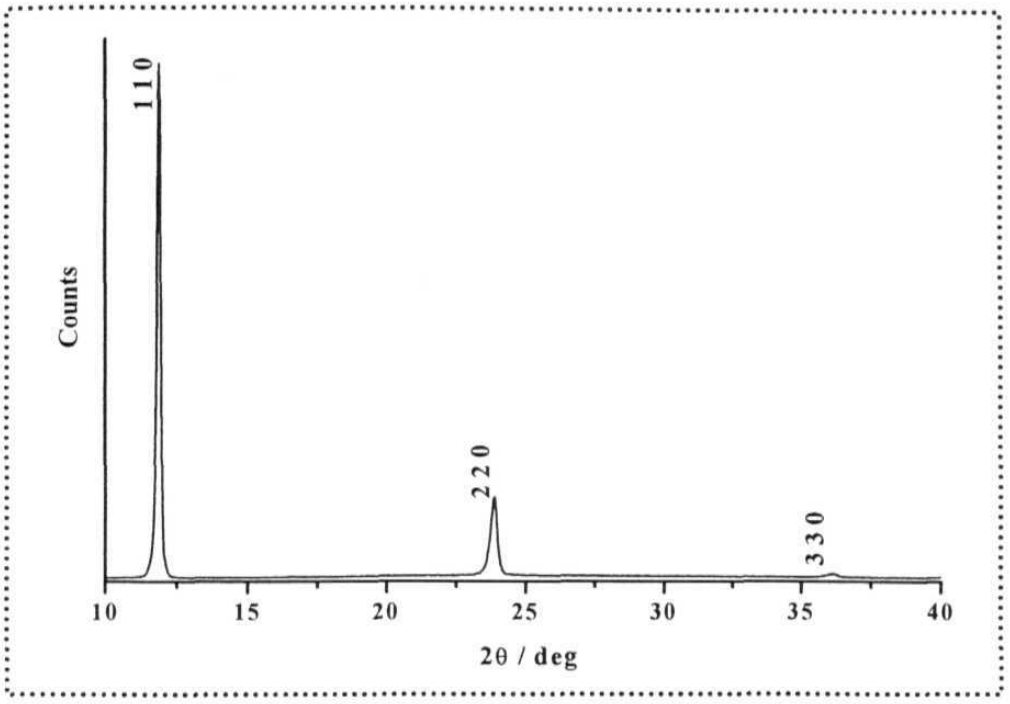

Figure 2.23b *X-ray diffractogram of **ZNMPA** thin film fabricated at d = 7 cm*

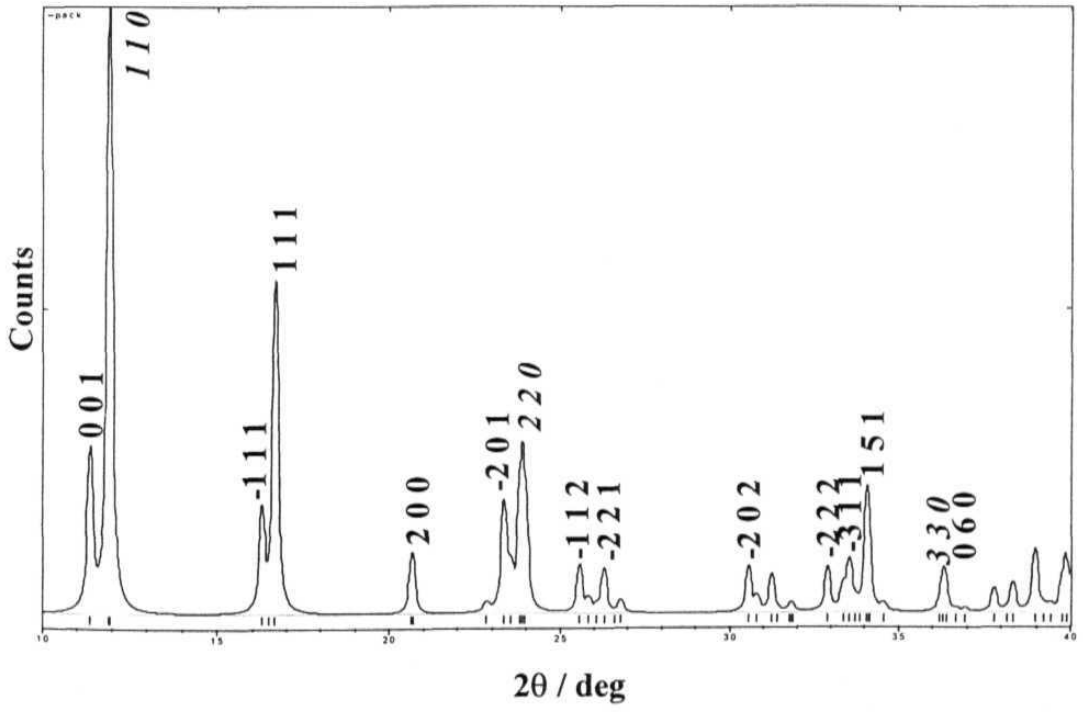

Figure 2.23c *Powder x-ray diffraction pattern simulated using **ZNMPA** crystal structure with peak indexing.*

centrosymmetric structure ZNPPA1 is exclusively formed, with the *c* axis oriented normal to the substrate (Fig. 2.24b). It is significant to note that the noncentrosymmetric structure could not be obtained exclusively in the film at any of the substrate position; this is reminiscent of the rarer formation of ZNPPA2 structure in crystallization experiments. The peaks are indexed using the powder x-ray diffractograms based on single crystal structures of ZNPPA1 (Fig. 2.24c) and ZNPPA2 (Fig. 2.24d). It is significant to note that in ZNDA and both the forms of ZNPPA, the crystallites are oriented with the longest unit cell axis normal to the substrate. These observations provides direct demonstration of the uniaxial orientational ordering of the polar crystallites with respect to the substrate normal, in the thin films of this family of metal organic compounds.

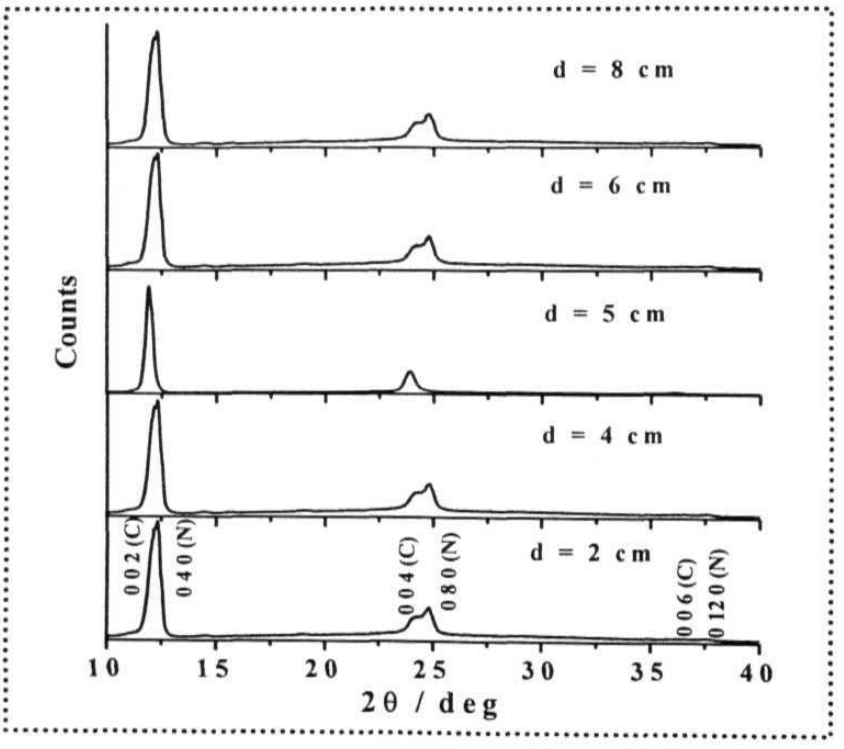

Figure 2.24a *X-ray diffractograms of **ZNPPA** films formed at different boat-substrate distances, d (C and N correspond to ZNPPA1 and ZNPPA2 respectively).*

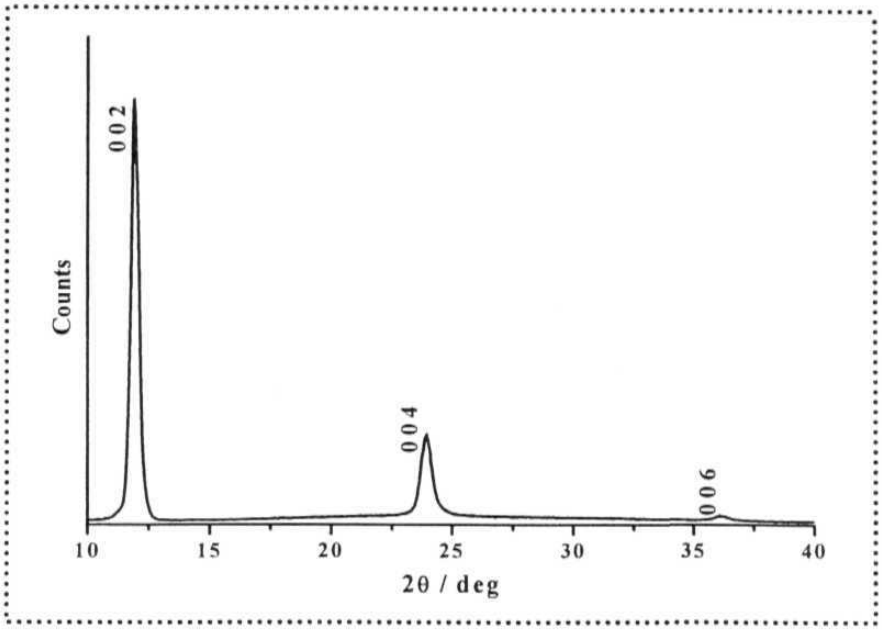

Figure 2.24b *X-ray diffractogram of **ZNPPA** thin film fabricated at d = 5 cm*

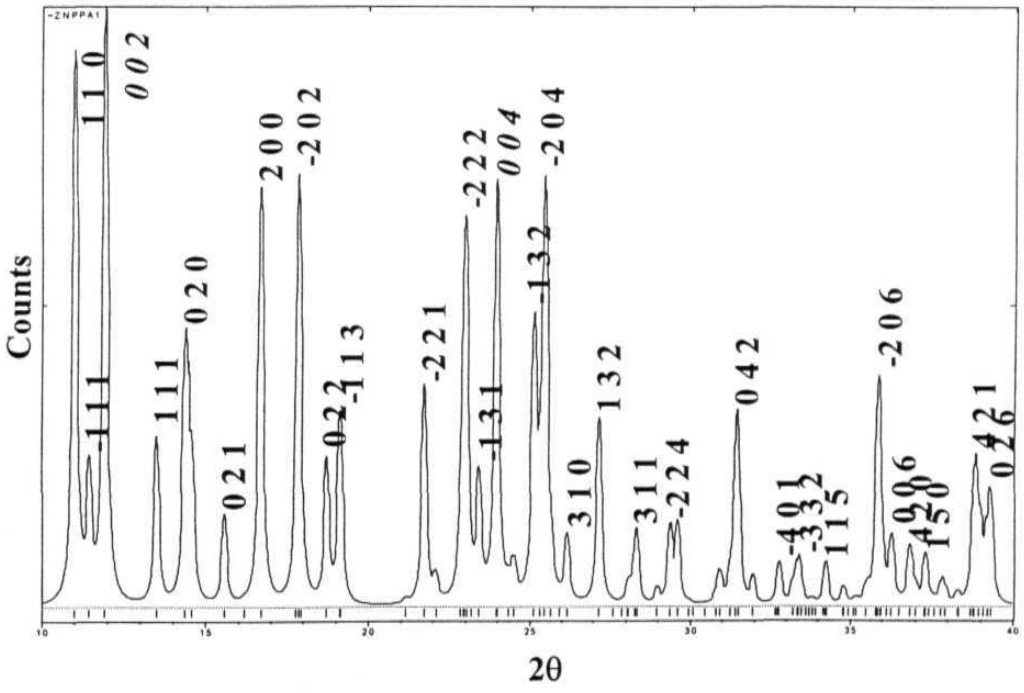

Figure 2.24c *Powder x-ray diffraction pattern simulated using **ZNPPA1** crystal structure with peak indexing.*

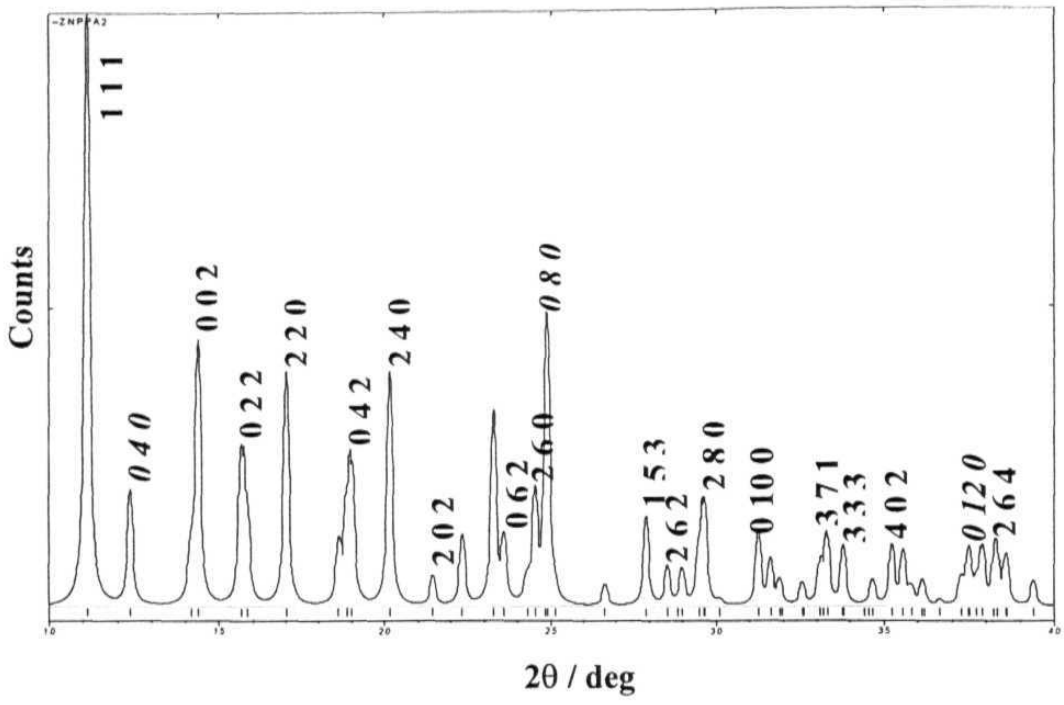

Figure 2.24d *Powder x-ray diffraction pattern simulated using* ***ZNPPA2*** *crystal structure with peak indexing.*

Morphology of the Thin Films

We have examined the morphology of the films to gain insight into the crystallite organization. Films having thickness of 0.4-0.6 μm were examined after providing a thin gold coating. ZNDA film shows square or rectangular crystallites with sizes in the range of 60-200 nm (Fig. 2.25a). The micrograph clearly reveals a face-on orientation of the crystallites, but little ordering of the crystallite axes parallel to the substrate plane. We have also observed micron-sized, flat crystallites when the film thickness is increased. Scanning electron micrograph of ZNMPA film is shown in Fig. 2.25b. It shows that the film is formed from well-packed, flat, micron-sized crystallites, resulting in a smooth surface. The crystallites reveal a clear orientational preference with their flat face parallel to the substrate. The SEM image shows that there is no ordering of crystallite orientations within the plane. ZNPPA shows needle-like crystallites in the films (Fig. 2.25c). The widths are typically 1 μm and length 10 μm. We have not observed any

difference in the morphology of the crystallites in films of exclusively centrosymmetric or dimorphic structures of ZNPPA. Preferential orientation of crystallites perpendicular to the substrate plane is not as clear in these films as in the previous cases. The SEM images of the ZNDA and ZNPPA also show that there is no ordering of crystallite orientations within the plane in the films.

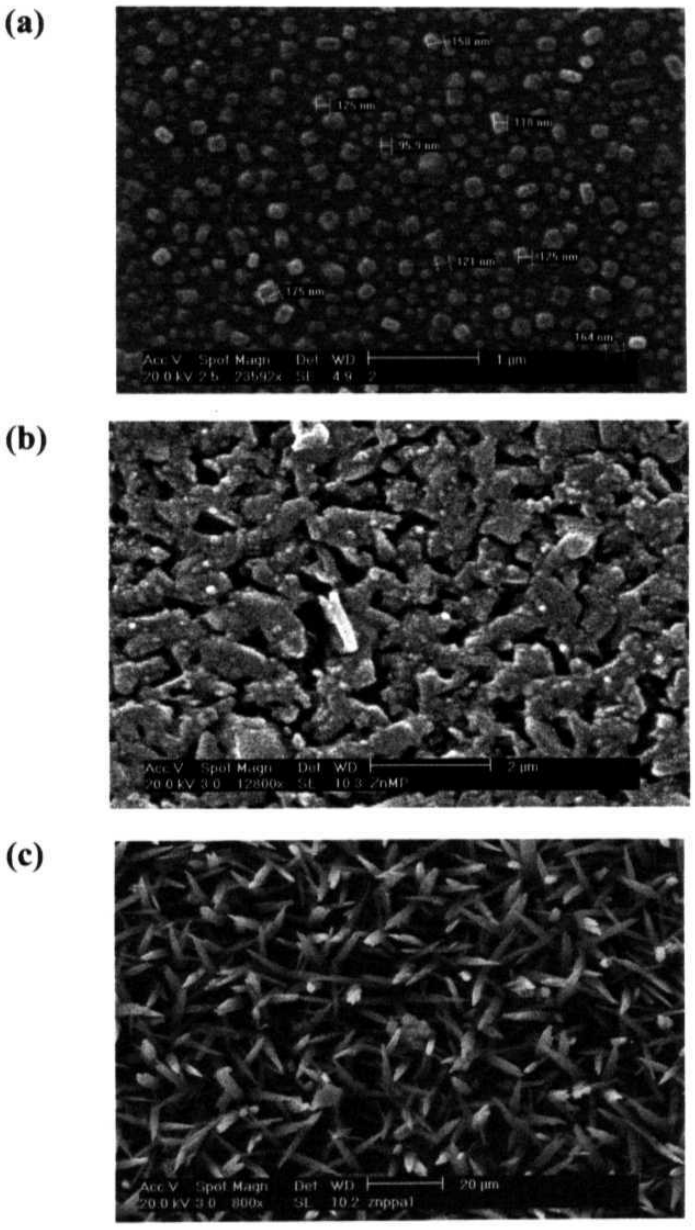

Figure 2.25 *SEM images of (a)* ***ZNDA****, (b)* ***ZNMPA*** *and (b)* ***ZNPPA*** *thin film on glass substrate*

Optical SHG Studies of Thin Films

SHG from the thin films on glass substrates was examined in transmission mode. Details of the experimental set up are provided in Appendix D. It was ascertained that the glass substrate alone produces no detectable SHG. Since films of pure ZNPPA2 could not be prepared, we have studied only the ZNDA and ZNMPA films. Films with different thickness were prepared and the thickness was measured by a profilometer. The

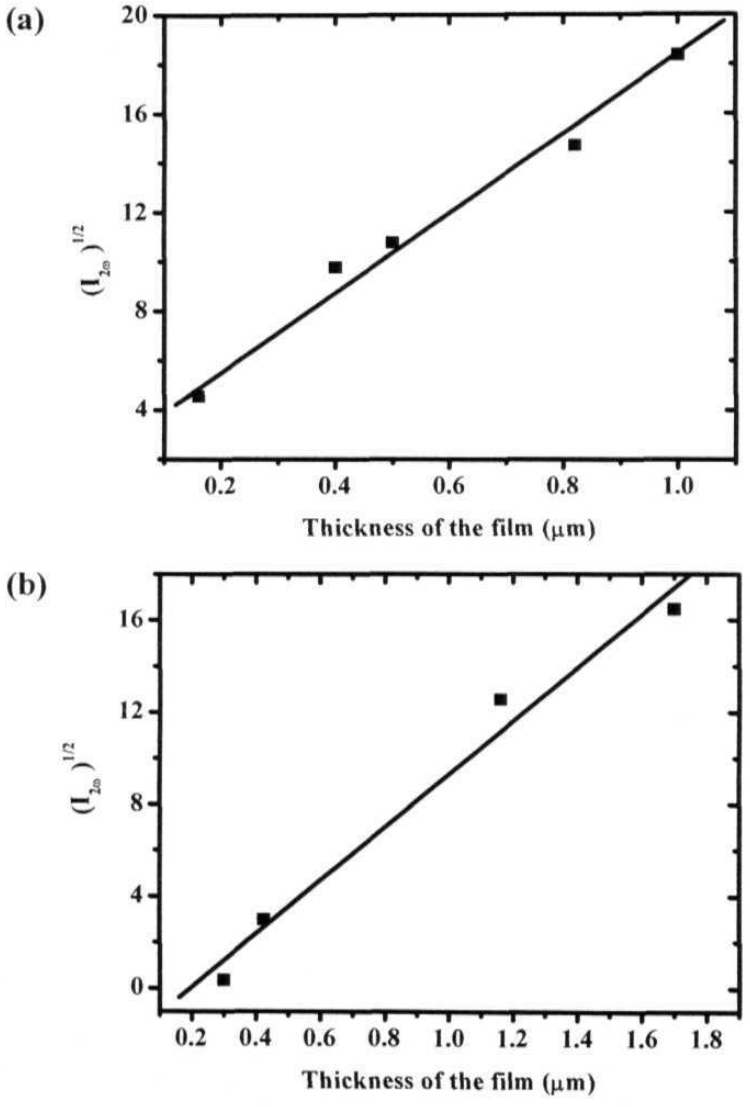

Figure 2.26 *Dependence of the SHG of (a)* ***ZNDA*** *and (b)* ***ZNMPA*** *films on the thickness*

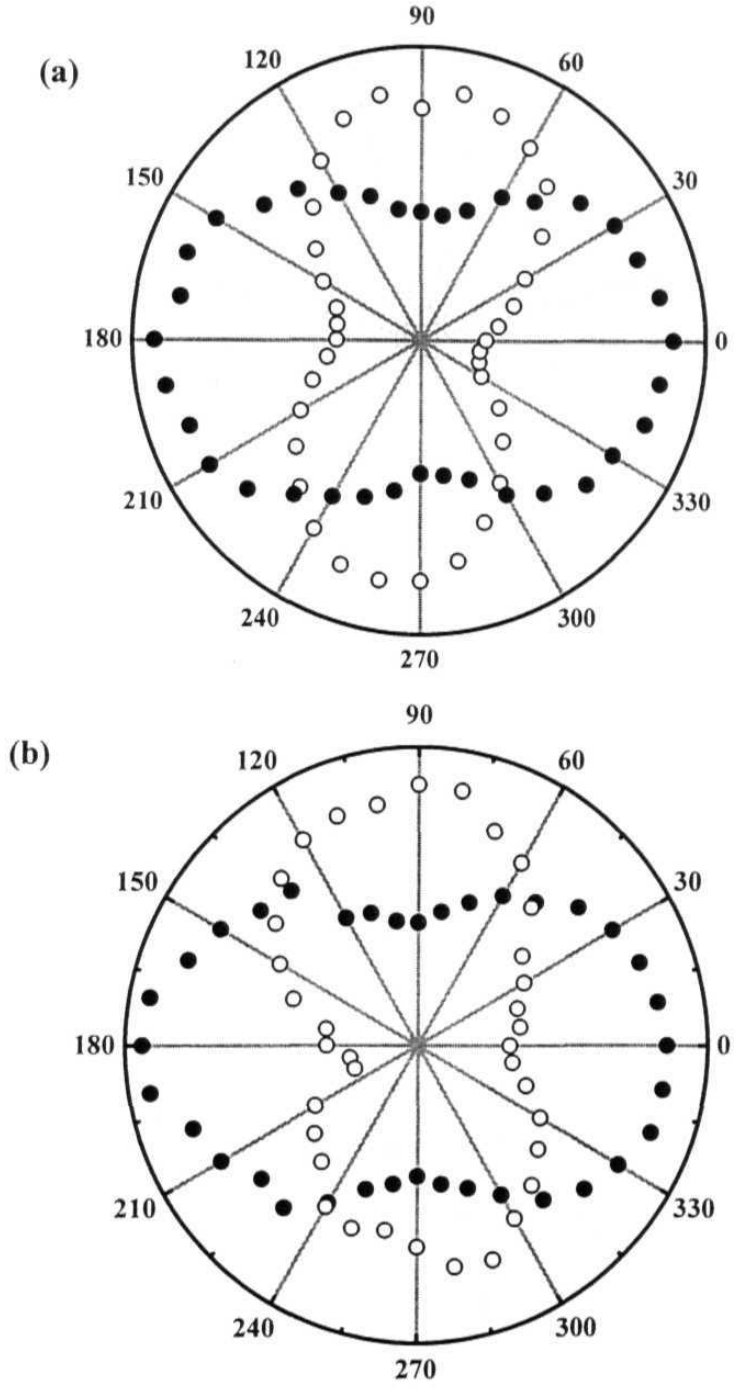

Figure 2.27 *Polar plots of the SHG of (a)* ***ZNDA*** *and (b)* ***ZNMPA*** *film in q-p (filled circle) and q-s (open circle) geometries (see text for details) as a function of the angle of rotation of the plane of polarization of the fundamental wave; the zero of the scale is chosen to coincide with one of the maxima in the q-p geometry., in each case.*

SHG was examined at different regions and the variation was found to be within the experimental error, indicating good homogeneity of the film over the area (~ 2 cm^2.). In addition, the SHG varies quadratically with the film thickness in both ZNDA and ZNMPA films (Fig. 2.26), indicating that the homogeneous organization is preserved with film growth.

Following the procedure developed by Zyss and coworkers,[45] the SHG was measured in p and s- polarizations, in the so-called q-p and q-s geometries, when the plane of polarization of the fundamental wave is rotated. It may be noted that there is no special axis in the plane of the film imposed either by the substrate or by the fabrication protocol. The SHG intensity variation for the q-p and q-s geometries shows a 90^o phase shift in both ZNDA and ZNMPA films (Fig. 2.27); this follows the pattern predicted for a collection of crystallites with uniaxial orientational ordering but random orientations within the plane.[45] Thus the SHG study further corroborates the crystallite orientations revealed by the x-ray diffraction and morphological studies in these films of metal-organic compounds which exhibit the rare phenomenon of perfectly polar supramolecular assembly.

2.7 SUMMARY

The novel 'screw'-shaped molecules with the 'push-pull' framework presented in this chapter exhibit the rare phenomenon of perfectly polar organization wherein the molecular dipoles are aligned parallel to one of the crystallographic directions. Examination of the crystal structures of ZNDA and ZNMPA in Sec. 2.3 revealed that these molecule form head-to-tail chains, promoted most likely, by dipolar interactions and polar sheet structures through weak intermolecular interactions between these chains. These sheets are organized into perfectly polar three-dimensional lattices. This bulk polar organization is in accord with the requirements put forth in the stochastic model[17] for the generation of polarity in supramolecular systems. These compounds demonstrate the formation of single component perfectly polar molecular crystals with high density of active components, without the involvement of a supporting structure based on a framework lattice, counterion or cocrystallization partner. We have found that even with

the 'screw' shaped dipolar molecules, if relatively stronger lateral H-bonding interactions are incorporated, it results in the formation of antiparallel alignment of molecular dipoles in the crystal lattice.[50] We have also observed that in a vanadyl complex, subtle modification of the ligand can have a drastic effect on the coordination geometry switching it between *cis* and *trans*, leading to a modification of the hierarchy of intermolecular interactions and changing the crystal organization from perfectly polar to a centrosymmetric one.[51]

In Sec. 2.4, we have presented an interesting case of dimorphism involving extreme molecular orientations in the two structures. The polar and centric packings exhibited by ZNPPA provide an interesting demonstration of the close and subtle energetics and kinetics involved in supramolecular assembly. The studies of the multidomain crystals suggest the possibility of obtaining different polarity in cogrowth domains of monolithic crystals. The domain structure built up of SHG active and inactive regions can be mapped using techniques such as second harmonic microscopy.[52] This would be an important direction for further work on these materials. If the orientational and spatial attributes of the domains can be controlled, it would be of considerable interest in developing crystals which simulate periodically poled structures for applications such as quasi phase-matched SHG.

In Sec. 2.6, we have described the fabrication of these novel compounds in the form of thin films by vapor deposition. Powder x-ray diffractogram studies demonstrated the orientational ordering of the perfectly polar microcrystallites in the films. The critical role of the substrate position with respect to the sublimation boat for effecting the crystallite orientation was demonstrated. Polarization dependence of the SHG from these films reveals the uniaxial orientational ordering of the crystallites with random orientation within the plane of the homogeneous thin films.[45] The fabrication of homogeneous thin films with orientationally ordered crystallites, through the physical vapor deposition of a family of metal-organic compounds which form perfectly polar assemblies in crystals, demonstrates the generality of this effect for this class of materials. In addition to projecting a fundamentally interesting phenomenon, the current study presents materials of potential utility in opto-electronic applications.

REFERENCES

1. (a) Simon, J; Bassoul, P. *Design of Molecular Materials : Supramolecular Engineering*, John Wiley: Chichester, 2000; (b) Moor, J. S.; Lee, S. *Chem. Ind.* **1994**, 556; (c) Desiraju, G. R. *Crystal Engineering; The Design of Organic Solids*, Elsivier, New York, 1989.
2. Bürgi, H.-B.; Hulliger, J.; Langley, P. *Curr. Opin. Solid State Mater. Sci.* **1998**, *3*, 425.
3. (a) Weber, M. J. (Ed.), *Handbook of Laser Science and Technology*, Supplement 2: Optical Materials, CRC Press, Boca Raton, 1995; (b) Chemla, D. S.; Zyss, J. (Eds.), *Nonlinear Optical Properties of Organic Molecules and Crystals*, Academic Press, New York, 1989, Vol. 1, 2.
4. Miyata, S.; Sasabe, H. (Eds.), *Poled Polymers and their applications to SHG and EO Devices*, Gorden and Breach, Amsterdam, 1997.
5. (a) Patel, K. M.; Sparrow, J. T. *Synthetic Commun.* **1979**, *9*, 251; (b) Lippert, E. L.; Truter, M. R. *J. Chem. Soc.* **1960**, 4996.
6. (a) Bosshard, C.; Günter, P. *Nonlinear Optics of Organic Molecular and Polymeric Materials*, (Eds.) S. Miyata and H. S. Nalwa, CRC Press, Boca Raton, 1997, p.391; (b) Moerner W. E.; Silence, S. M. *Chem. Rev.* **1994**, *94*, 127.
7 Martin, A. S.; Sambles, J. R.; Ashwell, G. J. *Phys. Rev. Lett.*, **1993**, *70*, 218.
8. König, O.; Bürgi, H.-B.; Armbruster, T.; Hulliger, J. *J. Am. Chem. Soc.* **1997**, *119*, 10632; (b) Ramamurthy, V.; Eaton, D. F. *Chem. Mater.* **1994**, *6*, 1128; (c) Hoss, R.; König, O.; Kramer-Hoss, V.; Berger, U.; Rogin, P.; Hulliger, J. *Angew. Chem. Int. Ed. Engl.* **1996,** *35*, 1664; (d) Hulliger, J.; Langley, P. J.; König, O.; Quintel, A.; Rechsteiner, P. *Pure Appl. Opt.* **1998**, *7*, 221.
9. The latest update (version 5.26) of the Cambridge Crystallographic Database shows 75.5% of the entries to be centrosymmetric.
10. Bosshard, C.; Spreiter, R.; Meier, U.; Liakatas, I.; Bösch, M.; Jäger, M.; Manetta, S.; Follonier, S.; Günter, P. *Crystal Engineering: From Molecules and Crystals to Materials*, (Ed.) D. Braga and F. Grepioni, Kluwer, 1991, p.261.
11. Wong, M. S.; Pan, F.; Bösch, M.; Spreiter, R.; Bosshard, C.; Günter, P.; Gramlich, V. *J. Opt. Soc. Am. B* **1998**, *15*, 426.

12. (a) Marder, S. R.; Perry J. W.; Schaefer, W. P. *Science* **1989**, *245*, 626; (b) Marder, S. R.; Perry, J. W.; Yakymyshyn, C. P. *Chem. Mater.* **1994**, *6*, 1137.
13. (a) Hulliger, J.; Roth, S. W.; Quintel, A.; Bebie, H. *J. Solid State Chem.* **2000**, *152*, 49; (b) Hulliger, J.; Langley, P. J.; Quintel, A.; Rechsteiner, P.; Roth, S. W. *Supramolecular Engineering of Synthetic Metallic Materials*, (Ed.) Veciana, J.; Rovira, C.; Amabilino, D. B. Kluwer, Dordrecht **1999**, p. 67; (c) Quintel, A.; Hulliger, J.; Wübbenhorst, M. *J. Phys. Chem. B* **1998,** *102*, 4277; (d) Hulliger, J.; König, O.; Hoss, R. *Adv. Mater.* **1995**, *7*, 719.
14. Holman, K. T.; Pivovar, A. M.; Ward, M. D. *Science* **2001**, *294*, 1907.
15. (a) Ohkita, M.; Suzuki, T.; Nakatani, K.; Tsuji, T. *Chem. Lett.* **2001**, 988; (b) Jouaiti, A.; Hosseini, M. W.; Kyritsakas, N. *Chem. Commun.* **2002**, 1896.
16. (a) Qin, J.; Su, N.; Dai, C.; Yang, C.; Liu, D.; Day, M. W.; Wu, B.; Chen, C. *Polyhedron* **1999**, *18*, 3461; (b) Qin, J.; Dai, C.; Zhang, J.; Su, N.; Yang, C.; Luo, B.; Liu, D.; Wu, B.; Chen, C.; Day, M. W. *Progress in Crystal Growth and Characterization of Materials* **2000**, 115.
17. Hulliger, J.; Langley, P. J.; Roth, S. W. *Cryst. Eng.* **1998**, *1*, 177.
18. (a) Anthony, S. P.; Radhakrishnan, T. P. *Chem. Commun.* **2001**, 931; (b) Anthony, S. P.; Naga Srinivas, N. K. M.; Narayana Rao, D.; Radhakrishnan, T. P. *J. Mater. Chem.* **2005**, *15*, 739.
19. Zhang, C.;. Chadha, R; Reddy, H. K.; Schrauzer, G. N. *Inorg. Chem.* **1991**, *30*, 3865.
20. Dewar, M. J. S.; Zoebisch, E. G.; Healy, E. F.; Stewart, J. J. P. *J. Am. Chem. Soc.* **1985**, *107*, 3902.
21. Desiraju, G. R. *Acc. Chem. Res.* **1996**, *29*, 441.
22. Miller, J. S.; *Adv. Mater*. **1998**, *10*, 1553.
23. (a) Bernstein, J. *Polymorphism in Molecular Crystals*, Oxford University Press, Oxford, 2002; (b) Zerkowski, J. A.; Macdonald, J. C.; Whitesides, G. M. *Chem. Mater.* **1997**, *9*, 1933; (c) Bernstein, J.; Etter, M. C.; Macdonald, J. C. *J. Chem. Soc. Perkin Trans.2* **1990**, 695.
24. (a) Gavezzotti, A. *Acc. Chem. Res.* **1994**, *27*, 309; (b) Lommerse, J. P. M.; Motherwell, W. D. S.; Ammon, H. L.; Dunitz, J. D.; Gavezzotti, A.; Hofmann, D. W. M.; Leusen, F. J. J.; Mooij, W. T. M.; Price, S. L.; Schweizer, B.; Schmidt, M. U.; van Eijck, B. P.; Verwer, P.; Williams, D. E. *Acta Cryst. B* **2000**, *56*, 697; (c)

Motherwell, W. D. S.; Ammon, H. L.; Dunitz, J. D.; Dzyabchenko, A.; Erk, P.; Gavezzotti, A.; Hofmann, D. W. M.; Leusen, F. J. J.; Lommerse, J. P. M.; Mooij, W. T. M.; Price, S. L.; Scheraga, H.; Schweizer, B.; Schmidt, M. U.; van Eijck, B. P.; Verwer, P.; Williams, D. E. *Acta Cryst. B* **2002**, *58*, 647; (d) Desiraju, G. R. *Nature Materials* **2002**, *1*, 77.

25. Bernstein, J.; Davey, R. J.; Henck, J. O. *Angew. Chem. Int. Ed. Engl.* **1999**, *38*, 3440.
26. (a) Kanis, D. R.; Ratner, M. A.; Marks, T. J. *Chem. Rev.* **1994**, *94*, 195; (b) Marks, T. J.; Ratner, M. A. *Angew. Chem. Int. Ed. Engl.* **1995**, *34*, 155; (c) Zyss, J.; Nicoud, J. F. *Curr. Opin. Solid State Mater. Sci.* **1996**, *1*, 533; (d) Gangopadhyay, P.; Radhakrishnan, T. P. *Angew. Chem. Int. Ed.Engl.* **2001**, *40*, 2451.
27. Bernstein, J. *Polymorphism in Molecular Crystals*, Oxford University Press: London, 2002, p.207.
28. Chemla, D. S.; Zyss, J. (Eds.), *Nonlinear Optical Properties of Organic Molecules and Crystals*, Academic Press: New York, 1987, Vol. 1, p.114.
29. (a) Zyss, J.; Ledoux, I.; Bertault, M.; Toupet, E. *Chem. Phys.* **1991**, *150*, 125; (b) Zyss, J.; Masse, R.;Bagieu-Beucher, M.; Levy, J. P. *Adv. Mater.* **1993**, *5*, 120.
30. Gong, B.; Zheng, C.; Zeng, H.; Zhu, J. *J. Am. Chem. Soc.* **1999,** *121*, 9766.
31. (a) Banister, A. J.; Bricklebank, N.; Clegg, W.; Elsegood, M. R. J.; Gregory, C. I.; Lavender, I.; Rawson, J. M.; Tanner, B. K. *Chem. Commun.* **1995**, 679; (b) Banister, A. J.; Bricklebank, N.; Lavender, I.; Rawson, J. M.; Gregory, C. I.; Tanner, B. K.; Clegg, W.; Elsegood, M. R. J.; Palacio, F. *Angew. Chem. Int. Ed. Engl.* **1996**, *35*, 2533.
32. Anthony, S. P.; Raghavaiah, P.; Radhakrishnan, T. P. *Crystal Growth & Design* **2003**, *3*, 631.
33. Freer, S. T.; Kraut, J. *Acta Cryst.* **1965**, *19*, 992.
34. (a) Green, B. S.; Knossow, M. *Science* **1981**, *214*, 795; (b) Ramdas, S.; Thomas, J. M.; Jordan, M. E.; Eckhardt, C. J. *J. Phys. Chem.* **1981**, *85*, 2421.
35. Sharma, S.; Radhakrishnan, T. P. *J. Phys.Chem. B* **2000,** *104*, 10191.
36. Jayanty, S.; Radhakrishnan, T. P. *Chem. Mater.* **2001**, *13*, 2460l.
37. Klamt, A.; Shüürmann, G. *Perkin Trans.* **1993**, 799.
38. Dupuis, M.; Karna, S. *J. Comput. Chem.* **1991**, *12*, 487.

39. Zyss, J.; Oudar, J. L. *Phys. Rev. A* **1982**, *26*, 2028.
40. Kurtz, S. K.; Perry, T. T. *J. Appl. Phys.* **1968**, *39*, 3798; (b) for details of our procedure, see : Gangopadhyay, P.; Radhakrishnan, T. P. *Chem. Mater.* **2000**, *12*, 3362.
41. (a) Bosshard, C.; Sutter, K.; Prêtre, P.; Hulliger, J.; Flörsheimer, M.; Kaatz, P.; Günter, P. *Organic Nonlinear Optical Materials*, Gorden & Breach, Amsterdam, 1995; (b) Kajzar, F.; Swalen, J. D. (Eds.), *Organic Thin Films for Waveguiding Nonlinear Optics*, Gorden & Breach, Amsterdam, 1996; (c) Tregold, R. H. *Order in Thin Organic Films*, Cambridge Univ. Press, Cambridge, 1994; (d) Whitsides, G. M.; Mathias, J. P.; Seto, C. T. *Science* **1991**, *254*, 1312.
42. (a) Roberts, M. J.; Lindsay, G. A.; Herman, W. N.; Wynne, K. J. *J. Am. Chem. Soc.* **1998**, *120*, 11202; (b) Wijekoon, W. M. K. P.; Wijayu, S. K.; Bhawalkar, J. D.; Prasad, P. N.; Penner, T. L.; Armstrong, N. J.; Ezenyilimba, M. C.; Williams, D. J. *J. Am. Chem. Soc.* **1996**, *118*, 4480.
43. (a) Lvov, Y.; Ariga, K.; Onda, M.; Ichinose, I.; Kunitake, T. *Colloids and surfaces A* **1999**, *146*, 337; (b) Cui, X.; Pei, R.; Wang, Z.; Yang, F.; Ma, Y.; Dong, S.; Yang, X. *Biosensors & Bioelectronics* **2003**, *18*, 59; (c) Park, S. Y.; Rubner, M. F.; Mayes, A. M. *Langmuir* **2002**, *18*, 9600; (d) Ulman, A. *Chem. Rev.* **1996**, *96*, 1533.
44. Forrest, S. R. *Chem. Rev.* **1997**, *97*, 1793.
45. Vallée, R.; Damman, P.; Dosière, M.; Toussaere, E.; Zyss, J. *J. Chem. Phys.* **2000**, *112*, 10556.
46. Ehara, T.; Hirose, H.; Kobayashi, H.; Kotani, M. *Synth. Metals* **2000**, *109*, 43.
47. Komatsu, K.; Nanjo, H.; Yamagishi, Y.; Kaino, T. *Thin Solid Films* **2001**, *393*, 1.
48. (a) Cai, C.; Bösch, M. M.; Tao, Y.; Müller, B.; Gan, Z.; Kündig, A.; Bosshard, C.; Liakatas, I.; Jäger, M.; Günter, P. *J. Am. Chem. Soc.* **1998**, *120*, 8563; (b) Cai, C.; Bösch, M. M.; Müller, B.; Tao, Y.; Kündig, A.; Bosshard, C.; Gan, Z.; Biaggio, I.; Liakatas, I.; Jäger, M.; Schwer, H.; Günter, P. *Adv. Mater.* **1999**, *11*, 745; (c) Rashid, A. N.; Erny, C.; Günter, P. *Adv. Mater.* **2003**, *15*, 2024.
49. Zhu, P.; Kang, H.; Facchetti, A.; Evmenenko, G.; Dutta, P.; Marks, T. J. *J. Am. Chem. Soc.* **2003**, *125*, 11496.
50. Anthony, S. P.; Radhakrishnan, T.P. unpublished results.

51. Anthony, S. P.; Srikanth, L.; Radhakrishnan, T.P. *Mol. Cryst. Liq. Cryst.* **2002**, 381, 133.

52. (a) Andreazza, P.; Lefaucheux, F.; Robert, M. C.; Josse, D.; Zyss, J. *J. Appl. Phys.* **1990**, *68*, 8; (b) Andreazza, P.; Josse, D.; Lefaucheux, F.; Robert, M. C.; Zyss, J. *Phys. Rev. B* **1992**, *45*, 7640.

CHAPTER 3

Hierarchical Structures of Coordination Polymers : Impact on Solid State Second Harmonic Generation

Papers published

- Anthony, S. P.; Radhakrishnan, T. P. *Chem. Commun.* **2004**, 1058.
  Helical and Network Coordination Polymers Based on a Novel C_2-Symmetric Ligand: SHG Enhancement Through Specific Metal Coordination.

- Anthony, S. P.; Radhakrishnan, T. P. *Cryst. Growth Des.* **2004**, *4*, 1223.
  Coordination Polymers of Cu(I) with a Chiral Push-Pull Ligand: Hierarchical Network Structures and Second Harmonic Generation.

3.1 INTRODUCTION

Rational approach to the design and realization of coordination polymers with network structures, through careful modulation of ligand structure, is of great interest since the topology of the network may be manipulated to dramatically influence the overall physical properties and functions of the resulting materials.[1-3] The flexibility and versatility of coordination polymers facilitates the realization of a variety of supramolecular organizations and a wide spectrum of materials attributes including electrical conductivity, magnetism and optical characteristics.[4] These properties are often directly related to the molecular organizations and the cooperative interactions between the molecules in the bulk materials. Infinite coordination polymers allow the construction of stable frameworks using rigid ligands with diverse structural motifs; examples include chains, ladders, helices and diamondoid and octahedral nets. The polymer formation leads to various modes of arrangement of organic molecules in the solid state. By choosing metal ions with specific coordination geometry, it is possible to organize the organic ligands in desired fashions through the supramolecular assembly.[4,5]

The mode of assembly of molecules in crystals is strongly influenced by the nature of the intermolecular interactions. While in the case of small organic molecules and metal complexes these include primarily H-bond, dipolar and dispersion interactions, in the case of coordination polymers, relatively stronger metal-ligand coordination are also involved in an extended fashion. One of the basic factors that lead to the occurrence of extensive cases of polymorphism in molecular crystals is the relatively low and comparable magnitude of a range of intermolecular forces giving rise to a complex energy landscape representing varied patterns of molecular assemblies. The foregoing considerations imply that metal coordination polymers with a more robust structure are likely to show lower propensity towards polymorphic structures. This point has been noted in earlier work on structural/supramolecular isomerism in coordination polymers.[6-8] The concept of supramolecular isomerism is a general one and it has been pointed out that polymorphism should be viewed as a subset of supramolecular isomerism.[7] In a less rigorous sense, structural variations arising from differences in the mode of ligation,[9] ligand conformations[10-15] or both[16] and in the network topologies[17,18] have been described as cases of polymorphism. Coordination polymers which exhibit supramolecular

isomerism in the networks are of considerable current interest for both conceptual reasons and because of a wide range of materials properties they exhibit.[4] Since these properties are sensitively related to the supramolecular organization, and as noted above, the probability of polymorphism arising in these materials is relatively low, investigations of any occurrence of polymorphic or hierarchical structures and more significantly, their correlation with materials attributes are valuable for the design of novel materials. The combination of improved molecular and materials attributes that may be realized and the possibility of exploring fundamental structure-property correlations warrants the development of novel ligands that can lead to varied polymer architectures.

Nonlinear optical (NLO) properties of organized molecular assemblies is one of the key targets of current investigations in materials chemistry.[19] Appreciable thermal stability and optical transparency that can be achieved through a judicious choice of metal ions and ligands makes coordination polymers particularly attractive candidates for NLO applications.[19-21] The metals used most often are Zn and Cd and transition metals such as W, Ni, Cu and Ru; some of the popular ligands that have been employed in these materials are based on Schiff bases, pyridines and stilbenes (Sec. 1.5).[20-24] Owing to the ease of building structures with three-fold rotational symmetry around a metal center, several octupolar metal-organic chromophores based on tetrahedral, octahedral or trigonal bipyramidal systems have been synthesized and their second order NLO properties have been studied in solution as well as in the solid state.[24-26] The possibility of fine-tuning the hyperpolarizability at the molecular level is an added advantage for quadratic applications such as second harmonic generation. Coordination of metal ions can be effectively exploited to enhance the nonlinearity at the molecular[27] and bulk[28,29] levels.

Chirality in general and helicity in particular are interesting phenomena and are of intense current interest in chemistry, biochemistry, pharmocology, agrochemistry and materials science.[30,31] C_2-symmetric molecules are useful building blocks for helical assemblies the chirality of which extends over the whole molecular superstructure. Enhancement of nonlinear optical properties has been demonstrated in polymers,[3] mesoscopic systems[32] and Langmuir-Blodgett[33] films through supramolecular aggregates and chirality. Study of the LB films based on helicenes[34] showed that the chiral

supramolecular organization of the nonracemic materials led to second order NLO susceptibility 30 times higher than that of the racemic materials with the same chemical structure. Strong enhancement of SHG in the helical superstructure of a C_2-symmetric molecule has been reported from our laboratory.[35] Among the molecular design approaches for quadratic NLO materials discussed in Sec. 1.2, only chirality guarantees the realization of a noncentrosymmetric structural organization in the solid state. Donor-acceptor substituted conjugated systems generally possess large β which can be further enhanced by coordination of electropositive metals at the acceptor site. Considering this factor and the fact that homochirality ensures the formation of noncentrosymmetric lattice structures we have investigated the deployment of N,N'-bis(4-cyanophenyl)-(1*R*,2*R*)-diaminocyclohexane (BCDC) as a novel C_2-symmetric ligand with a 'push-pull' framework. The axial symmetry of this ligand coupled with the multiple ligation sites have allowed the fabrication of different coordination polymer topologies. The different modes of coordination exhibited by the BCDC ligand in the coordination polymers are shown in Fig 3.1. In view of the optical transparency and possibility of forming coordination polymers we have chosen Cu(I) and Ag(I) for complexation.

We have investigated the crystal structures and SHG capability of the free ligand as well as its coordination polymers and analyzed the interesting trends that they exhibit.[36,37] The mode of coordination are strikingly different with the two metal ions Ag(I) and Cu(I). The Ag(I)-BCDC complex (SBP) shows linear coordination environment around Ag(I) with the two cyano nitrogens, leading to the formation of one-dimensional helical superstructures in the crystals. Since Cu(I) generally shows tetrahedral coordination, we anticipated that the Cu(I)-BCDC complex may be amenable to different structural organizations in the solid state. The solvent plays a role in the formation of two different architectures. The polymer topologies are two-dimensional network in one case (CBPT) and three-dimensional architecture built up of three interwoven diamondoid structures in the other (CBP). Diamondoid networks possess the connectivity of a diamond lattice, but the local symmetry at the vertices may not be strictly T_d; SHG active materials have been developed based on noncentric interwoven diamondoid structures.[38,21,26] The BCDC ligand adopts different conformations in the one-dimensional helical and two-dimensional network coordination polymer topologies. In the three-dimensional diamondoid structure, combination of two different

conformations leads to the formation of a helical superstructure in the crystal lattice. CBPT and CBP could be described as dimorphic structures, following earlier reports[13,14,17,39] of polymorphic forms with focus on the metal-ligand combination rather than on the specific stoichiometry or ligand structure. More significantly, we explore the consequence of the hierarchy in these noncentrosymmetric structures for their solid state optical SHG capability. We have analyzed the influence of the ligand conformation on the solid state second harmonic generation with respect to that of the ligand. A simple computational approach is used to understand the influence of the conformation of BCDC and the coordination of the metal ion on the hyperpolarizability (β) of these metal-organic systems.

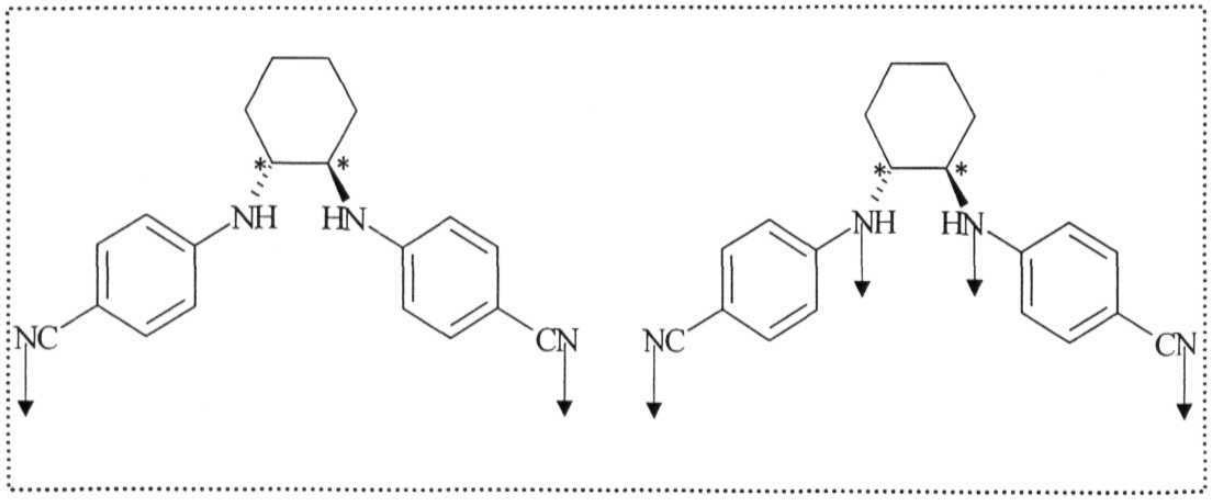

Figure 3.1 *Different modes of ligation exhibited by BCDC ligand in the silver(I) and copper(I) complexes we have developed.*

3.2 SYNTHESIS AND CHARACTERIZATION

Resolution of 1,2-diaminocyclohexane

The resolution was carried out following the methodology reported by Jacobsen *et al.* (Scheme 3.1).[40] A 100 ml beaker equipped with magnetic stirrer was charged with a solution of 20 g (1.332 mol) of L(+) – tartaric acid in 35 ml of distilled water at room

temperature. After the complete dissolution of the acid, 30 ml (0.245 mol) of 1,2-diaminocyclohexane (*cis* and *trans* mixture) was added dropwise with thorough stirring over a period of 30 min, maintaining the solution temperature below 65°C. White precipitate started appearing soon. 15 ml (0.2665 mol) glacial acetic acid was added to this mixture at such a rate that the reaction temperature just reached 75°C. The thick white precipitate formed upon addition of the acid was stirred vigorously as it cooled down to 30°C over a period of 2 h. The mixture was then cooled to ≤ 5°C in an ice bath for 2 h and the precipitate was collected by vacuum filtration. The wet cake was washed with (3 × 10 ml) water (5°C), (5 × 10 ml) chilled methanol (5°C) and then (3 × 20 ml) acetone (26°C). The residue was dried in air for 2 h and then recrystallized from water (1:20 w/v) and water–methanol (1:1 w/v). The recrystallized product was crushed and dried at 60°C under reduced pressure for several hours to yield 24 g (90% yield) of shining white (1*R*, 2*R*)-cyclohexanediammonium L (+) tartarate [M.P. 276 – 278°C (d); $[\alpha]^{D}_{20}$ (water) = +132 deg cm^2 g^{-1}]. 24 g of (1*R*,2*R*)-cyclohexanediammonium L (+) tartarate was dissolved in concentrated KOH solution (25 g of KOH in 10 ml of water) and the organic layer containing (1*R*,2*R*)-1,2-diaminocyclohexane was separated out. This fraction was dried over CaO; multiple distillations yielded 7 g (55% recovery) of the free amine.

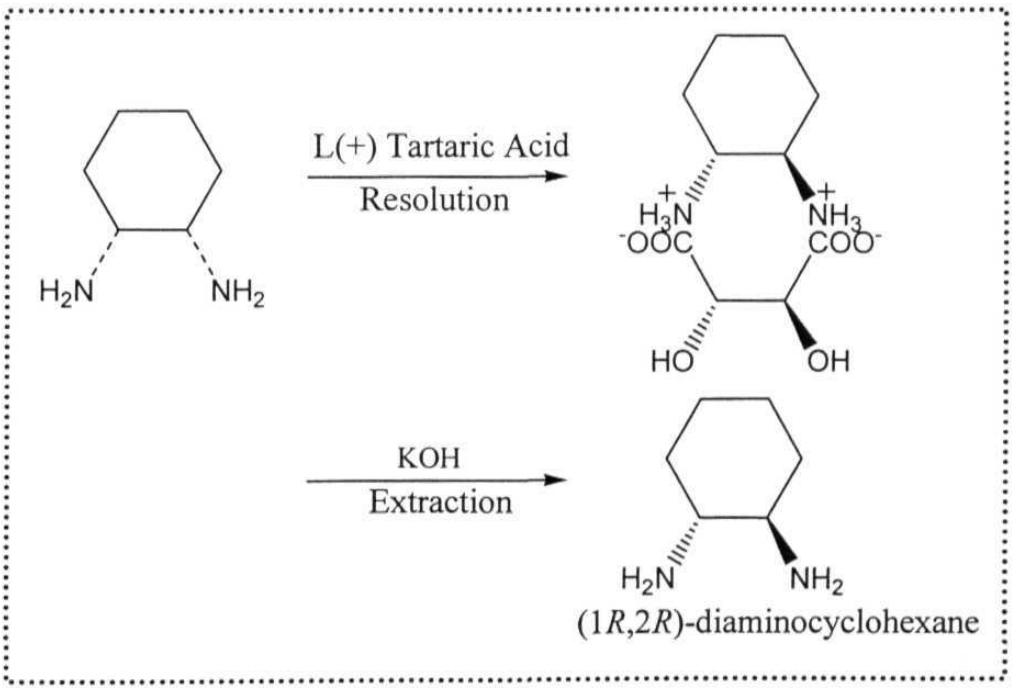

Scheme 3.1. *Resolution of 1,2- diaminocyclohexane.*

(1*R*,2*R*)-diaminocyclohexane: M. P: 46°C; B. P: 44-45°C/4mm Hg; $[\alpha]^{D}_{20}$ = -22 deg cm^2 g^{-1} (4 N HCl); FTIR (neat): $\bar{\upsilon}/cm^{-1}$ = 3354.5, 3348.7 (N-H stretch), 2924.4, 2856.8 (C-H stretch); ^{1}H NMR ($CDCl_3$): δ/ppm = 0.91 – 1.43 (m, 4H), 1.52 – 2.35 (m, 6H), 2.28 – 2.50 (m, 4H); ^{13}C NMR ($CDCl_3$): δ/ppm = 21.8, 25.4, 31.0, 35.5, 51.9, 57.7.

Synthesis of N,N'-bis(4-cyanophenyl)-(1R,2R)-diaminocyclohexane (BCDC).

Synthesis of BCDC has been reported by Kwiit and Gawronski.[41] We have developed a simpler protocol as follows. 0.37 g (3.2 mmol) of (1*R*,2*R*)-diamino-cyclohexane was dissolved in 5 ml DMSO and 2 g anhydrous K_2CO_3 was added with efficient stirring at 140°C; 1 g (8.2 mmol) of 4-fluorobenzonitrile was added slowly. The reaction mixture was stirred at 140°C for 10 h, cooled to 30°C and poured into ice-water with vigorous stirring. The precipitate formed was filtered and washed with ice-cold water. The crude product was purified by column chromatography (neutral alumina; ethyl acetate/hexane 20:80). The reaction procedure is shown in Scheme 3.2. Yield : 0.6 g (60%); M. P: 150°C ; UV-Vis (acetonitrile solution) λ_{max} = 216.2, 293.4 nm; FT-IR (KBr): $\bar{\upsilon}/cm^{-1}$ = 3335.2, 2212.6, 1604.9, 1520.0; ^{1}H-NMR ($CDCl_3$): δ/ppm = 1.20-1.80 (m, 6H), 2.29 (d, 2H), 3.32-3.79 (m, 2H), 4.46-4.52 (m, 2H), 6.55 (d, 4H), 7.29 (d, 4H); ^{13}C-NMR ($CDCl_3$): δ/ppm = 24.5, 32.3, 56.6, 98.5, 112.5, 120.5, 133.7, 150.7.

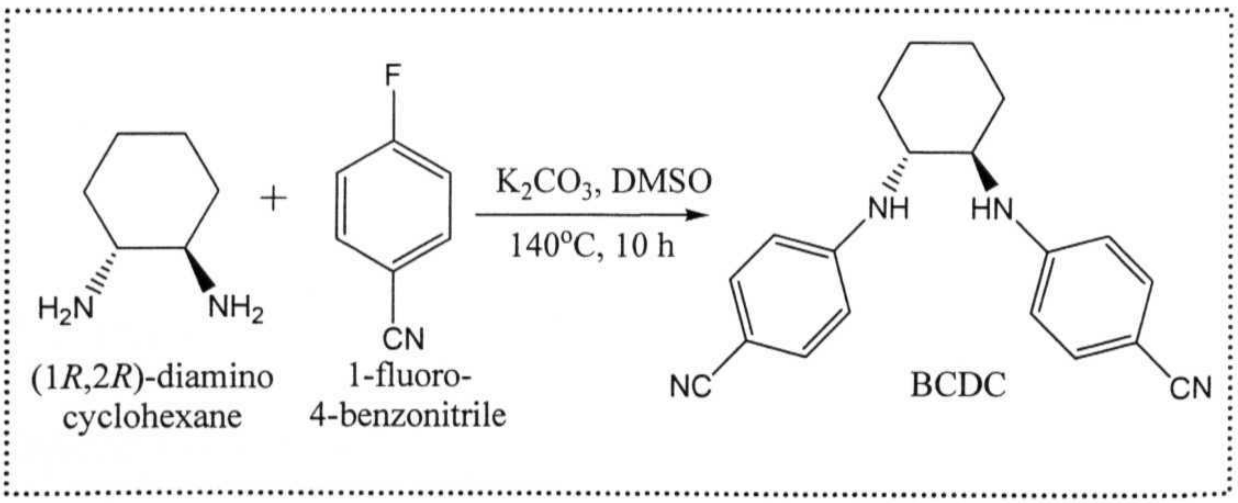

Scheme 3.2. *Synthesis of* ***BCDC***

Synthesis of the coordination polymers

[Ag(BCDC)]ClO_4. 0.05 g (0.22 mmol) of $AgClO_4.H_2O$ dissolved in 5 ml of acetone was added to a solution of 0.07 g (0.22 mmol) of BCDC in 5 ml of acetone. The mixture was stirred for 5 min at 30°C and the white product obtained was filtered, washed with acetone and dried. Yield: 0.1 g, (90%). Crystals were obtained by slow evaporation of acetonitrile solution. M. P: 195°C (dec); UV-Vis (solid pellet; reflectance mode); λ_{max} = 263.4, 348.6 nm; FT-IR (KBr): $\bar{\upsilon}/cm^{-1}$ = 3352.6, 2247.3, 1599.1, 1523.9, 1074.5.

[Cu(BCDC)]PF_6.THF. 0.08 g (0.26 mmol) of BCDC in THF was layered on a solution of 0.1 g (0.26 mmol) of $[Cu(CH_3CN)_4]PF_6$ in dry dichloromethane. Colorless crystals formed in about 48 h. The solution was decanted and the crystals were washed with dichloromethane and THF and dried. Yield : 0.13 g, (80%); M. P: 205°C (dec); UV-Vis (solid pellet; reflectance mode) : λ_{max} = 275.6, 362.2 nm; FT-IR (KBr): $\bar{\upsilon}/cm^{-1}$ = 3414.3, 2243.4, 1597.2,1506.5, 843.0.

[Cu(BCDC)$_2$]PF_6 0.08 g (0.26 mmol) of BCDC in dry dichloromethane was slowly added to a solution of 0.05 g (0.13 mmol) of $[Cu(CH_3CN)_4]PF_6$ in dry dichloromethane. Colorless crystals formed in about 2-3 days. The crystals were removed and washed with dichloromethane and dried. Yield: 0.10 g, (89%); M. P: 170°C (dec); UV-Vis (solid pellet; reflectance mode) : λ_{max} = 263.5, 334.4 nm; FT-IR (KBr): $\bar{\upsilon}/cm^{-1}$ = 3406.6, 2233.7, 1602.9, 1510.4, 846.8.

3.3 ROLE OF THE LIGAND CONFORMATION AND MODE OF LIGATION ON THE FORMATION OF HELICAL AND NETWORK STRUCTURES : CRYSTAL STRUCTURE INVESTIGATIONS

N, N'-bis (4-cyanophenyl)-(1R,2R)-diaminocyclohexane (BCDC)

Crystals were grown by diffusion of hexane into ethyl acetate solution of BCDC. X-ray analysis showed that the crystals belong to the orthorhombic space group $P2_12_12_1$ with one molecule in the asymmetric unit. A water molecule of crystallization is also present. The basic crystallographic data are presented in Table 3.1. The molecular structure of BCDC.H_2O is shown in Fig. 3.2. The water molecule included in the crystal lattice leads to N-H...O ($r_{N7...O25}$ = 3.035 Å, $\theta_{N7-H7...O25}$ = 154.9°) and O-H...N ($r_{O25...N24}$ = 2.999 Å, $\theta_{O25-H25A...N24}$ = 122.7°) hydrogen bond bridges which together with direct N-H...N ($r_{N8...N24}$ = 3.136 Å, $\theta_{N8-H8...N24}$ = 161.8°) hydrogen bonds lead to extended supramolecular networks in the *ab* plane (Fig. 3.3). In contrast to the nitro analog BNDC synthesized in our laboratory earlier,[35] BCDC does not show any helical superstructure. The conformation of the cyanophenyl groups in BCDC may be characterized by the

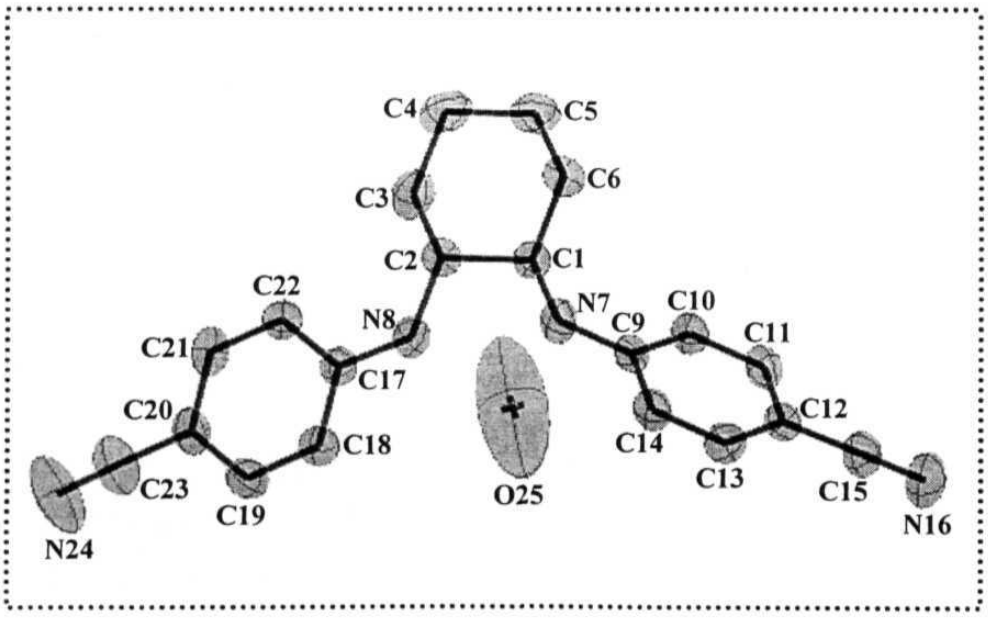

Figure 3.2 *Molecular Structure of* ***BCDC*** *obtained from single crystal analysis. 95% probability thermal ellipsoids are indicated; H atoms are omitted for clarity.*

torsion angle, τ (C_{phenyl}-N-C_{chiral}-C_{chiral}), formed by the phenyl carbon (C9), amino nitrogen (N7), the stereogenic carbon to which the amino group is attached (C1) and the other stereogenic carbon (C2′). The value of τ in the BCDC ligand is 157.9° indicating an *exo* conformation.

Table 3.1 *Crystallographic data for* ***BCDC.H_2O***

Empirical formula	$C_{20}H_{22}N_4O$
Formula weight	334.42
Crystal system	Orthorhombic
Space group	$P2_12_12_1$ (No. 19)
a / Å	7.886(3)
b / Å	15.27(3)
c / Å	15.765(9)
V / $Å^3$	1898(4)
Z	4
$\rho_{calc.}$ / g cm^{-3}	1.170
μ, cm^{-1}	0.70
λ / Å	0.71703
2θ range / deg.	1.86-30.96
Unique reflections	3405
Reflections with $I \geq 2\sigma_I$	1520
No. of parameters	242
GOF	1.026
R [for $I \geq 2\sigma_I$]	0.0535
wR^2[for $I \geq 2\sigma_I$]	0.1204

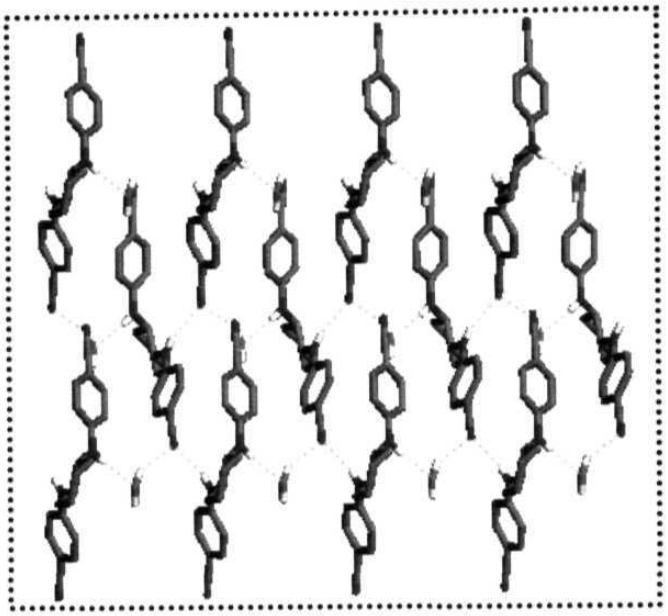

Figure 3.3 *Molecular packing in* ***BCDC.H_2O*** *from single crystal analysis; C(grey), N(Blue), O(red) and H(white) and H-bonds (broken cyan lines) are shown. Amino and water hydrogen atoms alone are shown.*

[Ag(BCDC)]ClO_4 (SBP)

Colorless crystals of SBP were grown from acetonitrile solution by slow evaporation. X-ray analysis revealed orthorhombic space group $P2_12_12_1$ with two molecules in the asymmetric unit. The basic crystallographic data are collected in Table 3.2. The molecular structure of SBP is shown in Fig. 3.4. The silver is coordinated by two cyano nitrogens from two different BCDC ligand molecules. Unlike the majority of known Ag(I)-aryl cyano complexes with tetrahedral coordination,[42] the present complex shows linear coordination environment around the metal center; even when excess of the BCDC ligand is employed in the reaction, the same complex with 1:1 mole ratio of metal and ligand is obtained. Significant bond lengths and bond angles in SBP around the metal site are listed in Table 3.3.

Significantly, the conformation of the cyanophenyl groups in BCDC are now oriented *endo* ($\tau = 89.3^{\circ}$), leading to a helical polymer chain formation through the Ag(I)

links (Fig. 3.5). The perchlorate counterions reside in the channels formed by the helical structure (Fig. 3.6a). H-bonding interactions between the amino nitrogen atoms of BCDC and oxygen atoms of the perchlorate ions ($r_{N2...O4}$ = 3.311 Å; $\theta_{N2-H2...O4}$ = 144.3°, $r_{N2...O5}$ = 3.401 Å; $\theta_{N2-H2...O5}$ = 157.1°, $r_{N3...O6}$ = 3.083 Å; $\theta_{N3-H3...O6}$ = 157.9°) connect the helical chains of the SBP along the *b* direction (Fig. 3.6b).

Table 3.2 *Crystallographic data for* ***SBP, CBPT*** *and* ***CBP.***

Identification code	**SBP**	**CBPT**	**CBP**
Empirical formula	$C_{40}H_{40}Ag_2Cl_2N_8O_8$	$C_{14}H_{18}Cu_{0.5}F_3N_2OP_{0.5}$	$C_{40}H_{40}CuF_6N_8P$
Formula Weight	1047.44	334.56	841.31
Crystal system	Orthorhombic	Orthorhombic	Orthorhombic
Space group	$P2_12_12_1$ (No. 19)	$P22_12_1$ (No. 18)	$P2_12_12_1$ (No. 19)
a / Å	9.488(3)	9.5577 (9)	10.0500 (6)
b / Å	14.094(3)	10.4800 (12)	18.3035 (10)
c / Å	31.354(4)	15.639 (2)	24.8967 (13)
V / $Å^3$	4193.0(16)	1566.5 (3)	4579.8 (4)
Z	8	4	4
$\rho_{calc.}$ / g cm^{-3}	1.659	1.419	1.220
μ / mm^{-1}	11.2	0.82	0.57
T_{min}, T_{max}	0.955, 0.999	0.975, 0.999	0.753, 0.899
λ / Å	0.71703	0.71703	0.71703
2θ range / deg.	1.3-25.47	2.13-31.96	1.64-28.27
unique reflections	4368	3030	10764
Reflection with $I \geq 2\sigma_I$	3794	1530	7761
No. of parameters	561	196	505
GOF	1.198	1.155	0.996
R [for $I \geq 2\sigma_I$]	0.0445	0.0653	0.0540
WR^2 [for $I \geq 2\sigma_I$]	0.1194	0.1464	0.1468

Table 3.3. *Significant bond lengths and angles in **SBP**; see Fig. 3.4 for atom labeling.*

Bond / Bonds	Distance (Å) / Angle (°)
Ag(1)-N(8)	2.102(6)
Ag(1)-N(1)	2.105(7)
Ag(2)-N(5)	2.092(6)
Ag(2)-N(4)	2.106(6)
N(1)-C(1)	1.123(10)
N(4)-C(20)	1.132(9)
N(5)-C(21)	1.135(10)
N(8)-C(40)	1.125(10)
N(8)-Ag(1)-N(1)	163.4(4)
N(5)-Ag(2)-N(4)	169.9(4)

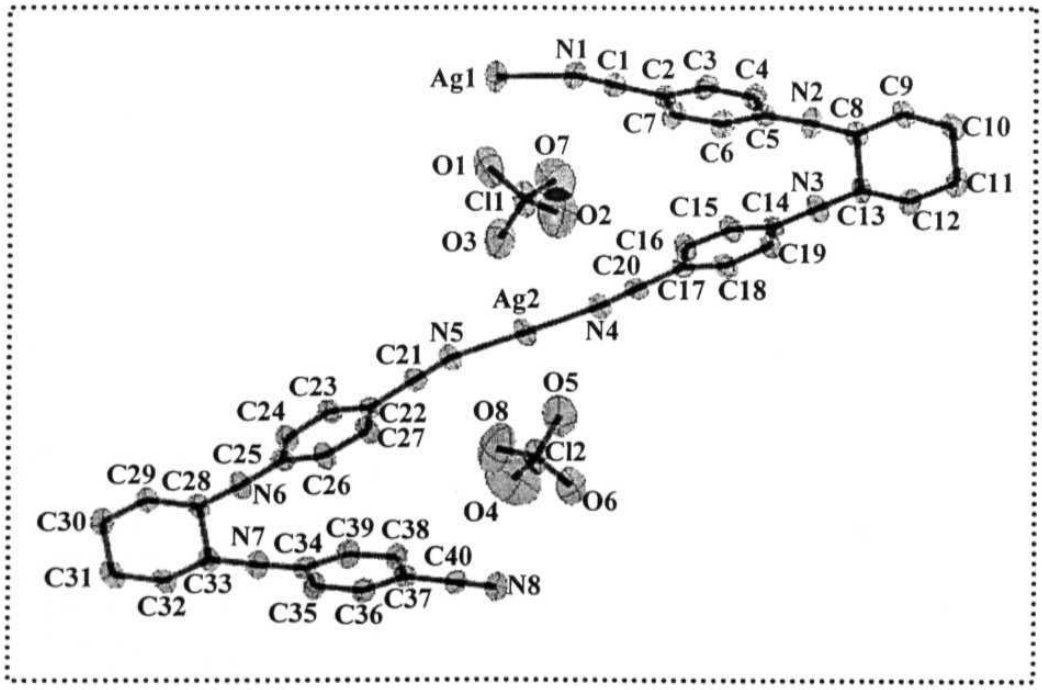

Figure 3.4 *Molecular Structure of **SBP** obtained from single crystal analysis. 95% probability thermal ellipsoids are indicated; H atoms are omitted for clarity.*

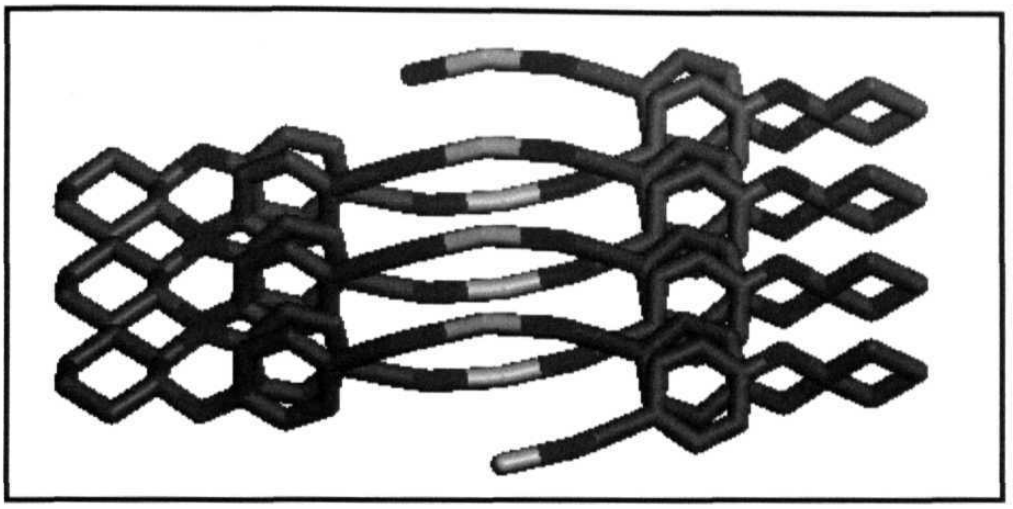

Figure. 3.5a *Helical polymeric chain in **SBP** along b axis; hydrogen atoms and perchlorate ions are omitted for clarity; C (grey), N (blue), Ag (Cyan).*

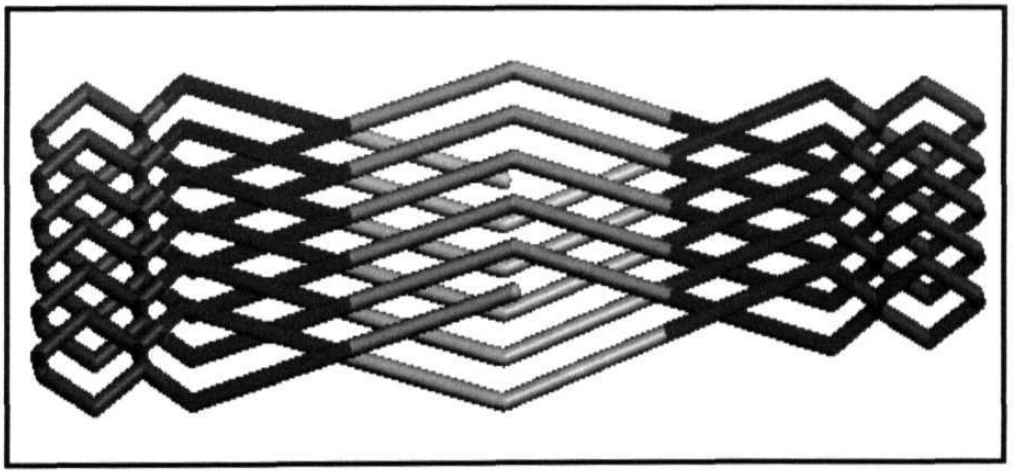

Figure. 3.5b *Schematic diagram of the helical chain; the cyanophenyl groups have been removed and amino nitrogens are connected directly to silver to demonstrate the helical structure.*

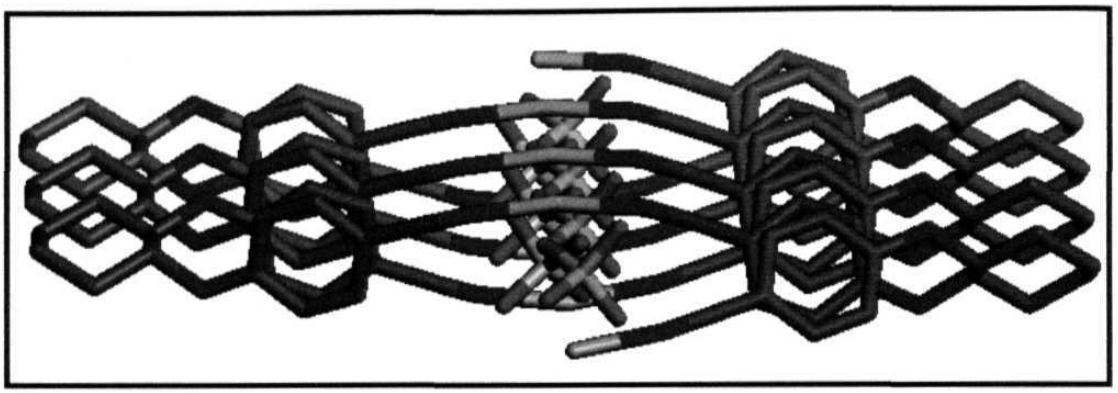

Figure 3.6a *The helical channel occupied by the perchlorate ions in* ***SBP****.*

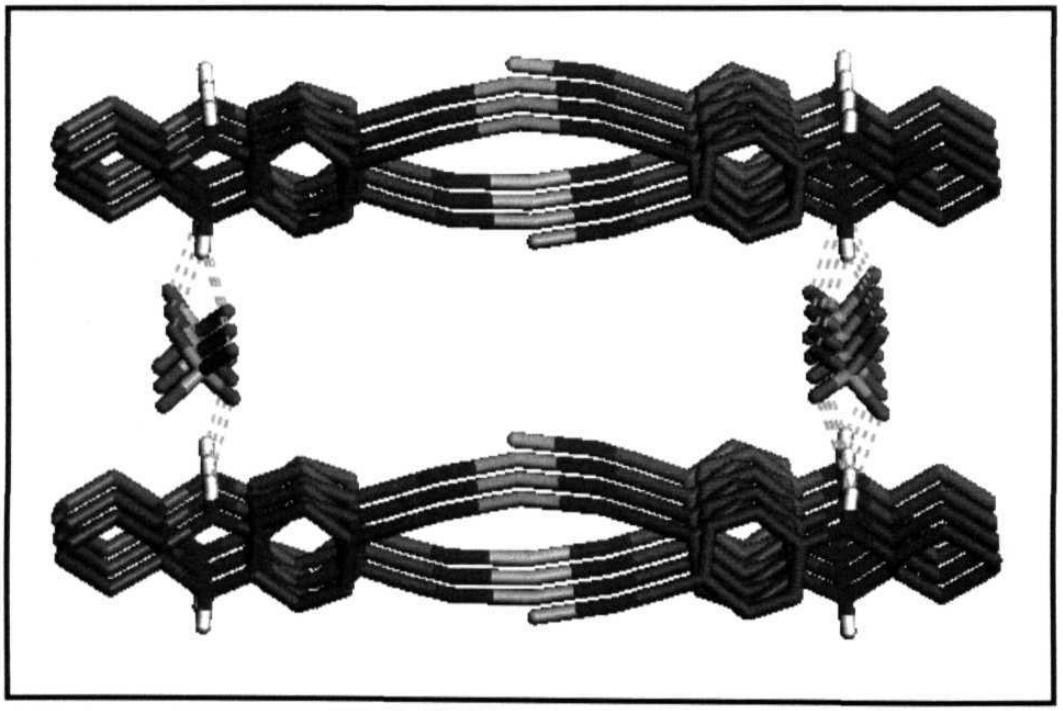

Figure 3.6b *Linking of helical chains through H-bond interactions.*

[Cu(BCDC)]PF_6.THF (CBPT)

Layering a solution of BCDC in THF on top of a solution of $[Cu(CH_3CN)_4]PF_6$[12] in dichloromethane yielded crystals of $[Cu(BCDC)]PF_6$ at the interface. The crystals belong to $P22_12_1$ space group with half the molecule and a molecule of THF in the asymmetric unit. The basic crystallographic data are presented in Table 3.2. The molecular structure of CBPT is given in Fig. 3.7. Cu(I) is tetrahedrally coordinated to the two amino nitrogens of BCDC and the cyano nitrogens of two other BCDC ligand molecules. The significant bond lengths and bond angles near the metal center given in Table 3.4 show values typical of Cu(I) - cyano and Cu(I) – amino coordination.[43] In CBPT the BCDC retains the *exo* conformation of the cyanophenyl groups to accommodate the Cu(I) coordination at the amino sites and the τ is 164.9°. The metal coordination leads to extended two-dimensional networks (Fig. 3.8). Hexafluoro-phosphate ions and THF appear in the channels formed by network. The hexafluorophosphate ions are not involved in any short intermolecular contacts. The amino groups of BCDC are engaged in H-bonds with the oxygen atom of the THF

Table 3.4. *Significant bond lengths and angles in **CBPT**; see Fig. 3.7 for atom labeling.*

Bond / Bonds	**Distance (Å) / Angle (°)**
Cu1-N3′	2.213(6)
Cu1-N3″	2.213(6)
Cu1-N4	1.897(6)
Cu1-N4′	1.897(6)
N4-C14	1.124(8)
N4′-C14′	1.124(8)
N3′-Cu1-N3″	79.0(3)
N3′-Cu1-N4	106.8(2)
N3′-Cu1-N4′	107.3(2)
N3″-Cu1-N4	107.3(2)
N3″-Cu1-N4′	106.8(2)
N4-Cu1-N4′	135.2(4)

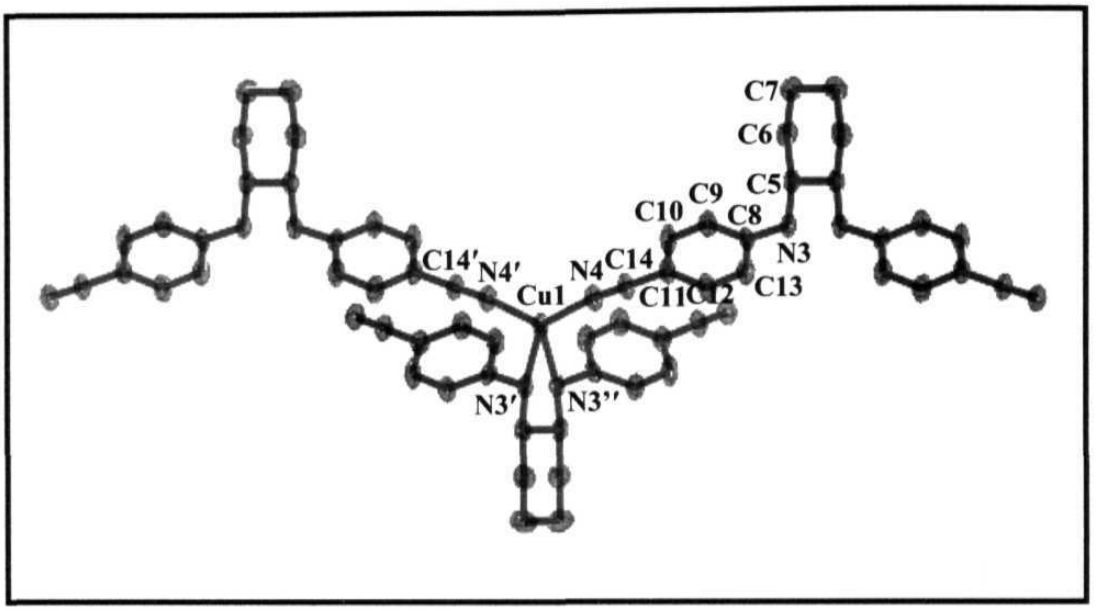

Figure 3.7 *Molecular Structure of* ***CBPT*** *from single crystal analysis. 95% probability thermal ellipsoids are indicated; H atoms are omitted for clarity.*

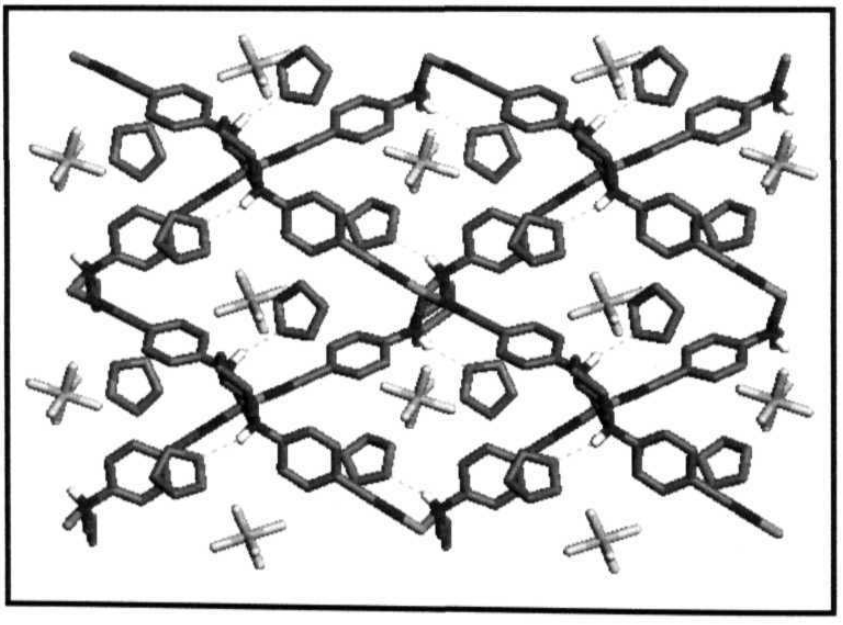

Figure 3.8 *Crystal structure of* ***CBPT*** *viewed along the a axis; hydrogen atoms are omitted for clarity. C (grey), N (blue), Cu (orange), P (magenta), F (cyan), O (red), H-bonds (broken cyan line).*

molecules in the lattice. The individual strands in the network have a *zig-zag* structure; no helical superstructure is observed. Fig. 3.9 provides a schematic representation of the two-dimensional rhombus network in CBPT; the BCDC (in *exo* conformation) connecting the Cu(I) sites are represented using straight lines, the Cu(I)....Cu(I) distances being 9.467 Å.

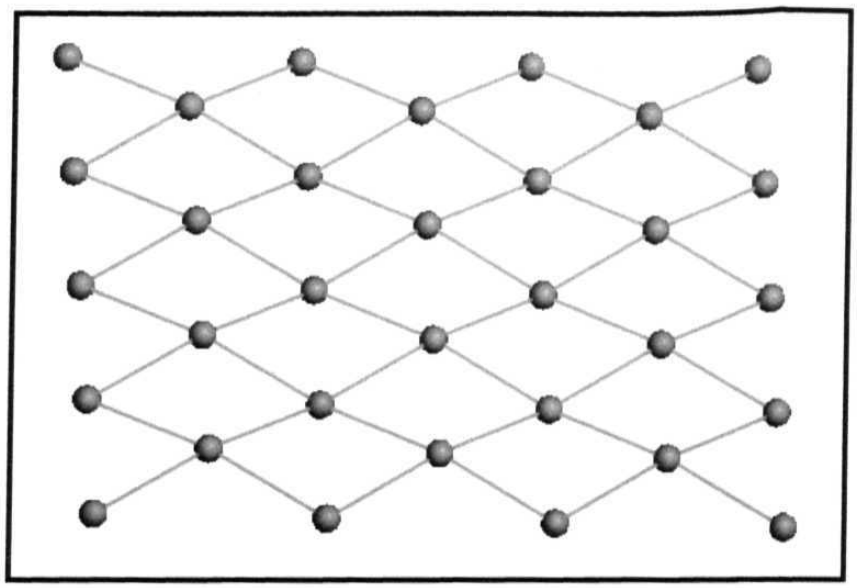

Figure 3.9 *Schematic diagram of the network topology in* ***CBPT****. The spheres represent Cu(I) and the lines, the bridging* ***BCDC*** *ligands in exo conformation.*

[Cu(BCDC)]PF_6 (CBP)

Colorless crystals of CBP were grown from dichloromethane solution containing BCDC and $[Cu(CH_3CN)_4]PF_6$. X-ray analysis showed that CBP belongs to orthorhombic $P2_12_12_1$ space group with half the molecule in the asymmetric unit. The basic crystallographic data are collected in Table 3.2. The molecular structure is presented in Fig. 3.10. In CBP, four BCDC ligands are coordinated tetrahedrally to Cu(I) through one of the cyano nitrogen atoms from each. CBP also shows an extended network structure as in CBPT, but with a three-dimensional connectivity. Interestingly, the CBP crystal lattice shows the presence of different conformations of the ligand BCDC. Two of the

BCDC's are in *exo* conformation ($\tau = 161.0^{\circ}$) and the other two in *endo* conformation ($\tau = 93.1^{\circ}$, since the BCDC's are close to, but not exactly C_2 symmetric, these τ are average values). The significant bond lengths and bond angles near the metal center in the CBP crystals listed in Table 3.5 show values typical of Cu(I) - cyano coordination.[43] It is seen that the local symmetry at the metal in CBP is close to, but not exactly T_d.

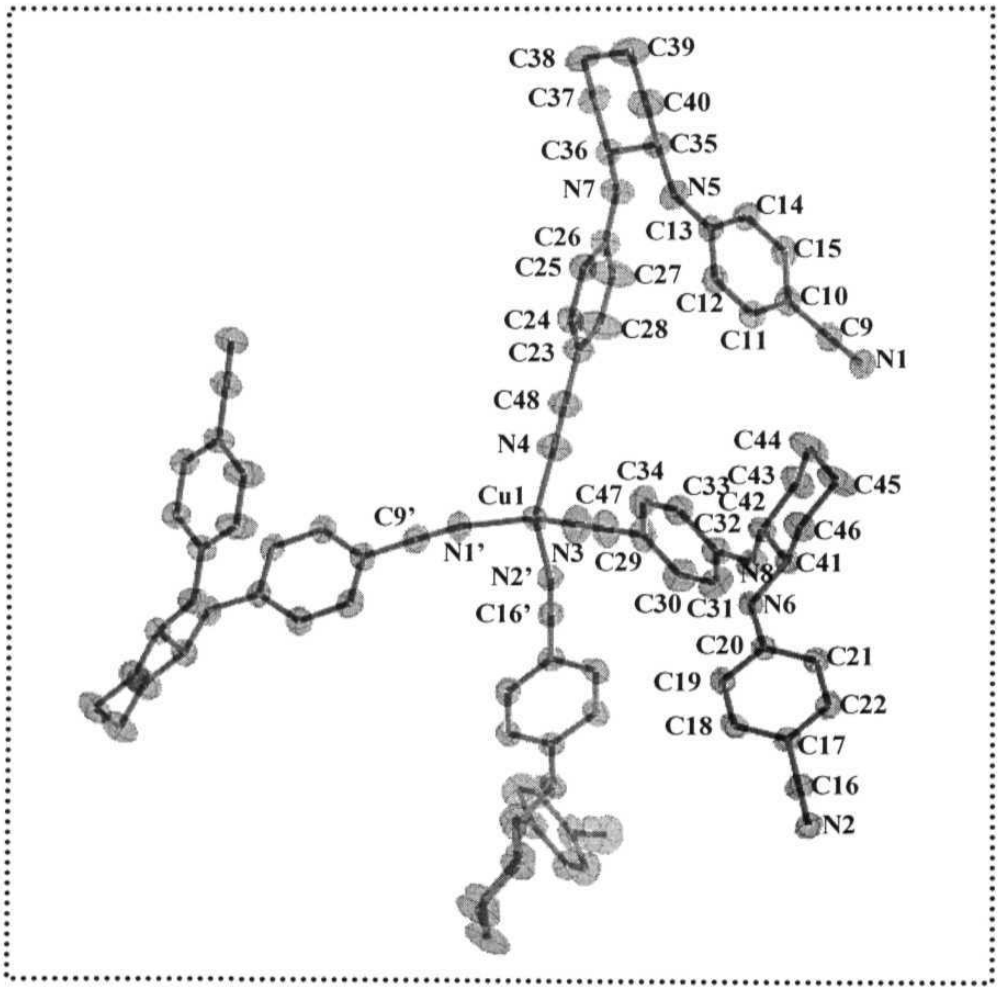

Figure 3.10 *Molecular Structure of **CBP** obtained from single crystal analysis. 95% probability thermal ellipsoids are indicated; H atoms are omitted for clarity.*

Table 3.5. *Significant bond lengths and angles in **CBP**; see Fig. 3.10 for atom labeling.*

Bond / Bonds	**Distance (Å) / Angle (°)**
Cu1-N1′	1.986(3)
Cu1-N2′	1.981(3)
Cu1-N3	1.980(3)
Cu1-N4	1.979(3)
N1-C9	1.131(5)
N2-C16	1.148(4)
N3-C47	1.142(5)
N4-C48	1.140(5)
N1′-Cu1-N2′	102.43(12)
N1′-Cu1-N3	112.64(15)
N1′-Cu1-N4	113.42(15)
N2′-Cu1-N3	110.50(15)
N2′-Cu1-N4	115.93(15)
N3-Cu1-N4	102.29(18)

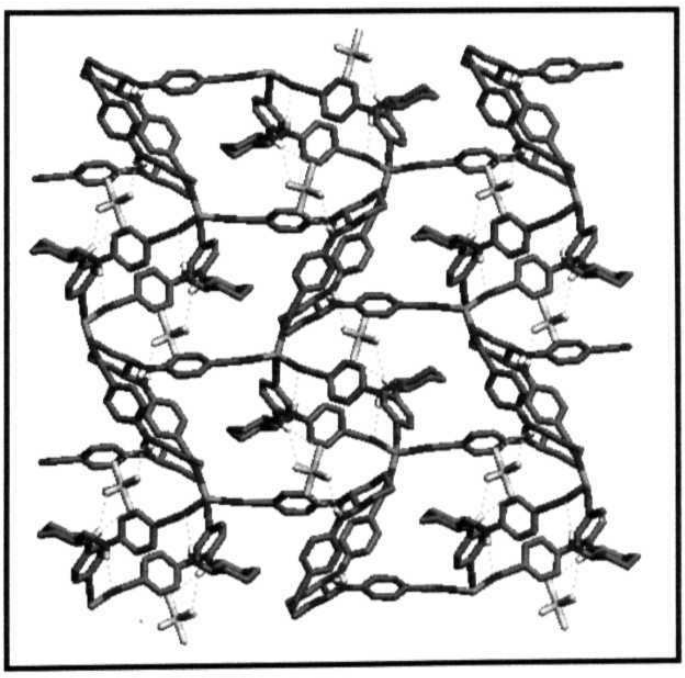

Figure 3.11 *Crystal structure of **CBP** viewed along the a axis; hydrogen atoms are omitted for clarity. C (grey), N (blue), Cu (orange), P (magenta), F (cyan), H-bonds (broken cyan line).*

The extended structures of the coordination polymers of CBP and CBPT are grossly different in the two crystals. In the CBP structure, the PF_6^- ions as well as the cyano groups of BCDC form H-bonds with the amino groups of the BCDC leading to extended structures (Fig. 3.11). Comparison of the structures of CBPT and CBP shows that the presence of THF in the crystallization medium has led to its inclusion in the structure of CBPT and considerable variation in the conformation of BCDC and ligation around Cu(I). The net impact may be visualized in terms of the network topology arising in the crystals. The topology of CBP is more fascinating than that in the CBPT. The tetrahedrally coordinated BCDC's around the Cu(I) sites in CBP, lead to a three-dimensional architecture that can be described as an interwoven structure of three diamondoid networks (Fig. 3.12). There is a succession of layers, constituted of six-member rings in elongated chair conformation, from each of the diamondoid networks; the interconnections between the layers are also elongated. The Cu(I)....Cu(I) distances within the layer are 10.406 and 18.148 Å and that between the layers is 18.148 Å; the short and long distances correspond respectively to the bridging BCDC in *endo* and *exo* conformations.

The structure of CBP can also be visualized as a combination of helical superstructure formations involving Cu(I) and BCDC ligands in different directions. The two different conformations of the BCDC ligand in CBP lead to different helical chain formations in three directions. Interestingly, in one direction both conformations are involved and in the other two directions either one of the conformations of the BCDC ligand is involved in the helical structure formation. A 2_1 chain structure is formed along the *a* axis mediated by the BCDC in *exo* conformation. The topological representation and the space-filling model of the 2_1 chains are given Figs. 3.13a and 3.14a respectively. Similarly, an extended 2_1 chain structure is formed along the *b* direction by BCDC in *endo* conformation (Figs. 3.13b and 3.14b). The helical assembly along the *c* axis is built up of *exo* and *endo* conformations of the BCDC ligands alternating along each chain. The topological representation of the helical structure is given in Fig 3.13c and the space-filling model in Fig. 3.14c.

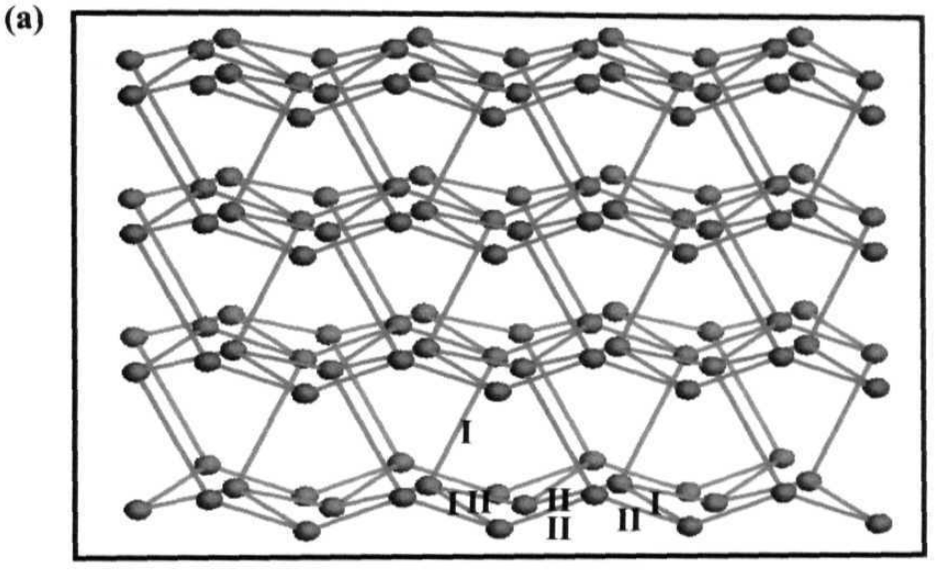

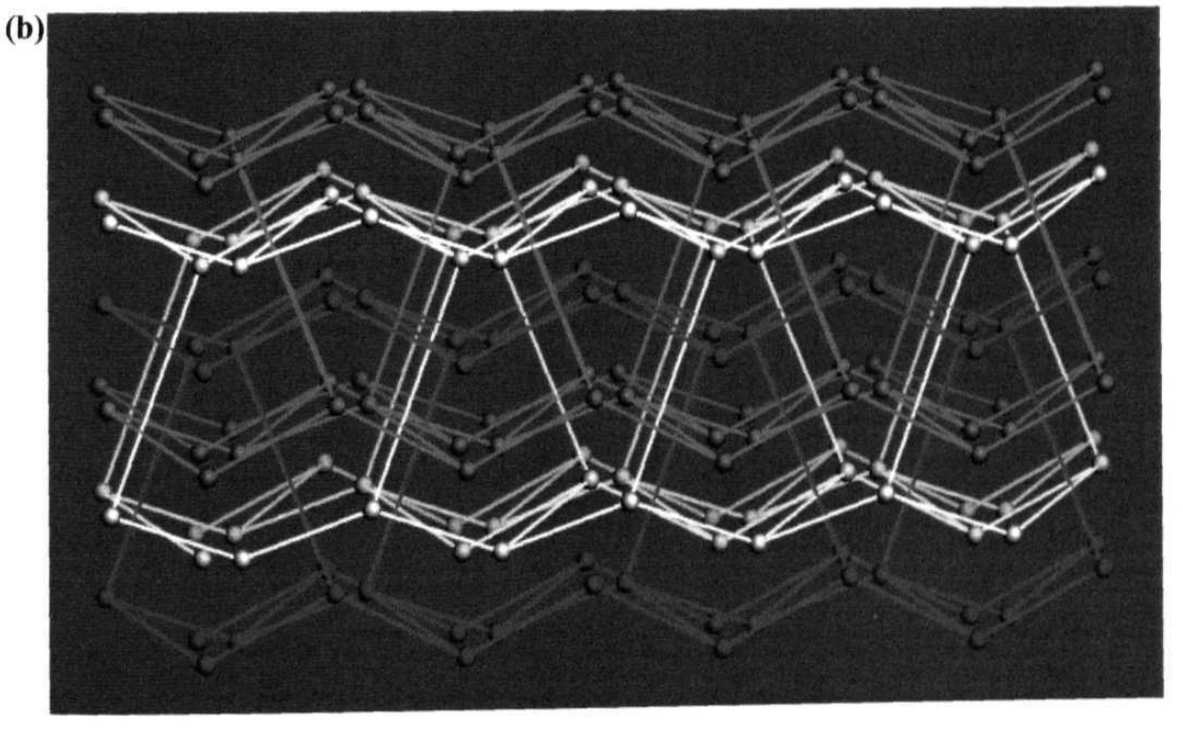

Figure 3.12 *Schematic diagram of the network topology in* ***CBPT****; (a) a single diamondoid network and (b) the interwoven diamondoid networks (the three networks are shown in different colors). The spheres represent Cu(I) and the lines, the bridging BCDC ligands in exo (I) and endo(II) conformations.*

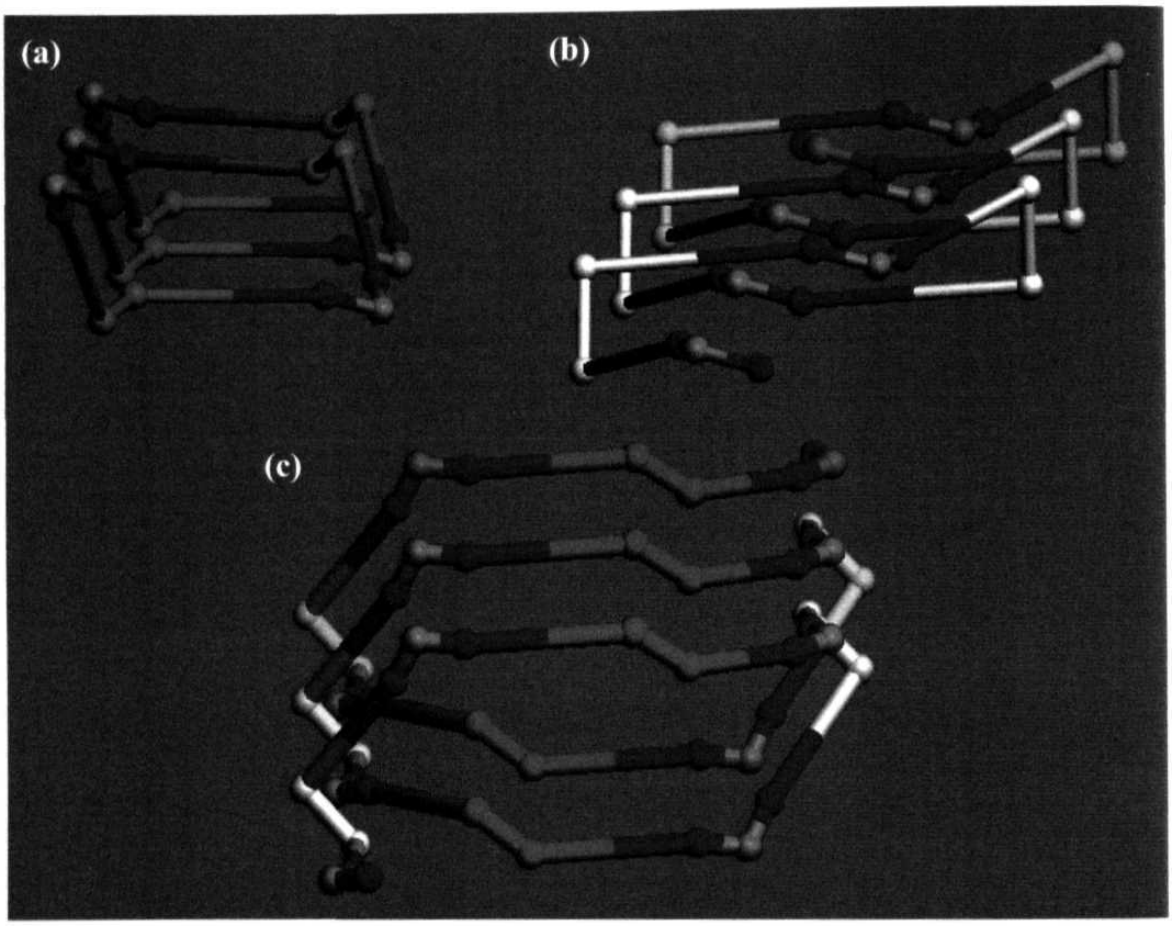

Figure 3.13 *Schematic diagram of the helical formations in **CBPT** along (a) a, (b) b and (c) c axes. The orange spheres represent Cu(I), the blue spheres, the cyano nitrogen atoms and the green and and white spheres the amino nitrogen atoms; the nitrogen atoms with the connecting lines denote the **BCDC** ligand. The green and white nitrogen atoms relate to **BCDC** in exo and endo conformations respectively.*

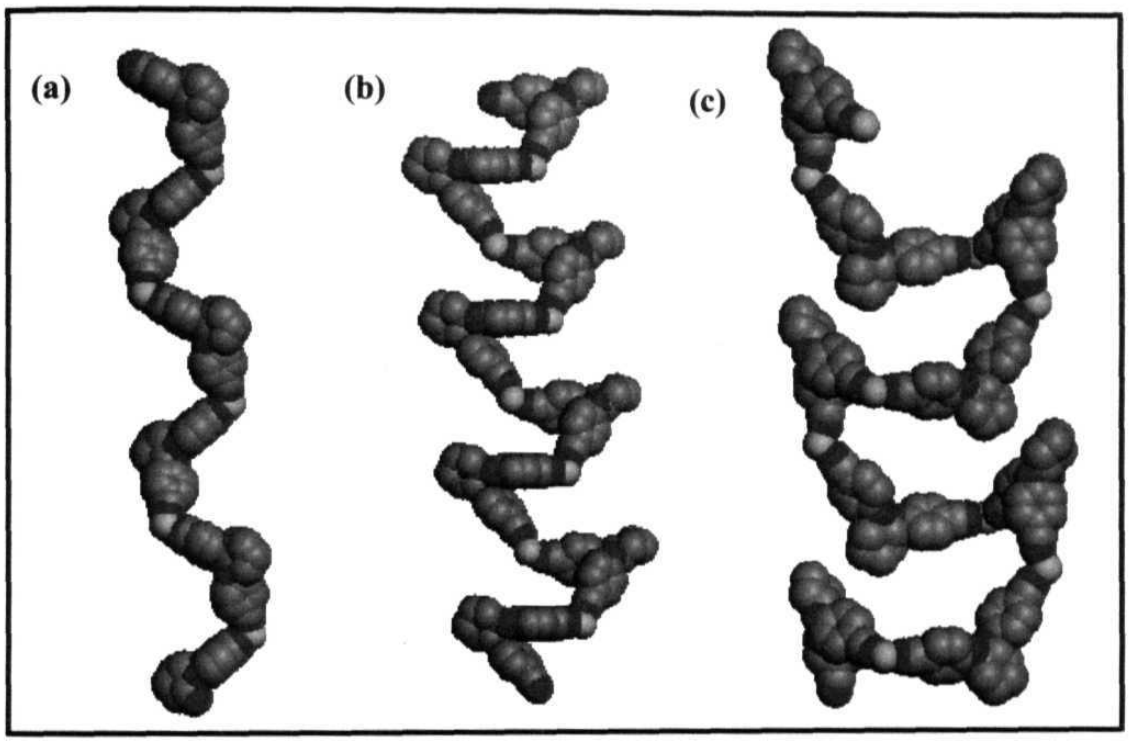

Figure 3.14 *Space-filling representations of (a) 2_1 chain along a, (b) 2_1 chain along b axis and (c) helical chain along the c axis in crystals of* ***CBP****.*

3.4 OPTICAL SECOND HARMONIC GENERATION : IMPACT OF THE STRUCTURAL MOTIFS

Donor-acceptor conjugated systems generally possess large hyperpolarizability which can be enhanced further by the coordination of electropositive metals at the acceptor site. The chirality coupled with multiple ligation sites of BCDC ligand has allowed us to fabricate coordination polymer topologies with noncentrosymmetric solid state organization and exhibiting different dimensionalities. This factor and push-pull nature of the BCDC-metal ion combination, suggests potential second order nonlinear optical effects in these materials and the possibility of investigating potential structure-property correlations in the coordination polymers. We have carried out Kurtz-Perry SHG measurements[44] on BCDC and the metal complexes; SHG variation with particle

size indicates phase-matchable behavior in all cases. The details of the experimental procedure are given in Appendix C. BCDC shows a moderate value saturating at 0.3 U (1U = SHG of urea). Interestingly, the complexation of Ag(I) at the cyano sites alone in $[Ag(BCDC)]ClO_4$ causes a nearly ten-fold increase in the SHG to 2.9 U compared to the free ligand BCDC. Complexation of Cu(I) at the amino and cyano sites in $[Cu(BCDC)]PF_6$ leads to a small reduction in the SHG to 0.2 U. Repeated experiments[44] with CBP, however, showed that it has no measurable SHG. The SHG data on BCDC and its coordination polymers are collected in Table 3.6.

The bulk SHG from materials are controlled by the molecular hyperpolarizability as well as the molecular organization. The difference in the SHG observed between BCDC ligand, SBP, CBPT and CBP coordination polymers can be analyzed by considering the different coordination modes and local metal-ligand structure as well as the very different network topologies in the three structures. The enhanced SHG observed in SBP is possibly linked to the formation of the helical superstructure.[27,35] It is interesting to note that the SHG reported in several helical coordination polymers[27,45] is ~ 1U.

The linear coordination of BCDC around Ag(I) gives it a nonpolar character whereas the asymmetric nature of ligation around Cu(I) in CBPT gives it appreciable dipolar character. The corresponding unit in CBP can be described formally as an octupolar system even though the dipolar component does not strictly vanish. The potential utility of octupolar systems in quadratic NLO applications was first highlighted by the seminal work of Zyss,[46] wherein a systematic appraisal of the dipolar/octupolar contributions to the nonlinear response of molecules and materials was presented. Large hyperpolarizabilities have since then been demonstrated in octupolar molecules.[47] At the bulk level, SHG has been obtained in polymer films with optically oriented octupolar molecules[48] as well as a host of two and three-dimensional coordination polymers based on octupolar building blocks.[37] The fundamental question of optimal molecular organization that would lead to enhanced bulk nonlinearity has been addressed in the case of dipolar systems early on[49] and for the two-dimensional octupolar systems more recently.[50] In the present study, it appears that the evolution from one-dimensional organization in SBP and two-dimensional organization in CBPT to a three-dimensional

one in CBP has had an adverse impact on the SHG capability. If we consider the SHG observed in the three coordination polymers of three different dimensionality, a correlation emerges between the dimensionality of the network topology and the nonlinear optical response; in this family of coordination polymers based on BCDC, lower dimensionality is more favorable. It is pertinent to note that mutually orthogonal helical motifs leading to three-dimensionally connected structures have been found to exhibit relatively lower SHG capability than helical superstructures formed along a single crystallographic direction, in polymorphs of an organic material studied in our laboratory.[35] The structure around the metal, dipolar in CBPT, octupolar in CBP and linear and nonpolar in the Ag(I) polymer, does not appear to have a direct correlation to the observed SHG. These arguments provide a framework to visualize the difference in the solid state SHG capability of SBP, CBPT and CBP in the context of the hierarchy in their network structural motifs.

Table 3.6 *SHG of microcrystalline powders of* ***BCDC, SBP*** *and* ***CBPT*** *at various particle sizes. 1 U = SHG of urea having particle size > 150 μm.*

Compound	SHG (U)				
	Particle size (μm)				Average value at saturation
	100-150	150-200	200-250	250-300	
$BCDC.H_2O$ (BCDC)	0.21	0.22	0.19	0.28	0.22
$[Ag(BCDC)]ClO_4$ (SBP)	2.4	2.4	2.5	2.9	2.5
$[Cu(BCDC)PF_6]THF$ (CBPT)	0.19	0.18	0.22	0.20	0.20

The anion can influence the formation of the extended structures. However, investigation of the hexafluorophosphate and perchlorate salts of the Cu(I) complex and the nitrate and perchlorate salts of the Ag(I) complex indicated that the SHG is largely independent of the anion. In view of the discussion of optimal organization of dipolar and octupolar systems referred to above, cognizance should be taken of the fact that

neither of the individual structures of one, two and three-dimensional networks in the present study have been optimized through any systematic approach. Hence, exploration of several more families with different dimensionality of the systems is essential to test the generality of the present observations.

3.5 INFLUENCE OF THE LIGAND CONFORMATION AND COORDINATION OF THE METAL ION ON THE HYPERPOLARIZABILITY : A COMPUTATIONAL STUDY

We have carried out some simple computational studies to gain insight into the influence of the conformation of BCDC and the coordination of the metal ion on the β. As stated earlier, the conformation of the cyanophenyl groups in BCDC may be characterized by the torsion angle, τ (C_{phenyl}-N-C_{chiral}-C_{chiral}). In the molecular structure from single crystal analysis, the τ are respectively 157.9, 89.3 and 164.4 in BCDC, SBP and CBPT respectively, representing *exo*, *endo* and *exo* conformations. In CBP, the Cu(I) metal ions are coordinated to four cyano nitrogens of four different BCDC molecules. Two of the BCDC's are in *exo* conformation ($\tau = 161.0^{o}$) and the other two in *endo* conformation ($\tau = 93.1^{o}$) (as noted above, since the BCDC's are close to, but not exactly C_2 symmetric, these τ are average values).

Several studies[25] have employed semiempirical as well as *ab initio* methods to compute β of metal-organic systems. We have computed the static hyperpolarizability of the ligand structures using the AM1/TDHF[51] method; the geometries from crystal structure were used and H atom positions alone were optimized. The influence of the metal ions were assessed by placing point positive charges at the relevant sites, since parameters for Ag(I) and Cu(I) are not available in this program. The computed β are collected in Table 3.7. The trends are in tune with classical push-pull concepts.[18] They are further confirmed using *ab initio* computations[52] at the B3LYP/3-21G* level carried out on the same structures, but now with Cu(I) and Ag(I) metals in place.[36] It is observed that the *endo* orientation of the phenyl rings leads to larger β. More significantly, the β is reduced by the coordination of Cu(I) at the cyano and amino groups whereas it is enhanced by coordination of Ag(I) at the cyano groups alone. Most notably, the

computed β parallel the observed solid state SHG values in BCDC, SBP and CBPT; the molecular nonlinearity appears to exert a dominant influence on the bulk property. This investigation shows that the SHG of these materials is primarily controlled by the ligand conformation and the mode of metal coordination, and not so much affected by the specific metal itself. In the case of CBP, the computations showed that the *exo* and *endo* forms possess respectively, β_0 values 14.17 x 10^{-30} and 21.66 x 10^{-30} esu. The higher β_0 of *endo* conformation compared to that of the *exo* conformation once again point to impact of the conformation of the BCDC on the β. In spite of the higher hyperpolarizability of the units in the polymer, CBP shows no observable SHG. This indicates the significant role of the mode of coordination around the metal ion and the resulting connectivity and network topology in these materials.

Table 3.7 *Computed static hyperpolarizabilities of* ***BCDC*** *(in the free form and as ligands in the metal complexes) and the* ***BCDC/metal*** *systems. In the AM1/TDHF computations on the complexes, the metal ions are replaced by point charges. Geometries are taken from the appropriate crystal structures with H atoms alone optimized in the AM1 method.*

Structure		β / 10^{-30}esu
BCDC	**Ligand**	7.49
CBPT	**Ligand**	4.44
	Ligand/3Cu(I)†	3.99
SBP	**Ligand**	9.66
	Ligand/2Ag(I)‡	22.35
CBP	**Ligand/2Cu(I)**†	14.17
	Ligand/2Cu(I)‡	21.66

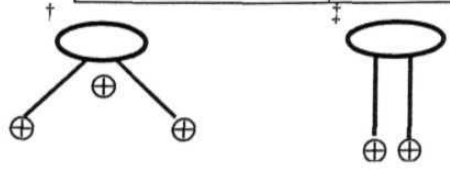

3.6 SUMMARY

We have synthesized a novel C_2-symmetric ligand with 'push pull' framework coupled with multiple ligation sites. The capability of multiple ligation of BCDC has been utilized to fabricate a series of fascinating coordination polymer topologies. The ligand is shown to adopt different conformations in the different systems. The coordination of BCDC ligand with Ag(I) metal ions leads to one-dimensional helical chains which show an enhanced SHG capability compared to the ligand. The structures of the Cu(I)-BCDC complex arising as a result of the difference in the crystallization solvent, manifest clearly different conformations of the ligand, modes of ligation and polymer network topologies. The Cu(I) coordination with BCDC in presence of THF leads to the inclusion of the solvent in the lattice as well as the formation of two-dimensional network structure that shows reduction in the bulk SHG, with respect to the ligand. The second Cu(I)-BCDC complex shows three-dimensional interwoven diamondoid coordination network structure. The molecular structure contains both *exo* and *endo* conformation of the BCDC leading to the formation of helical superstructure along each Cartesian direction and no observable SHG.

The consequence of the helical one-dimensional chain and hierarchical, two-dimensional network and three-dimensional diamondoid structures for the solid state SHG is quite interesting. The increase in dimensionality shows an adverse effect on the bulk SHG in these systems. Influence of the conformation of the ligand and the mode of coordination of the metal ions on β has been analyzed by simple computational investigations. The simple models involved provide meaningful insight into the trends of molecular nonlinearity in these polymeric systems and suggest a convenient approach to the design of coordination polymers for SHG applications.

REFERENCES

1. (a) Hoskins, B. F.; Robson, R. *J. Am. Chem. Soc.* **1990**, *112*, 1546; (b) Kawata, S.; Konda, M.; Furuchi, L.; Munakata. *Chem. Int. Ed. Engl.* **1994**, *33*, 1759.
2. Cheetham, A. K.; Ferey, G.; Louseau, T. *Angew. Chem. Int. Ed. Engl.* **1999**, *38*, 3268.
3. Kauranen, K.; Verviest, T.; Bouttoon, C.; Teerenstra, M. N.; Clays, K.; Schouten, A. J.; Nolte, R. J. M.; Pearsons, A. *Science* **1995**, *270*, 966.
4. (a) Janiak, C. *Dalton Trans.* 2003, 2781; (b) Kitagawa, S.; Noro, S. *Coord. Chem. II* **2004**, *7*, 231; (c) James, S. L. *Chem. Soc. Rev.* **2003**, *32*, 276.
5. (a) Batten, S. R.; Robson, R. *Angew. Chem. Int. Ed. Engl.* **1998**, *37*, 1461; (b) Hirsch, K. A.; Wilson, R. S.; Moore, J. S. *Chem. Eur. J.* **1997**, *3*, 765.
6. Hennigar, T. L.; MacQuarrie, D. C.; Losier, P.; Rogers, R. D.; Zaworotko, M. J. *Angew. Chem. Int. Ed. Engl.* **1997**, *36*, 972.
7. Moulton, B.; Zaworotko, M. J. *Chem. Rev.* **2001**, *101*, 1629.
8. Barnett, S. A.; Blake, A. J.; Champness, N. R.; Wilson, C. *Chem. Commun.* **2002**, 1640.
9. Janiak, C.; Hemling, H. *J. Chem. Soc. Dalton Trans.* **1994**, 2947.
10. Soldatov, D. V.; Zanina, A. S.; Enright, G. D.; Ratcliffe, C. I.; Ripmeester, J. A. *Cryst. Growth Des.* **2003**, *3*, 1005.
11. Soldatov, D. V.; Ripmeester, J. A.; Shergina, S. I.; Sokolov, I. E.; Zanina, A. S.; Gromilov, S. A.; Dyadin, Y. A. *J. Am. Chem. Soc.* **1999**, *121*, 4179.
12. Muthu, S.; Yip, J. H. K.; Vittal, J. J. *J. Chem. Soc. Dalton Trans.* **2001**, 3577.
13. Tong, M.; Chen, X.; Batten, S. R. *J. Am. Chem. Soc.* **2003**, *125*, 16170.
14. Colacio, E.; Lloret, F.; Kivekas, R.; Suárez-Varela, J.; Sundberg, M. R.; Uggla, R. *Inorg. Chem.* **2003**, *42*, 560.
15. Cheng, D.; Khan, M. A.; Houser, R. P. *Cryst. Growth Des.* **2004**, *4*, 599.
16. Bowden, T. A.; Milton, H. L.; Slawin, A. M. Z.; Lightfoot, P.*J. Chem. Soc. Dalton Trans.* **2003**, 936.
17. Reger, D. L.; Semeniuc, R. F.; Smith, M. D. *Eur. J. Inorg. Chem.* **2003**, 3480.
18. Shin, D. M; Lee, I. S.; Chung, Y. K.; Lah, M. S. *Chem. Commun.* **2003**, 1036.
19. (a) Chemla, D. S.; Zyss, J. (Eds.) *Nonlinear Optical Properties of Organic Molecules and Crystals* Academic Press, New York, 1989, vol. 1, 2; (b) Nie, W.

Adv. Mater. **1993**, *5*, 520; (c) Zyss, J.; Nicoud, J. F. *Curr. Opin. Solid State Mater. Sci.* **1996**, *1*, 533.

20. Qin, J.; Liu, D.; Dai, C.; Chen, C.; Wu, B.; Yang, C.; Zhan, C. *Coord. Chem. Rev.* **1999**, *188*, 23.
21. Evans, O. R.; Lin, W. *Acc. Chem. Res.* **2002**, *35*, 511.
22. Long, N. J. *Angew. Chem. Int. Ed. Engl.* **1995**, *34*, 21.
23. Di Bella, S. *Chem. Soc. Rev.* **2001**, *30*, 355.
24. Le Bozec, H.; Renouard, T. *Eur. J. Inorg. Chem.* **2000**, 229
25. (a) Whittall, I R.; McDonagh, A. M.; Humphrey, M G.; Samoc, M. *Adv. Organomet. Chem.* **1998**, *42*, 291; (b) Whittall, I R.; Humphrey, M G.; Houbrechts, S.; Maes, J.; Persoons, A.; Schmid, S.; Hockless, D. C. R. *J. Organomet. Chem.* **1997**, *544*, 277; (c) McDonagh, A. M.; Humphrey, M. G.; Samoc, M.; Luther-Davies, B.; Houbrechts, S.; Wada, T.; Sasabe, H.; Persoons, A. *J. Am. Chem. Soc.* **1999**, *121*, 1405; (d) Dhenaut, C.; Ledoux, I.; Samual, I. D. W.; Zyss, J.; Bourgault, M.; Bozec, H. L. *Nature* **1995**, *374*, 339; (e) Renouard, T.; Bozec, H. L.; Ledoux, I.; Zyss, J. *Chem. Commun.* **1999**, 871.
26. Lin, W.; Wang, Z.; Ma, L. *J. Am. Chem. Soc.* **1999**, *121*, 11249.
27. (a) Kanis, D. R.; Lacroix, P. G.; Ratner, M. A.; Marks, T. J. *J. Am. Chem. Soc.***1994**, *116*, 10089; (b) Lacroix, P. G.; Bella, S. D.; Ledoux, I. *Chem. Mater.* **1996**, *8*, 541; (c) Roberto, D.; Ugo, R.; Bruni, S.; Cariati, E.; Cariati, F.; Fantucci, P.; Invernizzi, I.; Quici, S.; Ledoux, I.; Zyss, J. *Organometallics* **2000**, *19*, 1775; (d) Senechal, K.; Maury, O.; Le Bozec, H.; Ledoux, I.; Zyss, J. *J. Am. Chem. Soc.* **2002**, *124*, 4560.
28. (a) Anthony, S. P.; Radhakrishnan, T. P. *Chem. Commun.* **2001**, 931; (b) Evans, C.; Luneau, D. *J. Chem. Soc. Dalton Trans.* **2002**, 83.
29. (a) Xie, Y. R.; Xiong, R. G.; Xue, X.; Chen, X. T.; Xue, Z.; You, X. Z. *Inorg. Chem.* **2002**, *41*, 3323; (b) Han, L.; Hong, M.; Wang, R.; Luo, J.; Lin, Z.; Yuan, D. *Chem. Commun.* **2003**, 2580.
30. (a) Bowyer, P. K.; Porter, K. A.; Rae, A. D.; Willis, A. C.; Wild, S. B. *Chem. Commun.* **1998**, 1153; (b) Ellis, W. W.; Schmitz, M.; Arif, A. A.; Stang, P. J. *Inorg. Chem.* **2000**, *39*, 2547; (c) Prins, L. J.; Huskens, J.; Jong, F. De.; Timmerman, P. *Nature* **1999**, *398*, 498; (d) Soghomonian, V.; Chen, Q.; Haushalter, R. C.; Zubieta, J.; O'Conner, C. J. *Science* **1993**, *259*, 1596.

31. (a) Chin, J.; Lee, S. S.; Lee, K. J.; Park, S.; Kim, D. H. *Nature* **1999**, *401*, 254; (b) Engelkamp, H.; Middelbeek, S.; Nolte, R. J. M. *Science* **1999**, *284*, 785; (c) Wu, B.; Zhang, W.-J.; Yu, S.-Y.; Wu, X.-T.; *J. Chem. Soc. Dalton Trans.* **1997**, 1795.
32. Clays, K.; Hendrick, E.; Verbiest, T.; Persoons, A. *Adv. Mater.* **1998**, *10*, 643.
33. Verbiest, T.; Elshocht, S. V.; Kauranen, M.; Hellemans, L.; Snauwaert, J.; Nuckolls, C.; Katz, T. J.; persoons, A. *Science* **1998**, *282*, 913.
34. Kauranen, M.; Verbiest, T.; Elshocht, S. V.; Persoons, A. *Opt. Mater.* **1998**, *9*, 286.
35. Gangopadhyay, P.; Radhakrishnan, T. P. *Angew. Chem. Int. Ed.* **2001**, *40*, 2451.
36. Anthony, S. P.; Radhakrishnan, T. P. *Chem. Commun.* **2004**, 1058.
37. Anthony, S. P.; Radhakrishnan, T. P. *Cryst. Growth Des.* **2004**, *4*, 1223.
38. (a) Lin, W.; Evans, O. R.; Xiong, R.; Wang, Z. *J. Am. Chem. Soc.* **1998**, *120*, 13272; (b) Evans, O. R.; Xiong, R.; Wang; Z.; Wong, G. K.; Lin, W. *Angew. Chem. Int. Ed.* **1999**, *38*, 536; (c) Lin, W.; Ma, L.; Evans, O. R. *Chem. Commun.* **2000**, 2263; (d) Evans, O. R.; Lin, W. *Chem. Mater.* **2001**, *13*, 2705.
39. Soldatov, D. V.; Henegouvwen, A. T.; Enright, G. D.; Ratcliffe, C. I.; Ripmeester, J. A. *Inorg. Chem.* **2001**, *40*, 1626.
40. Larrow, J. F.; Jacobson E. N.; Gao, Y.; Hong, Y, Nie, X.; Zepp, C. M. *J. Org. Chem.* **1994**, *59*, 1939.
41. Kwit, M.; Gawronski, J. *Tetrahedron* **2003**, *59*, 9323.
42. Cambridge Crystallographic Database (version 5.24) shows 192 hits for silver-cyano complexes; the number of complexes showing near linear coordination (N...Ag....N angle = 160-180°) is only 6.
43. (a) Tisato, F.; Retosco, F.; Bandoli, G.; Corain, B. *J. Chem. Soc. Dalton Trans.* **1994**, 2471; (b) Munakata, M.; Ning, G. L.; Karoda-Sowa, T.; Maekawa, M.; Suenaga, Y.; Horino, T. *Inorg. Chem.* **1998**, *37*, 5651.
44. Kurtz, S. K.; Perry, T. T. *J. Appl. Phys.*, **1968**, *39*, 3798.
45. Evans, O. R.; Wang, Z.; Lin, W. *Chem. Commun*, **1999**, 1903.
46. (a) Zyss, J. *J. Chem. Phys.* **1993**, *98*, 6583; (b) Zyss, J.; Ledoux, I. *Chem. Rev.* **1994**, *94*, 77.
47. (a) Dhenaut, C.; Ledoux, I.; Samuel, I. D. W.; Zyss, J.; Bourgault, M.; Le Bozec, H. *Nature* **1995**, *374*, 339; (b) Sénéchal, K.; Mauri, O.; Le Bozec, H.; Ledoux, I.; Zyss, J. *J. Am. Chem. Soc.* **2002**, *124*, 4561.

48. Viau, L.; Bidault, S.; Maury, O.; Brasselet, S.; Ledoux, I.; Zyss, J.; Ishow, E.; Nakatani, K.; Le Bozec, H. *J. Am. Chem. Soc.* **2004**, *126*, 8386.
49. Zyss, J.; Oudar, J. L. *Phys. Rev. A*, **1982**, *26*, 2028.
50. Zyss, J.; Brasselet, S.; Thalladi, V. R.; Desiraju, G. R. *J. Chem. Phys.* **1998**, *109*, 658.
51. (a) Dewar, M. J. S.; Zoebisch, E. G.; Healy, E. F.; Stewart, J. J. P. *J. Am. Chem. Soc.* **1985**, *107*, 3902; (b) MOPAC93 © Fujitsu Inc., Japan; (c) Dupuis, M.; Karna, S. *J. Comput. Chem.* **1991**, *12*, 487.
52. Gaussian 03, Revision B.04. Gaussian, Inc., Pittsburgh PA, 2003.

CHAPTER 4

Vicinal Chiral Bis(amide) Molecules Based Organic and Metal-Organic Materials : Assembly Through H-bonding and Second Harmonic Generation

Papers published

- Anthony, S. P.; Basavaiah, K.; Radhakrishnan, T. P. (Submitted).
  Chiral Vicinal Bis(Amide) Molecules: Polar/Helical Assemblies in Crystals and SHG.

4.1 INTRODUCTION

Last few decades have witnessed extensive research efforts directed towards the design and development of NLO materials. To be suitable for NLO applications such as optical SHG, materials have to satisfy several requirements including noncentrosymmetric organization, strong nonlinear response (molecular hyperpolarizability or bulk susceptibility), low absorbance in the spectral range of the fundamental and SHG and thermal and mechanical stability.[1] It is very difficult to achieve all of these characteristics in a single material. For instance, high molecular hyperpolarizability is often accompanied by strong absorbance at the SHG wavelength and high ground state molecular dipole moment; the former affects the SHG efficiency adversely and the latter often encourages the formation of centrosymmetric bulk materials. The thermal stability of materials is related to both the molecular structure and intermolecular interactions. The application potential of molecular materials for NLO applications is often limited by their low thermal stability. All these factors point out that an acceptable tradeoff between the molecular properties and materials attributes needs to be realized to develop specific materials for application.

Even though organic materials have been extensively investigated due to their inherent advantages over the traditional inorganic materials, such as strong NLO response and low refractive indices, they are yet to find practical applications because of the low thermal stability, low damage threshold under laser irradiation and absorption in the spectral range of SHG which makes the applications at these wavelengths inefficient. The NLO materials being used commercially are mostly based on inorganic materials such as potassium dihydrogen phosphate, lithium niobate and β-barium borate; they posses high thermal and mechanical stability along with good optical transparency.[2] Recently, increasing attention has been focused on the development of molecular NLO materials having high thermal and mechanical stability with good optical transparency. The thermal stability has been enhanced in dipolar chromophores in which donor and accepter groups are linked by a long π-conjugated polyene bridge; a synthetic route for ring-locked polyenes has been developed.[3] Among the polymer systems studied for NLO applications, aromatic imides are promising materials due to their high thermal stabilities and glass transition temperatures.[4] Highly thermally stable octupolar polyimide NLO

materials exhibiting large solution second order nonlinearity have also been reported.[5] Octupolar metal complexes based on bipyridyl ligands show large hyperpolarizability and better optical transparency than the corresponding dipolar metal complexes.[6] Thermally stable imines based on diaminomaleonitrile derivatives have been reported recently.[7]

Molecular assembly in crystals is controlled by the molecular structure and intermolecular interactions. For example, molecular chirality ensures noncentro-symmetricity in the bulk material and conformational flexibility can have profound influence on the molecular organization in the solid state.[8,9] Development of general routes for supramolecular assembly is one of the fundamental problems in engineering solid state structures. Hydrogen bonds represent one of the most prominent strategies in this respect,[10] their application in the synthesis of extended organic networks is well documented;[11] their use in the assembly of coordination compound networks has been fewer.[12,13] Molecular networking through interactions such as H-bonds and metal coordination can be exploited to generate a range of fascinating solid state structures.[14] The strength and directionality of the hydrogen bond, as compared to other intermolecular forces, account for its importance and have made it one of the most promising protocols for molecular recognition and supramolecular synthesis.[15] Many of the strategies have relied on the complementarity of hydrogen bond interactions. Carefully selected hydrogen bond interactions can not only assemble discrete molecules and ions but also constrain their relative orientations in the bulk materials,[8,9] a critically important consideration in the design of materials for quadratic NLO effects. Hydrogen bonding has been successfully utilized in the development of noncentrosymmetric structures from achiral molecules[16-19] for applications as NLO crystals. Hydrogen bonding can also often impart higher thermal stability to the materials.[20-22] Even though several approaches have been developed to obtain noncentrosymmetric structures, special motifs such as polar and helical structures remain important targets because of their great potential in materials applications related to nonlinear optics and opto-electronics.[1,23,24]

The construction of metal-containing networks has been achieved using different design approaches: the metal complexes can be linked either through coordinate covalent bonds[25] or weaker intermolecular forces such as hydrogen bonds or stacking interactions of aromatic groups.[26] Coordination chemistry can be employed as a powerful method for

the synthesis of metal-organic macromolecules or polymeric structures with metals in the backbone; there is great interest in developing methodologies to further organize these macromolecules into functional molecular materials.[27] The combination of coordination chemistry with non-covalent interactions such as hydrogen bonding provides great scope for creating complex structures from simple building blocks.[12,28-32] Weak hydrogen bonding interactions in organic-inorganic hybrid materials have been shown to lead to chiral network structures that exhibit solid state SHG.[33] Synthesis of supramolecular architectures by assembling discrete metal complexes bearing hydrogen bonding sites in the ligand has been reported.[34]

Coordination polymers are highly suited for the construction of materials based on extended inorganic-organic assemblies. They also facilitate considerable structural control. An early example involving coordination polymers along with hydrogen bonding approaches is that of Ag(I) ions with ligands based on pyridyl derivatives of ureas and oxalamides. The tetrahedral Ag(I) ions are connected into two-dimensional polymers by bridging bipyridine-like ligands and the complementary ligand based N-H…O hydrogen bonds extend the assembly process to a three-dimensional network.[35] Ag(I) networks formed by complementary self assembly using bipyridine ligands, anions and hydrogen bonding amide groups have also been reported recently.[9] Zn(II) dicarboxylate coordination polymers can be interconnected through hydrogen bonds between coordinated thiourea ligands and carboxylate moieties on neighboring chains.[36]

A strategy based on additional ligands capable of forming self complementary hydrogen bonds that are independent of the ligands required to assemble the coordination polymer has also been devised. Cu(II) halides can form linear coordination polymers via bridging halide groups, and simple pyridine based ligands with carboxylic acid, carboxamide and oxime substituents were used to generate two-dimensional assemblies.[37] Similarly, one and two-dimensional coordination polymers of Cd(II) thiocyanate were connected via self complementary ligand based hydrogen bonds, resulting in two and three-dimensional networks.[38] Linear Cu(II) dicyanamide coordination polymers have been cross-linked via complementary 2-aminopyrimidine hydrogen bonds.[39] Co(II) and Ni(II) complexes of dicyanamide which create infinite network structures through coordinate covalent bonds, have been connected into three-dimensional assemblies

through hydrogen bonds between additional 2-aminopyrimidine ligands located on the periphery.[40]

Following our studies of the chiral ligand BCDC discussed in Chapter 3, we have developed a new series of C_2-symmetric bis(amide) derivatives : N,N'-bis-(benzoyl)-(1*R*,2*R*)-diaminocyclohexane (BBDC), N,N'-bis(4-fluorobenzoyl)-(1*R*,2*R*)-diaminocyclohexane (BFBDC), N,N'-bis(4-nitrobenzoyl)-(1*R*,2*R*)-diaminocyclohexane (BNBDC), N,N'-bis(4-methoxybenzoyl)-(1*R*,2*R*)-diaminocyclohexane (BMBDC), N,N'-bis(4-aminobenzoyl)-(1*R*,2*R*)-diaminocyclohexane (BABDC) and N,N'-bis(isonicotinoyl)-(1*R*,2*R*)-diaminocyclohexane (BINDC). We have investigated their crystal structure and solid state SHG. All the compounds exhibit complementary amide hydrogen bond intermolecular interactions that lead to the formation of extended structures in the crystal lattice. BBDC exhibits the rare *syn* conformation of the bis(amide) group and forms interesting polar organization in the three-dimensional structure with all the carbonyl groups oriented in the same direction in the crystal.[41] This is unusual in the case of free vicinal bis(amide) structures because the *anti* conformation is energetically stabler; it has been observed earlier, only due to constraints of metal coordination[42] or cyclic structure formation.[43] Subtle molecular structure variations in the case of BINDC gives rise to helical organizations in crystals and the bis(amide) group shows the normal *anti* conformation. BFBDC, BNBDC, BMBDC and BABDC also show helical assembly through hydrogen bonding interactions in the crystal lattice. The substituent in the *para* position also seems to affect the conformation of the bis(amide) changing it back to *anti* from the *syn* in BBDC. The circular dichroism studies of BBDC and its derivatives in methanol solution show that the bis(amide) group has *anti* conformation and negative helicity in solution as reported earlier.[44] Significantly, these bis(amide) molecules exhibit solid state SHG when electron donating group is present in the *para* position of the aromatic ring and become SHG inactive if there is an electron withdrawing substituent. We have also fabricated coordination polymers based on BINDC and demonstrated the utilization of complementary amide hydrogen bonding interactions to organize the coordination polymers in the solid state. The coordinate covalent bonds lead to one-dimensional coordination polymers and the complementary hydrogen bonding between the amide groups result in two-dimensional network structures. The coordination polymers show reduction in the SHG value compared to the free ligand BINDC due to

the electron withdrawing character of the metal ions. This is consistent with the observation in the BBDC family. The BBDC and BINDC based families of compounds show appreciable thermal stability and good optical transparency in the visible range.

4.2 SYNTHESIS AND CHARACTERIZATION

The resolution of 1,2-diaminocyclohexane was carried out following the methodology reported by Jacobsen *et al.*[45] and the detailed procedure was given in Sec. 3.2. The synthesis of BBDC has been reported earlier.[46] We have adopted a slightly modified procedure.

N,N'-bis(benzoyl)-(1*R*,2*R*)-diaminocyclohexane (BBDC)

Benzoyl chloride (1.35 g, 9.63 mmol) was added dropwise over 15 min to the vigorously stirred solution of (1*R*,2*R*)-diaminocyclohexane (0.5 g, 4.37 mmol) in 10% NaOH (8 ml) solution (Scheme 4.1). The reaction mixture was stirred at room temperature for 1 h more; the white precipitate formed was filtered, washed with water

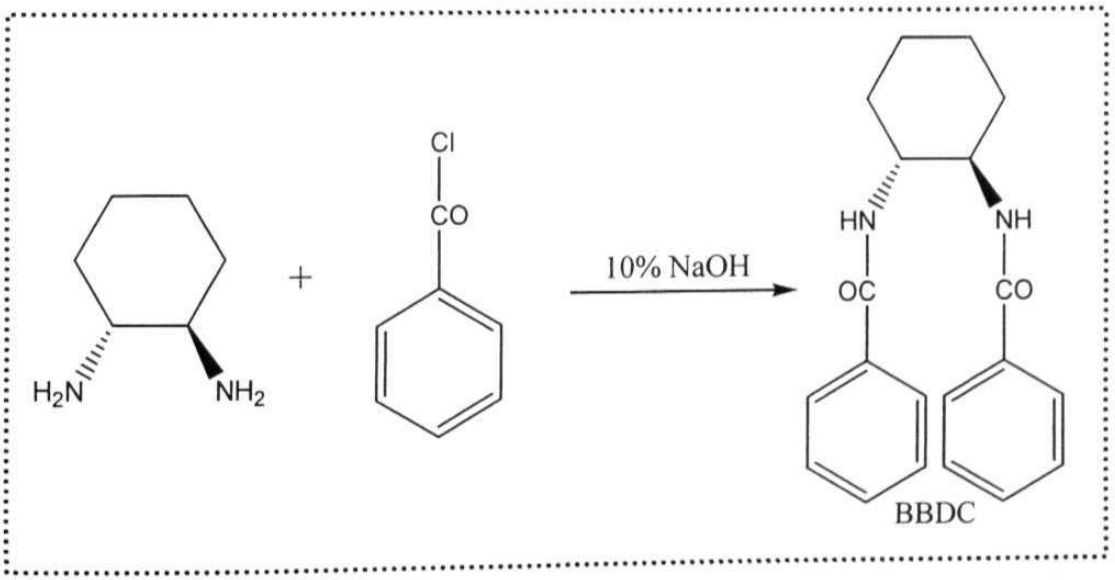

Scheme 4.1

thoroughly to remove any trace amount of NaOH solution in the compound and dried under vacuum. The product was purified by recrystallization from methanol. Yield: 1.13 g, 81%; M. P: 265-267°C; UV-Vis (methanol solution) λ_{max} ($\lambda_{cut\text{-}off}$): 224.8 nm (287 nm); IR (KBr pellet): $\bar{\upsilon}/cm^{-1}$: 3304.4, 2932.1, 2858.7, 1631.9, 1531.6, 1331.0, 694.4, 663.5; ^{1}H NMR (d_6-DMSO): δ/ppm = 1.29 (m, 2H), 1.5 (m, 2H), 1.75 (m, 2H), 1.92 (m,2H), 3.36 (s, 2H), 3.94 (m, 2H), 7.43 (m, 4H), 7.70 (m, 4H), 8.28 (m, 2H); ^{13}C NMR (d_6-DMSO): δ/ppm = 24.9, 31.8, 53.3, 117.3, 128.7, 131.1, 135.1, 166.7.

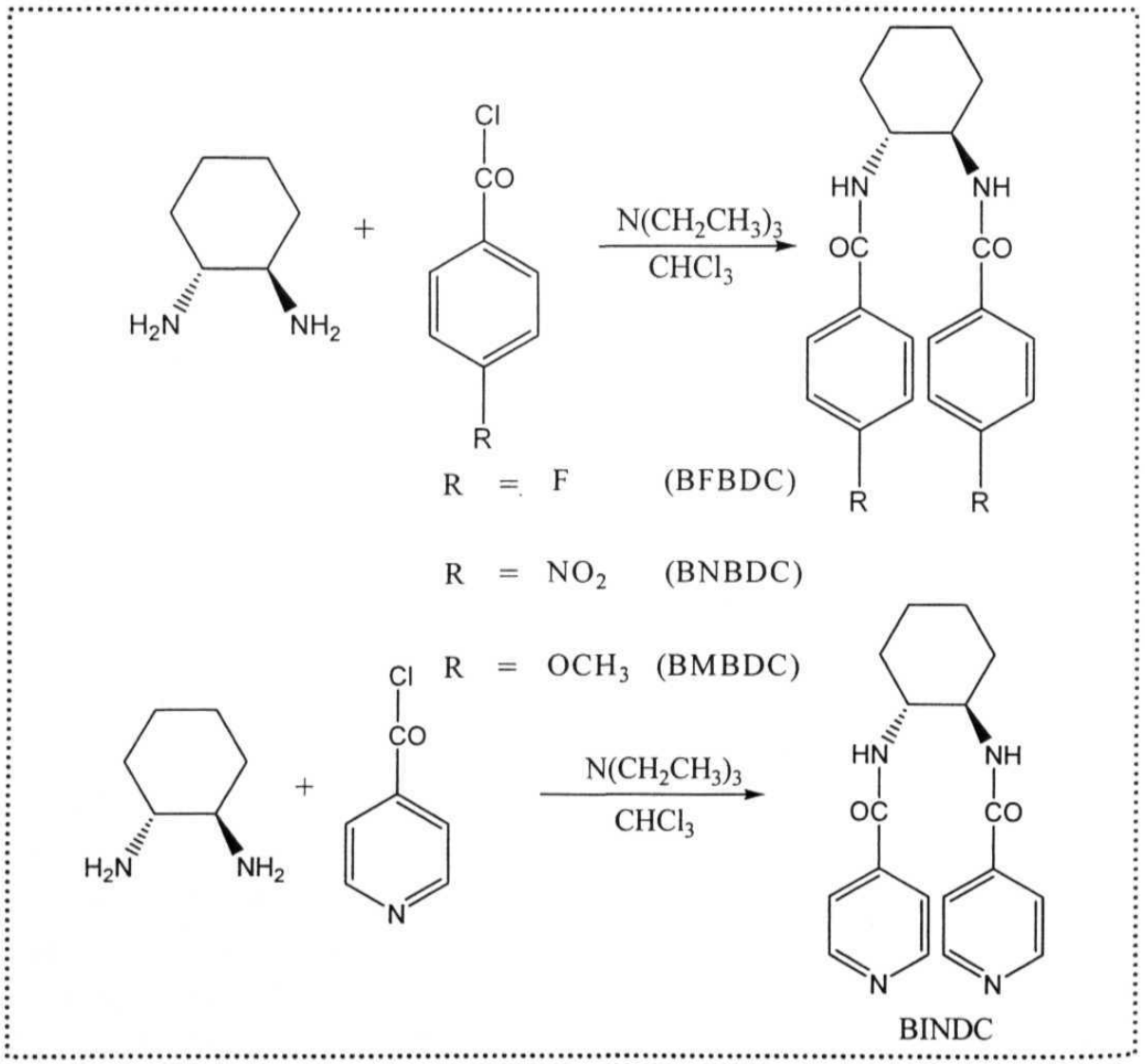

Scheme 4.2

BNBDC, BFBDC, BMBDC and BINDC : General synthesis procedure

2 mmol of the aroyl chloride and 2.4 mmol of triethylamine were dissolved in chloroform and stirred for 10 min. 1 mmol of (1*R*,2*R*)-diaminocyclohexane in chloroform was slowly added to the resulting solution (Scheme 4.2). Addition was carried out slowly due to the exothermic nature of the reaction. A white precipitate was obtained. The reaction mixture was heated at reflux for 14 h. The solution was then cooled to room temperature and the solid was filtered. In some cases, the solvent was evaporated to recover the solid. The resulting off-white solid was washed with water, saturated sodium bicarbonate solution and then again water. The product was vacuum dried and purified by recrystallization from methanol solution.

N,N'-bis(4-nitrobenzoyl)-(1*R*,2*R*)-diaminocyclohexane (BNBDC). Yield: 95%; M. P: 339°C (dec); UV-Vis (methanol solution) λ_{max} ($\lambda_{cut\text{-}off}$) : 263.6 nm (352 nm); IR (KBr pellet): $\bar{\upsilon}$/cm^{-1} : 3288.9, 2930.1, 2856.8, 1637.7, 1597.2, 1537.4, 1516.2, 1340.6, 869.9, 846.8, 692.5; ^{1}H NMR (d_6-DMSO): δ/ppm = 1.28 (m, 2H), 1.57 (m, 2H), 1.78 (m, 2H), 1.91 (m, 2H), 3.99 (m, 2H), 7.93 (d, 4H), 8.26 (d, 4H), 8.68 (d, 2H); ^{13}C NMR (d_6-DMSO): δ/ppm = 24.9, 31.6, 53.3, 123.6, 128.8, 140.8, 149.0, 164.9.

N,N'-bis(4-flurobenzoyl)-(1*R*,2*R*)-diaminocyclohexane (BFBDC). Yield : 90%. M. P: 268°C; UV-Vis (methanol solution) λ_{max} ($\lambda_{cut\text{-}off}$): 225.6 nm (279.4 nm); IR (KBr pellet) : $\bar{\upsilon}$/cm^{-1} : 3304.3, 2941.7, 2858.7, 1631.9, 1606.8, 1541.2, 1502.7, 1332.9, 846.8, 765.8, 665.5; ^{1}H NMR (d_6-DMSO): δ/ppm = 1.43-1.48 (m, 4H), 1.87 (m, 2H), 2.22 (m, 2H), 4.04 (m, 2H), 6.9 (d, 4H), 6.96 (m, 2H), 7.68 (d, 4H); ^{13}C NMR (d_6-DMSO): δ/ppm = 24.8, 32.2, 54.6, 115.2, 115.6, 129.1, 129.3, 130.2, 165.2.

N,N'-bis(4-methoxybenzoyl)-(1*R*,2*R*)-diaminocyclohexane (BMBDC). Yield: 90%; M. P: 269°C; UV-Vis (methanol solution) λ_{max} ($\lambda_{cut\text{-}off}$): 251.2 nm (289.8 nm); IR (KBr pellet): $\bar{\upsilon}$/cm^{-1} : 3310.1, 2934.0, 2852.9, 1628.1, 1606.8, 1537.4, 1504.6,1329.1, 1253.8, 1176.1, 1024.1, 839.1, 767.7, 665.5; ^{1}H NMR (d_6-DMSO): δ/ppm = 1.28 (m, 2H), 1.50 (m, 2H), 1.72 (m, 2H), 1.93 (m, 2H), 3.76 (s, 6H), 3.88 (m, 2H), 6.92 (d, 4H), 7.40 (d, 4H), 8.10 (m, 2H); ^{13}C NMR (d_6-DMSO): δ/ppm = 19.9, 27.4, 49.5, 50.2, 108.6, 121.7, 123.7, 157.1, 162.8.

N,N'-bis(isonicotinoyl)-(1*R*,2*R*)-diaminocyclohexane (BINDC). Yield: 85%; M. P: 268-270°C; UV-Vis (methanol solution) λ_{max} ($\lambda_{cut\text{-}off}$): 248.8 nm (304.6 nm); IR (KBr pellet): $\bar{\upsilon}$/cm^{-1} : 3292.8, 2941.7, 2858.7, 1639.6, 1597.2, 1537.4, 1408.2, 1329.1, 841.0, 758.1, 659.7; ^{1}H NMR (d_6-DMSO): δ/ppm = 1.32-1.44 (m, 4H), 1.5 (m, 2H), 2.22 (m, 2H), 4.05 (m, 2H), 7.26 (m, 2H), 7.53 (d, 4H), 8.6 (d, 4H); ^{13}C NMR (d_6-DMSO): δ/ppm = 24.7, 32.1, 54.78, 120.7, 141.1, 150.5, 166.3.

N,N'-bis(4-aminobenzoyl)-(1*R*,2*R*)-diaminocyclohexane (BABDC)

BNBDC (0.5 g, 1.2 mmol) was dissolved in dry methanol and catalytic amount of Pd/C (0.075g) was added and stirred for 15 min at room temperature. $NaBH_4$ (0.5 g, 13.2 mmol) was slowly added over 1 h (Scheme 4.3). The reaction mixture was further stirred for 3 h at room temperature. The progress of the reaction was monitored by TLC. After the completion of the reaction, the Pd/C was removed by filtration. The colorless methanol solution was completely evaporated under reduced pressure and water was added to the resulting semisolid to yield a white precipitate. The precipitate was filtered and washed with sodium bicarbonate solution and excess of water; it was then dried under vacuum. The product was purified by recrystallization from methanol. Yield: 0.38

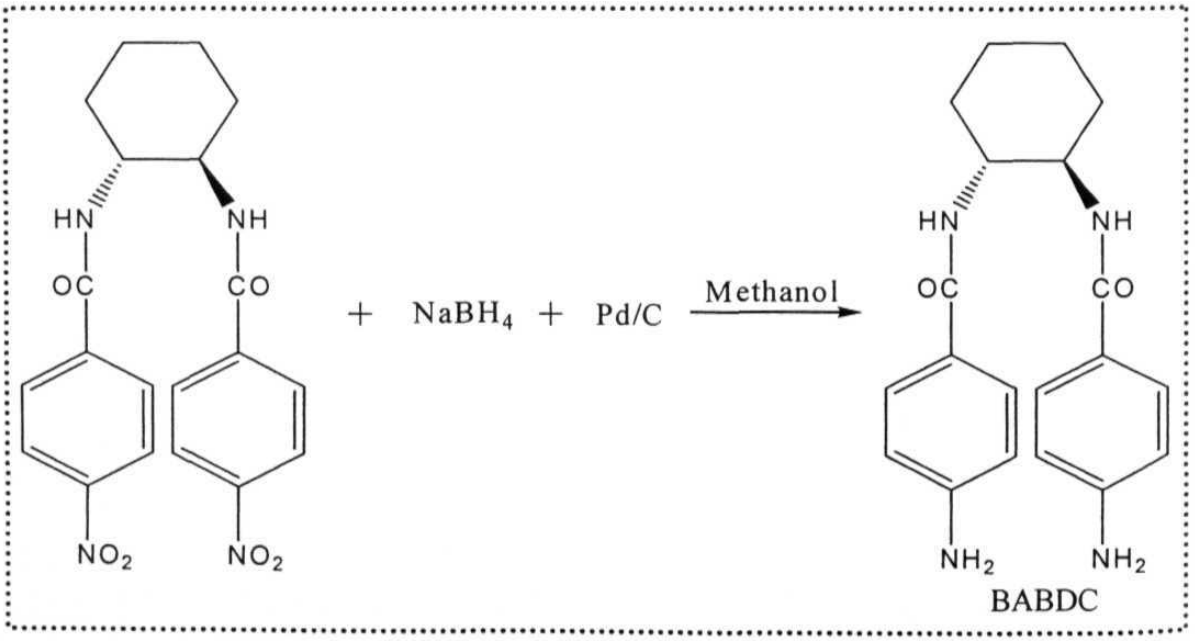

Scheme 4.3

g, 90%; M. P: 288-290°C (dec); UV-Vis (methanol solution) λ_{max} ($\lambda_{cut\text{-}off}$): 295.5 nm (327.5 nm); IR (KBr pellet): ν/cm^{-1} : 3468.3, 3356.4, 3288.9, 2932.1, 2854.9, 1612.6, 1537.4, 1506.5, 1323.3, 1184.4, 839.1, 767.7, 574.8; ^{1}H NMR (d_6-DMSO): δ/ppm = 1.26- 1.38 (m, 4H), 1.70 (m, 2H), 1.92 (m, 2H), 3.74 (s, 2H), 5.55 (s, 4H), 6.47 (d, 4H), 7.46 (d, 4H). 7.81 (s, 2H); ^{13}C NMR (d_6-DMSO) : δ/ppm = 24.8, 32.07, 53.6, 112.7, 121.4, 128.8, 151.7, 163.6.

(N,N'-bis(isonicotinoyl)-(1*R*,2*R*)-diaminocyclohexane)zinc chloride ($Zn(BINDC)Cl_2$)

BINDC (0.3 g, 0.92 mmol) dissolved in methanol was added to the aqueous solution of zinc chloride (0.12 g, 0.92 mmol). The resulting solution was kept at room temperature. Slow evaporation led to the formation colorless crystals of the complex. The crystalline product was filtered and washed with water and methanol, and dried under vacuum. Yield: 0.33 g, 80%; M. P: 373°C (dec); UV-Vis (aqueous solution) λ_{max} ($\lambda_{cut\text{-}off}$) : 262, 238 nm (302 nm); IR (KBr pellet): $\bar{\upsilon}/cm^{-1}$: 3317.8, 3287.0, 2920.5, 2858.7, 1647.7, 1618.4, 1537.4, 1423.6, 1332.9, 1221.1, 1089.9, 1062.8, 1026.2, 858.4, 640.4.

(N,N'-bis(isonicotinoyl)-(1*R*,2*R*)-diaminocyclohexane)zinc bromide ($Zn(BINDC)Br_2$)

Similar procedure was followed as used in the preparation of $ZnCl_2$(BINDC) complex with $ZnBr_2$ (0.2 g, 0.92 mmol) in place of $ZnCl_2$. Yield: 0.43 g, 85%; M. P: 410°C (dec); UV-Vis (aqueous solution) λ_{max} ($\lambda_{cut\text{-}off}$): 260.6, 236.6 nm (306.8 nm); IR (KBr pellet): $\bar{\upsilon}/cm^{-1}$: 3323.6, 3288.9, 2922.4, 2854.9, 1647.7, 1614.5, 1537.4, 1421.8, 1024.3, 858.4, 763.9.

(N,N'-bis(isonicotinoyl)-(1*R*,2*R*)-diaminocyclohexane)silver nitrate ($Ag(BINDC)NO_3$)

0.3 g (0.92 mmol) of BINDC dissolved in methanol was carefully layered on top of a solution of 0.16 g (0.92 mmol) of $AgNO_3$ in water and the solution was allowed to stand at room temperature without disturbing. Even though the solvents by themselves are miscible, the two solutions do not mix unless agitated. Colorless crystals were

formed in about 3 days. The solution was decanted and the crystals were washed with methanol and dried. Yield: 0.32 g, 70%; M.P: 310°C (dec); UV-Vis (aqueous solution) λ_{max} ($\lambda_{cut\text{-}off}$): 258, 235.4 nm (379.8 nm); IR (KBr pellet): $\bar{\upsilon}/cm^{-1}$: 3337.1, 3051.7, 2935.9, 2854.9, 1645.4, 1606.8, 1531.6, 1338.7, 1068.6, 842.9, 758.1.

4.3 POLAR / HELICAL ASSEMBLIES OF CHIRAL VICINAL BIS(AMIDE) MOLECULES : MOLECULAR AND CRYSTAL STRUCTURE INVESTIGATIONS

BBDC and BINDC posses closely related molecular structures. The only difference is the presence of the nitrogen atom in the pyridine rings of BINDC in place of the carbon atoms in BBDC. However the molecular organization in the two crystals turns out to be very different. The structures of this pair of vicinal bis(amide) molecules provide a fine illustration of the influence of subtle molecular structural features on supramolecular organization.

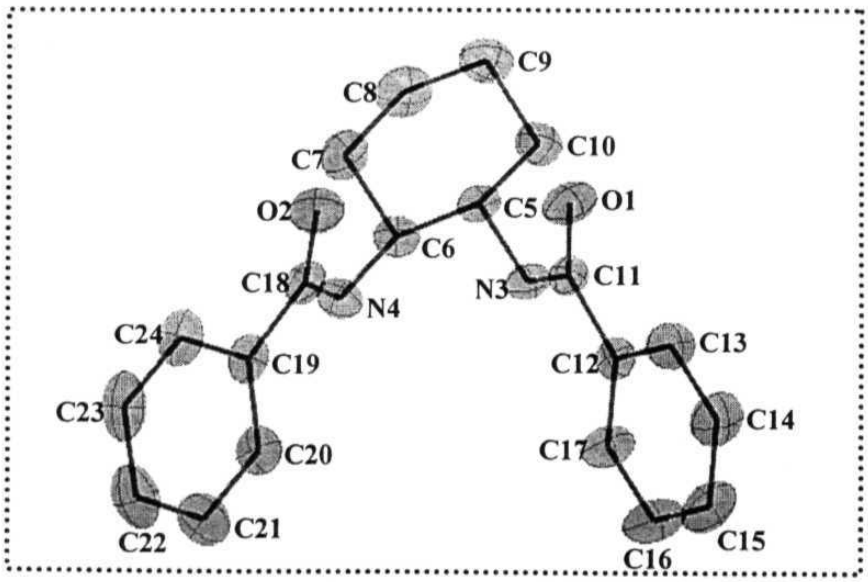

Figure 4.1 *Molecular structure of **BBDC** from single crystal analysis. 95% probability thermal ellipsoids are indicated; H atoms are omitted for clarity.*

Table 4.1. *Crystallographic data for* ***BBDC*** *and* ***BINDC***

Identification code	**BBDC**	**BINDC**
Empirical formula	$C_{20}H_{22}N_2O_2$	$C_{18}H_{20}N_4O_2$
Formula weight	322.40	324.38
Crystal system	Monoclinic	Orthorhombic
Space group	$P2_1$ (No. 4)	$P2_12_12_1$ (No. 19)
A / Å	9.2636(9)	5.1328(4)
b / Å	9.7900(9)	17.2924(14)
c / Å	10.7319(10)	18.9976(15)
β /°	115.0250(10)	90.0
V / $Å^3$	881.91(14)	1686.2(2)
Z	2	4
$\rho_{calc.}$ / g cm^{-3}	1.214	1.278
μ / mm^{-1}	0.079	0.086
λ / Å	0.71073	0.71073
2θ range / deg.	2.09 - 28.23°	1.59 - 28.25°
Unique reflections	4044	3904
Reflection with $I \geq 2\sigma_I$	3120	2183
No. of parameters	217	217
GOF	0.928	0.880
R [for $I \geq 2\sigma_I$]	0.0407	0.0440
wR^2[for $I \geq 2\sigma_I$]	0.0801	0.0788

Crystals of BBDC were grown from methanol solution by slow evaporation. They are found to belong to the monoclinic $P2_1$ space group with one molecule in the asymmetric unit. The basic crystallographic data are presented in Table 4.1. The molecular structure is shown in Fig. 4.1. The molecule possesses unusual *syn* orientation

of the bis(amide) groups. The short intermolecular N-H...O bonds ($r_{N4...O1}$ = 2.793 Å, $\theta_{N4-H4...O1}$ = 153.6°; $r_{N8...O2}$ = 2.959 Å, $\theta_{N8-H8...O2}$ = 164.1°) lead to extended polar chains along the *b* direction (Fig. 4.2). The screw rotation being the only symmetry element present, all the chains in the crystal are oriented in the same direction. No recognizable strong

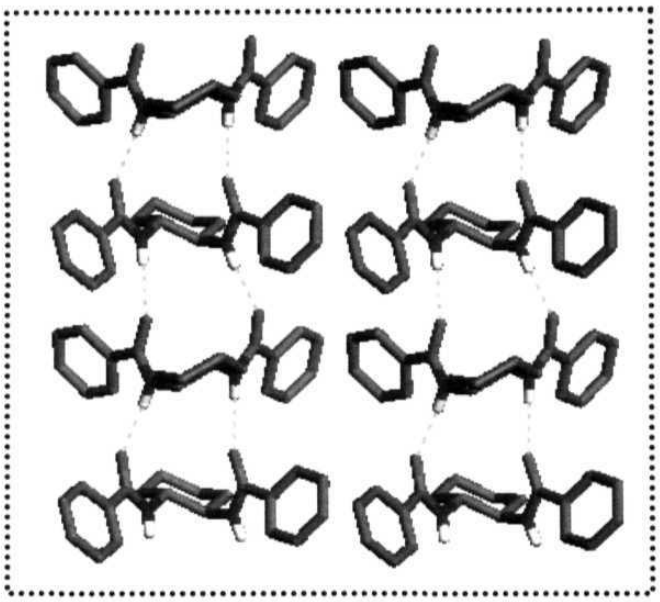

Figure 4.2. *Polar chains in crystals of **BBDC**; C (grey), N (blue), O (red), H (white) and H-bonds (broken cyan lines) are shown; H of amide groups alone are shown for clarity.*

Table 4.2. *Computed enthalpies of formation / energies of **BBDC** and **BINDC** conformers.*

Structure	**Conformation of the bis(amide) group**	**ΔH_f (AM1) / kcal mol^{-1}**	**E (B3LYP/ 6-31G*) / Hartrees**
BBDC	*syn*	-33.8	-1035.377
	anti	-39.4	-1035.389
BINDC	*syn*	-11.8	-1067.446
	anti	-15.9	-1067.459

intermolecular interactions are observed along the *a* and *c* directions. Cyclohexane ring of adjacent molecules along *b* are in opposite directions, but all the carbonyl groups are oriented in the same direction, leading to polar organization in the three-dimensional lattice structure.

The *syn* conformation of BBDC in the solid state is unique. We have carried out semiemprical computations using the AM1 method;[47] molecular structure from crystal structure and the alternate conformer obtained by rotating one of the amide groups were used as initial geometries for the full optimization calculations. Ab initio[48] computations were also carried out in which the AM1 optimized structures were used as the initial geometry for the full optimization calculations. The computations show that the *anti* conformer is stabler than the *syn* conformer by 6 – 8 kcal/mol (Table 4.2). The CD spectrum of BBDC in methanol solution (Fig. 4.3) is consistent with an earlier report [44] and suggests *anti* conformation and negative helicity in solution. This is confirmed by the similar CD spectra of the various derivatives of BBDC discussed in Sec. 4.4, which show *anti* conformation in the solid state as well. From the computational results and CD spectra, we infer that the *syn* conformer in the crystals of BBDC results from solid state effects alone, making the polar assembly through amide H-bonds possible.

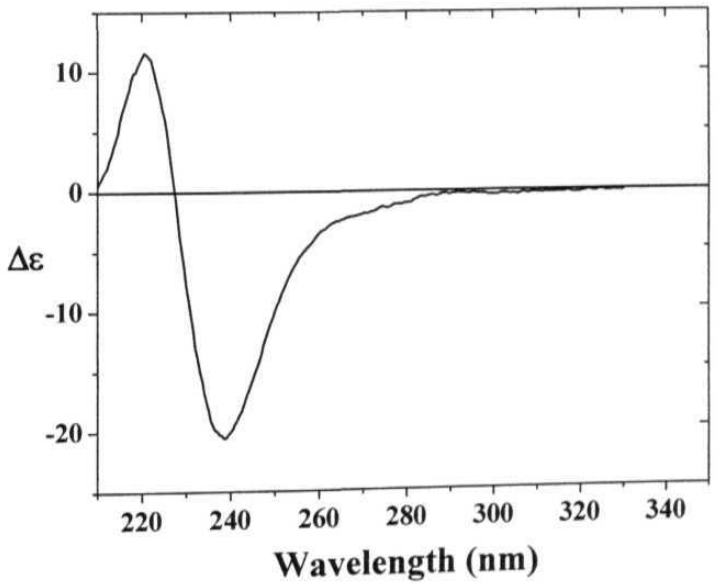

Figure 4.3 *CD spectrum of* ***BBDC*** *in methanol solution.*

Crystals of BINDC grown by slow evaporation of methanol solution are found to belong to the orthorhombic $P2_12_12_1$ space group with one molecule in the asymmetric unit. The basic crystallographic data are presented in Table 4.1. The molecular structure

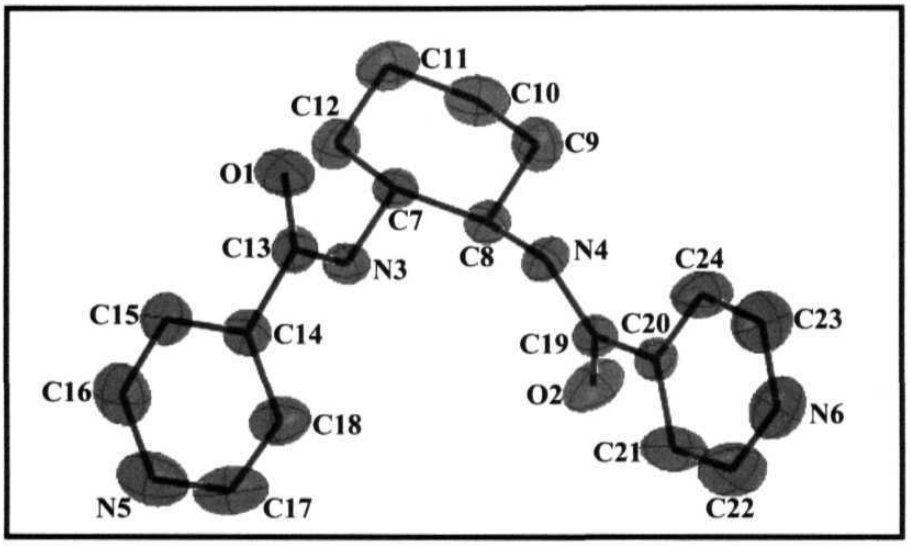

Figure 4.4 *Molecular structure of **BINDC** from single crystal analysis. 95% probability thermal ellipsoids are indicated; H atoms are omitted for clarity.*

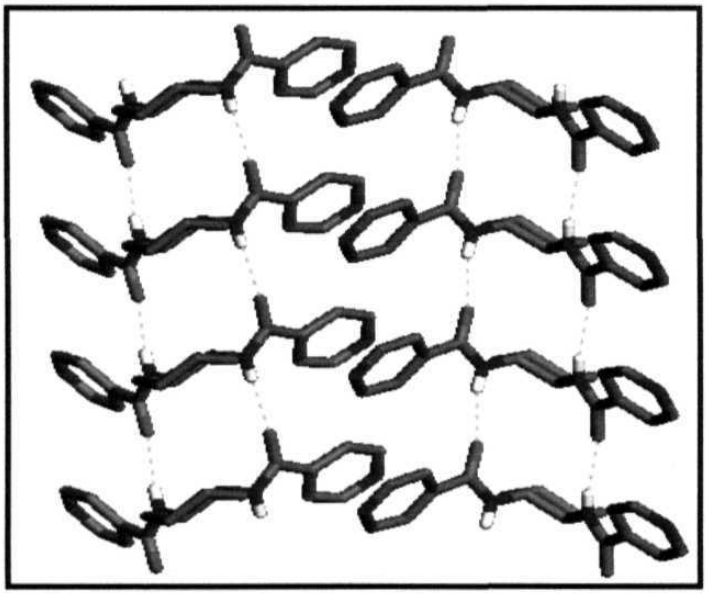

Figure 4.5 *Complementary amide hydrogen bonding interactions in crystals of **BINDC**. C (grey), N (blue), O (red), H (white) and H-bonds (broken cyan lines) are shown; H of amide groups alone are shown for clarity.*

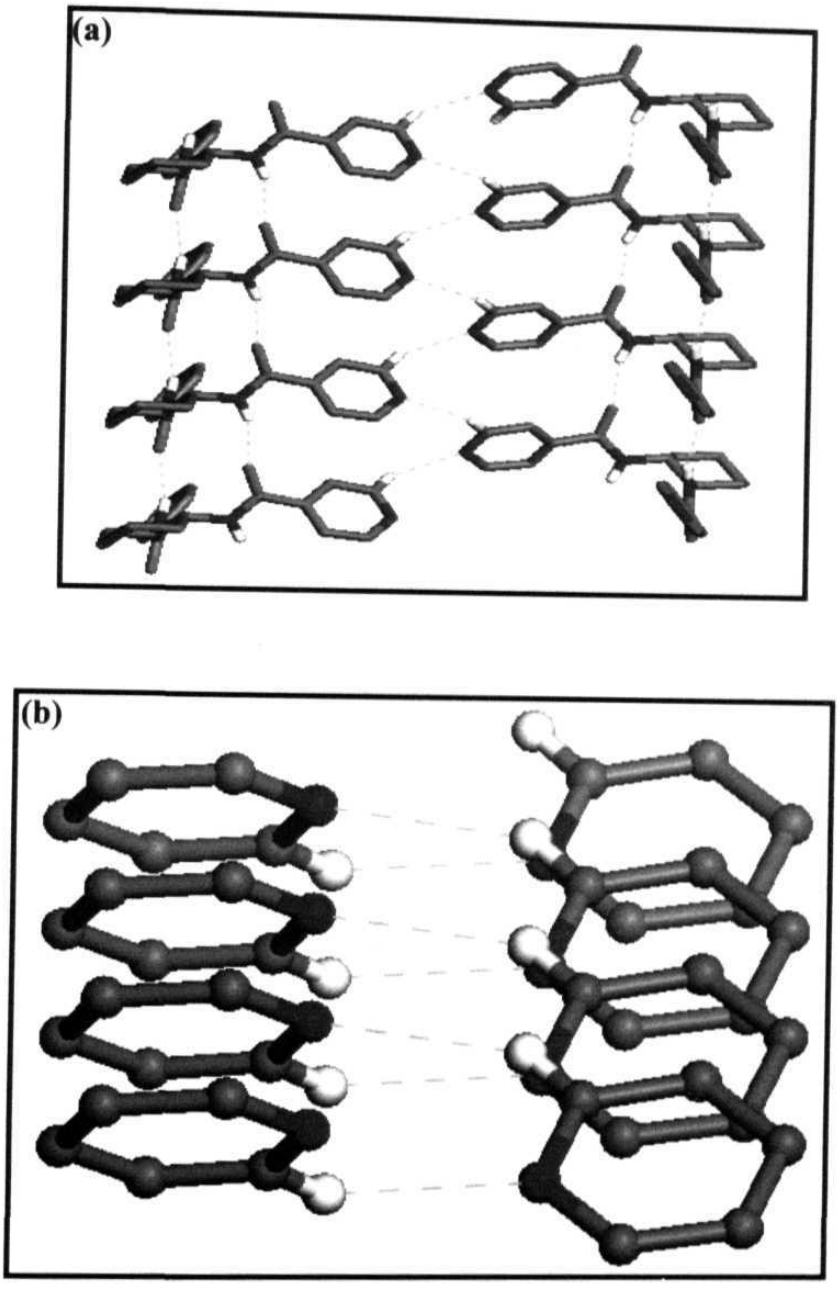

Figure 4.6 *(a) N-H…O and C-H…N intermolecular interactions in crystals of* ***BINDC*** *and (b) the helical motif arising from the latter interactions (the relevant pyridine ring and hydrogen atom alone are shown). C (grey), N (blue), O (red), H (white) and intermolecular contacts (broken cyan lines) are shown. Most H atoms are omitted for clarity.*

is given in Fig. 4.4. The amide groups in BINDC are disposed in the normal *anti* conformation. This is as expected for a free molecule as well (Table 4.2). As in BBDC, the amide groups enter into strong H-bond interactions ($r_{N4...O2}$ = 2.972 Å, $\theta_{N4-H4...O2}$ = 160.2°; $r_{N3...O1}$ = 3.033 Å, $\theta_{N3-H3...O1}$ = 162.4°) leading to an extended structure along the *a* axis (Fig. 4.5). In addition, there are relatively short intermolecular contacts involving the pyridine nitrogen atom and one of the hydrogen atoms *ortho* to it ($r_{C22...N6}$ = 3.453 Å, $\theta_{C22-H22...N6}$ = 149.8°). These interactions lead to a helical motif extending along the *a* direction (Fig. 4.6). The intermolecular hydrogen bonding interactions involving the amide groups and one of the pyridine units lead to the formation of one-dimensional extended network structure. The second pyridine ring is not involved in any recognizable intermolecular interactions. The subtle variation in the molecular structure from BBDC to BINDC and the introduction of intermolecular contacts through the ring nitrogen in latter changes the molecular assembly pattern completely with the conformation reverting back to *anti*. Semiempirical[47] and ab initio[48] computations show that the *anti* conformer is stabler than the *syn* conformer (Table 4.2); therefore the solid state interactions do not have any special role in this case of stabilizing an alternate conformation. The CD

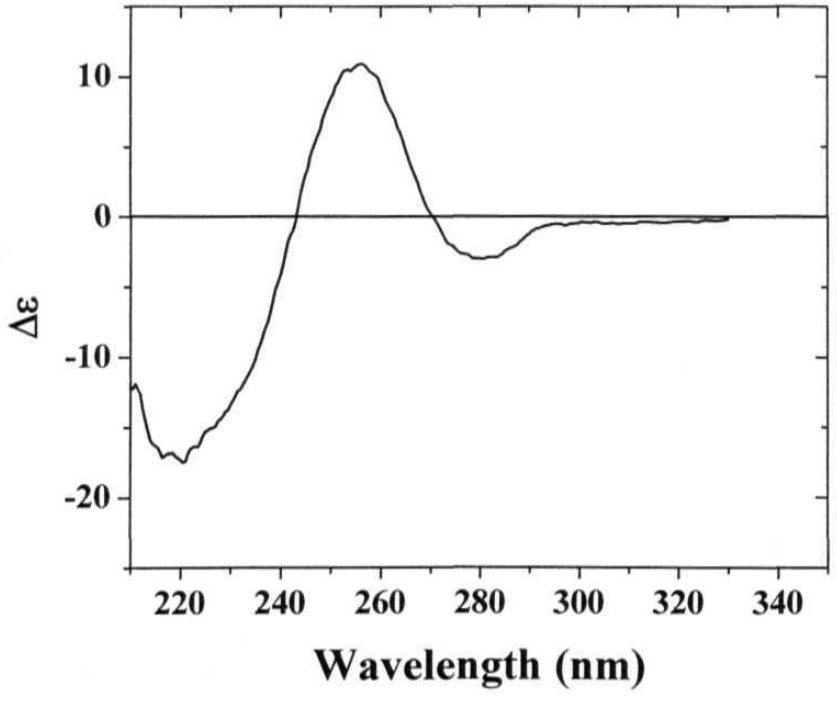

Figure 4.7 *CD spectrum of **BINDC** in methanol solution.*

spectrum of BINDC in methanol solution shows positive helicity (Fig. 4.7). Based on the synthesis we know that the stereochemistry of BINDC is (*R*,*R*); the helicity reversal compared to BBDC may be attributed to the reorientation of the transition dipoles in the amide-pyridine combination with respect to that in the amide group of BBDC.

4.4 DERIVATIVES OF BBDC : MOLECULAR AND CRYSTAL STRUCTURE INVESTIGATIONS

The carbonyl moiety attached to the phenyl groups in BBDC acts as potential electron sink, although the amino group tend to reduce the electron withdrawing effect. Therefore, the molecular hyperpolarizability of BBDC can be influenced by the nature of the substituents in the *para* position of the phenyl ring. We have synthesized two derivatives with electron withdrawing groups (fluoro and nitro) and two with electron donating groups (methoxy and amino). In this section, we describe the assembly of these molecules in their crystals.

BFBDC

Crystals were grown by slow evaporation of methanol solution. X-ray analysis showed that the crystals belong to the orthorhombic space group $P2_12_12_1$ with one molecule in the asymmetric unit. The basic crystallographic data are presented in Table 4.3 and the molecular structure is depicted in Fig. 4.8. The bis(amide) group in BFBDC adopts the *anti* conformation. The amide groups are involved in strong H-bond interactions ($r_{N5\cdots O3}$ = 3.026 Å, $\theta_{N4\text{-}H4\cdots O2}$ = 163.5°; $r_{N6\cdots O4}$ = 2.937 Å, $\theta_{N3\text{-}H3\cdots O1}$ = 158.3°) in the crystal lattice and lead to an extended network structure along the *a* axis (Fig. 4.9). Intermolecular close contacts involving fluorine atoms are observed in the crystal lattice. Fluorine atom on one of the phenyl rings (F1) is involved in such intermolecular F…F interactions [49] with two neighboring molecules ($r_{F1\cdots F1}$ = 2.862 Å); it may be noted that the sum of the van der Waals radii is 2.94 Å. The F…F contacts leads to an extended one-dimensional chain along the *a* direction (Fig. 4.10a). The fluorine atom in the second phenyl ring (F2) is involved in weak intermolecular interactions with one of the hydrogen atoms *ortho* to F ($r_{C18\cdots F2}$ = 3.506 Å, $\theta_{C18\text{-}H18\cdots F2}$ = 133.9°). Interestingly these

interactions result in the formation of a helical motif along the *a* direction (Fig. 4.10b). The amide hydrogen bonds coupled with the intermolecular interactions involving the fluorine atoms lead to the formation of a two-dimensional extended network structure. The CD spectrum of BFBDC in methanol solution (Fig. 4.11) has similar pattern as that reported for BBDC.[44]

Table 4.3. *Crystallographic data for* ***BFBDC*** *and* ***BNBDC***

Identification code	**BFBDC**	**BNBDC**
Empirical formula	$C_{20}H_{20}F_2N_2O_2$	$C_{20}H_{20}N_4O_6$
Formula weight	358.38	412.40
Crystal system	Orthorhombic	Orthorhombic
Space group	$P2_12_12_1$ (No. 19)	$P2_12_12_1$ (No. 19)
a / Å	5.0889(3)	5.0133(9)
b / Å	18.8303(11)	17.922(3)
c / Å	18.8509(11)	22.016(4)
V / Å^3	1806.40(18)	1978.1(6)
Z	4	4
$\rho_{calc.}$ / g cm^{-3}	1.318	1.385
μ / mm^{-1}	0.100	0.104
λ / Å	0.71073	0.71073
2θ range / deg.	1.53 – 28.26	1.47 – 28.23
Unique reflections	4321	4273
Reflection with $I \geq 2\sigma_I$	2290	2267
No. of parameters	236	272
GOF	1.009	0.980
R [for $I \geq 2\sigma_I$]	0.0615	0.0580
wR^2[for $I \geq 2\sigma_I$]	0.0952	0.0837

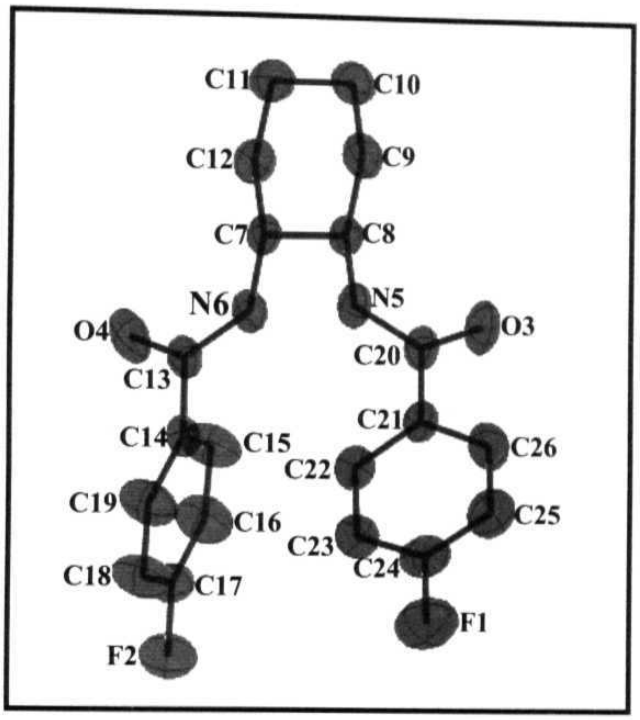

Figure 4.8 *Molecular structure of **BFBDC** from single crystal analysis. 95% probability thermal ellipsoids are indicated; H atoms are omitted for clarity.*

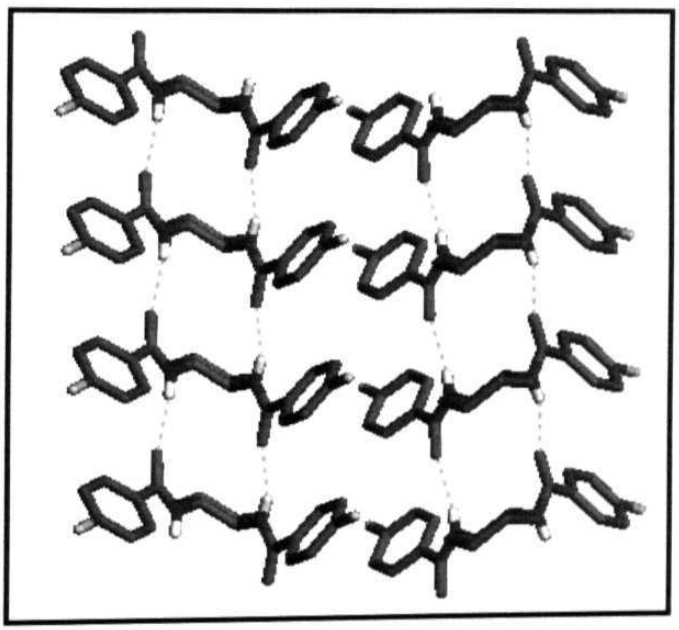

Figure 4.9. *Complementary amide hydrogen bonding interactions in crystals of **BFBDC**; C (grey), N (blue), O (red), H (white), F (light cyan) and H-bonds (broken cyan lines) are shown; H of amide groups alone are shown for clarity.*

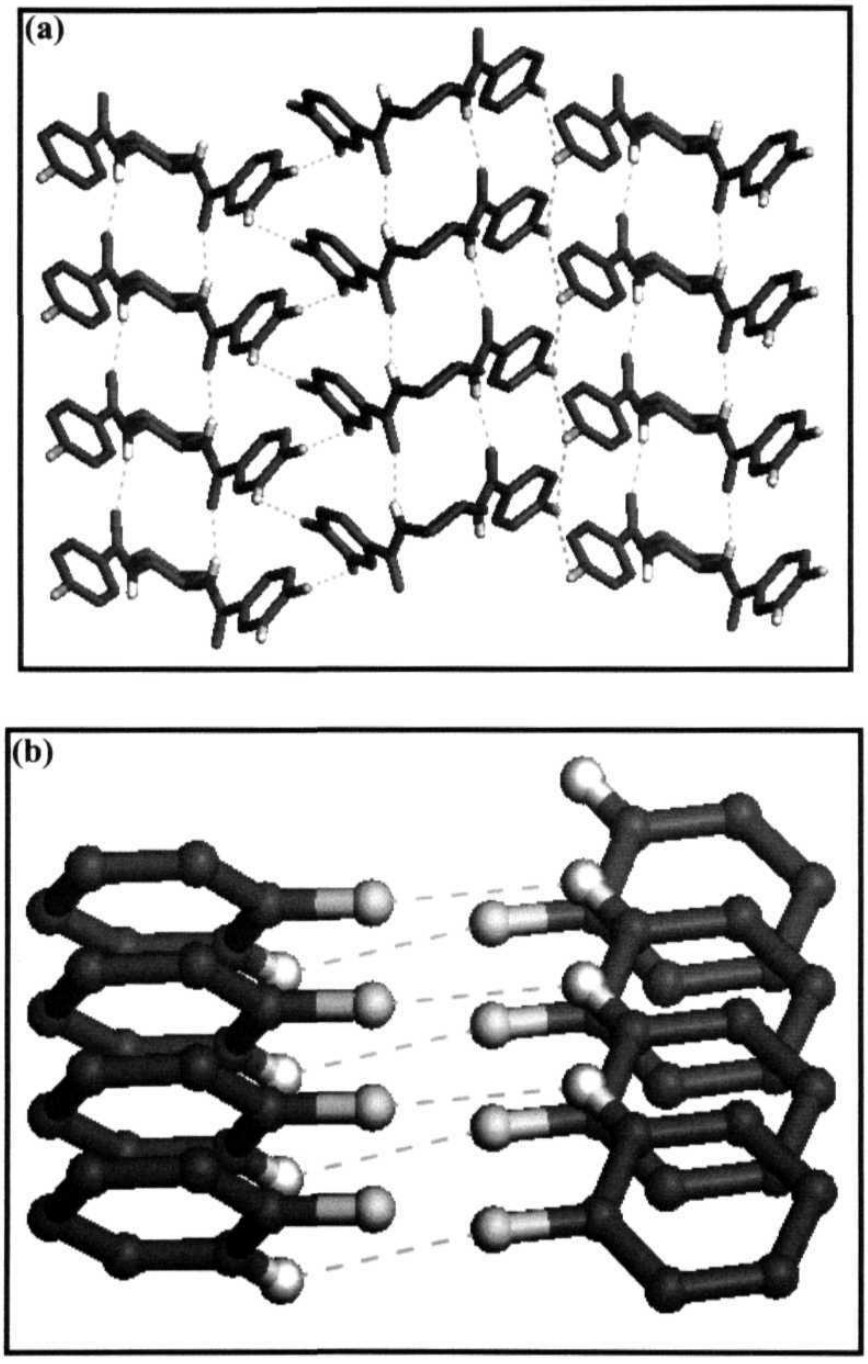

Figure 4.10 *(a) N-H...O, C-H...F and F...F intermolecular interactions in crystals of* ***BFBDC*** *and (b) the helical motif arising from the CH...F contacts (the relevant fluorophenyl ring and hydrogen alone are shown). C (grey), N (blue), O (red), H (white), F (light cyan) and intermolecular contacts (broken cyan lines) are shown. Most H atoms are omitted for clarity.*

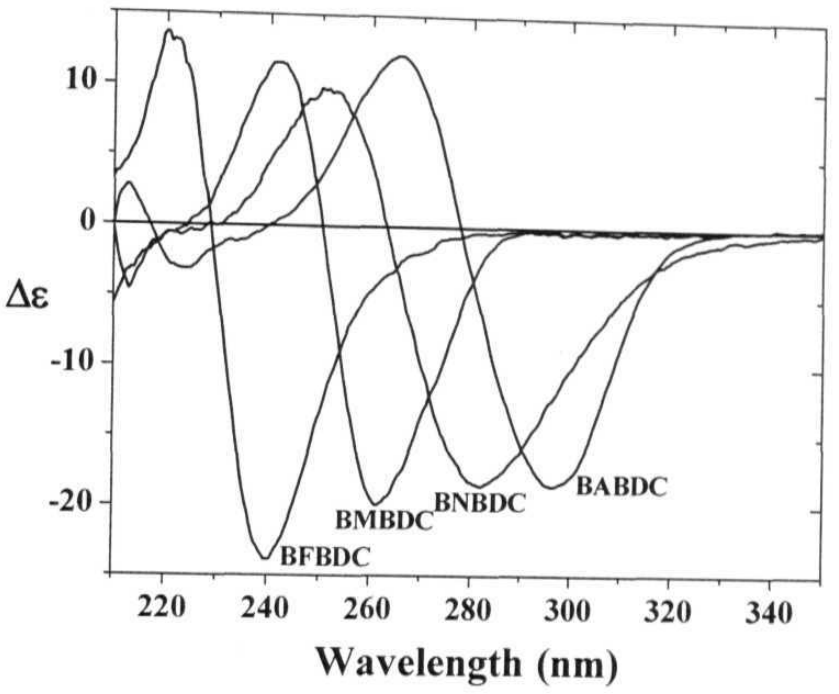

Figure 4.11 *CD spectra of* ***BFBDC, BNBDC, BMBDC*** *and* ***BABDC*** *in methanol solution.*

BNBDC

Crystals grown by slow evaporation of methanol solution belong to the orthorhombic space group $P2_12_12_1$ with one molecule in the asymmetric unit. The basic crystallographic data are provided in Table 4.3. The molecular structure is shown in Fig. 4.12. The amide groups in BNBDC are in the *anti* conformation. Once again, the amide groups forms strong intermolecular H-bond interactions ($r_{N7...O1}$ = 2.852 Å, $\theta_{N7-H7...O1}$ = 159.6°; $r_{N8...O2}$ = 2.975 Å, $\theta_{N8-H8...O2}$ = 150.4°) leading to an extended structure along the *a* axis (Fig. 4.13). The nitro group provides another H-bonding option and leads to interactions between one oxygen atom of one of the nitro groups and hydrogen atoms of the phenyl ring *meta* to the nitro group ($r_{C23...O4}$ = 3.579 Å, $\theta_{C23-H23...O4}$ = 152.4°) (Fig. 4.14). The CD spectrum of BNBDC molecules in methanol solution (Fig. 4.11) again follows the general pattern.[44]

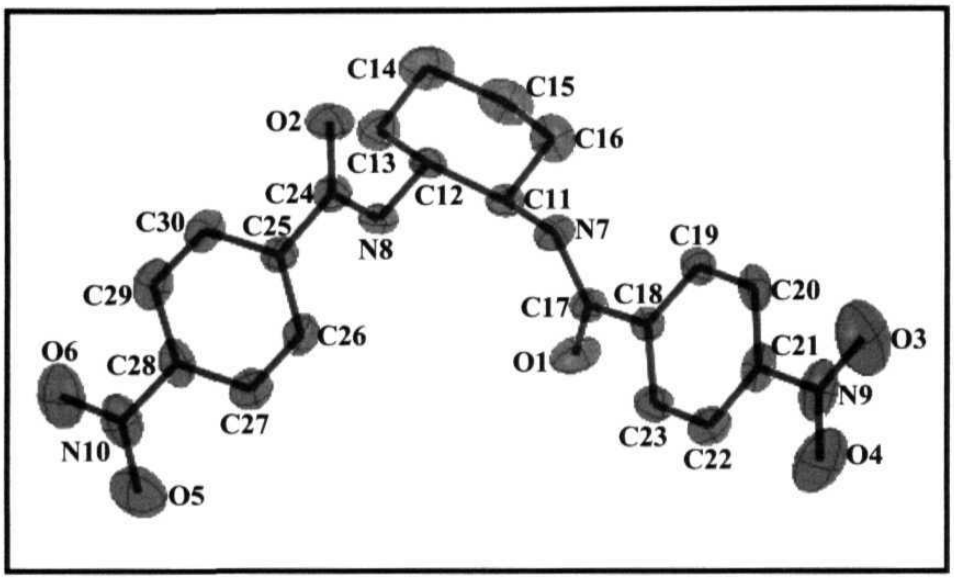

Figure 4.12 *Molecular structure of **BNBDC** from single crystal analysis. 95% probability thermal ellipsoids are indicated; H atoms are omitted for clarity.*

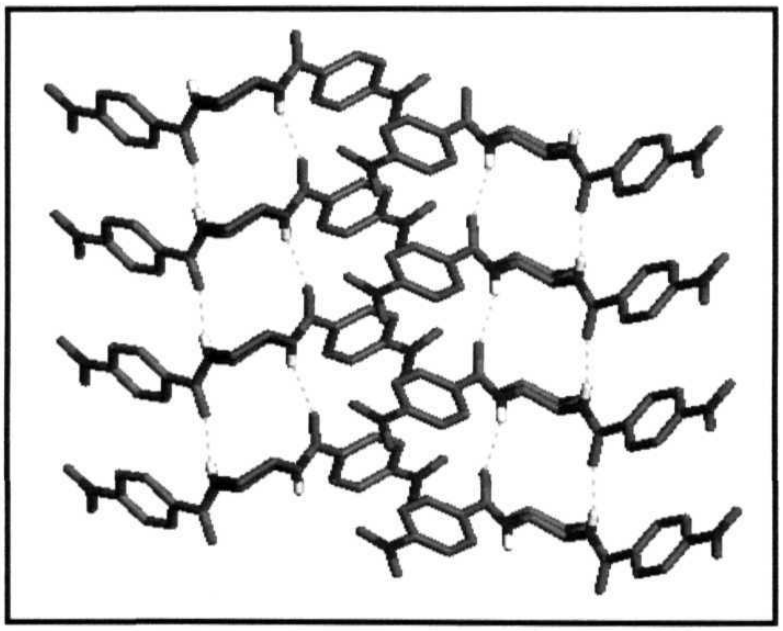

Figure 4.13 *Complementary amide hydrogen bonding interactions in crystals of **BNBDC**; C (grey), N (blue), O (red), H (white) and H-bonds (broken cyan lines) are shown; H of amide groups alone are shown for clarity.*

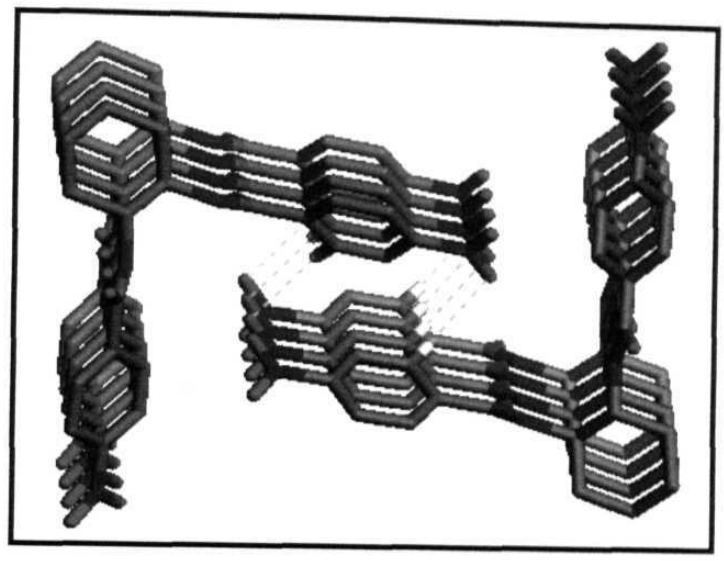

Figure 4.14 *Helical assembly through C-H...O interactions in crystals of* ***BNBDC****; C (grey), N (blue), O (red), H (white) and H-bonds (broken cyan lines) are shown; relevant hydrogen atoms alone are shown for clarity.*

BMBDC

Crystals were grown by slow evaporation of methanol solution. X-ray analysis revealed that the crystals belong to the orthorhombic space group $P2_12_12_1$ with one molecule in the asymmetric unit. The basic crystallographic data are presented in Table 4.4. The molecular structure is shown in Fig. 4.15. The bis(amide) group in BMBDC also occurs in *anti* conformation. Strong complementary H-bond interactions ($r_{N5...O1}$ = 2.934 Å, $\theta_{N5-H5...O1}$ = 157.0°; $r_{N6...O2}$ = 2.953 Å, $\theta_{N6-H6...O2}$ = 158.3°) are observed in the *a* direction (Fig. 4.16). Weak intermolecular C-H...O interactions between the methoxy groups of neighboring molecules ($r_{C28...O3}$ = 3.397 Å, $\theta_{C28-H28B...O3}$ = 157.8°) lead to the formation of left handed helical assembly along the *c* axis (Fig. 4.17a). Another intermolecular interaction between the oxygen atom of a carbonyl group and hydrogen atom of the methoxy group ($r_{C28...O2}$ = 3.515 Å, $\theta_{C28-H28C...O4}$ = 167.0°) lead to right handed helical structure formation along the *a* axis (Fig. 4.17b). The CD spectrum of BMBDC molecules in methanol solution shows negative helicity of the amide groups and resembles that of the earlier derivatives (Fig. 4.11).

Table 4.4. *Crystallographic data for* ***BMBDC*** *and* ***BABDC***

Identification code	**BMBDC**	**BABDC. $2H_2O$**
Empirical formula	$C_{22}H_{26}N_2O_4$	$C_{20}H_{28}N_4O_4$
Formula weight	382.45	388.43
Crystal system	Orthorhombic	Monoclinic
Space group	$P2_12_12_1$ (No. 19)	$P2_1$ (No. 4)
a / Å	5.0789(5)	5.1297(4)
b / Å	19.1500(18)	21.2093(17)
c / Å	20.9714(19)	9.4739(8)
β /°	90.0	99.158(2)
V / $Å^3$	2039.7(3)	1017.60(14)
Z	4	2
$\rho_{calc.}$ / g cm^{-3}	1.245	1.150
μ / mm^{-1}	0.086	0.076
λ / Å	0.71073	0.71073
2θ range / deg.	1.44 – 28.27	1.92 – 28.31
Unique reflections	4778	4722
Reflection with $I \geq 2\sigma_I$	2388	3615
No. of parameters	255	269
GOF	0.859	1.066
R [for $I \geq 2\sigma_I$]	0.0443	0.0592
WR^2[for $I \geq 2\sigma_I$]	0.0681	0.1122

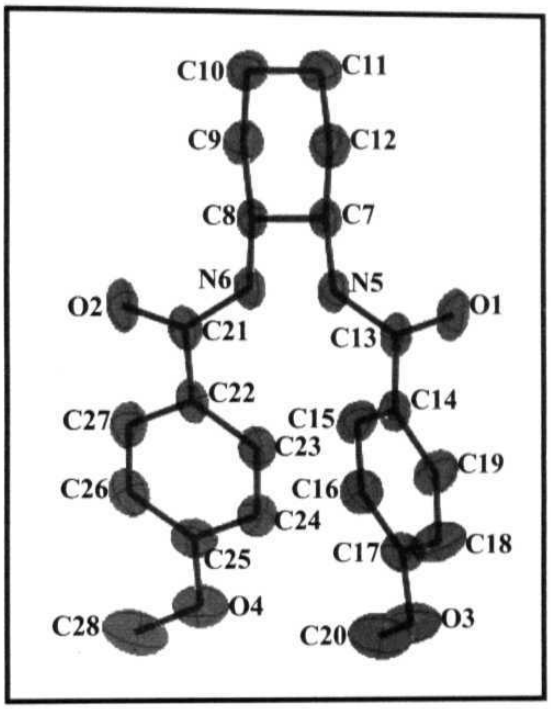

Figure 4.15 *Molecular structure of* ***BMBDC*** *from single crystal analysis. 95% probability thermal ellipsoids are indicated. H atoms are omitted for clarity.*

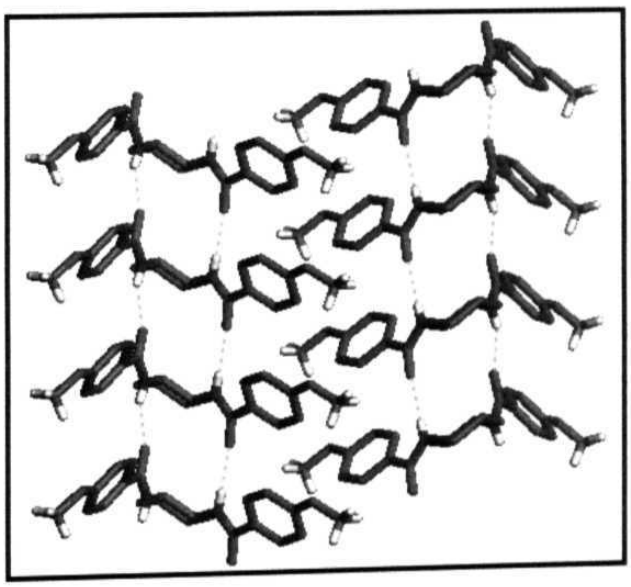

Figure 4.16 *Complementary amide hydrogen bonding interactions in crystals of* ***BMBDC****; C (grey), N (blue), O (red), H (white) and H-bonds (broken cyan lines) are shown; H of amide and methoxy groups alone are shown for clarity.*

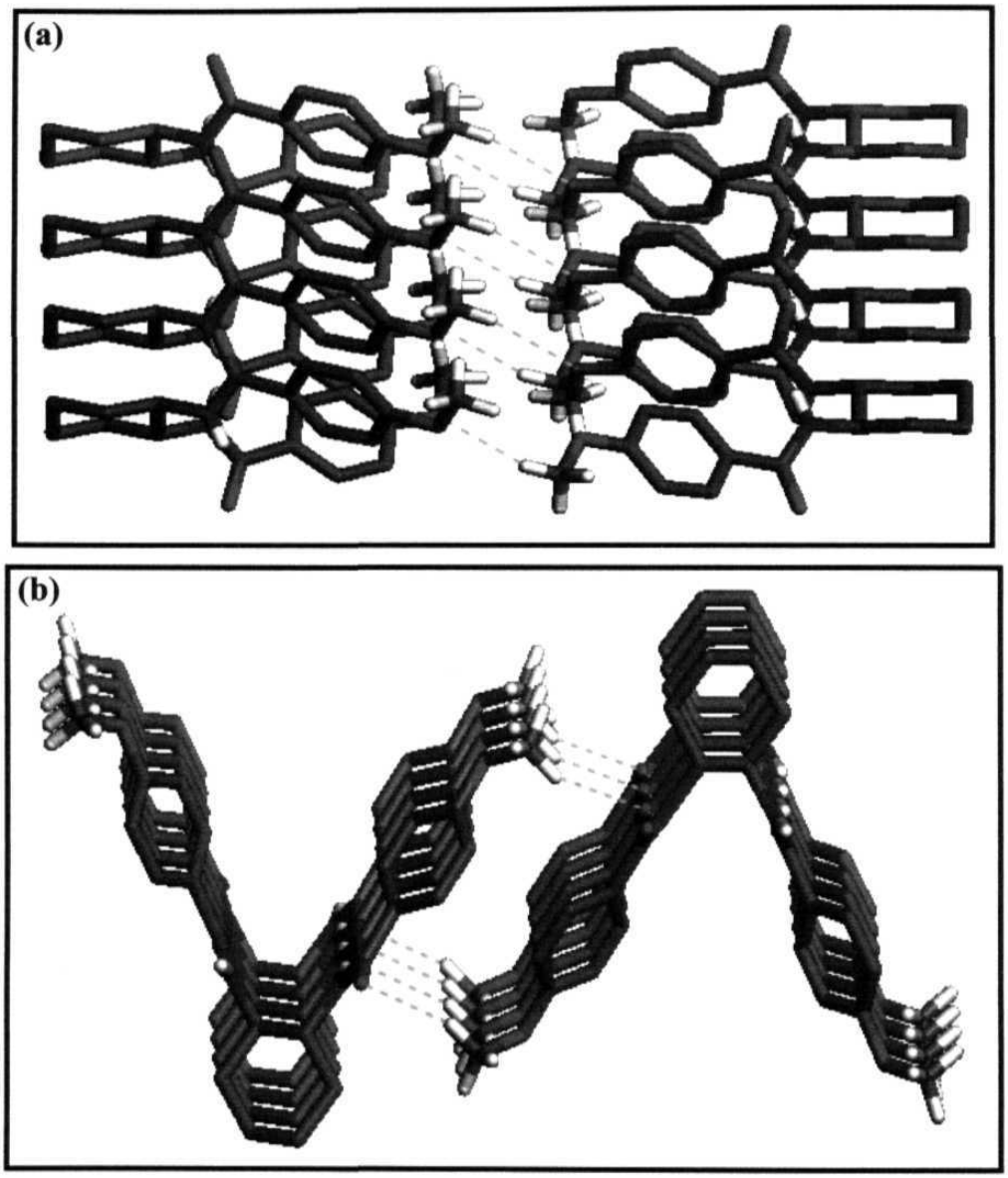

Figure 4.17 *Helical assembly in crystals of* ***BMBDC*** *formed through C-H...O interactions between (a) methoxy groups and (b) methoxy-carbonyl groups.*

BABDC

Crystals of BABDC were grown from methanol solution by slow evaporation. X-ray analysis revealed that the crystals belong to the monoclinic space group $P2_1$ with one molecule in the asymmetric unit. Two water molecule are also included in the lattice

The basic crystallographic data are presented in Table 4.4. The molecular structure of BABDC.$2H_2O$ is shown in Fig. 4.18. The amide groups in BABDC are disposed in the usual *anti* conformation. There is a large number of strong intermolecular H-bonds in the crystal. The geometric features of these H-bonds are summarized in Table 4.5. Complementary H-bonds occur between amide groups. Further there are strong interactions between the amide groups and water molecules (Fig. 4.19). Extended H-bonds involving amino group, water molecules and amide group leads to helical structures extending along the *a* axis (Fig. 4.20). The CD spectrum of BABDC in methanol solution (Fig. 4.11) also conforms to those of other molecules in the family. The collection of CD spectrum of the BBDC derivatives (Fig. 4.3 and Fig. 4.11) indicates that all molecules have similar conformation in solution. Since *anti* conformation is seen in the crystal structure of all the derivatives and is shown to be stabler energetically, we conclude that the conformation is *anti*.

Table 4.5 *Strong intermolecular H-bonds in* ***BABDC****. D and A are the H-bond donor and accepter atoms respectively in the D-H...A bond; r and θ are the relevant distance and angle.*

D-H	A	$r_{D...A}$ (Å)	$\theta_{D-H...A}$ (°)
N5-H5	O1	2.978	153.3
N6-H6	O2	2.976	162.2
O3-H3A	O1	2.820	168.5
O4-H4A	O2	2.868	170.7
N7-H7A	O3	2.981	139.6
N8-H8A	O3	3.097	163.8
N7-H7B	O4	3.195	157.0
N8-H8B	O4	2.999	154.7
O3-H3B	N8	2.983	163.3
O4-H4B	N7	3.039	168.7

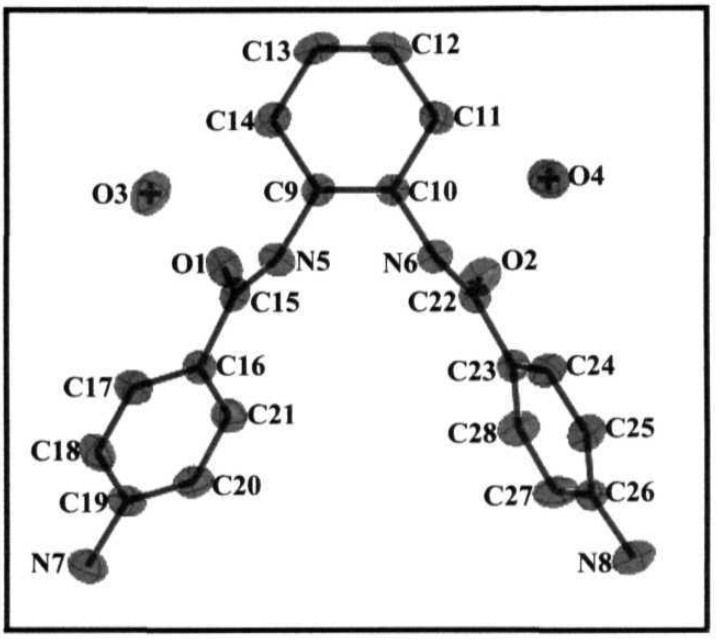

Figure 4.18 *Molecular structure of* ***BABDC.2H$_2$O*** *from single crystal analysis. 95% probability thermal ellipsoids are indicated; H atoms are omitted for clarity.*

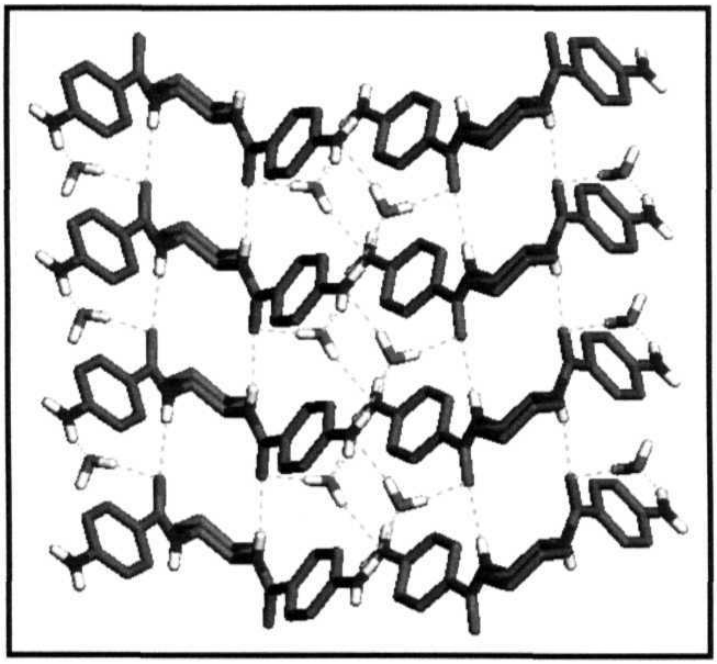

Figure 4.19 *Complementary hydrogen bonding interactions involving amide and water in crystals of* ***BABDC.2H$_2$O****; C (grey), N (blue), O (red), H (white) and H-bonds (broken cyan lines) are shown; H atoms involved in H-bonds alone are shown for clarity.*

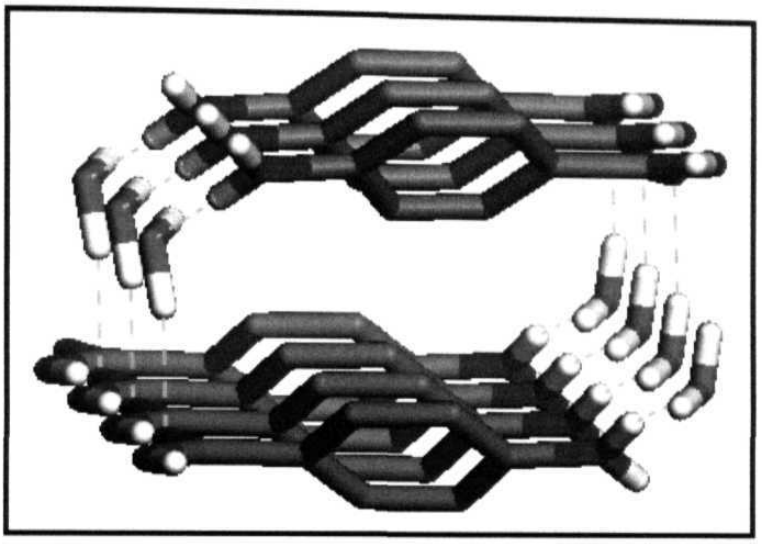

Figure 4.20 *Helical motif in crystals of* ***BABDC*** *arising through hydrogen bonding interactions between water, amide and amino groups; only one 4-aminobenzamide unit from each* ***BABDC*** *molecule is shown for clarity.*

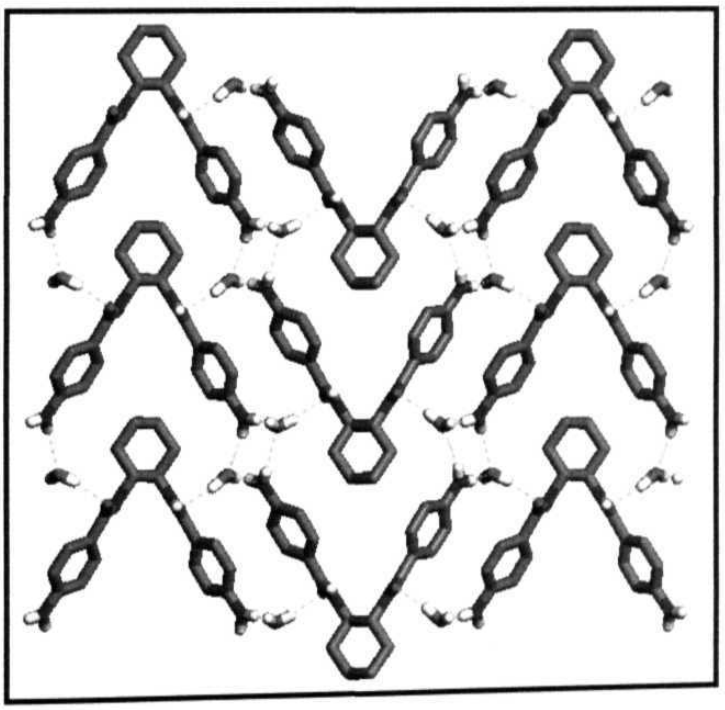

Figure 4.21 *H-bonding interactions in the* ***BABDC*** *molecules in the bc plane; H of amide, water and amino groups alone are shown for clarity.*

4.5 COORDINATION POLYMERS BASED ON BINDC LIGAND : CRYSTAL STRUCTURE INVESTIGATIONS

As described in Sec. 4.2, crystals of Zn(BINDC)Cl_2 and Zn(BINDC)Br_2 were grown by slow evaporation of methanol-water solution, whereas Ag(BINDC)NO_3 crystals were grown at the interface of methanol-water solution by layering a methanol solution of BINDC on top of an aqueous solution of silver nitrate. X-ray analysis showed that all the three crystals belong to the orthorhombic space group $P2_12_12$ with one molecule in the unit cell. The basic crystallographic data of the three compounds are presented in Table 4.6.

The molecular structures of Zn(BINDC)Cl_2 and Zn(BINDC)Br_2 are shown in Fig. 4.22. Zn(II) is tetrahedrally coordinated to the two halogen atoms and two pyridine nitrogens from different BINDC molecules. This coordination leads to the formation of extended one-dimensional polymers in Zn(BINDC)Cl_2 and Zn(BINDC)Br_2. The strong complementary hydrogen bonding interaction observed between the amide groups in the BINDC ligand is intact in the coordination polymer as well. In Zn(BINDC)Cl_2, N-H...O interactions ($r_{N6...O4}$ = 3.075 Å, $\theta_{N6-H6...O4}$ = 176.7°; $r_{N7...O5}$ = 2.893 Å, $\theta_{N7-H7...O4}$ = 160.8°) along *c* directs the one-dimensional coordination polymer to self assemble into a two-dimensional corrugated sheet like structure (Fig. 4.23). Moreover the chlorine atoms form close contacts with the hydrogen atoms of the pyridyl groups; the hydrogen atoms *ortho* ($r_{C19...Cl2}$ = 3.563 Å, $\theta_{C19-H19...Cl2}$ = 149.7) and *meta* ($r_{C27...Cl2}$ = 3.759 Å, $\theta_{C27-H27...Cl2}$ = 165.0°) to the nitrogen of the pyridyl ring are involved (Fig. 4.24). The coordinate bond, amide H-bonds and chlorine-hydrogen interactions lead to the formation of a three-dimensional network structure. In Zn(BINDC)Br_2, the amide groups enter into strong intermolecular interactions ($r_{N6...O4}$ = 3.098 Å, $\theta_{N6-H6...O4}$ = 175.2°; $r_{N7...O5}$ = 2.900 Å, $\theta_{N7-H7...O5}$ = 148.0°) and assemble the *zig-zag* coordination polymer chains into two-dimensional corrugated network structure (Fig. 4.25).

The molecular structure of Ag(BINDC)NO_3 is shown in Fig. 4.26. Ag(I) is coordinated tetrahedrally to two oxygen atoms from different nitro groups and two pyridine nitrogens from different BINDC molecules leading to the formation of a two-dimensional network polymer. The amide hydrogen bond interactions ($r_{N6...O4}$ = 3.046 Å,

$\theta_{N6\text{-}H6\ldots O4}$ = 157.0°) appear within this network structure and probably enhance its stability (Fig. 4.27). The anionic nitro group acts as a bidentate ligand and coordinates two silver metal centers in the formation of the extended network structure. Weak intermolecular interactions between the oxygen atoms of the nitro group and hydrogen atom *meta* to pyridine nitrogen ($r_{C16\ldots O2}$ = 3.554 Å, $\theta_{C16\text{-}H16\ldots O2}$ =161.6°) are also observed in the crystal lattice (Fig.4.28).

Table 4.6. *Crystallographic data for* ***Zn(BINDC)Cl$_2$, Zn(BINDC)Br$_2$*** *and* ***Ag(BINDC)NO$_3$***

Identification code	**Zn(BINDC)Cl_2**	**Zn(BINDC)Br_2**	**Ag(BINDC)NO_3**
Empirical formula	$C_{18}H_{20}Cl_2N_4O_2Zn$	$C_{18}H_{20}Br_2N_4O_2Zn$	$C_{18}H_{20}N_4O_5Ag$
Formula weight	460.65	549.57	480.25
Crystal system	Orthorhombic	Orthorhombic	Orthorhombic
Space group	$P2_12_12$ (No. 18)	$P2_12_12$ (No. 18)	$P2_12_12$ (No. 18)
a / Å	15.0824(9)	15.1119(18)	5.1990(4)
b / Å	25.3484(15)	25.855(3)	12.6951(9)
c / Å	5.0566(3)	5.0689(4)	14.4281(10)
V / Å^3	1933.2(2)	1980.5(4)	952.28(12)
Z	4	4	2
$\rho_{calc.}$ / g cm^{-3}	1.583	1.843	1.675
μ / mm^{-1}	1.568	5.296	1.096
T_{min}, T_{max}	0.737, 0.921	0.617, 0.948	0.720, 0.898
λ / Å	0.71073	0.71073	0.71073
2θ range / deg.	1.57-28.25	1.56 – 28.33	1.41 - 28.26
Unique reflections	4588	4736	2261
Reflection with I $\geq 2\sigma_I$	2913	4021	2175
No. of parameters	245	244	133
GOF	0.873	0.979	1.113
R [for I $\geq 2\sigma_I$]	0.0469	0.0355	0.0341
wR^2[for I $\geq 2\sigma_I$]	0.0666	0.0739	0.0816

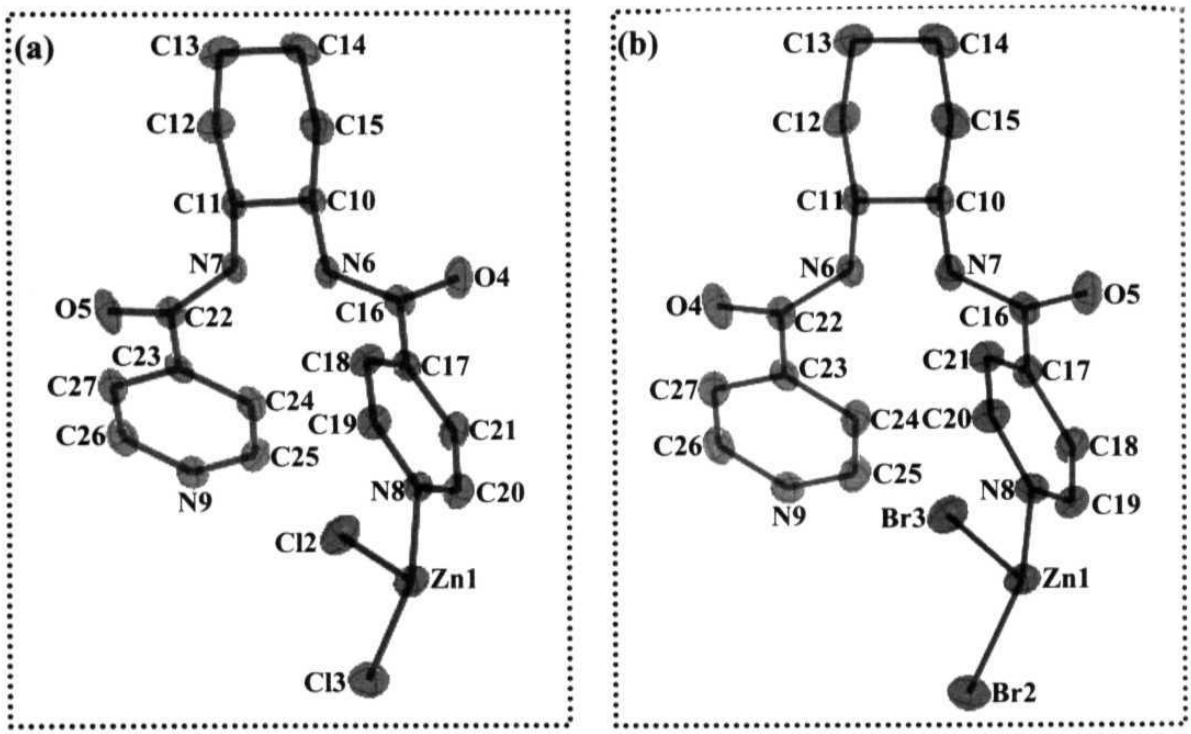

Figure 4.22 *Structure of the asymmetric unit in the coordination polymers, (a)* ***Zn(BINDC)Cl$_2$*** *and (b)* ***Zn(BINDC)Br$_2$*** *from single crystal analysis. 95% probability thermal ellipsoids are indicated; H atoms are omitted for clarity.*

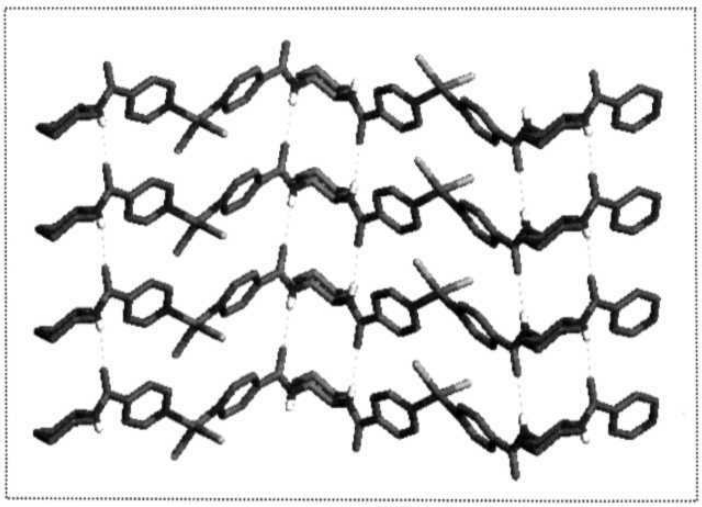

Figure 4.23 *Metal coordination and N-H...O interactions in the crystal of* ***Zn(BINDC)Cl$_2$****; C (grey), N (blue), O (red), H (white), Cl (green), Zn (slate gray) and H-bonds (broken cyan lines) are shown; H of amide groups alone are shown for clarity.*

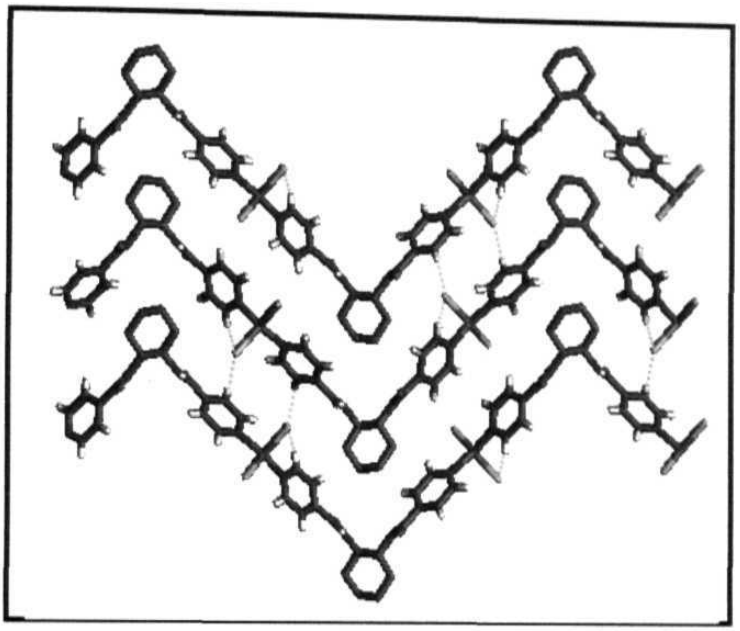

Figure 4.24 *C-H…Cl interactions in the crystal of* ***Zn(BINDC)Cl$_2$;*** *C (grey), N (blue), O (red), H (white), Cl (green), Zn (slate gray) and H-bonds (broken cyan lines) are shown; H of amide and phenyl groups alone are shown for clarity.*

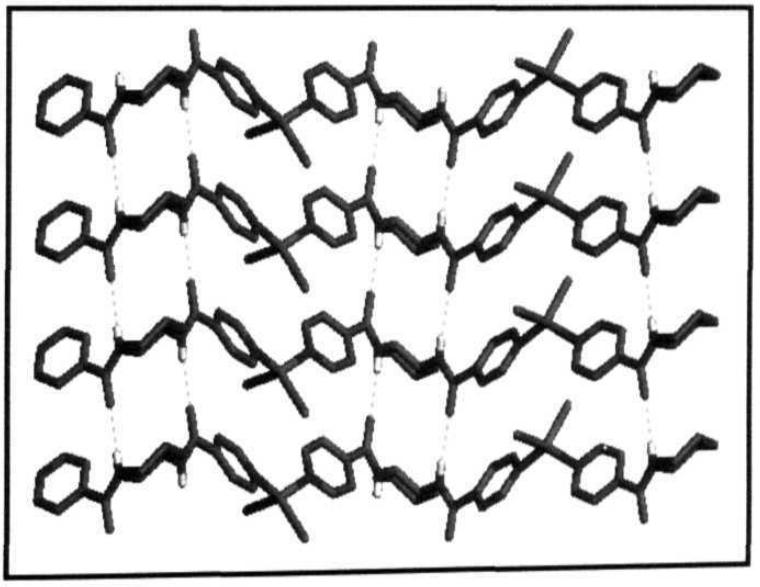

Figure 4.25 *Metal coordination and N-H…O interactions in the crystal of* ***Zn(BINDC)Br$_2$****; C (grey), N (blue), O (red), H (white), Br (wine), Zn (slate gray) and H-bonds (broken cyan lines) are shown; H of amide groups alone are shown for clarity.*

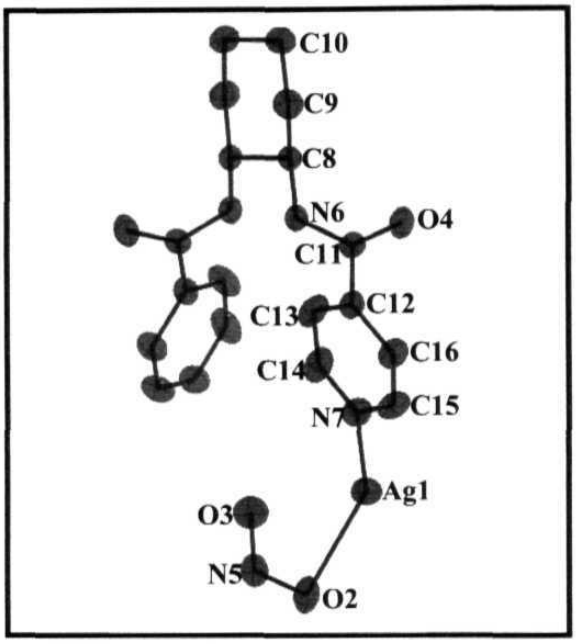

Figure 4.26 *Structure of the asymmetric unit in the coordination polymer,* ***Ag(BINDC)NO$_3$*** *from single crystal analysis. 95% probability thermal ellipsoids are indicated. . H atoms are omitted for clarity.*

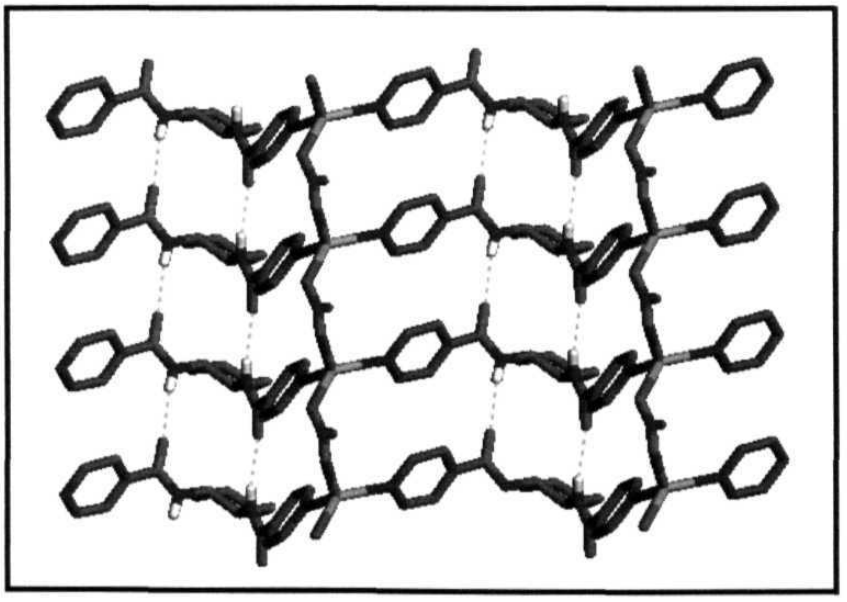

Figure 4.27 *Metal coordination and N-H...O interactions in the crystal of* ***Ag(BINDC)NO$_3$****; C (grey), N (blue), O (red), H (white), Ag (light steel blue) and H-bonds (broken cyan lines) are shown; H of amide groups alone are shown for clarity.*

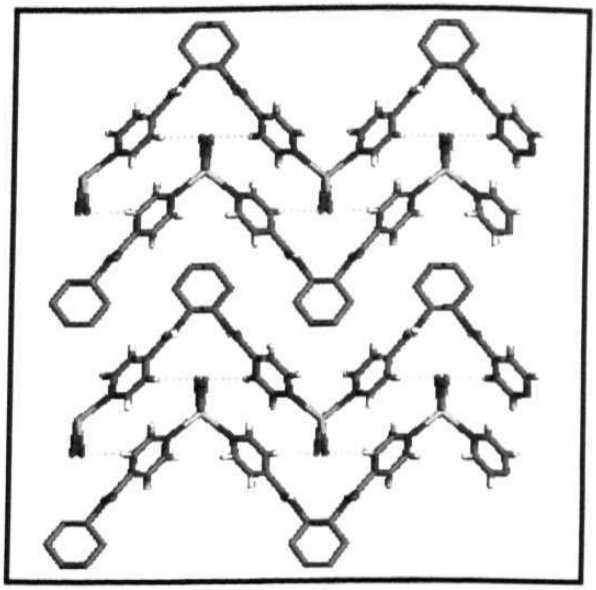

Figure 4.28 *C-H…O interactions in the crystal of* ***Ag(BINDC)NO$_3$****; C (grey), N (blue), O (red), H (white), Ag (light steel blue) and H-bonds (broken cyan lines) are shown; H of amide and phenyl groups alone are shown for clarity.*

4.6 OPTICAL SECOND HARMONIC GENERATION STUDY AND THERMAL STABILITY

The molecular structure of BBDC and BINDC do not possess any special features that enhance hyperpolarizabilities. The β values were estimated using AM1/TDHF[50] computations on AM1 optimized structure. The results are collected in Table 4.7. BBDC and BINDC possess small hyperpolarizabilities, irrespective of the conformation. However, the methoxy and amino substituted BBDC show higher values as suggested earlier. Since the BBDC and BINDC families of molecules assemble in interesting noncentrosymmetric structures, SHG from microcrystalline powders were examined using the Kurtz-Perry technique.[51] Details of the experiment are provided in Appendix C. The data for the different compounds discussed in the earlier sections are collected in Table 4.8. The particle size dependence of SHG indicates phase-matchable behavior in all the cases. BBDC shows no measurable SHG, but BINDC shows a moderate value of 0.8 U. This possibly owes its origin to the helical superstructure in BINDC; as noted in Chapter 3, the significance of helical organization for quadratic NLO effects has been

Table 4.7. ***AM1/TDHF*** *computed hyperpolarizabilities, β (static and at 1.17eV) of* ***BBDC****, its derivatives and* ***BINDC***

Structure	β (0 eV) (x 10^{-30} esu)	β (1.17 eV) (x 10^{-30} esu)
BBDC (*syn*)	0.86	1.22
BBDC (*anti*)	0.90	1.22
BINDC (*anti*)	0.87	1.24
BINDC (*syn*)	0.90	1.27
BFBDC	1.44	2.11
BNBDC	1.81	2.83
BMBDC	4.02	6.37
BABDC	6.47	11.29

Table 4.8. *SHG data for* ***BMBDC****,* ***BABDC****,* ***BINDC****,* ***Zn(BINDC)Cl$_2$****,* ***Zn(BINDC)Br$_2$*** *and* ***Ag(BINDC)NO$_3$*** *(1U = SHG of urea with average particle size of 150 μm)*

Compound	SHG (U)				
	Particle size (μm)				Average value at saturation
	100-150	150-200	200-250	250-300	
BMBDC	0.87	0.89	0.87	0.90	0.9
BABDC	1.79	1.81	1.87	1.80	1.82
BINDC	0.79	0.78	0.81	0.83	0.80
Zn(BINDC)Cl$_2$	0.37	0.35	0.39	0.37	0.38
Zn(BINDC)Br$_2$	0.34	0.36	0.37	0.36	0.37
Ag(BINDC)NO$_3$	0.36	0.34	0.37	0.37	0.37

highlighted in several investigations from our laboratory and elsewhere.[23,52] While the derivatives of BBDC with electron withdrawing groups produce no SHG, the methoxy and amino substituted ones show SHG of 0.9 and 1.8 U respectively. Since the general crystal packing are similar, the SHG of the bulk materials reflect the trends in molecular

nonlinearity. The SHG from all the coordination polymers of BINDC are ~ 0.4 U; the reduction from that of BINDC appears to result from the electron withdrawing effect of the coordinated metal and the extended structure formation. The observed impacts of the electron rich groups connected to the amide functionality in improving the solid state SHG and that of the electron withdrawing groups or metal complexation in reducing it are consistent with the classical 'push-pull' concepts.[1.22]

High thermal stability is an important attribute of the various materials developed in this investigation. As noted in Sec. 4.2, the new organic materials show melting temperatures above 250°C. The metal coordination polymers decompose above 300°C. The thermal stability of the compounds was investigated by differential scanning calorimetry; the melting transition temperatures are provided in Table 4.9. The extended intermolecular interactions ranging from weak H-bonds to strong ones and metal coordination lay the basis for the thermal robustness of these materials. This important characteristic coupled with high transparency of all these materials in the visible range should make them important candidates to develop quadratic nonlinear optical materials.

Table 4.9 *The melting transition temperatures of organic bis(amides) and coordination polymers.*

Compound	Onset temperature (°C)	Phase transition temperature (°C)
BBDC	257.5	265.6
BFBDC	265.0	270.0
BNBDC	338.2	340.0
BMBDC	264.7	269.0
BABDC	285.5	290.0
BINDC	267.8	270.0
Zn(BINDC)Cl_2	369.3	373.4
Zn(BINDC)Br_2	406.0	411.3
Ag(BINDC)NO_3	307.3	310.4

4.7 SUMMARY

We have developed a series of bis(amide) compounds based on axially chiral diaminocyclohexane. The molecule incorporating pyridine moiety is shown to be a versatile new ligand to build coordination polymers based on Zn(II) and Ag(I) ions. In Sec. 4.3, we presented the crystal structure of the simplest member of this family, BBDC in which, the rare *syn* conformer of the bis(amide) group is observed. The CD studies however, suggest that the amide groups orient in *anti* conformation in solution.[44] Interestingly, the molecule exhibits polar molecular organization with all the carbonyl groups oriented in the same direction in the crystal lattice. This crystal adds a new dimension to our investigation of perfectly polar crystals presented in Chapter 2. In the case BINDC, the subtle molecular structure variation causes complete change in the crystal lattice leading to helical motifs formed through weak intermolecular H-bonds. Strong intermolecular hydrogen bonding interactions between the amide groups are observed in the crystal lattice of all the compounds.

In Sec. 4.4, we described a family of derivatives of BBDC and structural network formation through various intermolecular interactions. In BFBDC, in addition to the complementary amide hydrogen bond interactions, F...F and H...F interactions are observed leading to helical assembly. Similarly, a range of weak intermolecular interactions lead to helical superstructures in the different derivatives involving nitro, methoxy and amino substituents. In Sec.4.5, we demonstrated the utility of the amide functionality to assemble the coordination polymer chains or networks through hydrogen bonding. The different coordination polymers are assembled into two-dimensional networks with interesting topologies.

We have investigated the optical second harmonic generation capability of the new family of organic crystals and coordination polymers in Sec. 4.6. Even though all the bis(amide) compounds form noncentrosymmetric crystal lattices, only those possessing electron donating group in the *para* position of the aromatic ring exhibit solid state SHG. Further, the SHG depends on the strength of the donor substituent in the phenyl group. In the case of the metal coordination polymers of BINDC, the electron withdrawing nature of the metal ions appears to affect the SHG capability of the free

ligand adversely. We have demonstrated that the strong hydrogen bonding interactions in bis(amide) molecules coupled with coordinate bond in coordination polymers make these materials thermally very stable and the right choice of metal ion leads to good optical transparency. The current study establishes these new series of organic and metal-organic compounds as viable systems to develop stable NLO materials.

REFERENCES :

1. (a) Chemla, D. S.; Zyss, J. (Eds.), *Nonlinear Optical Properties of Organic Molecules and Crystals*, Academic Press, New York, 1989, Vol. 1, 2; (b) Prasad, P. N.; Williams, D. J. *Introduction to Nonlinear Optical Effects in Molecules and Polymers*, John Wiley: New York, 1991; (c) Günter, P. *Nonlinear Optical Effects and Materials, Springer Series in Optical Sciences, Vol. 72*, Springer-Verlag, Heidelberg, 2000.
2. (a) Shen, H. Y.; Zhou, Y. P.; Lin, W. X.; Zeng, Z. D.; Zeng, R. R.; Yu, G. F.; Huang, C. H.; Jiang, A. D.; Jia, S. Q.; Shen, D. Z. *IEEE J. Quant. Electron.* **1992**, *28*, 48; (b) Smith, R. G.; Geusic, J. E.; Levinstein, H. J.; Rubin, J. J.; Singh, S.; Uitert, L. G. V. *Appl. Phys. Lett.* **1968**, *12*, 308; (c) Lin, S.; Wu, B.; Xie, F.; Chen, C. *Appl. Phys. Lett.* **1991**, *59*, 1541.
3. (a) Shu, C. –F.; Shu, Y. –C.; Gong, Z. –H.; Peng, S. –M.; Lee, G. –H,; Jen, A. K. –Y. *Chem. Mater.* **1998**, *10*, 3284; (b) Shu, Y. –C.; Gong, Z. –H.; Shu, C. –F.; Breitung, E. M.; McMahon, R. J.; Lee, G. –H. *Chem. Mater.* **1999**, *11*, 1628; (c) Zhang, C.; Ren, A. S.; Wang, F.; Zhu, J.; Dalton, L. R.; Woodford, J. N.; Wang, C. H. *Chem. Mater.* **1999**, *11*, 1966.
4. (a) Saadeh, H.; Yu, D.; Wang, L. M.; Yu, L. P. J. *Chem. Mater.* **1999**, *9*, 1865; (b) Liang, Z.; Dalton, L. R.; Garner, S. M.; Kalluri, S.; Chen, A.; Steier, W. H. *Chem. Mater.* **1995**, *7*, 941; (c) Yu, D.; Gharayi, A.; Yu, L.; *J. Am. Chem. Soc.* **1995**, *117*, 11680.
5. Bouder, T. L.; Maury, O.; Bozec, H. L.; Leodoux, I.; Zyss, J. *Chem. Commun.* **2001**, 2430.
6. (a) Le Bozec, H.; Renourd, T. *Eur. J. Inorg. Chem.* **2000**, 229; (b) Sénéchal, K.; Maury, O,; Le Bozec, H.; Ledoux, I.; Zyss, J. *J. Am. Chem. Soc.* **2002**, *124*, 4560.
7. (a) Nesterov,.V. V.; Antipin, M. Y.; Nesterov, V. N.; Penn, B. G.; Frazier, D. O.; Timofeeva, T. V. *Cryst. Growth Des.* **2004**, *3*, 521; (b) Nesterov, V. V.; Antipin, M. Y.; Nesterov, V. N.; Moore, C. E.; Cardelino, B. H.; Timofeeva, T. V. *J. Phy. Chem. B* **2004**, *108*, 8531.
8. Bernstein, J. *Polymorphism in Molecular Crystals*, Oxford University Press: Oxford 2002, chapter 5.

9. (a) Bernstein, J. *Polymorphism in Molecular Crystals*, Oxford University Press: Oxford 2002, chapter 6; (b)Burchell, T. J.; Eisler, D. J.; Puddephatt, R. J. *Chem. Commun.* **2004**, 944.

10. (a) Aakeröy, C. B.; Beatty, A. M. *Aust. J. Chem.* **2001**, *54*, 409; (b) Aakeröy, C. B. *Acta Crystallogr., Sect. B* **1997,** *53*, 569; (c) Etter, M. C. *Acc. Chem. Res.* **1990**, *23,* 120.

11. (a) Huang, C.; Leiserowitz, L.; Schmidt, G. M. *J. Chem. Soc. Perkin Trans. 2* **1973**, 503; (b) Pan, F.; Wong, W. S.; Gramlich, V.; Bosshard, C.; Günter, P. *Chem. Commun.* **1996**, 1557; (c) Sarma, J. A. R. P.; Desiraju, G. R. *J. Chem. Soc. Perkin Trans.* 2. **1985**, 1905; (d) Aakeröy, C. B.; Beatty.; Nieuwenhuyzen, M.; Zou, M. *Tetrahedron* **2000,** *56,* 6693; (e) Aakeröy, C. B.; Beatty.; Helfrich, B. A. *Angew. Chem. Int. Ed. Engl.* **2001**, *40*, 3240; (f) Aakeröy, C. B.; Desper, J.; Helfrich, B. A. *Cryst. Eng. Comm.* **2004**, *6,* 19.

12. Beatty, M.; *Coord. Chem. Rev.* **2003,** *246*, 131.

13 (a) Brammer, L.; *Dalton Trans.* **2003**, 3145; (b) Ferlay, S.; Felix, O.; Hosseini, M. W,; Planeix, J. –M,; Kyritsaka, N. *Chem. Commun.* **2002**, 702; (c) Braga, D.; Maini,; Grepioni, A.; De cian, A.; Felix, F.; Fischer, J.; Hosseini, M. W. *New J. Chem.* **2000**, *24*, 547.

14. (a) Atwood, J. L.; Davies, J. E. D.; Lehn, J.–M.; MacNicol, D. D.; Vogtle, F. (Eds.), *Comprehensive Supramolecular Chemistry* Pergamon: Oxford, 1996; (b) Schneider, H.–J.; Yatsimirsky, A. K. *Principles and Methods in Supramolecular Chemistry* John Wiley: Chichester, 2000.

15. (a) Lehn, J. –M. *Supramolecular Chemistry* 1995, VCH: Weinheim; (b) Seto, C. T.; Whitesides, G. M. *J. Am. Chem. Soc.* **1991**, *113*, 712; (c) Zhao, X.; Chang, Y. –L.; Fowler, F. W.; Lauher, J. W. *J. Am. Chem. Soc.* **1990**, *112*, 6627; (d) Lehn, J. –M.; Moscal, M.; Decian, A.; Fischer, J. *J. Chem. Soc. Perkin Trans. 2* **1992**, 461.

16. Etter, M. C.; Frankenbach, G. M. *Chem. Mater.* **1989**, *1*, 10.

17. Wong, M. S.; Gramlich, V.; Bosshard, C.; Günter, P. *J. Mater. Chem.* **1997**, *7*, 2021.

18. Goeta, A. E.; Wilson, C. C.; Autino, J. C.; Ellena, J.; Punte, G. *Chem. Mater.* **2000**, *12*, 3342.

19. Broder, C. K.; Davidson, M. G.; Forsyth, V. T.; Howard, J. A. K.; Lamb, S.; Mason, S. A. *Cryst. Growth Des.* **2002**, *2*, 163.
20. Miller, R. D.; Betterton, K. M.; Burlang, D. M.; Lee, V. Y.; Moylan, C. R.; Twieg, R. J.; Walsh, C. A.; Volksen, W. *Proc. SPIE.* **1994**, *354*, 2042.
21. Timofeeva, T. V.; Kuhn, G. H.; Nesterov, V. V.; Nesterov, V. N.; Frazier, D. O.; Penn, B. G.; Antipin, M. Yu. *Cryst. Growth Des.* **2003**, *3*, 383.
22. Nesterov, V. N.; Montoya, N. G.; Antipin, M. Yu.; Sanghadasa, M.; Clark, R. D.; Timofeeva, T. V. *Acta Crystallogr., Sect. C: Cryst. Struct. Commun.* **2002**, *58*, 72.
23. (a) Nie, W. *Adv. Mater.* 1993, *5*, 520; (b) Zyss, J.; Nicoud, J. F. *Curr. Opin. Solid State Mater. Sci.* **1996**, *1*, 533.
24. (a) Verbiest, T.; Elshocht, S. V.; Kauranen, M.; Hellemans, L.; Snauwaert, J.; Nuckolls, C.; Katz, T. J.; Persoons, A. *Science* **1998**, *282*, 913; (b) Hoss, R.; König, O.; Kramer-Hoss, V.; Berger, U.; Rogin, P.; Hulliger, J. *Angew. Chem., Int. Ed. Engl.* **1996**, *35*, 1664; (c) Gangopadhyay, P.; Radhakrishnan, T. P. *Angew. Chem. Int. Ed.* **2001**, *40*, 2451; (d) Anthony, S. P.; Radhakrishnan, T. P. *Chem. Commun.* **2001**, 931.
25. (a) Wang, Z.; Xiong, R. –G.; Foxman, S. R.; Wilson, S. R.; Lin, W. *Inorg. Chem.* **1999**, *38,* 1523; (b) Shimizu, K. H.; Enright, G. D.; Ratcliffe, C. I.; Ripmeester, J. A.; Wayner, D. D. *Angew. Chem. Int. Ed. Engl.* **1998**, *37,* 1407; (c) Biradha, K.; Seward, C.; Zaworotko, M. J. *Angew. Chem. Int. Ed. Engl.* **1999**, *38,* 492; (d) Hirsch, K. A.; Wilson, S. R.; Moore, J. S. *Chem. Commun.* **1998**, 13; (e) Keller, S. W. *Angew. Chem. Int. Ed. Engl.* **1997**, *36*, 247.
26. (a) Aakeröy, C. B.; Beatty, A. M.; Leinen, D. S. *Angew. Chem. Int. Ed. Engl.* **1999**, *38*, 1815; (b) Aakeröy, C. B.; Beatty, A. M.; Leinen, D. S. *J. Am. Chem. Soc.* **1998**, *120*, 7383; (c) Aakeröy, C. B.; Beatty, A. M. *Chem. Commun.* **1998**, 1067; (d) Batasanov, A. S.; Hubberstey, P.; Russel, C. E.; Walton, P. H. *Dalton Trans.* **1997**, 2667; (e) Chang, C. –W.; Mingos, D. M. P.; Williams, D. J. *Dalton Trans.* **1995**, 2469; (f) Munkata, M.; Wu, L. P.; Yamamoto, M.; Kuroda-Sowa, T.; Maekawa, M. *J. Am. Chem. Soc.* **1996**, *118*, 3117; (g) Rivas, J. C. M.; Brammer, L. *New J. Chem.* **1998**, *22*, 1315; (h) Scudder, M.; Dance, I. *Dalton Trans.* **1998**, 3167.
27. Steed, J. W.; Atwood, J. L. *Supramolecular Chemistry*, VCH, New York, 2000.
28. Braga, D. *Chem. Commun.* **2000**, 2751.

29. Brammer, L.; Rivas, J. C. M.; Atencio, R.; Fang, S.; Pigge, F. C. *Dalton Trans.* **2000**, 3855.

30. Burchell, T. J.; Eisler, D. J.; Jennings, M. C.; Puddephatt, R. J. *Chem. Commun.* **2003**, 2228.

31. Qin, Z.; Jennings, J. C.; Puddephatt, R. J. *Inorg. Chem.* **2002**, *41*, 5174.

32. (a) Muthu, S.; Yip, J. H. K.; Vittal, J. J. *Dalton Trans.* **2001**, 3577; (b) Muthu, S.; Yip, J. H. K.; Vittal, J. J. *Dalton Trans.* **2002**, 456; (c) Lavalette, H.; Tuna, F.; Clarkson, G.; Alcock, N. W.; Hannon, M. J. *Chem. Commun.* **2003**, 2666; (d) Matwey, E.; Fowler, F. W.; Lauher, J. W. *J. Am. Chem. Soc.* **1997**, *119*, 10245.

33. Chen, H. –J.; Zhang, L. –Z.; Cai, Z. –G.; Yang, G.; Chen, X. –M. *Dalton Trans.* **2000**, 2463.

34. (a) Lavalette, H.; Tuna, F.; Clarkson, G.; Alcock, N. W.; Hannon, M. J. *Chem. Commun.* **2003**, 2666; (b) Brammer, L.; Rivas, J. C. M.; Atencio, R.; Fang, S.; Pigge, F. C. *Dalton Trans.* **2000**, 3855; (c) Qin, Z.; Jennings, M. C.; Puddephatt, R. J. *Chem. Commun.* **2001**, 2676; (d) Aakeröy, C. B.; Desper, J.; Valdés-Martínez. *Cryst. Eng. Comm.* **2004**, *6*, 413.

35. (a) Schauer, C. L.; Matway, E.; Fowler, F. W.; Lauher, J. W. *J. Am. Chem. Soc.* **1997**, *119*, 10245; (b) Schauer, C. L.; Matway, E.; Fowler, F. W.; Lauher, J. W. *Crystal Eng.* **1998**, *1* 213.

36. Burrows, A. D.; Harrington, R. W.; Mahon, M. F.; Price, C. E. *Dalton Trans.* **2000,** 3845.

37. (a) Aakeröy, C. B.; Beatty, A. M.; Leinen, D. S.; Lorimer, K. R. *Chem. Commun.* **2000**, 935; (b) Aakeröy, C. B.; Beatty, A. M.; Lorimer, K. R. *Dalton Trans.* **2000,** 3869.

38 Yang, G.; Zhu, H. –G.; Liang, B. –H.; Chen, X. –M. *Dalton Trans.* **2001**, 580.

39. van Albada, G. A.; Quiroz-Castro, M. E.; Mutikainen, I.; Turpeinen, U.; Reedijk, *J. Inorg. Chim. Acta* **2000**, *298*, 221.

40. Jensen, P.; Batten, S. R.; Moubaraki, B.; Murray, K. S. *Chem. Commun.* **2000**, 793.

41. Anthony, S. P.; Basavaiah, K.; Radhakrishnan, T. P. (Submitted).

42. (a) Yamamura, T.; Kuroda, R.; Tadokoro, M. *Chem. Lett.* **1989**, 1807; (b) Cornman, C. R.; Zorinka, E. P.; Boyajian, Y. D.; Olmstead, M. M.; Noll, B. C. *Inorg. Chim. Acta* **1999**, *285*, 134.

43. (a)Moberg, C.; Warnmark, K.; Csoregh, I.; Ertan, A. *J. Org. Chem.* **1991**, *56*, 3339; (b) Szumna, A.; Jurczak, J. *Eur. J. Org. Chem.* **2001**, 4031.
44. Gawronski, J.; Kolbon, H.; Kwit, M. *Enantiomer* **2002**, *7*, 85.
46. Larrow, J. F.; Jacobson E. N.; Gao, Y.; Hong, Y, Nie, X.; Zepp, C. M. *J. Org. Chem.* **1994**, *59*, 1939.
46. Whitener, G. D.; Hagadorn, J. R.; Arnold, J. *Dalton Trans.* **1999**, 1249.
47. (a) Dewar, M. J. S.; Zoebisch, E. G.; Healy, E. F.; Stewart, J. J. P. *J. Am. Chem. Soc.* **1985**, *107*, 3902; (b) MOPAC93 © Fujitsu Inc., Japan.
48. Gaussian 03, Revision B.04. Gaussian, Inc., Pittsburgh PA, 2003.
49. Reichenbächer, K.; Süss, H. I,; Hulliger, J. *Chem. Soc. Rev.* **2005**, *34*, 22.
50. Dupuis, M.; Karna, S. *J. Comput. Chem.* **1991**, *12*, 487. The AM1 optimized geometries were used in the calculations.
51. Kurtz, S. K.; Perry, T. T. *J. Appl. Phys.* **1968**, *39*, 3798.
52. (a) Anthony, S. P.; Radhakrishnan, T. P. *Chem. Commun.* **2004**, 1058; (b) Xie, Y. R.; Xiong, R. G.; Xue, X.; Chen, X. T.; Xue, Z.; You, X. Z. *Inorg. Chem.* **2002**, *41*, 3323; (c) Han, L.; Hong, M.; Wang, R.; Luo, J.; Lin, Z.; Yuan, D. *Chem. Commun.* **2003**, 2580.

CHAPTER 5

Overview of the Present Work and Future Prospects

5.1 OVERVIEW OF THE WORK PRESENTED IN THE THESIS

Molecular materials afford great flexibility in their design and fabrication. This has led to the realization of a wide range of materials attributes in them. These materials therefore, are promising candidates for several technological applications. Development of novel molecular materials requires the knowledge and control of the structure at the molecular level and organization at the bulk level. The organization of molecular materials is critical since the bulk properties are often sensitively dependent on the orientation and mutual disposition of the molecules. Intermolecular interactions which play the crucial role in this event, continue to be a challenging phenomenon to understand and control. Even though molecular materials afford many advantages over the traditional materials in terms of fine-tuning the materials properties through molecular design, their thermal and mechanical stabilities are still limited and in many instances unsatisfactory for device applications. Currently, in addition to searching for novel ways to organize the molecules in the bulk materials to achieve desired properties, considerable attention is being paid to the development of more efficient and thermally and mechanically robust materials. Thus the search for new optimized molecular materials has become more fascinating and challenging a task. Careful investigation of the structural and materials attributes of each new class of materials provides important insights into structure-property correlations and helps in the development of more advanced materials with enhanced possibilities of real world applications.

We have presented in this thesis, the development of several new classes of molecular materials, the building blocks of which are easily synthesized metal-organic compounds. Uncommon assemblies such as single component perfectly polar crystals and uniaxially oriented thin films as well as extended network structures of coordination polymers are fabricated. Optical second harmonic generation capability of all the new materials is investigated. Based on the structural and SHG investigations and computational modeling studies, we have been able to propose some empirical structure-property correlations in the novel materials. We have tried to focus throughout, on the thermal stability and optical transparency attributes of the novel materials by careful selection of metal ions, ligand design and the incorporation of relevant intermolecular interactions.

In Sec. 2.3, we have presented the synthesis of novel 'screw' shaped molecules based on zinc complexes and discussed the perfectly polar assembly of molecular dipoles observed in their crystals. Examination of the crystal structure revealed that the hierarchy in the strength of intermolecular interactions in the crystal lattice plays a significant role in the assembly of the dipolar molecules into a three-dimensionally polar motif. The achievement of the perfectly polar molecular arrangement in crystals without the involvement of a supporting structure based on a framework lattice, counterion or cocrystallization partner can be described as a case of self-poling. In Sec. 2.4, we have described an interesting case of polymorphism involving extreme molecular orientation of dipoles in the crystal structures. The role of solvent polarity and rate of crystallization on the formation of perfectly polar and centric molecular assembly is discussed. The delicate balance of energetics involved in the polar and centric supramolecular assembly is addressed through a simple semiempirical computational approach. The unusual formation of multidomain crystals involving the dimorphic structures is a fascinating observation with these new molecules. The perfectly polar molecules are ideally suited for electro-optic applications. Due to limitation of experimental capabilities, we have opted to investigate only the quadratic NLO property of second harmonic generation. These studies are presented in Sec. 2.5. It may be noted that the SHG capabilities observed in our systems are comparable to that of typical metal-organic compounds of this type. Sec. 2.6 describes the physical vapor deposition technique for the fabrication of thin films of the new metal complexes. Optimization of the substrate position with respect to the sublimation boat is demonstrated to be a simple method to effect crystallite orientation control in the thin film. The uniaxial orientational ordering of the perfectly polar crystallites is demonstrated through x-ray diffraction and microscopy studies of the morphology as well as the polarization dependence of SHG.

The utilization of a novel multidentate C_2-symmetric ligand, BCDC with 'push-pull' framework, for the fabrication of a series of coordination polymers is presented in Sec. 3.3. The chirality coupled with the multiple ligation sites of the ligand allowed us to develop noncentrosymmetric one, two and three-dimensional coordination network structures. The mode of metal coordination and the one-dimensional helical superstructure formation in the silver(I) coordination polymer is shown to lead to enhanced SHG capability over the pure ligand. We have also observed, the impact of the

solvent of crystallization on the formation of different structures of the copper(I) coordination polymer in two-dimensional network and three-dimensional interwoven diamondoid lattice. The consequence of the mode of ligation and the conformation of the ligand on the bulk SHG capability of these novel coordination polymers is discussed in Sec. 3.4. The impact of the conformation of the ligand as well as the mode of metal coordination on the hyperpolarizability is discussed using a simple computational approach presented in Sec. 3.5. The coordination polymers based on BCDC, extending into structures of different dimensionalities allowed us to propose a correlation between the dimensionality of the network and the bulk SHG in this class of materials.

Thermally stable materials with good optical transparency have special significance for the development of materials for NLO applications. In this context, we have investigated a series of compounds based on the bis(amide) moiety and networked through metal coordinate bonds. In Sec. 4.3, we highlighted the unusual *syn* conformation of the bis(amide) group in the chiral compound BBDC leading to polar structure in the solid state. Subtle variation in the molecular structure reverts the bis(amide) group into the normal *anti* conformation in the other derivatives studied (Sec. 4.4). Solution CD studies and computational modeling suggest that all the bis(amide) molecules posses *anti* conformation in solution and the *syn* conformation in BBDC is a solid state effect. The fabrication of coordination polymers based on the chiral vicinal bis(amide) molecule, BINDC is described in Sec. 4.5. The BBDC derivatives and coordination polymers exhibit a variety of helical assemblies in the crystals, mediated by intermolecular H-bonds as well as metal coordination. The thermal stability of these materials is considerably enhanced by the extended interactions in the lattice. These materials also show appreciable transparency in the visible range. The SHG studies on the large family of organic crystals and metal coordination polymers are presented in Sec. 4.6. The SHG trends follow classical push-pull concepts as demonstrated through structural arguments and semiemprical computational modeling.

This thesis highlights the development of several families of metal-organic compounds exhibiting a range of fascinating molecular assemblies. It is significant to note that the building blocks of these materials are extremely simple. The molecular organization in crystals and thin films support the realization of SHG capability and in

most of the cases simple structure-property correlations could be delineated. Involvement of the specific metals, ligands and intermolecular interactions ensured that the new materials have good optical transparency and thermal stability. Thus, while demonstrating several structural organizations, these systems also hold appreciable application potential.

5.2 FUTURE PROSPECTS

Perfectly polar organization of molecular dipoles in crystals and thin films is not easily achieved through spontaneous self-assembly. Such molecular assemblies can have profound influence on the materials attributes. The single component perfectly polar crystals we have developed are based on simple metal complexes of pyridine ligands. It would be of great interest to incorporate ligands based on derivatives of pyridine with extended conjugation, such as stilbazole; such systems are expected to posses larger hyperpolarizability and if similar bulk organization is achieved, should give rise to enhanced bulk nonlinearities. This opens up the question of how general the role of the 'screw-shaped' molecules is, in the generation of perfectly polar materials. Several more related molecular structures need to be synthesized and structurally characterized to verify the generality of the current observations. The polar organization of molecular dipoles in bulk materials is very important for technologically useful solid state properties such as piezoelectricity, pyroelectricity and electro-optic effects; so it would be interesting to investigate the potential utility of the present systems as well as further derivatives in this context.

The investigation of the multidomain crystals we have presented, suggests the possibility of obtaining different polarity orientations in cogrowth domains of monolithic crystals. The domain structure built up of SHG active and inactive regions can be mapped using techniques such as second harmonic microscopy. The formation of twin polar domains (180° twinned structure) in the metal-organic crystals can be investigated using phase sensitive second harmonic or scanning pyroelectric microscopy. If one can control the orientational and spatial attributes of the domains, it would be of considerable

interest in developing crystals which simulate periodically poled structures for applications such as quasi phase-matched SHG.

The physical vapor deposition technique provides a convenient method to fabricate thin films of molecular materials. We have fabricated homogeneous thin films of metal-organic compounds and achieved uniaxial orientational ordering of polar crystallites through the optimization of the distance between the sublimation boat and substrate. Fabrication of thin films of orientationally ordered dipoles without special substrate functionalization or use of external fields or rubbing methods, but through chemical control of molecular structure, is an attractive proposition from fundamental materials chemistry as well as application perspectives. Since these films consist of perfectly polar crystallites with uniaxial orientation perpendicular to the substrate but random azimuthal orientations, it is important to investigate the influence of an external electric field imposed during the film fabrication. Electro-optic properties of the thin films also need to be investigated. It would also be of interest to control the crystallite sizes to still smaller, nanoscopic dimensions and observe the impact on the nonlinear optical phenomena.

Our current investigations of the C_2-symmetric ligands and their coordination polymers suggested that the impact of the conformation of the ligand and the mode of metal coordination, rather than the type of metal ions involved are the dominant factors controlling the SHG capability. It would be of fundamental interest to explore more systems to probe the generality of these concepts. The enhancement of solid state SHG in one-dimensional helical superstructures, the case presented in this thesis as well as reported earlier from our laboratory, point to the importance of helical assembly for quadratic nonlinear optical properties of the materials. Our current examples also suggest that the increase in the dimensionality of the network affect adversely, the solid state second harmonic generation capability. Several more families of coordination polymers need to be investigated to see if this correlation of dimensionality with the solid state second harmonic generation can be implemented as a general design strategy.

The bis(amide) molecules we have developed, provide a good starting point to generate H-bond networked coordination polymers with appreciable optical transparency,

thermal stability and SHG capability. The SHG from these materials are however rather weak. The several strategies known to enhance molecular hyperpolarizabilities can be deployed to get around this limitation. Such a strategy should hopefully lead to materials that are thermally robust, transparent and strongly SHG active.

The studies presented in this thesis have thrown up several possibilities for further exploration of metal-organic systems for nonlinear optical applications. Questions related to materials fabrication, molecular organization and structure-property correlations have been addressed. Continued efforts along the new directions proposed here, should culminate in new materials which will be of both academic and applications interest.

Appendices

APPENDIX A

Instrumentation for Characterization of New Materials

Melting temperatures of solids were determined using capillary melting point apparatus (Superfit, India); values reported are uncorrected. Boiling points refer to the temperature measured using short path distillation units and are uncorrected. Infra red spectra were recorded on a Jasco5300 FTIR spectrometer. All the spectra were calibrated against polystyrene absorption at 1601 cm^{-1}. Solid samples were recorded as KBr pellets and liquid samples as thin films between NaCl plates. Electronic absorption (UV-Vis) spectra were recorded on a Shimadzu UV 3101 PC spectrophotometer. Optical rotations were measured on a Jasco Digital Polarimeter (Model: DIP – 370) using sodium D-light as the source. Specular reflectance (8^{o} incidence) or diffuse reflectance spectra of solid pellets were recorded on the same spectrometer using the integrating sphere (ISR 3100) attachment. Circular dichroism spectra were recorded on a Jasco Spectropolarimeter Model J-810. The melting transition temperatures were recorded on a DSC 2010 differential scanning calorimeter. ^{1}H and ^{13}C NMR spectra were recorded on Bruker 200 MHz or 400 MHz NMR spectrometer. Sartorius BP211D balance was used for high precision weighing.

Morphology of films coated on glass substrates by the physical vapor deposition technique was examined using a Philips XL 30 ESEM Scanning Electron Microscope. Gold coating was provided on the films prior to examination. Thickness of the films was measured using an Ambios Technology XP-1 profilometer. X-ray diffraction pattern of the thin films as well as powder x-ray patterns of microcrystalline materials were recorded on a Philips Model PW 1830 Powder X-ray Diffractometer. CuK_{α} radiation was used. The powder pattern was simulated using the atom coordinates from single crystal x-ray study, using the PowderCell program.[1]

1. W. Kraus, G. Nolze, G. *PowderCell for Windows*, Version 2.3.

APPENDIX B

X-ray Crystallography

Several of the x-ray diffraction data were collected on an Enraf-Nonius MACH3 diffractometer. All were collected at 293K. MoK_α radiation (λ = 0.71073 Å) with a graphite crystal monochromator in the incident beam. Standard CAD4 centering, indexing and data collection programs were used. The general routine used for the data collection is as follows; minor variations in settings were done in specific cases. The unit cell dimensions were obtained by a least square fit of 24 centered reflections in the neighborhood of $\theta = 10^\circ$. Intensity data were collected using the ω scan method at a scan speed of 4.12°/min to a maximum 2θ of 50°. The scan width $\Delta\theta$, for each reflection was $0.80 + 0.35 \tan\theta$. During data collection the intensities of three standard reflections were monitored every 1.5 h of x-ray exposure. In all the cases we have studied, no decay was observed. In addition three orientation standards were monitored every 250 reflections to check the effects of crystal movement. Data was reduced using Xtal 3.4;[1] Lorentz and polarization corrections were included. All non-hydrogen atoms were found using the direct method analysis in SHELX-97[2] and after several cycles of refinement the positions of the hydrogen atoms were calculated and added to the refinement process. Empirical absorption correction was applied in the relevant cases, using ψ scan data. Refinement proceeded to convergence by minimizing the function $\sum \mathbf{w}(F_o^2 - F_c^2)$. A final difference Fourier synthesis map showed the largest difference peak and hole to be acceptably small. The R indices were calculated as $R = \sum \left| (|F_0| - |F_c|) \right| / \sum |F_0|$ and $wR^2 = \left[\sum w(F_0^2 - F_c^2)^2 / \sum (F_0^2)^2 \right]^{1/2}$. Graphics were handled using ORTEX6a,[3] Platon[4] and Materials Studio.

The X-ray intensity data for some of the crystals were measured on a Bruker SMART APEX CCD area detector system equipped with a graphite monochromator and a MoK_α fine-focus sealed tube (λ = 0.71073 Å) operated at 1750 W power (50 kV, 35 mA). All data were collected at 293K. The detector was placed at a distance of 6.003 cm from the crystal. Required number of frames were collected depending upon the crystal systems with a scan width of 0.3° in ω; exposure time was set based on the data quality. The frames were integrated with the Bruker SAINT software package[5] using a narrow-

frame integration algorithm. Analysis of the data showed negligible decay during data collection. Data were corrected for absorption effects using the multi-scan technique (SADABS). The structure was solved and refined using the Bruker SHELXTL (Version 6.14) Software Package.[6]

Table B.1 lists the space groups and REFCODE (Cambridge Crystallographic Database) or deposition number from Cambridge Crystallographic Data Centre[7] for the new crystal structures presented in this thesis. The crystal structure of BBDC, BINDC, BFBDC, BNBDC, BMBDC, BABDC, Zn(BINDC)Cl_2, Zn(BINDC)Br_2 and Ag(BINDC)NO_3 described in Chapter 4 are not yet deposited in CCDC. The fractional atomic coordinates (x 10^4) and isotropic displacement parameters, U_{eq} (Å^2 x 10^3) of these crystals are provided in Tables B.2-B.11. U_{eq} is defined as one third of the trace of the orthogonal U_{ij} tensor. Estimated standard deviations (e.s.d) are given in parenthesis.

Table B.1 *Space groups and the REFCODE / deposition number from CSD and the reference in the thesis.*

Compound	Space Group	REFCODE / Deposition No.	Page no.
ZNDA	Fdd2	QOLWUJ	57
ZNMPA	Cm	253976	62
ZNPPA1	C2/c	ULAVUYO1	67
ZNPPA2	Fdd2	ULAVUY	67
BCDC.H_2O	$P2_12_12_1$	228200	106
SBP	$P2_12_12_1$	228201	108
CBPT	$P22_12_1$	228202	113

References

1. *Xtal 3.4*, Hall, S. R.; King, G. S. D.; Stewart, J. M. (Eds.), University of Western Australia, Perth, Australia, **1995**.
2. *SHELX-97*, Sheldrick, G. M. University of Göttingen, Göttingen, Germany, **1997**.
3. McArdle, P. *J. Appl. Cryst.* **1995**, *28*, 65.
4. Spek, A. L. Utretcht University, The Netherlands, **2000**.
5. SAINT Version 6.2, Bruker AXS Inc., Madison, Wisconsin, USA.
6. SHELXTL Version 6.14, Bruker AXS Inc., Madison, Wisconsin, USA.
7. Cambridge Structural Database, Version 5.24 (November 2002 Update).

Table B.2 CBP

Atom	x	y	z	U(eq)
Cu(1)	9477(1)	5684(1)	11528(1)	57(1)
C(36)	10240(3)	696(2)	9655(1)	56(1)
N(8)	2003(3)	6997(2)	8459(1)	62(1)
C(20)	5421(3)	6951(2)	9277(1)	50(1)
C(41)	4374(3)	6760(2)	8373(1)	51(1)
N(1)	9458(3)	4648(2)	11293(1)	65(1)
N(2)	8411(3)	6171(2)	10962(1)	61(1)
C(17)	7029(3)	6547(2)	10142(1)	54(1)
N(6)	4630(3)	7167(2)	8863(1)	55(1)
N(3)	11295(3)	6099(2)	11554(2)	83(1)
C(26)	11153(3)	983(2)	10576(1)	58(1)
C(34)	-465(4)	8383(2)	8072(2)	68(1)
N(5)	8422(3)	1519(2)	9952(1)	61(1)
C(16)	7806(4)	6341(2)	10592(1)	58(1)
C(22)	6787(4)	6059(2)	9724(2)	64(1)
N(7)	11182(3)	1014(2)	10033(1)	63(1)
C(33)	714(4)	7995(2)	8083(2)	64(1)
C(24)	10149(4)	612(2)	11411(1)	63(1)
C(21)	5995(4)	6263(2)	9301(1)	60(1)
N(4)	8850(4)	5825(2)	12275(1)	83(1)
C(29)	-1511(3)	8188(2)	8406(2)	66(1)
C(13)	8706(3)	2142(2)	10221(1)	51(1)
C(42)	3134(3)	7059(2)	8104(1)	54(1)
C(35)	9147(4)	1231(2)	9487(1)	58(1)
C(14)	9580(4)	2683(2)	10033(1)	61(1)
C(19)	5713(4)	7453(2)	9686(1)	60(1)
C(10)	9130(4)	3430(2)	10798(2)	60(1)
C(32)	857(3)	7389(2)	8413(1)	56(1)
C(25)	10116(4)	645(2)	10857(1)	62(1)
C(23)	11188(4)	913(2)	11696(1)	71(1)

C(15)	9774(4)	3316(2)	10311(2)	62(1)
C(9)	9314(4)	4107(2)	11082(2)	62(1)
C(11)	8278(4)	2894(2)	10995(2)	65(1)
C(46)	5564(4)	6800(2)	7995(1)	69(1)
C(30)	-1360(4)	7586(2)	8739(2)	75(1)
C(12)	8052(4)	2273(2)	10715(2)	62(1)
C(18)	6502(4)	7254(2)	10109(1)	62(1)
C(28)	12210(5)	1242(4)	11415(2)	103(2)
C(27)	12187(5)	1284(3)	10872(2)	95(2)
C(37)	10973(5)	425(3)	9160(2)	77(1)
C(44)	4078(5)	6736(4)	7192(2)	102(2)
C(43)	2893(4)	6682(3)	7562(2)	83(1)
C(40)	8193(5)	869(3)	9090(2)	85(1)
C(31)	-229(4)	7194(2)	8738(2)	72(1)
C(38)	10014(6)	68(3)	8766(2)	99(2)
C(45)	5294(5)	6394(3)	7465(2)	94(2)
C(39)	8901(6)	577(3)	8607(2)	99(2)
C(47)	12281(4)	6408(2)	11574(2)	76(1)
C(48)	8803(5)	5868(2)	12731(2)	76(1)
P(49)	6052(2)	9876(1)	664(1)	159(1)
F(52)	7038(8)	10124(5)	266(4)	277(5)
F(50)	6185(12)	10656(3)	842(4)	295(5)
F(55)	5010(7)	9710(4)	1094(4)	251(4)
F(54)	7132(7)	9656(4)	1057(3)	231(3)
F(51)	5946(9)	9066(3)	464(3)	242(4)
F(53)	4938(8)	10081(4)	278(4)	289(5)

Table B.3 BBDC

Atom	x	y	z	U(eq)
O(1)	1474(1)	2875(1)	7444(1)	57(1)
O(2)	-677(2)	2789(1)	3547(1)	59(1)
C(18)	-489(2)	1604(2)	3242(2)	44(1)
C(11)	1737(2)	1664(2)	7305(2)	39(1)
N(4)	-1038(2)	513(1)	3646(1)	45(1)
N(3)	564(1)	804(1)	6577(1)	43(1)
C(19)	376(2)	1312(2)	2371(2)	44(1)
C(5)	-1072(2)	1277(2)	5845(2)	42(1)
C(6)	-1922(2)	498(2)	4495(2)	44(1)
C(12)	3405(2)	1134(2)	7991(2)	41(1)
C(17)	3870(2)	-136(2)	7747(2)	55(1)
C(10)	-2014(2)	1154(2)	6714(2)	53(1)
C(20)	1133(2)	79(2)	2422(2)	52(1)
C(7)	-3626(2)	1013(2)	3714(2)	57(1)
C(13)	4538(2)	1983(2)	8929(2)	57(1)
C(23)	1152(2)	2038(2)	601(2)	71(1)
C(15)	6543(2)	295(2)	9378(2)	69(1)
C(8)	-4553(2)	963(2)	4586(2)	69(1)
C(24)	414(2)	2297(2)	1457(2)	57(1)
C(14)	6095(2)	1564(2)	9618(2)	69(1)

C(22)	1886(2)	811(2)	670(2)	71(1)
C(9)	-3688(2)	1710(2)	5937(2)	64(1)
C(21)	1894(2)	-160(2)	1586(2)	65(1)
C(16)	5436(2)	-551(2)	8434(2)	70(1)

Table B.4 BINDC

Atom	x	y	z	U(eq)
N(3)	6142(3)	9448(1)	8258(1)	52(1)
N(4)	7275(3)	9417(1)	6778(1)	50(1)
C(8)	7528(3)	8731(1)	7214(1)	48(1)
C(12)	5748(4)	8030(1)	8266(1)	67(1)
C(7)	5642(3)	8769(1)	7831(1)	48(1)
C(14)	4998(4)	10522(1)	9007(1)	53(1)
C(20)	8648(4)	10462(1)	6031(1)	48(1)
C(17)	7549(5)	11615(1)	9304(2)	87(1)
C(9)	7063(5)	8006(1)	6776(1)	68(1)
O(2)	11556(3)	9632(1)	6633(1)	77(1)
N(5)	6078(5)	11818(1)	9839(1)	89(1)
C(10)	7178(5)	7274(1)	7218(1)	75(1)
C(18)	7114(4)	10979(1)	8879(1)	70(1)
N(6)	7704(5)	11676(1)	5095(1)	84(1)
C(11)	5256(5)	7321(1)	7816(1)	73(1)
C(13)	4234(4)	9835(1)	8577(1)	53(1)
C(16)	4054(6)	11376(2)	9957(1)	87(1)
C(23)	6257(6)	11060(2)	5115(1)	98(1)
C(19)	9288(4)	9803(1)	6510(1)	50(1)
C(15)	3437(5)	10730(1)	9560(1)	70(1)
C(22)	9635(7)	11691(1)	5542(2)	100(1)
C(21)	10196(5)	11099(1)	6004(1)	85(1)
C(24)	6618(5)	10447(1)	5575(1)	83(1)
O(1)	1928(3)	9640(1)	8532(1)	75(1)

Table B.5 BFBDC

Atom	x	y	z	U(eq)
N(5)	301(4)	-751(1)	6685(1)	51(1)
N(6)	1337(4)	728(1)	6752(1)	52(1)
C(7)	56(4)	-311(1)	6058(1)	45(1)
C(8)	1869(5)	331(1)	6110(1)	45(1)
C(13)	-1729(5)	-973(1)	7079(1)	49(1)
O(4)	5546(4)	1036(1)	6947(1)	74(1)
C(12)	581(6)	-725(1)	5383(1)	61(1)
O(3)	-3999(3)	-835(1)	6918(1)	82(1)
C(20)	3219(5)	1032(1)	7139(2)	53(1)
C(9)	1670(6)	793(1)	5452(1)	62(1)
C(21)	2421(5)	1375(1)	7816(1)	51(1)

F(1)	375(4)	-2516(1)	9538(1)	97(1)
C(14)	-1082(5)	-1380(1)	7728(1)	46(1)
C(11)	411(6)	-261(2)	4726(1)	66(1)
F(2)	508(4)	2361(1)	9683(1)	114(1)
C(17)	-131(7)	-2147(2)	8937(2)	64(1)
C(26)	3856(6)	1940(2)	8071(2)	73(1)
C(24)	1148(7)	2035(2)	9064(2)	75(1)
C(10)	2224(6)	371(2)	4783(2)	67(1)
C(22)	319(6)	1148(2)	8213(2)	72(1)
C(18)	-2117(8)	-1678(2)	8930(2)	90(1)
C(23)	-301(7)	1477(2)	8846(2)	83(1)
C(19)	-2605(6)	-1298(2)	8321(2)	80(1)
C(15)	889(7)	-1861(2)	7757(2)	78(1)
C(16)	1356(7)	-2260(2)	8365(2)	80(1)
C(25)	3205(8)	2279(2)	8695(2)	81(1)

Table B.6 BNBDC

Atom	x	y	z	U(eq)
O(1)	13275(4)	4145(1)	1467(1)	63(1)
C(17)	10958(6)	3942(2)	1416(1)	42(1)
C(18)	10335(5)	3175(1)	1176(1)	37(1)
C(23)	12041(5)	2875(2)	747(1)	48(1)
C(19)	8234(5)	2749(2)	1390(1)	47(1)
N(8)	7996(4)	5802(1)	975(1)	45(1)
C(22)	11660(6)	2162(2)	528(1)	53(1)
O(2)	3743(4)	6104(1)	745(1)	68(1)
C(20)	7845(6)	2032(2)	1176(1)	53(1)
C(11)	9141(5)	5069(1)	1891(1)	42(1)
C(13)	7766(6)	6398(2)	1970(1)	61(1)
C(25)	6937(5)	6199(2)	-44(1)	45(1)
C(24)	6104(6)	6024(2)	592(1)	48(1)
C(15)	8640(7)	5675(2)	2923(1)	73(1)
C(12)	7424(5)	5675(1)	1617(1)	41(1)
N(7)	8891(4)	4362(1)	1573(1)	45(1)
C(14)	7048(7)	6300(2)	2636(2)	75(1)
N(9)	9110(8)	992(2)	515(2)	76(1)
O(3)	7299(7)	640(1)	727(1)	127(1)
C(28)	8389(7)	6573(2)	-1205(1)	54(1)
O(4)	10604(7)	762(1)	120(1)	111(1)
C(16)	8417(6)	4963(2)	2556(1)	61(1)
C(27)	9714(6)	6003(2)	-921(1)	60(1)
C(21)	9556(6)	1755(2)	744(1)	52(1)
C(26)	8986(6)	5828(2)	-334(1)	54(1)
C(30)	5649(6)	6766(2)	-353(2)	62(1)
C(29)	6356(7)	6959(2)	-933(2)	69(1)
N(10)	9165(8)	6778(2)	-1831(1)	72(1)
O(6)	7769(6)	7206(2)	-2112(1)	104(1)
O(5)	11189(7)	6509(2)	-2037(1)	101(1)

Table B.7 BMBDC

Atom	x	y	z	U(eq)
N(6)	825(3)	3785(1)	1854(1)	51(1)
N(5)	2060(3)	3798(1)	3168(1)	51(1)
C(7)	2368(4)	4430(1)	2786(1)	47(1)
C(8)	461(3)	4418(1)	2225(1)	46(1)
O(1)	6360(3)	3556(1)	3220(1)	75(1)
O(2)	-3462(3)	3654(1)	1621(1)	71(1)
C(13)	4073(4)	3395(1)	3337(1)	51(1)
C(9)	763(4)	5072(1)	1821(1)	62(1)
C(21)	-1191(4)	3435(1)	1596(1)	51(1)
C(22)	-535(4)	2766(1)	1268(1)	51(1)
C(10)	402(4)	5729(1)	2218(1)	68(1)
O(4)	942(4)	895(1)	334(1)	88(1)
C(12)	2031(4)	5090(1)	3179(1)	65(1)
C(14)	3457(4)	2738(1)	3685(1)	48(1)
C(17)	2686(5)	1508(1)	4364(1)	60(1)
C(11)	2327(4)	5741(1)	2773(1)	70(1)
C(23)	1565(4)	2338(1)	1433(1)	62(1)
C(25)	345(5)	1516(1)	626(1)	64(1)
O(3)	2526(4)	885(1)	4671(1)	89(1)
C(19)	5060(5)	2168(1)	3593(1)	67(1)
C(27)	-2167(4)	2550(1)	782(1)	61(1)
C(15)	1454(4)	2675(1)	4122(1)	63(1)
C(16)	1074(5)	2067(1)	4467(1)	66(1)
C(24)	1970(5)	1720(1)	1118(1)	68(1)
C(18)	4666(5)	1561(1)	3919(1)	79(1)
C(26)	-1728(5)	1934(1)	455(1)	67(1)
C(20)	669(6)	806(1)	5163(1)	103(1)
C(28)	-743(6)	660(1)	-168(1)	112(1)

Table B.8 BABDC

Atom	x	y	z	U(eq)
O(1)	-521(3)	6796(1)	2729(2)	46(1)
C(9)	3063(4)	7395(1)	1266(2)	35(1)
N(5)	3706(4)	7018(1)	2562(2)	38(1)
C(15)	1868(4)	6760(1)	3230(3)	36(1)
C(10)	5064(4)	7927(1)	1285(2)	34(1)
N(6)	5106(4)	8303(1)	2577(2)	37(1)
C(22)	7322(4)	8527(1)	3340(3)	36(1)
O(2)	9485(3)	8453(1)	2945(2)	50(1)
C(16)	2778(5)	6414(1)	4584(3)	37(1)
C(11)	4467(6)	8329(1)	-64(3)	47(1)
C(13)	2316(5)	7406(2)	-1422(3)	52(1)
C(23)	7078(4)	8875(1)	4675(3)	37(1)
N(8)	6984(5)	9935(1)	8396(2)	56(1)
C(18)	1918(5)	5590(1)	6188(3)	50(1)
N(7)	5010(5)	5354(1)	8320(2)	56(1)

C(14)	2936(6)	7001(1)	-94(3)	51(1)
C(21)	5111(5)	6542(1)	5496(3)	46(1)
C(17)	1204(5)	5933(1)	4962(3)	47(1)
C(25)	4966(5)	9626(1)	6019(3)	49(1)
C(19)	4253(5)	5722(1)	7100(3)	44(1)
C(27)	8993(6)	9147(2)	7074(3)	54(1)
C(24)	5019(5)	9278(1)	4798(3)	47(1)
C(20)	5816(5)	6208(1)	6735(3)	47(1)
C(28)	9062(5)	8817(1)	5848(3)	50(1)
C(26)	6952(5)	9568(1)	7178(3)	41(1)
C(12)	4347(6)	7924(2)	-1401(3)	53(1)
O(4)	40(5)	9543(1)	1226(2)	62(1)
O(3)	8024(5)	5681(1)	1181(3)	67(1)

Table B.9 Zn(BINDC)Cl_2

Atom	x	y	z	U(eq)
C(12)	12294(2)	6972(1)	1305(8)	41(1)
C(13)	13132(2)	7303(2)	1406(9)	45(1)
C(14)	13013(3)	7755(2)	3330(9)	48(1)
N(7)	4294(2)	11945(1)	-764(6)	29(1)
C(20)	9196(2)	9468(2)	-706(8)	34(1)
C(16)	10142(3)	8361(1)	3419(8)	32(1)
C(18)	8685(3)	8831(1)	3264(8)	38(1)
C(17)	9529(2)	8776(1)	2284(7)	29(1)
C(10)	11366(2)	7758(1)	2447(7)	27(1)
C(19)	8118(3)	9199(2)	2160(8)	39(1)
C(21)	9797(3)	9107(1)	282(8)	35(1)
C(11)	11469(2)	7289(1)	626(7)	26(1)
C(23)	5342(2)	11297(1)	704(7)	27(1)
C(15)	12212(2)	8084(1)	2595(8)	40(1)
C(24)	5937(2)	11366(2)	-1338(8)	32(1)
C(27)	5434(3)	10850(1)	2251(8)	35(1)
C(26)	6094(3)	10492(2)	1645(8)	38(1)
O(5)	4395(2)	11770(1)	3606(5)	45(1)
C(22)	4627(2)	11692(1)	1319(8)	28(1)
O(4)	10175(2)	8283(1)	5822(5)	47(1)
N(8)	8371(2)	9515(1)	167(6)	32(1)
N(6)	10633(2)	8100(1)	1656(7)	32(1)
C(25)	6587(2)	11000(1)	-1760(8)	34(1)
N(9)	6674(2)	10563(1)	-316(6)	32(1)
Zn(1)	7490(1)	9984(1)	-1806(1)	36(1)
Cl(2)	6436(1)	9410(1)	-3010(2)	47(1)
Cl(3)	8326(1)	10421(1)	-4750(2)	48(1)

Table B.10 $Zn(BINDC)Br_2$

Atom	x	y	z	U(eq)
C(24)	3957(2)	-1387(1)	3685(8)	34(1)
Br(2)	1546(1)	-438(1)	29(1)	42(1)
Br(3)	3628(1)	577(1)	1971(1)	45(1)
Zn(1)	2459(1)	1(1)	3149(1)	33(1)
C(21)	1364(2)	1168(1)	8153(8)	37(1)
C(11)	-1380(2)	2720(1)	5589(7)	27(1)
C(18)	220(2)	925(1)	5220(8)	34(1)
C(20)	1891(2)	804(1)	7028(8)	36(1)
C(22)	5267(2)	-1701(1)	6328(7)	28(1)
N(6)	-559(2)	1921(1)	6627(6)	32(1)
N(8)	1613(2)	495(1)	5066(6)	31(1)
C(16)	-73(2)	1659(1)	8374(7)	31(1)
O(4)	-89(2)	1739(1)	10751(5)	44(1)
C(13)	-3040(3)	2720(2)	6390(8)	42(1)
C(10)	-1283(2)	2262(1)	7431(7)	28(1)
N(9)	3244(2)	-586(1)	4629(6)	32(1)
C(26)	3820(2)	-515(1)	6591(8)	38(1)
C(27)	4477(2)	-867(1)	7210(8)	35(1)
C(25)	3315(2)	-1023(1)	3227(8)	36(1)
C(14)	-2930(3)	2278(2)	8309(9)	46(1)
C(17)	512(2)	1249(1)	7224(7)	30(1)
C(23)	4552(2)	-1315(1)	5704(7)	29(1)
C(19)	780(2)	554(1)	4226(8)	35(1)
N(7)	5605(2)	-1946(1)	4257(6)	29(1)
O(5)	5494(2)	-1777(1)	8612(5)	47(1)
C(12)	-2199(2)	3036(1)	6260(9)	40(1)
C(15)	-2134(2)	1946(2)	7562(9)	42(1)

Table B.11 $Ag(BINDC)NO_3$

Atom	x	y	z	U(eq)
Ag(1)	10000	0	5144(1)	47(1)
N(5)	5000	0	6154(2)	42(1)
O(2)	7032(5)	179(2)	6564(2)	62(1)
O(4)	5166(5)	3542(2)	1583(2)	47(1)
C(11)	7397(5)	3453(2)	1829(2)	33(1)
C(8)	9066(5)	4539(2)	564(2)	32(1)
N(6)	9397(4)	3903(2)	1397(2)	36(1)
C(12)	8094(6)	2760(2)	2638(2)	35(1)
C(10)	9145(7)	4517(3)	-1184(2)	51(1)
C(9)	9470(7)	3872(2)	-302(2)	47(1)
C(15)	7157(7)	2016(3)	4109(2)	47(1)
C(16)	6527(7)	2712(3)	3409(2)	43(1)
N(7)	9202(5)	1372(2)	4089(2)	44(1)
O(3)	5000	0	5295(3)	84(1)
C(14)	10671(6)	1430(3)	3342(3)	52(1)
C(13)	10228(9)	2113(3)	2608(2)	50(1)

APPENDIX C

Powder Second Harmonic Generation Measurement

We have measured the second harmonic generation from microcrystalline powders of the various compounds using the Kurtz and Perry[1] method with minor modifications of the original layout. Particle sizes were graded using standard sieves; sizes ranging from 50 – 420 μm were studied. Samples were loaded in glass capillaries having an inner diameter of 600 μm. Fundamental beam (1064 nm) of a Q-switched ns-pulsed (6 ns, 10 Hz) Nd:YAG laser (Spectra Physics, Model INDI 40) was used. The beam was split and approximately 10% was passed through a 200 μm thick powder sample of N-4-nitrophenyl-(*S*)-prolinol, NPP (average particle size ~ 175 μm) to monitor pulse to pulse fluctuation of the beam. The main beam was split further into two halves and focused onto the sample from opposite directions. The scattered SHG signal was collected using a concave mirror and lens combination with a 45° disposition to the incident beams (Fig. C.1). The second harmonic signal from reference and the sample were collected using appropriate optics and detected using a monochromator (Jobin-Yvon Model HRS–2), PMT (Hamamatsu, Model C956-06/131) and oscilloscope (Tektronix, Model TDS 210, 60MHz). Calibrated neutral density filters were used when needed, so that the signal measured on the oscilloscope was in the same range for all samples and the reference; this ensures that readings are taken in a linear regime of the PMT. Microcrystalline urea having particle sizes 150 - 350 μm was used as the reference in all SHG measurements. The measured SHG signal from the sample is first corrected for the background noise and the fluctuation in reference before comparing with similarly corrected signal of the standard, urea. Measurements for the sample and the standard were carried out for different particle sizes. Our setup is calibrated by measurements on urea and NPP. The SHG measured for NPP is 138 U (1U = SHG of urea) at saturation. The errors in the measurements are ~ 10 – 15 %.

The compounds we have studied showed good stability under laser irradiation and no sign of decomposition was detected, even on continuous irradiation with a laser power of 1 GW cm^{-2}. Each measurement was repeated at least three times over a period of time and the value of SHG reported is the average of such measurements. In all cases we have

studied, the SHG saturated at higher particle sizes, indicating phase matchable behavior of the materials.

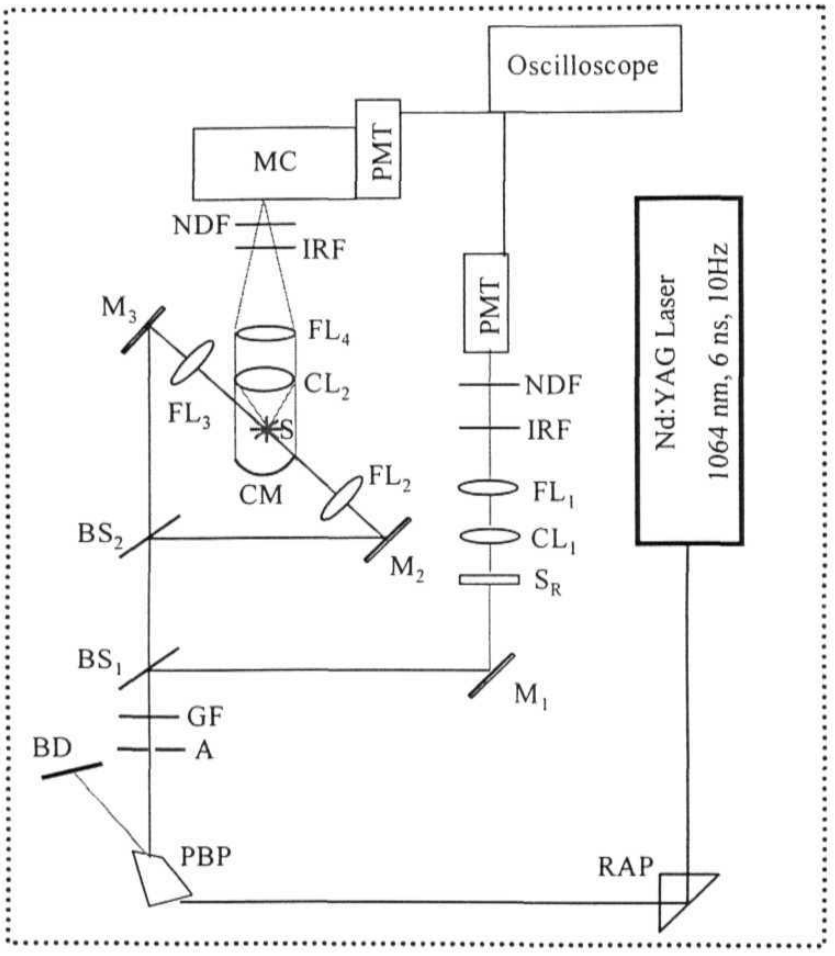

A: Aperture, BD: Beam Dump, BS_1, BS_2: Beam Splitters, CL1, CL2: Collecting Lenses, CM: Concave Mirror, FL_n: Focussing Lenses, GF: Green Filter, IRF: IR Filter, M_n: Mirrors, MC: Monochromator, NDF: Neutral Density Filters, PBP: Pellin-Broca prism, PMT: Photomultiplier Tube, RAP: Right angle prism, S: Sample, S_R: Reference Sample.

Figure C.1 *Setup for measurements of SHG from microcrystalline powders*

Reference

1. Kurtz, S. K.; Perry, T. T. *J. Appl. Phys.* **1968**, *39*, 3798.

APPENDIX D

Thin Film Second Harmonic Generation Measurement

SHG from the thin films on glass substrates was examined in transmission mode. Fundamental beam (1064 nm) of a Q-switched, ns-pulsed (6 ns, 10 Hz) Nd:YAG laser (Spectra Physics Model INDI-40) was used. The SHG signal was collected using appropriate optics and detected using a monochromator, PMT and boxcar averager

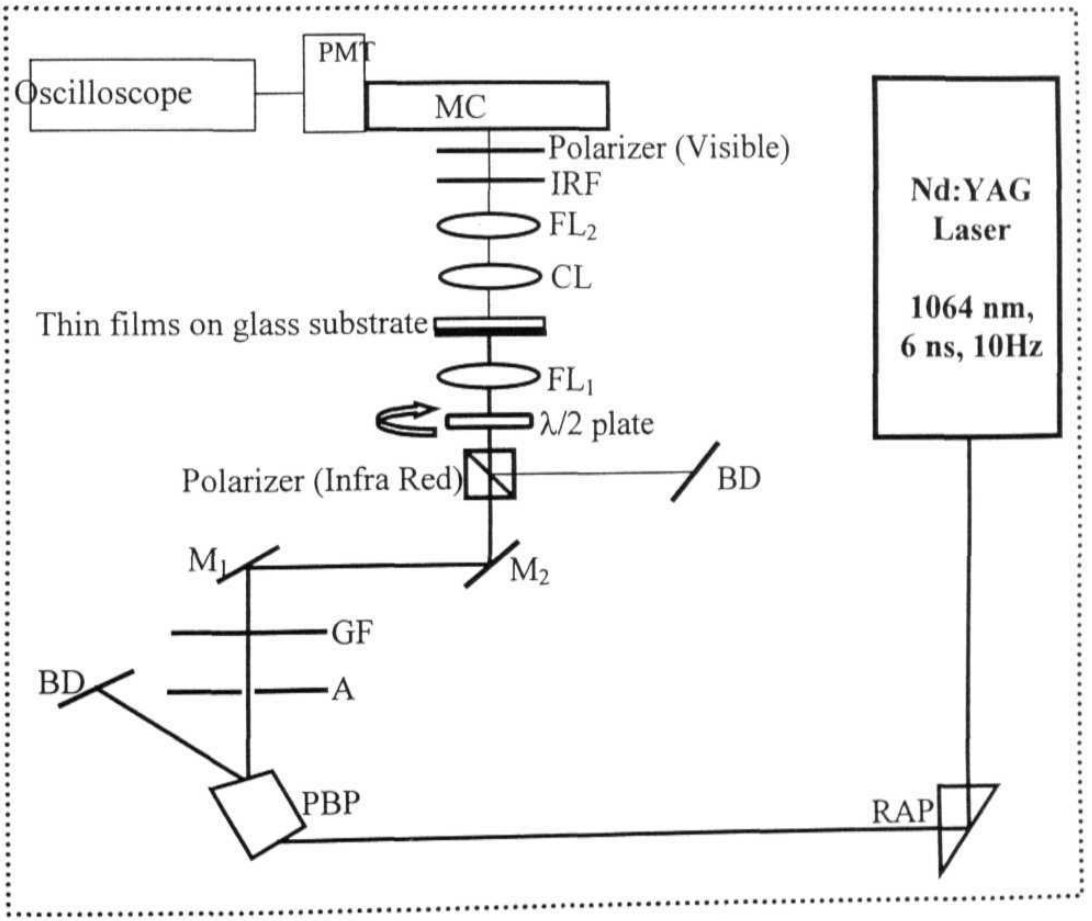

A: Aperture, BD: Beam Dump, CL: Collecting Lense, FL_n: Focussing Lenses, GF: Green Filter, IRF: IR Filter, M_n: Mirrors, MC: Monochromator, PBP: Pellin-Broca prism, PMT: Photomultiplier Tube, RAP: Right angle prism.

Figure D.1 *Setup for measurement of SHG from thin films*

(Stanford Research Systems Model SR250). The fundamental beam was plane polarized and the plane of polarization was rotated through 360^{o} using a half-wave plate. The transmitted SHG was detected in p- and s-polarizations, the so-called q-p and q-s geometries.[1] It was ascertained that the glass substrate alone produces no detectable SHG.

Reference

1. R. Vallée, P. Damman, M. Dosière, E. Toussaere, J. Zyss, *J. Chem. Phys.* **2000**, *112*, 10556.

Publications and Presentations

PUBLICATIONS

1. Anthony, S. P.; Radhakrishnan, T. P. *Chem. Commun*, **2001**, 931.
Perfectly polar assembly of molecular dipoles in crystals of Zn(II)(DMAP)$(acac)_2$: a case of self-poling.

2. Anthony, S. P.; Srikanth, L.; Radhakrishnan, T. P. *Mol. Cryst. Liq. Cryst.*, **2002**, *381,* 133.
Impact of molecular structure change on the hierarchy of intermolecular interactions leading to polar / centrosymmetric crystals.

3. Anthony, S. P.; Raghavaiah, P.; Radhakrishnan, T. P. *Cryst. Growth Des.* **2003**, *3*, 631.
Extreme molecular orientations in a dimorphic system : polar / centric and polar / polar cogrowth crystal architectures.

4. Anthony, S. P.; Radhakrishnan, T. P. *Chem. Commun.* **2004**, 1058.
Helical and network coordination polymers based on a novel C_2-symmetric ligand: SHG enhancement through specific metal coordination.

5. Anthony, S. P.; Radhakrishnan, T. P. *Cryst. Growth Des.* **2004**, *4*, 1223.
Coordination polymers of Cu(I) with a chiral push-pull ligand: hierarchical network structures and second harmonic generation.

6. Anthony, S. P.; Naga Srinivas, N. K. M.; Rao, D. N.; Radhakrishnan, T. P. *J.Mater.Chem.* **2005**, *15*, 739.
Thin films of perfectly polar crystallites with uniaxial orientational ordering.

7. Srinivas, K.; Sitha, S.; Rao, V. J.; Bhanuprakash, K.; Ravikumar, K.; Anthony, S. P.; Radhakrishnan, T. P. *J.Mater.Chem.* **2005**, *15*, 965.
First hyperpolarizability of some nonconjugated donor-acceptor 3D molecules: noncentrosymmetric crystal through conformational flexibility.

8. Anthony, S. P.; Basavaiah, K.; Radhakrishnan, T. P. (Submitted).
Chiral vicinal bis(amide) molecules : polar / helical assemblies in crystals and SHG.

9. Anthony, S. P.; Porel, S.; Rao, D. N.; Radhakrishnan, T. P. (Submitted).
Thin Films of Metal-Organic Compounds and Metal Nanoparticle Embedded Polymer for Nonlinear Optical Applications.

PRESENTATIONS

1. Poster presented at the National Laser Symposium, Center for Advanced Technology, Indore, India, December, **2002**.
Naga Srinivas, N. K. M.; Anthony, S. P.; Rao, D, N.; Radhakrishnan, T. P. "Self assembly of $Zn(acac)_2(DMAP)$: SHG from thin film grown by physical vapour deposition."

2. Poster presented at the National Laser Symposium, Center for Advanced Technology, Indore, India, December, **2002**.
Gangopadhyay, P.; Naga Srinivas, N. K. M.; Anthony, S. P.; Rao, D. N.; Radhakrishnan, T. P. "Internal cancellation of second harmonic signals in solvent mixtures and solutions : a new analysis protocol for EFISH study."

3. Poster presented at the Modern Trends in Inorganic Chemistry, Indian Institute of Technology, Bombay, India, December, **2003**.
Anthony, S. P.; Radhakrishnan, T. P. "Perfectly polar crystals of zinc complexes and dimorphic structures with extreme dipole orientations."

4. Poster presented at the International Topical Conference on Optical Probes of Conjugated Polymers and Biosystems, Indian Institute of Science, Bangalore, India, January, **2005**.
Anthony, S. P.; Naga Srinivas, N. K. M.; Rao, D. N.; Radhakrishnan, T. P. "Thin films of perfectly polar crystallites with uniaxial orientational ordering: optical second harmonic generation."